

130 187 909

2003 LE MA 1019

A STUDY OF PREPARATION OF LIGHT COLORED PHOTSENSITIVE  
LIQUID NATURAL RUBBER

CHOR.WAYAKRON PHETPHAISIT



A THESIS SUBMITTED IN PARTIAL FULFILLMENT  
OF THE REQUIREMENTS FOR  
THE DEGREE DOCTOR OF PHILOSOPHY  
(POLYMER SCIENCE AND TECHNOLOGY)  
FACULTY OF GRADUATE STUDIES  
MAHIDOL UNIVERSITY  
200X

ISBN XXX-XX-XXXX-X  
COPYRIGHT OF MAHIDOL UNIVERSITY

BIBLIOTHEQUE UNIVERSITAIRE DU MANS  
\*M062848\*

## CONTENTS

Page

ACKNOWLEDGEMENT

ABSTRACT ( in English )

ABSTRACT ( in Thai )

LIST OF TABLES

LIST OF FIGURES

LIST OF ABBREVIATIONS

CHAPTER

I	INTRODUCTION	1
II	OBJECTIVE	4
III	LITERATURE REVIEW	6
	1. Natural Rubber	6
	1.1 Fresh natural rubber latex	6
	1.2 Concentrated natural rubber latex	10
	1.3 Purification of natural rubber	12
	1.4 Analysis of proteins	14
	1.5 Stability of natural rubber latex	15
	2. Liquid Natural Rubber	18
	2.1 Oxidative chain scission	19
	2.2 Chemical accelerated chain scission	21
	3. Epoxidised Natural Rubber	26
	3.1 Mechanism of epoxidation	27
	3.2 Side reactions of epoxidation	28
	3.3 Parameters affecting epoxidation reaction	30
	3.3.1 Amount of formic acid	30
	3.3.2 Amount of hydrogen peroxide	31
	3.3.3 Effect of reaction temperature	31
	3.3.4 Effect of pH, latex stability and concentration of latex	32

	<b>Page</b>
4. Acrylated Natural Rubber	33
5. Photoinduced polymerization or crosslinking reaction	38
5.1 UV sources	38
5.2 UV irradiation polymerization mechanism	39
5.2.1 Initiation stage	40
5.2.2 Propagation stage	40
5.2.3 Termination stage	40
5.3 Photoinitiator	42
5.3.1 Free radical initiator	43
5.3.2 Cationic photoinitiator	44
5.4 Functionalized oligomers or prepolymers	45
5.5 Reactive diluents	46
5.6 Analytical method for studying the photopolymerization	48
5.6.1 Infrared spectroscopic method	48
5.6.2 Ultraviolet spectroscopic method	50
5.6.3 Calorimetric method	51
<b>IV MATERIALS AND METHODS</b>	<b>54</b>
1. Materials and Instruments	54
2. Preparation of Purified Natural Rubber	56
3. Degradation of Purified Natural Rubber Latex by Using Potassium Persulfate and Propanal	56
4. Epoxidation Reaction of Liquid Purified Natural Rubber	57
4.1 By in-situ performic acid	57
4.2 By m-chloroperbenzoic acid	59
5. Degradation Reaction of Epoxidized Purified Natural Rubber by Using Periodic Acid	59
6. Addition Reaction of Acrylic Acid onto Epoxidized Molecules	60
6.1 Addition reaction of acrylic acid onto 4,5-epoxy-4- methyloctane	60

	Page
6.2 Addition reaction of acrylic acid onto epoxidized liquid synthetic rubber	61
6.3 Addition reaction of acrylic acid onto epoxidized liquid purified natural rubber	62
7. Analysis	63
7.1 Chemical structure characterization	63
7.1.1 By infrared spectroscopy	63
7.1.2 By <sup>1</sup> H-NMR and <sup>13</sup> C-NMR spectroscopy	64
7.2 Separation characterization technique	64
7.2.1 By supercritical fluid chromatography (SFC)	64
7.2.2 By Gas chromatography-mass spectrometer (GC-MS)	64
7.3 Determination of nitrogen content by micro-Kjeldahl method	64
7.4 Determination of epoxide content	65
7.4.1 By <sup>1</sup> H NMR spectroscopy	65
7.4.2 By <sup>13</sup> C NMR spectroscopy	66
7.5 Determination of acrylate content	66
7.6 Molecular Weight Determination	66
7.6.1 By viscometric method	66
7.6.2 By gel permeation chromatography	67
8. Photocrosslinking Reaction of Acrylate Elastomer	67
8.1 Operating apparatus	67
8.2 Preparation of samples for the study of photoreaction	69
<b>V RESULTS AND DISCUSSION</b>	74
1. Purified Natural Rubber	74
2. Degradation of Purified Natural Rubber by Using Potassium Persulfate and Propanal	76
2.1 Proposed reaction mechanism	78
2.2 Parameter effecting the degradation reaction	81
2.2.1 Effect of concentration of K <sub>2</sub> S <sub>2</sub> O <sub>8</sub>	81

	<b>Page</b>
2.2.2 Effect of concentration of propanal	83
2.2.3 Effect of Na <sub>3</sub> PO <sub>4</sub>	85
2.2.4 Effect of reaction temperature	85
2.2.5 Effect of dry rubber content (DRC)	87
2.2.6 Effect of oxygen	88
2.2.7 Effect of surfactant	90
2.3 Kinetics study of degradation reaction	91
3 Epoxidation Reaction of Liquid Purified Natural Rubber	98
3.1 Epoxidation by using m-chloroperbenzoic acid	
3.2 Epoxidation by using in-situ performic acid	
3.2.1 Chemical structure of epoxidized product	
3.2.2 Parameters effecting epoxidation reaction	
3.2.2.1 Effect of surfactant	
3.2.2.2 Effect of hydrogen peroxide	
3.2.2.3 Effect of formic acid	
3.3 Kinetics study of epoxidation reaction	
3.4 Degradation reaction of epoxidized purified natural rubber by using periodic acid	
3.4.1 Preparation of epoxidized natural rubber	
3.4.2 Degradation reaction	
3.4.3 Parameters affecting the degradation reaction	
3.4.3.1 Amount of periodic acid	
3.4.3.2 Amount of epoxide content of starting material	
3.4.3.3 Effect of type of rubber and chemical reagent	
3.4.3.4 Proposed degradation mechanism of rubber by periodic acid	
4 Addition Reaction of Acrylic Acid onto Epoxidized Molecules	144

## CHAPTER I

### INTRODUCTION

Natural rubber (NR) is a very high molecular weight polymer ( $>1 \times 10^6$ ), having highly cis-1,4-polyisoprenic structure that cannot be easily produced by synthetic method. The NR has been widely used for manufacturing of various industrial and medicinal products requiring high elasticity and flexibility such as tyres, rubber seals, gloves and condoms. Among 2500 plant species known to produce natural rubber, *Hevea brasiliensis* is the only tree that produces natural rubber in high quantity for industrial applications. Thailand is the first natural rubber producing country in the world. The production ratio is about 32% per year over the world production as shown in Table 1.1. However, the price of raw natural rubber is not effectively controlled by the country, it is mostly due to the fluctuation of the world economic. The researches on improving the quality of raw natural rubber, finding new rubber products and varieties of usable natural rubber are the ways to increase the need of NR as well as its price.

**Table 1.1** The world production of natural rubber in 2001 and 2002 (January-May): data supplied by the Department of Foreign Trade, Thailand (all values in thousands of metric tones)

Country	2001		2002 (January-May)	
	Production	Ratio of production	Production	Ratio of production
Thailand	2357	33.15	902	31.99
Indonesia	1576	22.17	684	24.26
India	631	8.87	222	7.87
Malaysia	547	7.69	219	7.77
China	451	6.34	199	7.06
Vientiane	317	4.46	163	5.78
Other	1231	17.31	431	15.28
World total	7110	100.00	2820	100.00

Natural rubber is originally obtained in latex form and it can be then transformed into solid stage for further specific utilizations. Chemical modification of NR would increase the areas of application and it can be done both in the form of solid and latex, depending on the reaction involved. Degradation of NR into lower molecular weight will wider the field of utilization of NR such as binder, plasticizer, adhesive and surface coating materials [1-4]. Functionalization of NR by epoxidation is one of the most interesting methods for property modification of NR. The presence of oxirane structure will increase the polarity of NR, leading to increasing of oil and wear resistance. The introduction of the epoxide group on the molecular chain of NR will also offer varieties of further exploitation of NR as the epoxide group is a reactive intermediate for addition reaction by nucleophilic reagents. The second step modification of the NR will wider the application of existing NR. Addition of photosensitive moieties, flame retardable moieties are examples of the successful modification of NR [1,5,6].

Nowadays, the field of surface coating materials is increasingly applied under irradiation particularly the use of ultraviolet light source because of the rapid process and the possibility to provide variety of formulations with the presence of non-volatile organic solvent. The materials subjected to be used by this technology should contain a certain amount of photosensitive groups in the compound formulation. Generally, the base materials can be oligomers or polymers containing mono- or polyphotopolymerisable functional groups. The photosensitive monomers often involved in this system are cinnamic, methacrylic and acrylic molecules. Acrylated epoxies, acrylated urethanes and acrylated polyester are three types of photosensitive oligomes used in industrial applications such as flooring (paper upgrading, laminating adhesive) and thin film coating in electronics applications [7-10]. Another type of oligomer being developed is (metha) acrylated elastomers. These materials have promising interest because the resulting product will combine the distinct characteristics of elastomeric character of the elastomer and the toughness of acrylate. They should produce high resistance to impact and scratching, great flexible and good adhesion to substrates [1,5,11-13].

The introduction of the NR into the field of surface coating particularly by using ultraviolet irradiation technique would offer a great potential in development of

new photosensitive material which will certainly wider the exploitation of NR. However, the NR is a very high molecular weight material, therefore the use of NR for surface coating application requires the method to lower its molecular weight or viscosity suitable for the process to be further involved. In this study, the degradation of NR into low molecular weight has to be investigated. The NR also contains a small amount of non-rubber constituents which may induce coloration to the final product as well as the allergic problem, therefore purified natural rubber by treatment of NR with an enzyme and followed by double centrifugations was employed.

The acrylic group is considered as a very sensitive function to photoreaction. This study is focused on fixation of certain amount of this molecule on the NR having low molecular weight. The addition of the acrylic acid on the rubber chain has been planned through the epoxide ring opening reaction of prior epoxidised liquid rubber. The study of photocrosslinking of the liquid rubber containing the acrylate function has planned to be investigated by using photocalorimetry system. The system is based on the use of modified differential scanning calorimetry which is equipped with ultraviolet light source. The internal change during the photopolymerization of the samples such as heat released from the formation of carbon-carbon linkage will be directly detected. The data of the heat change can be used to relate the kinetic and extent of photoreaction of the materials. The photocalorimetry is a convenient method for study of photopolymerisation and photocrosslinking reaction as small quantity of material is needed and the measurement of the heat released can be directly compared to the amount of the photosensitive group added.

## CHAPTER II

### OBJECTIVES

The present thesis aims to find value added for natural rubber (NR) by modification of the NR into photosensitive material, which has potential use in the field of surface coating application, particularly by using ultraviolet irradiation. For this, it is necessary to transform the NR into suitable molecular weight and viscosity. The NR should also contain photosensitive functions which fit well with the technology of photocuring. The molecular weight of the NR in the order of 5 000 to 20000 will be promising for further being used in surface coating area. The introduction of acrylic function onto the NR molecule can be done by second step modification via epoxide ring. Therefore, the addition reaction of acrylic acid onto epoxidized low molecular weight NR will be the strategy for introduction of the photosensitive group onto the NR molecular chain. Generally, the materials used in the field of surface coating applications contain diluents for viscosity modifier and photoinitiators for acceleration of the rate of curing. The study of the photocuring of various compound formulations is necessary in order to find the optimum conditions for further application of the photosensitive materials prepared from natural rubber.

The objectives of this work are the followings;

1. Preparation of photosensitive material from natural rubber (NR) by introduction of certain amount of acrylic groups onto the molecular chain of the NR.
2. Study of the photocrosslinking reaction of the prepared photosensitive rubber by photocalorimetry.

The scope of the work is divided into 4 main parts.

1. Preparation of liquid purified natural rubber (LPNR) by degradation reaction of purified natural rubber (PNR) using potassium persulfate and propanal.

The PNR is prepared by enzymatic treatment of natural rubber latex, following by twice centrifugation. Parameters effecting the degradation reaction such as the amount of the potassium persulfate and propanal as well as the reaction temperature are also studied.

2. Study of epoxidation reaction of LPNR in organic and latex medium by using m-chloroperbenzoic acid and in-situ performic acid, respectively.

The in-situ performic acid is generated by the reaction of hydrogen peroxide and formic acid. The kinetic of the epoxidation is also investigated. The purpose of this step is to prepare liquid natural rubber containing epoxide functional group. The study of degradation of epoxidized purified natural rubber by periodic acid is also carried out.

Parameters effecting the epoxidation reaction such as types and amount of surfactant, amount of hydrogen peroxide and formic acid are investigated.

3. Study of preparation of acrylated liquid natural rubber from the addition reaction of acrylic acid onto epoxidized liquid rubber prepared from the former section.

The addition reaction of acrylic acid onto 4,5-epoxy-4-methyloctane and liquid synthetic polyisoprene are also investigated as well as the parameters effecting the addition reaction such as the amount of acrylic acid and the reaction temperature.

4. Investigation of photocrosslinking reaction of acrylated liquid rubber and its kinetic reaction by photocalorimetry.

The effects of photoinitiators, reactive diluents and reaction temperature on the rate of photocrosslinking reaction are also studied.

## CHAPTER III

### LITERATURE REVIEW

#### 1. Natural Rubber

Natural rubber (NR) can be synthesized in numerous of plants, over 2,000 species but *Hevea brasiliensis* tree is the only one that can produce NR used industrially. The NR possesses excellent physical properties, especially high tensile and tear strength, remarkable elastic behavior, which have not yet been competed by synthetic elastomers. As the NR is produced naturally in latex form, exuded from the *Hevea* tree, it can be served for fabrication of dipping products such as gloves and balloons. The transformation of NR into solid form has expanded its applications to important industries such as manufacturing of tyres and rubber seals. The NR is a very high molecular weight polymer fabricated in plant. The rubber compositions in latex are varied among different types of plant. The rubber latex contains also some non-rubber constituents. It has been reported that the non-rubber components effect on the physical properties of the final products. Therefore, there have been many works continuously published by a numbers of scientists on the study of the nature, composition and manufacture of NR in order to optimize the exploitation of the NR.

##### 1.1 Fresh natural rubber latex

The fresh latex exuded from the *Hevea* rubber tree is white cytoplasmic fluid composed of spherical rubber particles dispersed in water. The plant has synthesized the rubber on the basis of the presence of the key enzyme, rubber transferase which transforms the carbon in the plant into long hydrocarbon chains of rubber. These chains are assembled and accumulated as rubber particles surrounded by an osmotically sensitive biomembrane, ranging in size from 5 nm to 3  $\mu\text{m}$ . suspended in water. The biomembrane is composed of lipid-protein interactions, which preserves an interface between the hydrophobic rubber core interior and the aqueous cytosol and

prohibit the aggregation of the rubber particles [14-16]. It has been reported and accepted that the chemical structure of the rubber is cis-1,4-polyisoprene with an average molecular weight of about  $1.0-1.3 \times 10^6$ . The *Hevea* exhibits bimodal distribution of the molecular weight with a major peak at ca.  $7 \times 10^5$  and a minor peak at ca.  $0.5-1.0 \times 10^5$  [17,18]. This may suggest that the polymerization in this plant undergoes a two-step process or the presence of some branching. It has also been reported by Othman AB and Hepburn C that the NR molecular chain contains some abnormal groups such as epoxide and carbonyl functions [19].

The fresh *Hevea* latex is generally consisting of about 30-45% w/v rubber hydrocarbon and about 4-5% w/v non-rubber constituents [19]. The variability of the latex composition depends on several factors such as clone source of rubber, tapping frequency and collected season. The non-rubber components have been identified as proteins, lipids, inorganic substances and others as presented in Table 3.1. They are positioned randomly in the latex. By using ultracentrifugation at 19500 rpm, the fresh latex can be separated into four fractions as shown in Figure 3.1. The upper white fraction is mainly composed of rubber particles with small quantities of protein, lipid and metals. The second layer is yellowish orange in color containing the Frey Wyssling particles. The third part is called C-serum fraction and the bottom fraction (lutoid) is grey yellow in color, sometime called B-serum. They contain some proteins and metals.

**Table 3.1** Composition of fresh natural rubber latex [20-22]

Composition	% by weight
Dry rubber content	30-45
Non-rubber constituents	
- Proteins	0.95-1.5
- Lipids	1.6
- Inorganic substances	0.5
- Inositols and carbohydrates	1
- Ash	Up to 1
- Sugar	1.0-1.5

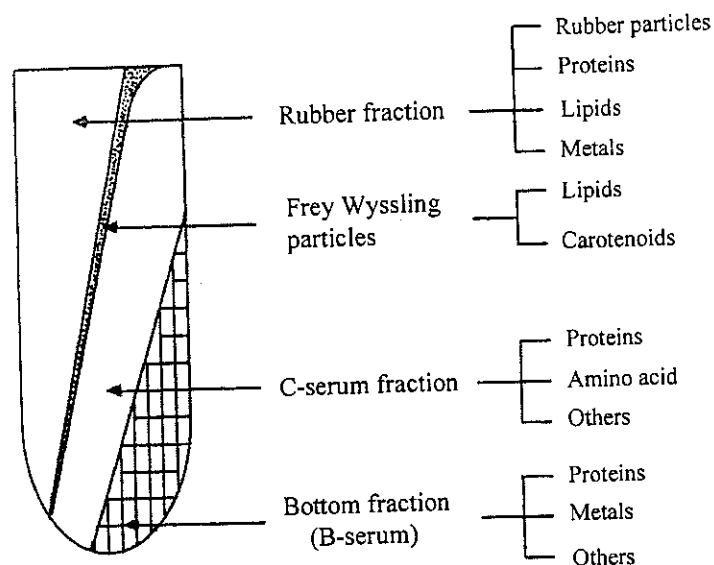


**Figure 3.1** Four fractions of fresh natural rubber latex separated by using ultracentrifugation [19]

Two major components of the non-rubber constituents which have been reported to effect on the physical and chemical properties of natural rubber are proteins and lipids [16,21-27]. About 27.2 % of proteins found in the *Hevea* latex are bound with the rubber particles, 47.5% are in serum fraction and 25.3% are in the bottom fraction. Normally, the *Hevea brasiliensis* contains up to 80 different types of proteins with the size range between 5 to over 200 kDa. However, only a few types of protein can be classified. Two proteins tightly bound with rubber particle are observed namely as 14.6 kDa (rubber elongation factor) and 24 kDa (small rubber particle protein). Rubber elongation factor enzyme (14.6 kDa) has been proposed to work with prenyl transferase (38 kDa) to effect on the polymerization of the isoprene unit. Hevamine (29 kDa) which is the basic protein from the bottom fraction and Hevin (N domain, 5 kDa and C domain, 14.2 kDa) which is found in serum fraction, acts as defense-related proteins. Two unrecognized latex proteins at 46 and 110 kDa are found and studied by several scientists and they are pointed as protein allergen to some people.

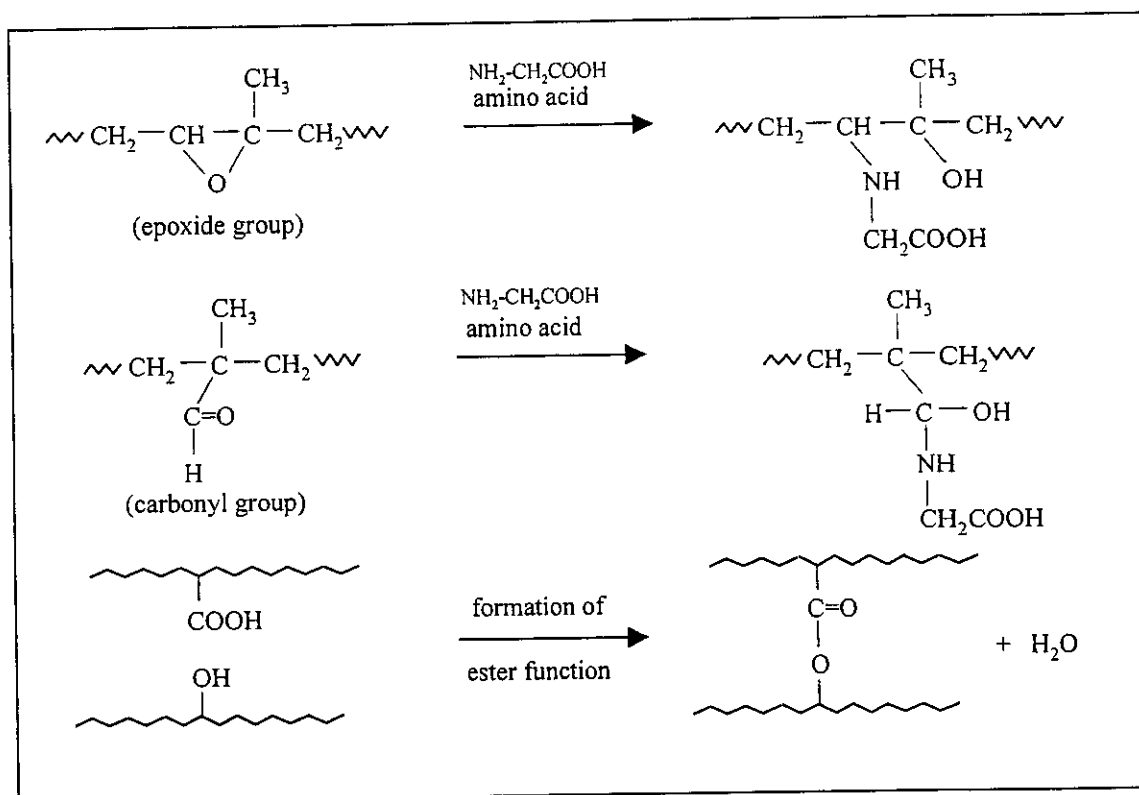


**Figure 3.2** Proposed reactions that cause the storage hardening of natural rubber [19]

For the physical properties of rubber, the presence of basic amino acids such as alanine show powerful effect on the fluctuation of modulus of the rubber with the humidity changed. It is believed that, proteins cause lightly crosslinking in the rubber, called storage hardening. This may come from the reaction of amino acid with the abnormal groups on the rubber chains such as epoxide or the carbonyl groups as well as the reaction between the abnormal groups (as shown in Figure 3.2).

In the case of about 1.6% of lipids found in the fresh *Hevea* latex, they compose of 54% neutral lipids, 33% glycolipids and 14% phospholipids [21]. The neutral lipids include tocotrienol, which are natural antioxidants, and phenolic compounds such as polyphenols and carotenoids, which cause discoloration of dry rubber. Glycolipids found are composed of four main components i.e. esterified sterol glycoside (ESG), monogalactosyl diglyceride (MGDG), sterol glucoside (SG) and digalactosyl diglyceride (DGDG). The role of these substances is not clear but it is believed to relate to the presence of sugar. The polar phospholipid is believed to adsorb on the surface of the rubber particles with the polar head groups facing



outwards to the surrounding aqueous medium and the hydrophobic tail of phospholipids is intermingling with the rubber core [14].

As reported that the surface layer of rubber particles are surrounded by lipid-protein monolayer biomembrane, Cornish K et al. had used electron- paramagnetic-resonance spin labeling (EPR) to indicate that proteins are positioned at the outer surface of the rubber particles with very little fraction penetrating into the biomembrane interior [14]. The proteins are believed to play more roles on the surface charge of rubber particles than the lipids as they can act as natural surfactant for the natural rubber latex. Kuhakarn S had studied the character of latex particles at various pH by using electrophoresis [28]. The results obtained indicated that the surface of latex is amphoteric in nature with an isoelectric point at pH 4. This amphoteric character confirms the presence of proteins on the latex particles [29-31]. At pH below 4, the protein exhibits the positive charge while the negative charge is dominated when the pH is above 4 as demonstrated in Figure 3.3.

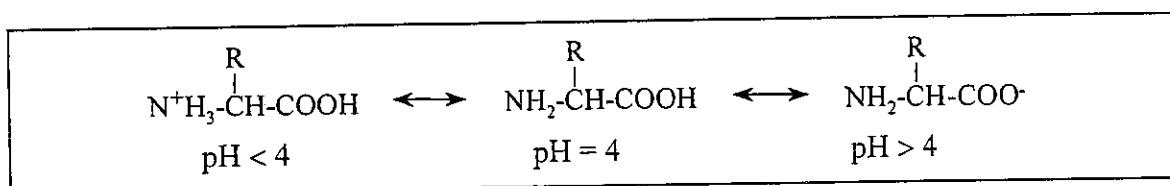


**Figure 3.3** Zwitterionic form of protein on rubber particles in latex phase at various pH [28-31]

## 1.2 Concentrated natural rubber latex

The variability of the rubber products is believed to depend on the non-rubber components, which are about 4-5% in fresh NR latex. Therefore partially removal of the non-rubber constituents which are sensitive to bacterial attack, may result in better uniformity in quality of the latex. This can be done by increasing the concentration of NR latex. The concentrated latex will gain some advantages in lowering the cost of storage and transportation. Three main methods for preparation of concentrated natural rubber latex are employed [20,32].

The first one is concentration by evaporation. For this the latex was stabilized with alkali i.e. potassium hydroxide and soap or ammonia before heating at 90°C

under reduced atmospheric pressure. Usually, 11 times of operation are required to obtain high total solid content (upto 75%) as each time the decrease of latex concentration is about 7%. By this method, the concentrated latex contains high level of non-rubber content (8%).

The second process is called creaming. The rubber particle can move to the upper phase by the density difference between the rubber dispersed phase ( $0.93 \text{ gcm}^{-1}$ ) and the serum continuous phase ( $1.02 \text{ gcm}^{-1}$ ) with the help of creaming agents such as ammonium alginate and sodium alginate to increase the viscosity which caused the acceleration of creaming process. High viscosity (1100 mPa, at 20 rpm) and high dry rubber content (66%) are collected by this process. However, this is a slow process and during storage or transportation, post-creaming can be inevitably occurred.

The most popular process which takes about 90% over other methods is concentration by centrifugation. The rubber latex is stabilized with ammonia before centrifugation into about 60% dry rubber content. The rate of the movement of the suspended rubber particles away from the aqueous phase depends on the angular velocity of the centrifugation. The latex is fractionated into cream fraction and serum fraction which includes skim latex. This process eliminates mainly soluble non-rubber constituents including water soluble proteins. In the skim latex, it contains about 3-6% of rubber particles. The concentrated latex obtained shows low level of non-rubber content of about 2%. Hasma H analyzed proteins from concentrated high ammonia latex (HANR) and proteins from C- and B-serum of fresh latex using isoelectric focusing (IEF) polyacrylamide gel [22]. The results from IEF image shown in Figure 3.4 reveal less number of band regions corresponding to the number of types of proteins in serum of HANR than in the serum of fresh latex. It can be postulated that the HANR prepared by centrifugation, some part of protein are eliminated i.e. reduction of non-rubber contents.

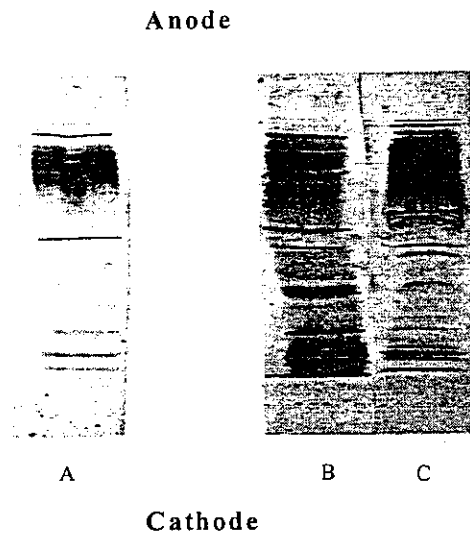


**Figure 3.4** Isoelectric focusing (IEF) of (A) serum proteins of high ammonia latex concentration, (B) the proteins from B-serum of fresh latex and (C) the proteins from C-serum of fresh latex [22]

### 1.3 Purification of natural rubber

As mentioned earlier that the rubber particles are coated with protein-lipid membrane. The lipid can be extracted from the solid rubber by using chloroform/methanol mixture. The proteins in fresh latex are believed to be both distributed in the serum fraction and bound with the rubber particles. The water soluble proteins can be partially removed by centrifugation during the concentration process, but not the proteins bound on the rubber particles. Therefore, the storage hardening behavior is unavoidable as well as the influence of proteins on physical properties of rubber i.e. hardness and modulus [19]. The presence of residual proteins may cause allergic problem to people contacting natural rubber product [23,26,27].

By using ultracentrifugation, Hasma H had isolated 2 main fractions of HANR i.e. rubber fraction and serum fraction [22]. The serum proteins separated from the first ultracentrifugation contained 14, 24, 29, 36, 45 and over than 100 kDa. The proteins, which are bound with the rubber particles (RP) in rubber cream fraction, can be further removed by using ammonia, sodium dodecyl sulphate (SDS) or organic solvent such as chloroform/methanol mixture. Hasma H had rinsed the rubber fraction with water before redispersing in water using 0.7% of ammonia or 0.2% sodium

dodecyl sulphate (SDS) and stirred over night. After recentrifugation at ultrahigh speed, the analysis of the serum fraction obtained showed the presence of 14, 24 and 29 kDa proteins. This may be postulated that ammonia and SDS can extract proteins bound on the RP. By using organic solvent extraction, the rubber fraction from the first centrifugation was dispersed in a minimum amount of water before adding of chloroform-methanol. The extract, separated from rubber coagulum, was washed with 0.6% sodium chloride and the resulting mixture was kept overnight before characterization. Similar types of proteins i.e. 14, 24 and 29 kDa are extracted by organic solvents. In addition, proteolipid was detected in the case of the use chloroform-methanol.

There are several works expressing the elimination of proteins from NR by determination of residual nitrogen content. The nitrogen content in fresh field NR latex is found to be 0.87%. Ichikawa N et al. had claimed the preparation of highly purified NR latex as they obtained very low nitrogen content of NR latex by using two techniques [33]. The first one is by washing the NR latex with 1% w/v of non-ionic surfactant, Triton X100, followed by ultracentrifugation (11000 rpm). They repeated the process for 5 times and found that the nitrogen content was reduced to 0.03%. They also found the decrease of weight average molecular weight ( $\bar{M}_w$ ) with respect to number of centrifugations. The  $\bar{M}_w$  of field latex was reduced from  $3.40 \times 10^6$  to  $1.80 \times 10^6$  for 5 times of centrifugations. Another method is by using enzymatic treatment (alkaline protease) with three times of washing with surfactant, sodium naphthenate, together with ultracentrifugation. By this method, they obtained very low nitrogen content of 0.009%. The  $\bar{M}_w$  of field latex was reduced from  $3.40 \times 10^6$  to  $1.76 \times 10^6$ . When they used high ammonia concentrated NR latex (HANR), they found the decrease of nitrogen content from 0.56% of HNAR to 0.03% by using non-ionic surfactant and 0.08% for enzymatic treatment. They also found the decrease of  $\bar{M}_w$  of high ammonia latex (HALx) from  $3.45 \times 10^6$  to  $2.69 \times 10^6$  and  $2.46 \times 10^6$ , respectively.

#### 1.4 Analysis of proteins

There are several methods having been developed for revealing the presence of proteins in NR. By electrophoresis technique using polyacrylamide gradient gels over 80 different types of proteins can be differentiated in NR latex, ranging in size between 5 to over 200 kDa [22,23,25,26,34,35].

As the protein is poly(amino acid), therefore, detection of amide function in the molecular chain by spectroscopic method should be possible. FTIR spectroscopy is a feasible easy method for qualitative measurement of proteins [36,37]. Lu FJ and Hsu SL had fractionated the NR into two fractions; the soluble part called sol and the insoluble fraction or gel [36]. They found that the infrared spectra of sol and gel of NR indicated the presence of proteins by the appearance of absorption bands at  $3280\text{ cm}^{-1}$ , which is characteristic of N-H stretching, at  $1630\text{ cm}^{-1}$  due to amide I vibration and at  $1540\text{ cm}^{-1}$  corresponding to amide II vibration, as shown in Figure 3.5. The spectra also presented the absorption band characteristic of fatty acid at  $1738\text{ cm}^{-1}$  due to C=O stretching. They found the disappearance of the absorption bands at  $3280\text{ cm}^{-1}$ ,  $1630\text{ cm}^{-1}$  and  $1540\text{ cm}^{-1}$  for the purified rubber obtained by using lauryl sodium sulfate solution (6%) and water/acetone extraction. However, the characteristic band of fatty acid at  $1738\text{ cm}^{-1}$  is still relevant.

Another method often used to represent the existence of proteins in NR is the determination of the amount of nitrogen in the rubber sample. It can be referred to protein content and it can be derived from 6.25 times of nitrogen content. CHN-elemental analysis and Kjeldahl method have been widely used for determine of the nitrogen content. However, the elemental analysis sometime shows negative values of nitrogen content as this method is very sensitive to purity of the material analyzed. Micro Kjeldahl method has been frequently used to determine the amount of nitrogen in NR with 0.001% accuracy. There are several works that reported the presence of proteins by giving the value of nitrogen content. Othman AB and Hepburn C reported nitrogen content (wt%) of standard Malaysian rubber (SMR) and deproteinized natural rubber (DPNR) prepared by ultracentrifugation at 195000 rev/min. to be 0.41 and 0.08 wt%, respectively [19]. Eng AH et al. had found 0.38 and 0.015 wt% nitrogen content

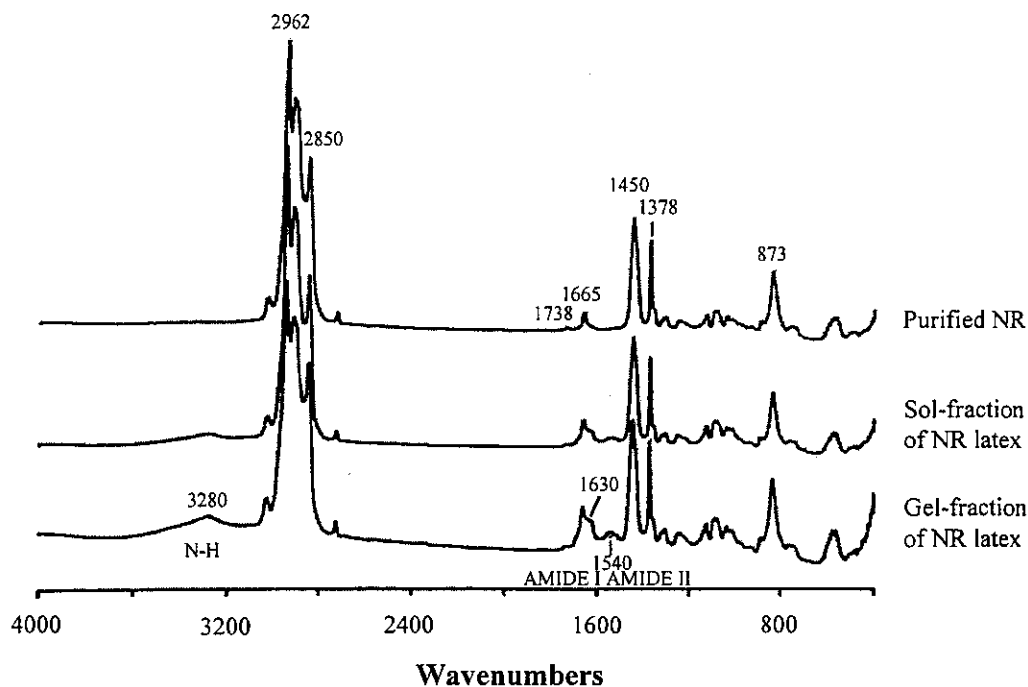


**Figure 3.5** Infrared spectra of sol and gel fraction of purified rubber natural [36]

in pale crepe rubber and DPNR obtained by enzymatic treatment and centrifugation, respectively [38].

Tanaka Y. et al. had investigated nitrogen content in several samples of DPNR [38,39]. They used FTIR analysis on the measurement of the intensity ratio of N-H stretching (between  $3347\text{-}3277\text{ cm}^{-1}$ ) to =CH out-of-plane deformation of isoprene structure (between  $907\text{-}780\text{ cm}^{-1}$ ) to quantify the nitrogen content, comparing to elemental analysis and Kjeldahl method. They found that FTIR method offers rapid determination and the result is comparative to the other two techniques. However, the limitation of FTIR is the humidity of the sample that may interfere to the signal of N-H stretching.

### 1.5 Stability of natural rubber latex

The rubber particle (RP) is found to be surrounded by biomembrane which are protein/lipid complex layer. This surface layer acts as natural surfactant making the rubber well dispersed in colloidal form of the latex. The isoelectric point of *Hevea*

latex is reported to be at pH 4 [28]. Above this point, the RP is stabilized by negative charge of adsorbed proteins [29,30]. This natural surfactant is sensible for bacterial attack, therefore, ammonia solution or aqueous base such as sodium hydroxide is practically added to freshly tapped latex as well as in the concentrated latex as partially proteins are removed during the centrifugation process.

In the preparation of purified natural rubber mentioned earlier, an important amount of protein is eliminated; therefore insufficient amount of natural surfactant for covering the surface of rubber particles will cause destabilization of NR latex. The loss of natural stability will bring about molecular interaction forces or Van der Waals' forces between two hydrocarbon molecules as well as the cohesive forces of strong hydrogen bonding between water-water which induced significant coagulation. The addition of chemical surfactants can modify the surface of the rubber particles or interface between the rubber particles and the water by reducing the energy difference between the rubber hydrocarbon chain and water to allow the stable colloidal mixture to be formed [40].

Surfactants used for emulsification of NR latex can be classified in three types; anionic, cationic and nonionic or amphoteric surfactants. Ionic surfactants provide good performance in increased water-solubility and stability of the products. While nonionic surfactants can provide the product stability in wide range of pH [40]. Each surfactant has two chemical behaviors; one as a hydrophilic character, which tends to coalesce with aqueous phase and a hydrophobic character, which will prefer to be expelled from the aqueous phase. The hydrophobic moiety tends to be adsorbed or transferred to the surface of non-polar molecules (in the case of oil/water emulsion). The behavior of surfactant depends upon concentration as shown in Figure 3.6. The long straight line represents the hydrophobic part of the surfactant while the circle signifies the hydrophilic end-chain. At very low concentration (I), the surfactant molecules lie flat on the particle surface. As the concentration increases (II), there are not enough places for lying flat due to the surfactant molecules increases so they begin to orient upward. When the amount of surfactant is high enough for covering all the surface of the particle, the surfactant will orient the hydrophilic part stand outward to the aqueous phase or hydrophobic part to the organic phase. This concentration is

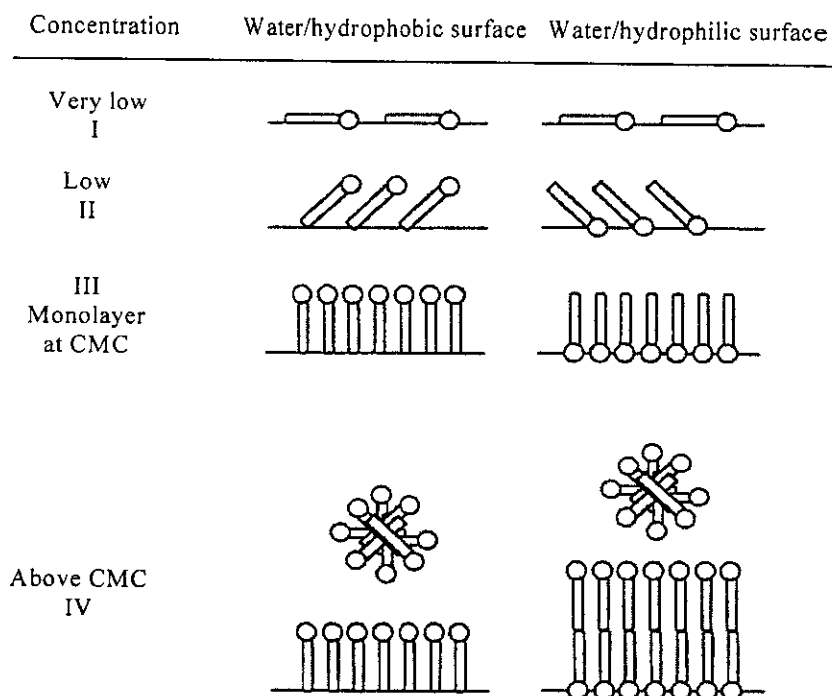


**Figure 3.6** Adsorption behaviors of surfactant at various concentrations [40]

called critical micelle concentration (CMC). At the concentration IV (above CMC), there is no apparent change in the adsorption on the substrates, but more than one layer of surfactant molecules can be formed at the particle surface for forming of micelle.

The stability of colloidal particles covering with surfactants depends on the type of surfactant [41,42]. Figure 3.7 shows three mechanisms of stabilization of particles by different types of surfactant. The ionic surfactant will follow the electrostatic repulsion while the nonionic surfactant can behave as steric repulsion which included osmotic and entropic repulsion. The surfactant containing ionic charge on the hydrophilic part will stabilize the droplets from aggregation by electrostatic repulsion. This repulsion can overcome the interfacial attraction of Van der Waals forces between the molecules. Some examples of surfactant usually used for stabilization of NR latex are sodium dodecyl sulfate (SDS), which has negative charge on the hydrophilic part. While the nonionic surfactants such as nonyl phenol ethoxylated (sinnopal NP 307) that does not ionize, will stabilize the droplets by steric repulsion, which can be explained by osmotic effect and entropic of elastic effect. Osmotic repulsion can be occurred between interpenetration of chains of surfactant

which bring about the high osmotic pressure in the overlap zone. The outside water will be transported to reduce the pressure in the overlap zone, leading to the repulsion of two molecules. On the hand, when the two molecules move out until arrival of the short interparticles distance, the chains of surfactant will not be interpenetrated, the compression of the chains will bring about the decrease of conformation of the chains and reduce the entropy of the system. Then, the particles will be separated to increase the thermodynamic stability. This is call entropic or elastic repulsion.

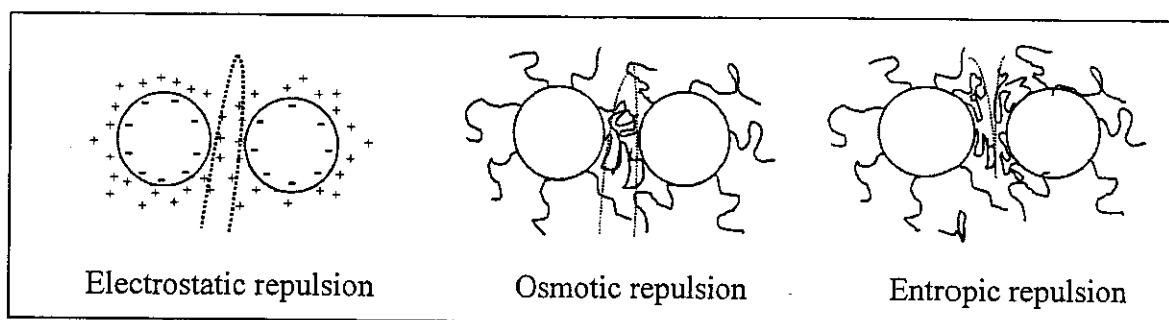


**Figure 3.7** Mechanism of stabilization on presentation of ionic and nonionic surfactant [41,42]

## 2. Liquid Natural Rubber

NR as obtained from *Hevea* tree is a very high molecular weight polymer of about one million and it is found in elastic solid form. By lowering the molecular weight, the NR will become viscous fluid so called liquid natural rubber (LNR). The molecular weight of LNR can be varied from about 10,000 to several ten-thousands, depending on the conditions of preparation. Because of its liquid-like character, LNR has various promising fields of application, such as adhesive, binder, sealant, reactive plasticizer and surface coating materials. There have been several works published on degradation of NR into LNR [43-47]. These methods include mechanical, thermal and chemical or photochemical degradation. Most of them indicated that the main chemical structure of LNR is cis-1,4-polyisoprene as the original NR. Some revealed also the presence of functional groups such as hydroxyl and carbonyl groups. Oxidative degradations by thermal and chemical reactions have been widely studied because controlled molecular weight can be obtained as well as the possibility to perform the degradation reaction in latex or organic medium.

## 2.1 Oxidative chain scission

Bevilacqua EM was one of the beginners who studied the oxidative chain scission of *Hevea* latex [48]. The reaction was carried out at 90°C and 1.8 atmospheric pressure, under shaking of 240 cycles per minute. He measured the intake oxygen used in this reaction. He found that the intrinsic viscosity,  $[\eta]$  of the rubber was decreased with the increasing of adsorbed oxygen in the latex. The results showed also the increase of small molecules such as carbon dioxide, formic acid and acetic acid. Bevilacqua EM had continued the work on oxidative degradation of dry rubber at 140°C [49]. He found that the chain scission of rubber resulted in volatile products i.e. levulinaldehyde ( $\text{CH}_3\text{COCH}_2\text{CH}_2\text{CHO}$ ) and formaldehyde. He suggested that levulinaldehyde could be the source of both acetic acid and carbon dioxide found in the case of degradation of *Hevea* latex.

Morand JL had studied the oxidative chain scission of synthetic polyisoprene in air at 100°C [50]. By using gas-phase chromatography, 26 different volatile species were detected and 11 of them were the same products identified by Bevilacqua EM. Thermal oxidation of synthetic cis- and trans-1,4-polyisoprenes and squalene were investigated by Golub MA and Hus MS [51]. They used nuclear magnetic resonance to analyze the resulting products, and then proposed the oxidative chain degradation mechanism as shown in Figure 3.8. At high temperature, carbon radical at allylic position of polyisoprene unit can be formed as well as its delocalized isomer. These radicals were then attacked by oxygen, leading to two cyclic peroxide intermediates (I and II). The breakage of carbon-carbon and carbon-oxygen bond of these intermediates will lead to rubber chain scission and formation of some small molecules. It was found that the degraded polyisoprene contained ketone and aldehyde functions.

Alam TM et al. had studied the thermal oxidative degradation of pentacontane ( $\text{C}_{50}\text{H}_{102}$ ) at 125°C, less than a day and polyisoprene (PI, 97% cis 1,4 structure) at 95°C for 31 days [52]. They used  $^{17}\text{O}$  NMR for determination of the non-volatile degradation species remaining in the polymer sample. They found that in the case of pentacontane, equal amount of ketone and alcohol or ether functions were found. But for the PI, the concentrations of alcohols/ether species were higher than ketones. They

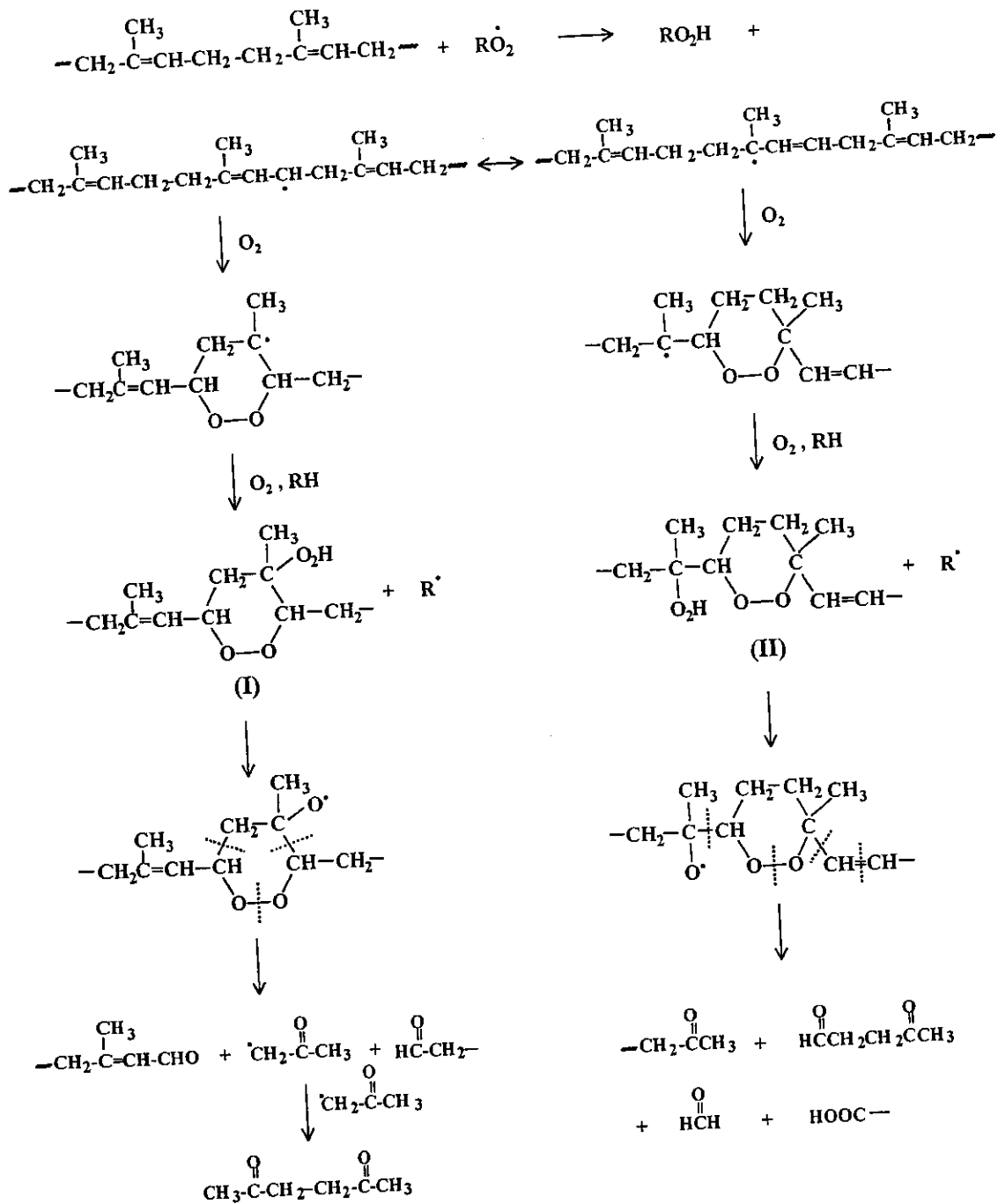
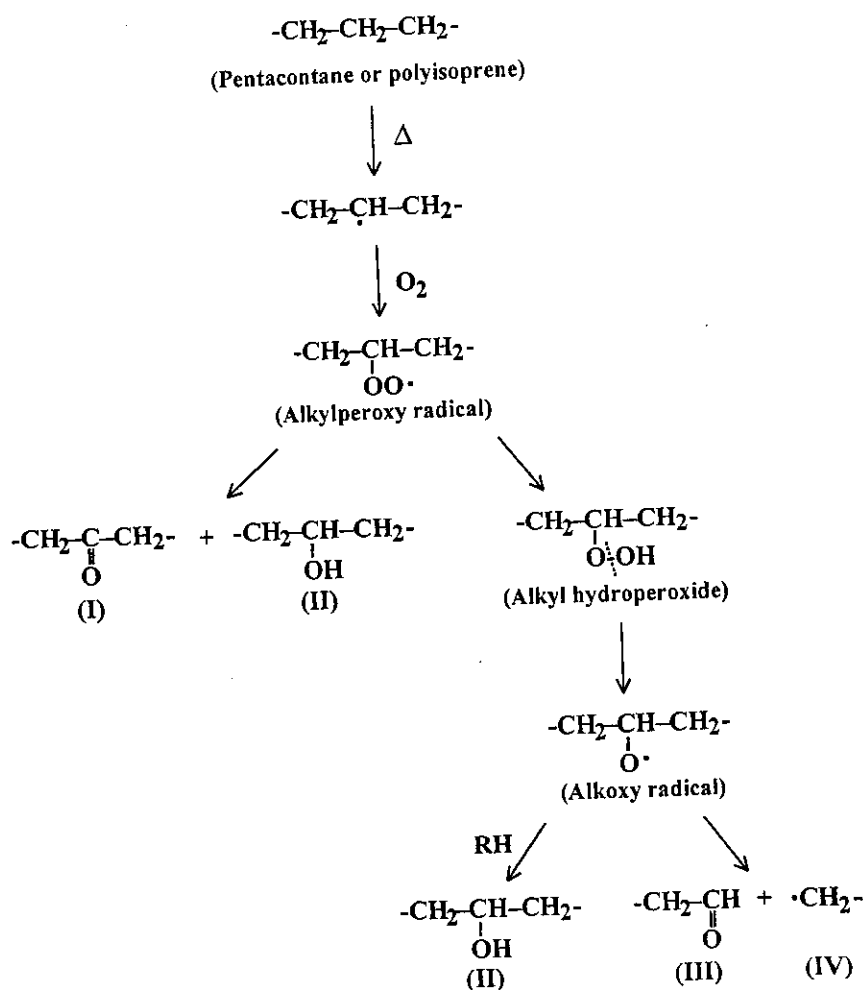


Figure 3.8 Thermal oxidation of polyisoprene [53]



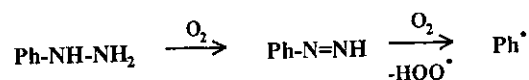
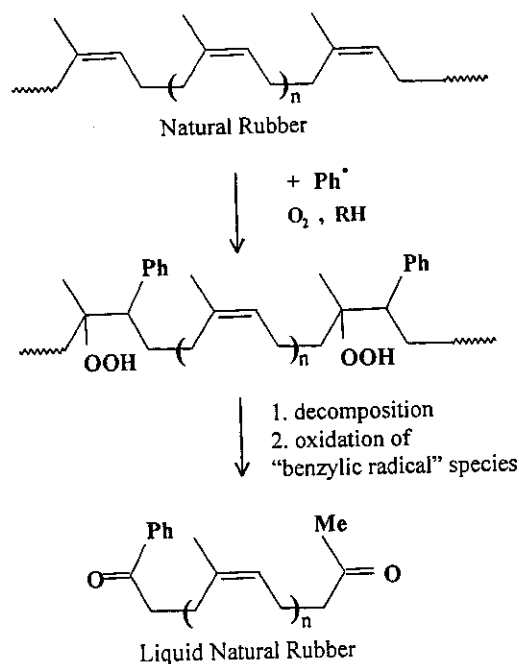
**Figure 3.9** Proposed reaction pathway of chain degradation of pentacontane and polyisoprene [52]

proposed the oxidative degradation mechanism as shown in Figure 3.9. The pentacontane should follow the mechanism of formation of alkylperoxy radical (ROO $\cdot$ ) which leads to chain scission of species I and II. The PI would go to the formation of alkyl hydroperoxide (ROOH), followed by alkoxy radical (RO $\cdot$ ) before chain cleavage to the structures II, III and IV.

## 2.2 Chemical accelerated chain scission

According to the common mechanism of oxidative chain degradation of polymers involves prior generation of radical species on the molecular chains, chemical reagents capable of inducing such species fast at relative low temperature

## Oxidation of phenylhydrazine

Chain cleavage process initiated by radical  $\text{Ph}\cdot$ 

**Figure 3.10** Proposed degradation reaction pathway of natural rubber by using phenylhydrazine/ $\text{O}_2$  system [54]

should be used to accelerate the chain scission. Pautrat R had studied the oxidative degradation of natural rubber in latex phase in the presence of phenylhydrazine and oxygen at  $60^\circ\text{C}$  [45]. He found that the reduction of the molecular weight of the rubber depended directly on the amount of phenylhydrazine at the fixed amount of oxygen. The mechanism of degradation reaction of this system was elucidated by Reyx D et al. as shown in Figure 3.10 [47]. They indicated that the phenylhydrazine was decomposed into phenyl radical which then reacted with the double bond of the polyisoprene, leading to the formation of radical species on the polymeric chain. These active sites were attacked by oxygen, forming hydroperoxide intermediate before the breakage of the polymer chain. The resulting degraded rubber contains ketone functions at the extremity of the chain [47,54].

Tangpakdee J et al. had studied the degradation reaction of deproteinized natural rubber (DPNR) using different types of initiator such as AIBN, potassium persulphate ( $K_2S_2O_8$ ), benzoyl peroxide (BPO) and 2,2'-azobis(2,4-dimethylvaleronitrile (V-65), in the presence of carbonyl compounds such as acetone, formaldehyde or propanal [46]. They concluded that  $K_2S_2O_8$ /propanal system is the most effective for degradation of rubber at 60°C. They claimed that the rubber chain was oxidized by radical initiator and the propanal may react partly with the reactive aldehyde forming at the chain end of the degraded product as shown in Figure 3.11. The degraded rubber contained aldehyde and ketone groups at both terminal chains ends. They did not propose the mechanism of the degradation. The kinetic of the oxidative degradation was not mentioned.

In some cases, decreasing of molecular weight of NR was carried out with previously modified NR. Bac NV et al. had added  $NaNO_2$  to the prepared epoxidized NR as well as during the epoxidation process of NR [55]. They found that  $NaNO_2$  had acted as a reducing agent to scissor the molecular chain of NR. The intrinsic viscosity of the rubber sample reduced quickly in the first 10 hours from 4.1 to 1.08 in the presence of 3.4 phr of  $NaNO_2$  at low pH. However, the reaction mechanism of this parallel reaction was not proposed.

Lead tetraacetate,  $Pb(OAc)_4$  and periodic acid ( $H_5IO_6$ ) are another interesting chemicals used for degradation of polyisoprenic chain. Generally, both reagents can cleave vic-glycols to carbonyl compounds. Burfield DR and Gan SN had studied the chain cleavage of natural rubber and epoxidized synthetic rubber (EIR) by these compounds [56]. They found that  $Pb(OAc)_4$  degraded hydrolysed EIR faster than EIR. It can also slowly degrade the synthetic polyisoprene sample (IR) which presumably contains no 1,2-diols. The authors proposed that the chain scission by  $Pb(OAc)_4$  was occurred through radical oxidative degradation process. However, the author found that  $H_5IO_6$  did not cleave the chain of the controlled IR. However, the  $H_5IO_6$  can be used as a chemical to degrade NR and acid hydrolyzed NR. In the case of NR, it is believed that the degradation of the chain was occurred as the NR contained a few 1,2-diol groups in the molecular chain. The degradation of other epoxidized compounds

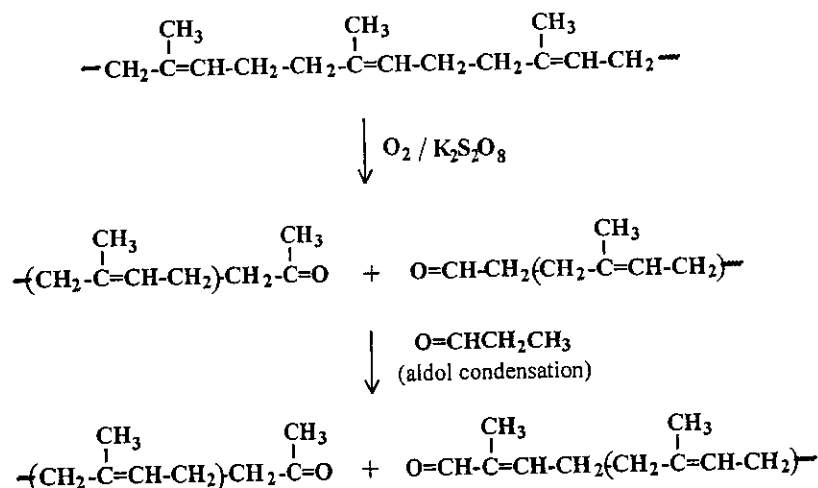


**Figure 3.11** Proposed degradation reaction pathway of deproteinized natural rubber by using  $\text{K}_2\text{S}_2\text{O}_8$ /propanal system [46]

by the  $\text{H}_5\text{IO}_6$  had also been demonstrated by Nagarkatti JP and Ashley KR [57]. They had studied the degradation of 5,6-epoxycyclooctene and 1,6-epoxycyclohexane with  $\text{H}_5\text{IO}_6$  (1/1 mole/mole) in water at  $45^\circ\text{C}$ . They proposed that the cleavage reaction had been occurred through the formation of periodate complex of the epoxide which was then subsequently cleaved to yield the aldehydes at the end of the molecular structure (see Figure 3.12). This oxidation does not necessarily proceed via glycol intermediate, the cleavage reaction may be occurred directly at the epoxide structure.

Mauler RS et al. investigated the chain cleavage of styrene-butadiene rubber (SBR) by using  $\text{H}_5\text{IO}_6$  and/or ultrasonic radiation [58]. They showed that the use of  $\text{H}_5\text{IO}_6$  could degrade the SBR chain much better than the use of only the ultrasonic radiation of 40 kHz. The  $\text{H}_5\text{IO}_6$  can induce degradation reaction of SBR from  $\bar{M}_w$  of 325,000 to 80,000. The condition of  $\text{H}_5\text{IO}_6$  in conjunction with 40 kHz of ultrasonic radiation, the  $\bar{M}_w$  of SBR was reduced to 40,000. Later on, Mauler RS and another coworkers had studied the chain cleavage of 1,4-cis-polyisoprene (*Hevea brasiliensis*), using  $\text{H}_5\text{IO}_6$  (2/10 v/v) in various solvents and reaction temperatures [59]. The effect of solvent and temperature on the degradation reaction are shown in Table 3.2. It can be seen that at low temperature the chain degradation using  $\text{H}_5\text{IO}_6$  is better in

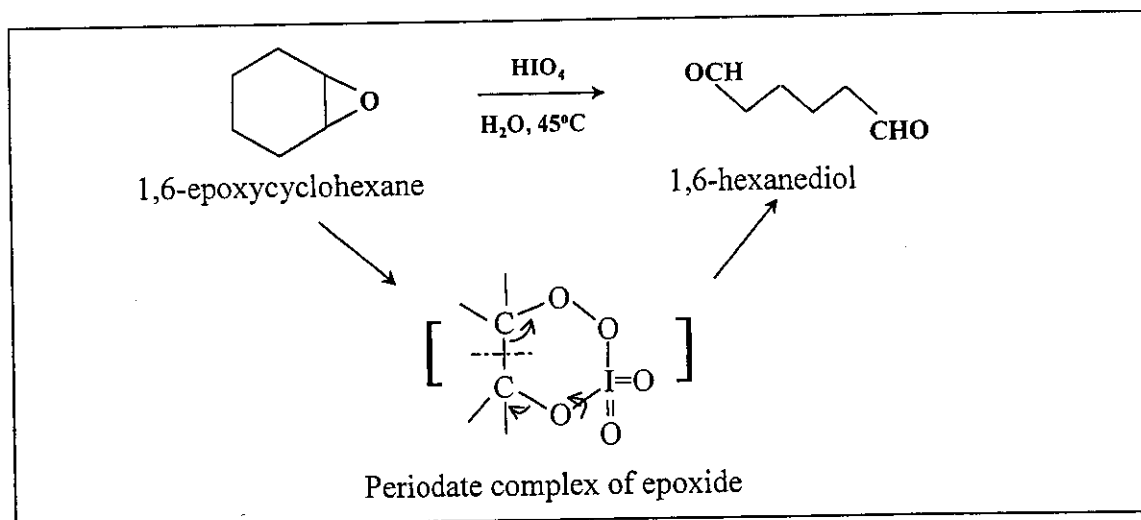


**Figure 3.12** Proposed the degradation reaction pathway of partially epoxidized compound with periodic acid [57]

chloroform than in toluene and n-hexane. They explained by solvent dielectric constant ( $\epsilon/D$ ) values that the increase of  $\epsilon/D$  value may bring about the increase of ionic activity coefficient, then the dissociation constant of electrolyte in solution increases. The  $\epsilon/D$  values of chloroform, toluene and n-hexane are found to be 4.806, 2.379 and 1.89 respectively. Therefore, the dissociation of the periodic acid ( $H_5IO_6$  activity) is expected to be highest in chloroform solution. Moreover, periodic acid dissociation increases with increased reaction temperature, resulting in increasing the reaction rate constant of chain degradation.

**Table 3.2** Molecular weight obtained after degradation reaction of NR using  $H_5IO_6$  in various types of solvent and reaction temperatures after 60 mins

MW	Starting NR	Degradation condition					
		Chloroform		Toluene		n-Hexane	
		10°C	50°C	10°C	50°C	10°C	50°C
$\bar{M}_w$	800,000	100,000	5,000	300,000	5,000	460,000	200,000

Reyx D and Campistron I had used  $H_5IO_6$  for preparation of telechelic liquid natural rubber [47]. They found the decrease of epoxide content from 25% of the starting rubber to 8% after degradation reaction. The molecular weight of degraded

rubber was found to be  $\overline{M}_n = 3100$  and  $\overline{M}_w = 17,600$  respectively.  $^1\text{H}$  NMR spectrum revealed the presence of aldehyde and methylketone at the chain ends, residual oxiranes and secondary furanic and cyclic structure. Gillier-Ritoit S et al. had studied chain degradation of polyisoprene (PI) and epoxidized polyisoprene (EPI) using  $\text{H}_5\text{IO}_6$  in organic solution (THF) [60]. The degraded rubber from PI showed similar  $^1\text{H}$  NMR results as the degraded rubber obtained from EPI. Both final products contained aldehyde and ketone terminal ends. They found that the degree of chain scission of this system were not the same. The cleavage reaction of PI with  $\text{H}_5\text{IO}_6$  was slower than in the case of EPI. They proposed that the  $\text{H}_5\text{IO}_6$  cleaved the EPI directly but in the case of chain degradation of PI, they proposed two-step mechanism. In the first step,  $\text{H}_5\text{IO}_6$  reacted with double bond resulting in epoxide or  $\alpha$ -glycol structure. Then, the epoxide or  $\alpha$ -glycol was cleaved by second equivalent of  $\text{H}_5\text{IO}_6$  (see Figure 3.13).

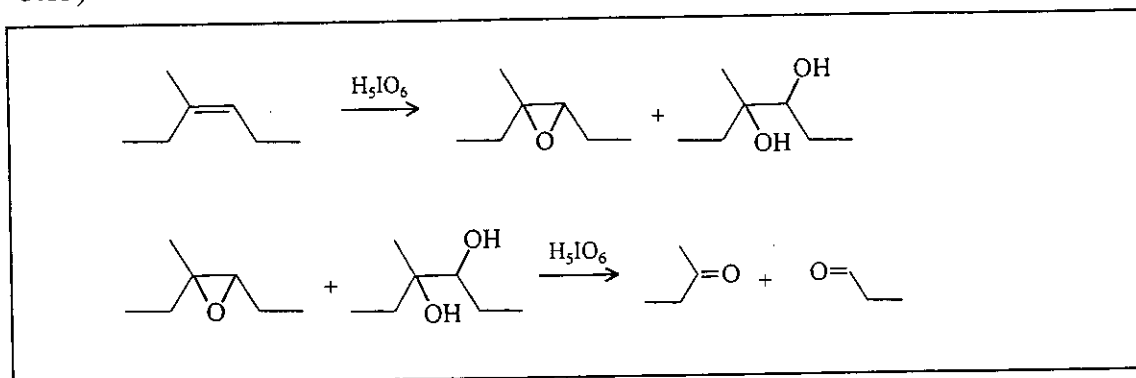


**Figure 3.13** Proposed degradation pathway of polyisoprene by periodic acid [60]

### 3. Epoxidized Natural Rubber

NR is highly *cis*-1,4-polyisoprenic structure, the double bond along the molecular chain is considered to be an active function for various chemical reactions, like other olefinic molecules. Investigations of functionalization of natural rubber (NR) have been started in mid-1970 as a result of the oil crisis. The aim of the scientists is to prepare new polymeric materials as well as to wider the application of NR. Epoxidation represents a particular convenient and promising method for transforming the NR into an interesting elastomeric material with improved oil and wear resistance [61]. This modification leads to the increase of the polarity of the NR

as well as to create another active functional group to the NR. The epoxidized NR has shown an improvement of the adhesion properties between non-polar and polar polymer such as the adhesion between rubber and nylon in tire industry [62]. The epoxide or oxirane ring on the rubber chain can be further used as an active intermediate for several reactions such as the reaction with phosphate groups, resulting in improvement of flame resistance of 1,4-polydienes, reaction with acrylic acid for development of photosensitive materials [1,3,63].

In the case of polydienes, both synthetic and natural materials, the epoxidation has been extensively studied as it can be performed in various ways, including in solid sheets, in solution or in latex medium [64-66]. Reagents used for epoxidation reaction of alkene molecules include preformed peracid such as m-chloroperbenzoic acid, perphthalic acid, peracetic acid and in-situ performic acid generated from hydrogen peroxide and formic acid. General reaction between peroxyacid and an alkene is shown in Figure 3.14.

### 3.1 Mechanism of epoxidation

The epoxidation reaction of alkenes has been widely studied with varieties of peroxy acids. Kwart H and Hoffman DM proposed two epoxidation mechanisms as Bartlett's mechanism and 1,3-dipolar mechanisms which depend on the polarity of the solution system, as shown in Figure 3.15 [67,68]. In non-polar solvent, the reaction between peroxyacid and the double bond can be occurred via Bartlett's mechanism. While the reaction which is carried out in polar solvent may undergo 1,3-dipolar mechanism. It has also been mentioned in the literature that the cis-alkene undergoes epoxidation more rapidly than the trans isomer [67]. The epoxidation reaction of diene polymers i.e. polyisoprene or polybutadiene result in a random distribution of epoxide groups along the polymer backbone. The reaction with cis-isomer structure is faster than with the trans-isomer structure [67,69].

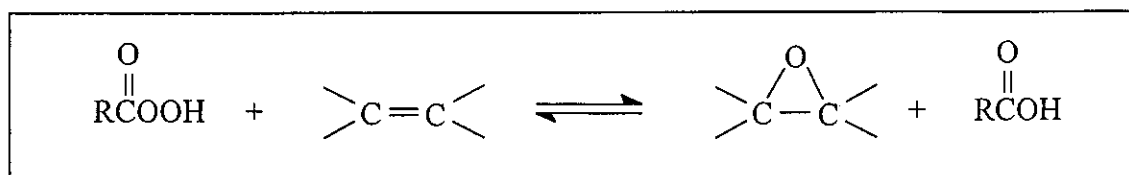
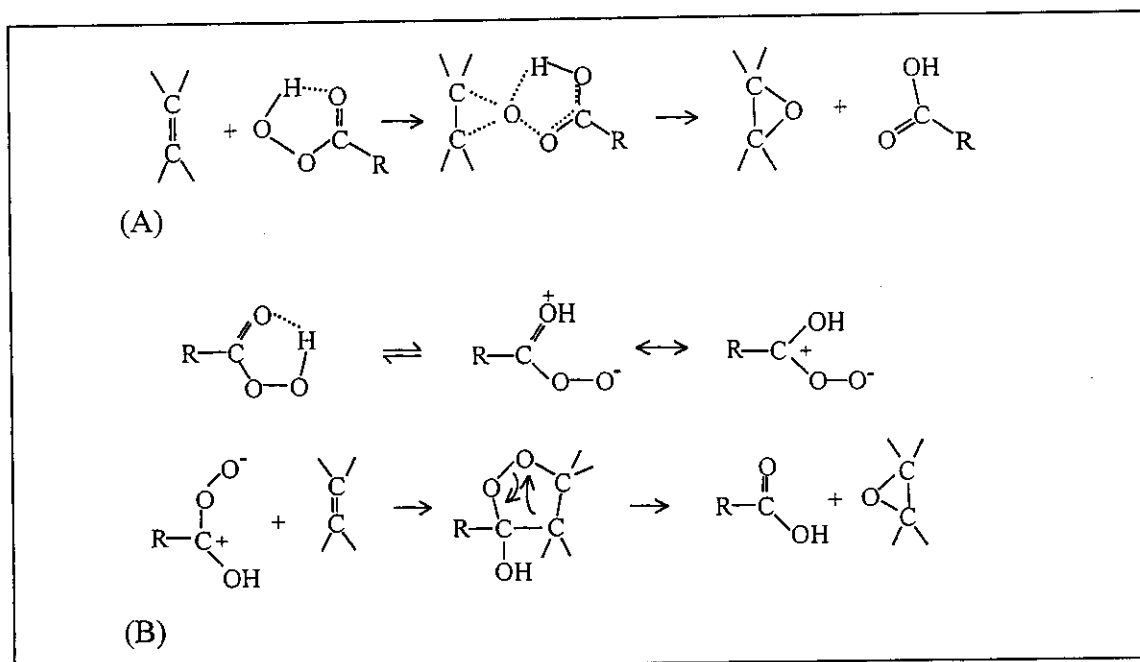


Figure 3.14 Epoxidation reaction of an alkene with peroxy acid [69]



**Figure 3.15** (A) Bartlett's mechanism and (B) 1,3-Dipolar mechanism of peroxyacid epoxidation [67]

### 3.2 Side reactions of epoxidation

The epoxidation of NR in latex medium is preferable for commercial development because of the ease of the reaction procedure and low cost of the reagents involved. However, some side reactions are usually occurred. The epoxidation in organic medium is also carried out as less secondary reaction is obtained. In aqueous solution, preformed peracetic acid or in-situ performic acid are generally used. As a consequence of epoxidation reaction, the peroxy acid is transformed into carboxylic acid. If it is not eliminated, it can react with epoxide ring, resulting in the epoxide ring opening reaction. The ring opened product intermediates may lead to various types of by-products such as diol structure, hydroxyl carboxylate and crosslinked by-products as shown in Figure 3.16 as well as the formation of hydrofuran (THF) in Figure 3.17 [64-66,69-72].

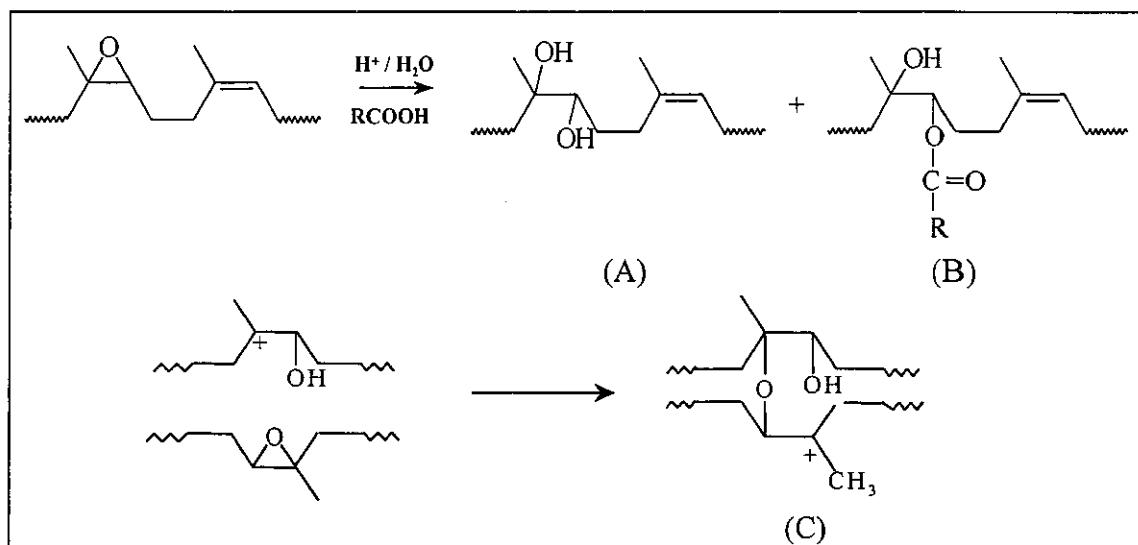


**Figure 3.16** Secondary ring opening reaction of isolated epoxide groups; (A) Diol structure, (B) Carboxylat structure and (C) Ether linkage structure [65,69]

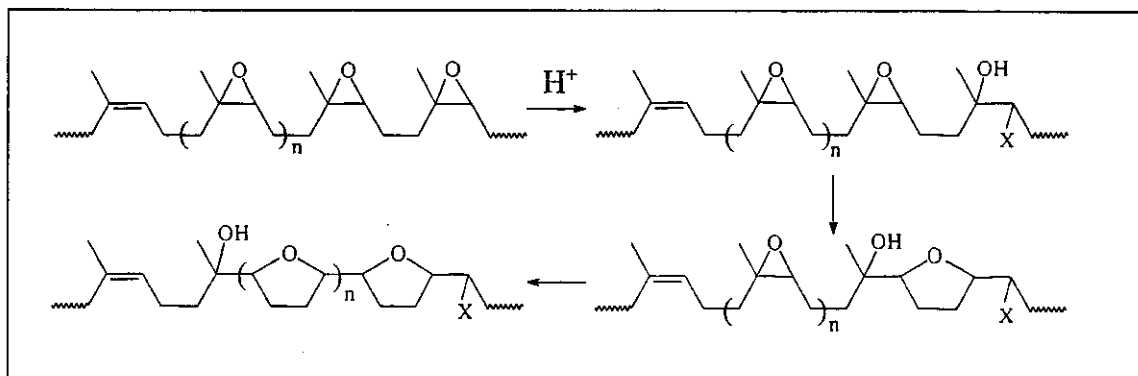


**Figure 3.17** Formation of five-membered cyclic ether reaction of adjacent epoxidized polyisoprenic units [69]

Bac NV et al. had investigated the epoxidation of NR, using peracetic acid [71]. They analyzed the epoxidized NR (ENR) and by-products of the reaction by using infrared spectroscopy. They found that the most important characteristic bands of epoxide group were observed at 870-880  $\text{cm}^{-1}$  (epoxide half ring stretching) and 1240-1260  $\text{cm}^{-1}$  (epoxide whole ring stretching). At higher epoxide level (>20%), the signal of cyclic ether at 1070  $\text{cm}^{-1}$  was observed, this band can be assigned to tetrahydrofuran (THF) ring formed by ring-opening side reaction. The authors titrated the ENR solution with hydrogen bromide (HBr) and found that with low epoxide contents (lower than 15%), the ring-opening intermediate was occurred, then followed by the addition of bromide ion. However, at higher epoxide contents, the titration of

ENR did not follow by the addition of bromide ion to the ring opened intermediate but it was followed by the formation of cyclic ether moieties (THF). The spectra of the products after titration show the strong band of hydroxyl group at 3200-3580  $\text{cm}^{-1}$  and THF at 1070  $\text{cm}^{-1}$ . These results were used to confirm that at high epoxide content of the ENR prepared, the formation of cyclic ether by-product can be occurred. These authors also pointed out that determination of epoxide content of the ENR at high epoxide content by HBr titration gave lower value than the use of  $^1\text{H-NMR}$ , which was due to the furanization during the titration.

Gelling IR had also demonstrated that beside the main epoxide structure of the reaction in latex medium of NR with peracetic acid, secondary products were also occurred depending on the level of epoxidation [69]. At low epoxide level, the majority of epoxide groups were isolated, probable side reactions expected can only be hydrolyzed derivatives such as vic-diol, hydroxyl carboxylate and ether linkage as shown earlier in Figure 3.16. When the modification level was increased, hence increasing of number of adjacent epoxide groups will bring about the formation of five-membered cyclic ether or hydrofuran formation as in Figure 3.17.

### **3.3 Parameters affecting epoxidation reaction**

As mentioned earlier that the preparation of epoxidized NR has preferably performed in aqueous media as it is the original media of the NR. Therefore, peroxy acids such as peracetic acid and in-situ performic acid generated from hydrogen peroxide and formic acid can be involved. It has been found in several papers that the amount of these acids have direct influence on the formation of epoxide structure, secondary products and the stability of the reaction medium [65,66,72-74]. The acidity usually representing in terms of pH and reaction temperature also involved in the epoxidation reaction. Some examples of these parameters are as the followings.

#### **3.3.1 Amount of formic acid**

Ng SC and Gan LH performed the epoxidation reaction of NR latex using in-situ performic acid generated from hydrogen peroxide and formic acid [65]. They experimented with excess amount of formic acid and found that the epoxidation was occurred only 7%. As most of the oxiranes formed were suddenly followed by ring opening reaction to form hydroxyformate and glycol. The latex had lost its stability

within 2 hours of reaction and the rubber coagulum was observed. This may be due to the formation of ether linkages and THF ring.

Perera MCS et al. had studied the effect of amount of formic acid on epoxidation reaction of natural rubber [72]. They used  $[PI]/[H_2O_2] = 0.65$  and  $[H_2O_2]/[HCOOH] = 2.9, 1.4$  and  $0.5$  under the presence of nonionic surfactant. The results showed the rate of epoxidation increased with increasing the amount of acid. However, the times for observation of the formation of secondary products are reduced as 52, 25 and 10 hours of reaction, respectively.

Roy S et al. noticed that the rate of epoxidation of NR latex increased with increasing the amount of formic acid [73]. By increasing the amount of formic acid, less epoxidation level was obtained. This may be due to the fact that at higher acid concentration, side reactions such as ring opening reaction and furanisation predominate over the epoxidation process. The maximum extent of epoxidation was obtained to be 70% in the case of using  $2.3 \text{ mol/dm}^3$ . All latex systems were stable through the reaction by the help of nonionic surfactant.

### 3.3.2 Amount of hydrogen peroxide

Hydrogen peroxide ( $H_2O_2$ ) is the controlled chemical reagent of the conversion of natural rubber to epoxidized natural rubber because of exhaustion after formation of peracid. However, the epoxide content obtained does not relate directly to the amount of hydrogen peroxide added because of the loss of some hydrogen peroxide due to reaction temperature and pH of the reaction medium. Gnecco S et al. reported the epoxidation reaction of low molecular weight *Euphorbia lactiflua* natural rubber by in-situ performic acid [75]. In this case, higher amount of  $H_2O_2$  led to a higher epoxidation level in the final product. The use of an excess amount  $H_2O_2$  allows the achievement of higher amount of epoxidized unit in the final product at an early stage of the reaction.

### 3.3.3 Effect of reaction temperature

Reaction temperature also influences on the rate of epoxidation using hydrogen peroxide and formic acid of NR latex. Swern D et al. proposed that formic acid react slowly with hydrogen peroxide to form peracid under the reaction temperature below

40°C without an acid catalyst [76]. However, the increase of reaction temperature may increase the rate of decomposition of hydrogen peroxide.

Gan LH and Ng SC had studied the kinetic of performic epoxidation of NR latex by using hexadecyltrimethylammonium chloride as cationic surfactant at 3, 15 and 25°C [70]. They found that the rate determining step was the formation of performic acid. At higher reaction temperature, higher epoxidation level could be occurred. The activation energy was found to be 55 +/- 6 KJ mol<sup>-1</sup> and the entropy of activation -172 +/- 22 Jmol<sup>-1</sup>K<sup>-1</sup>. Some ring opened structures were also detected at long epoxidation time (higher 40% epoxidation). It was purposed that the positive charged latex particles might have a role in inhibiting the secondary ring opening reaction.

Roy S et al. had studied the epoxidation reaction of NR latex using *in-situ* performic acid under acetic acid catalyst [73,77]. The reaction was carried out between 24 to 38°C. The results showed the increase of epoxide content and rate of reaction with increasing the temperature, whereas the extent of secondary reaction was also increased. In the Arrhenius plot, the straight line from the overall rate constant values (ln k) was falld after the reaction temperature higher than 32°C. It was due to the fast increase of amount of secondary product formation, thus the overall rate of epoxidation was decreased.

Mulder Houdayer S had studied the effect of reaction temperatures as 40, 60 and 70°C on epoxidation reaction of NR latex and synthetic rubber using the ratio of H<sub>2</sub>O<sub>2</sub>/HCOOH = 1 in the presence of 3 phr of sinnopal NP 307 non-ionic surfactant [78]. The rates of epoxidation of both rubbers were found increasing with increasing of reaction temperature. However, after 70-80 hours, the epoxide content using 60 and 70°C showed the same values as about 24 % epoxide content or 80% yield. In addition, the secondary reactions, forming cyclic furan and hydroxylated products were also found with the increase of the reaction temperature.

### 3.3.4 Effect of pH, latex stability and concentration of latex

Bac NV et al. reported the effect of pH on epoxidation reaction. They found that at high values of pH as 6-7, low rate and low epoxide content were observed due

to the decomposition of  $H_2O_2$  causing the decrease of active peracid. The suitable pH for the epoxidation should be 2.2-3 [55,74,79].

As the epoxidation reaction is well performed in acid media (low pH). This is not an easy process to control the reaction of natural rubber latex due to the ease of loss of stability in acidic condition. The study of the use of different types of surfactant has been considered by many researches. Bac NV et al. had studied the effect of nonionic surfactant on latex stability and epoxidation condition [74]. The use of nonionic surfactant resulted in ability to lower the pH of the latex system by acid to a suitable pH for epoxidation reaction without the loss of latex stability during the epoxidation. The authors found that increasing the amount of nonionic surfactant from 3 to 5 phr for high ammonia natural latex resulted better latex stability. However, the pH did not result in better lowering the pH of latex. Although, the use of nonionic surfactant can result in high values of epoxide content and good latex stability, the secondary products were also observed.

Mulder Houdayer S found the stability of natural rubber latex through the epoxidation reaction with four types of surfactant both anionic and nonionic surfactants [78]. While the use of cationic and amphoteric surfactants showed the loss of latex stability as the rubber coagulation was occurred. However, the results revealed the presence of oxiranes units in the case of cationic, amphoteric and non-ionic surfactants more than the use of anionic surfactant.

Bac NV et al. showed that the stability of latex depended on the initial dry rubber content [74]. They found that the more diluted latex quickly reduced the pH of the system therefore the formation of performic acid can be attained rapidly. This resulted in faster rate of epoxidation before the loss of its stability. Vernekar SP had also studied the effect of latex concentration on the epoxidation of NR latex [80]. They found that increasing latex concentration (20 to 60 wt%) stabilized with 3 phr of nonionic surfactant showed faster coagulation of rubber from 24 to 3 hours at 50°C.

#### **4. Acrylated Natural Rubber**

Natural rubber (NR) is a natural material possessing excellent elastic property. Introduction of acrylate groups into the NR molecule is a method to

transform the NR into new material so called acrylated natural rubber (ANR). The ANR is an attractive material as it increases the polarity of the rubber and has potential application in the field of photoreaction as the acrylate function is prone to be polymerized under ultraviolet radiation. The fixation of the acrylate function into high molecular weight like NR can be carried out by direct addition of the acrylic acid onto the C=C of isoprenic structure. Another method is to be carried out by creation of another active intermediate on the rubber chain such as an epoxide function which will be later easily reacted with an acrylic acid. Generally, epoxides can react with various types of nucleophile due to the strain of the three membered ring. Epoxidized unit can therefore be used as an active intermediate for second step modification. Additions of nucleophilic molecules into polydienes via ring opening reaction of oxirane unit previously introduced have been studied by several researchers.

Soutif JC had studied the addition of benzoic acid onto epoxidized 1,4-polybutadiene at 90°C in chloroform solution by the help of tetramethyl ammonium hydroxide (Me<sub>4</sub>NOH) as a catalyst [81]. The product mixture was analyzed by <sup>1</sup>H NMR spectroscopy. Figure 3.18 presented the spectra of the 1,4-polybutadiene (1,4-PB), the epoxidized PB and the product after 3.5 hours of addition reaction. He reported 6 different structures of the product obtained i.e. 19.4% 1,2-polybutadiene, 30.1% 1,4-polybutadiene, 16.4% residual epoxidized product, 15.5% of secondary products including diol and THF structures, and 18.6% benzolated polybutadiene. Soutif JC had also compared the influence of the temperature on the addition of benzoic acid onto epoxidized 1,4-PB and epoxidized 1,2-PB. He demonstrated that the epoxidized-1,4-polybutadiene showed lower activation energy of addition reaction (54 kJ.mol<sup>-1</sup>) than the epoxidized-1,2-PB (75 kJ.mol<sup>-1</sup>).

Derouet D et al. studied the fixation of methacrylic acid onto epoxidized liquid natural rubber (ELNR) at 100°C in chloroform solution in the presence of catalysts i.e. tetramethyl ammonium methacrylate, potassium hydroxide, triphenyl phosphine and pyridine [2]. The initial molar ratio of [acid]/[epoxide]/[catalyst] were 1/1/0.1 respectively. They found that only in the presence of pyridine as the catalyst, the methacrylated liquid natural rubber was obtained. The additional content was found to be about 13.3% after 75 hours of reaction, detected by titrations technique. <sup>1</sup>H NMR

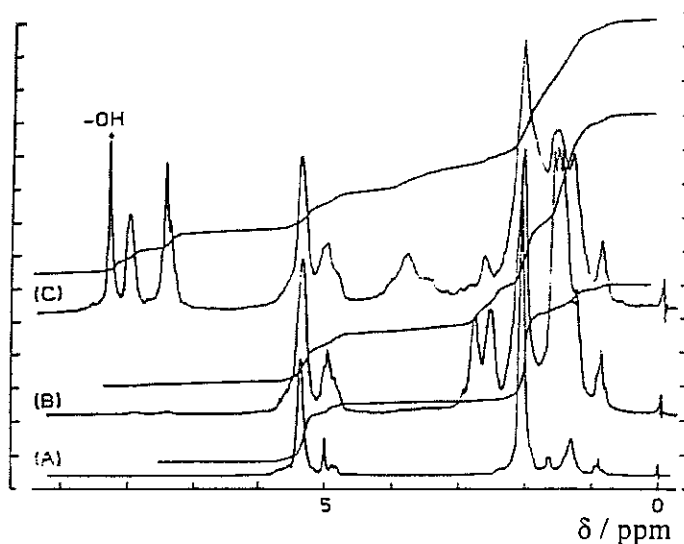


**Figure 3.18**  $^1\text{H}$  NMR spectra of (A) 1,4 polybutadiene ( $\overline{\text{DP}}_n = 14$ , 80.5% of 1,4-units), (B) Epoxidized-1,4-polybutadiene (50% epoxide content) and (C) After reaction with benzoic acid at  $90^\circ\text{C}$  after 3.5 hours ( $[\text{acid}] = 2 \text{ mol l}^{-1}$ ,  $[\text{acid}]/[\text{epoxide}]/[\text{catalyst}] = 1:1:0.1$ ) in  $\text{CCl}_4$  [81]

spectrum confirmed the fixation of methacrylic acid onto ELNR at 5.75 and 6.3 ppm corresponding to two protons attached to the double bond of methacrylate function.

Xuan HL and Decker C had studied the addition of acrylic acid onto epoxidized natural rubber (ENR) and ELNR [63]. The addition reaction was produced in an excess acid system (26 folds of mole/mole of acid/oxirane unit or 5 fold of weight/weight of acid/rubber solution) in toluene solution, carried out at  $35^\circ\text{C}$ . The reaction was followed and analyzed by FTIR spectroscopy. Acrylation of rubber was essentially completed within 16 hours which was noticed by the disappearance of the absorption bands characteristic of epoxy group at  $1250$  and  $870 \text{ cm}^{-1}$ . The acrylated rubber obtained revealed the addition of acrylic acid onto the rubber by the presence of absorption bands at  $3500 \text{ cm}^{-1}$  (OH stretching),  $1728 \text{ cm}^{-1}$  (ester stretching),  $1408 \text{ cm}^{-1}$  ( $=\text{CH}_2$  deformation),  $1190 \text{ cm}^{-1}$  (C-O ester) and  $805 \text{ cm}^{-1}$  ( $=\text{CH}_2$  twisting). The FTIR results showed the slightly faster consumption of epoxide units than the presentation of acrylated function. Therefore, the addition reaction was assumed to be composed of two steps, the first step is the ring opening of the epoxide unit by protonation,

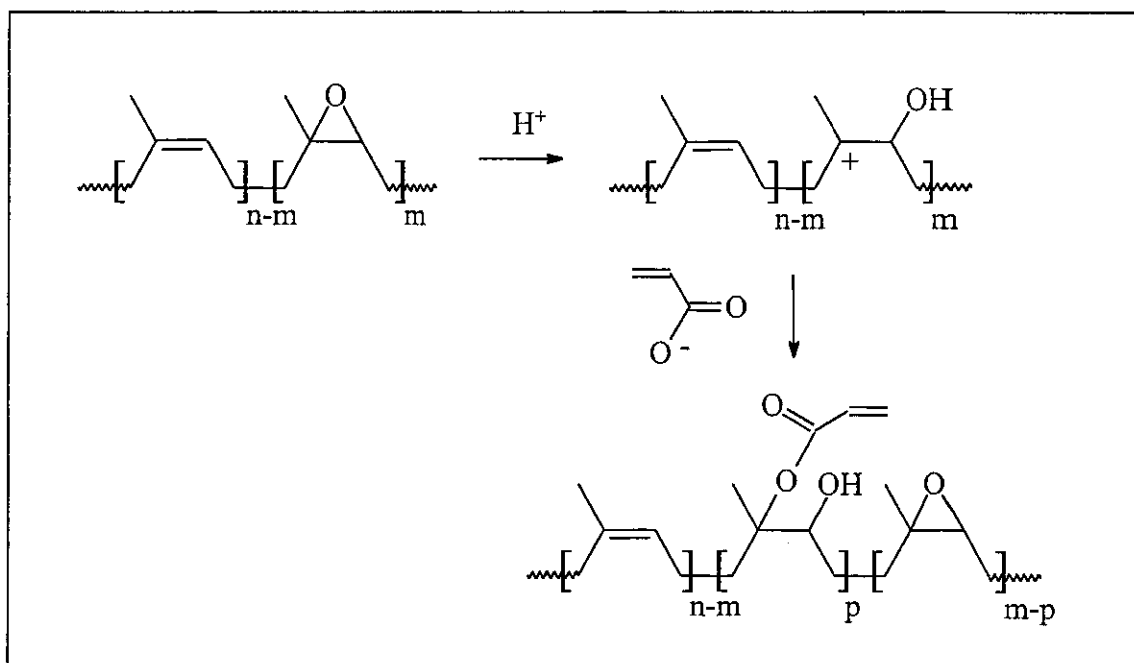


**Figure 3.19** Acrylation of epoxidized rubber [63]

followed by formation of tertiary carbonium ion intermediate. The later step is the addition of the acrylate anion to the intermediate. The reaction mechanism is given in Figure 3.19.

Decker C et al. also studied the ratio of acid per rubber, reaction temperature and effect of catalysts [82,83]. By using 10, 3 and 1 fold of weight of acrylic acid per weight of rubber, they found that faster and higher formation of acrylated rubber were obtained when increasing the amount of acrylic acid. The increase of reaction temperature from 20°C to 80°C in the condition of acrylic acid and rubber of 10:1 weight ratio resulted in speeding up the rate of addition reaction and increasing the acrylation level (as shown in Figure 3.20). The presence of a catalyst, like tetrabutyl ammonium bromide, resulted in an increase of rate and efficiency of the addition reaction. Moreover, the increase of reaction temperature up to 100°C in the presence of 2% of catalyst in the condition of acrylic acid and rubber of 2:1 weight ratio were found to increase the rate of the acrylation. The reaction was completed within 7 hours, as shown in Figure 3.21.

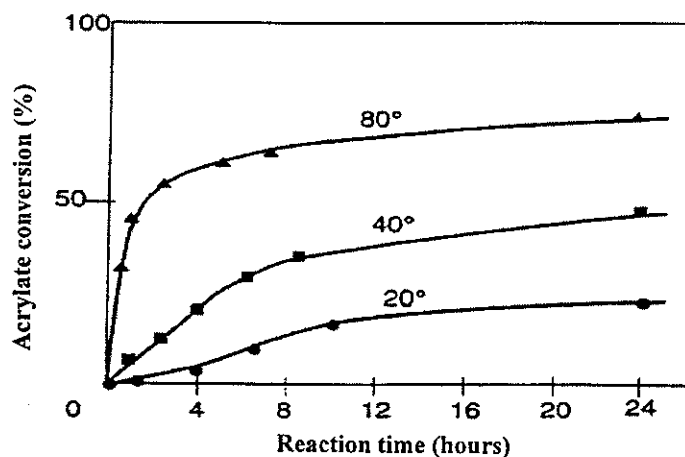


**Figure 3.20** Effect of reaction temperature on the acrylation reaction of epoxidized natural rubber by using formic acid/rubber = 10 w/w [82]

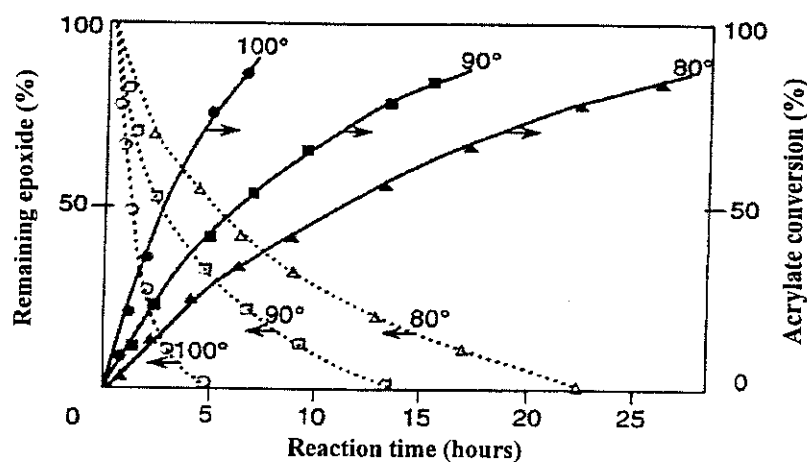


**Figure 3.21** Effect of reaction temperature on the acrylation reaction of epoxidized natural rubber in the presence of catalyst and using formic acid/rubber = 2 w/w [82]

Duangthong S had studied the effect of two different solvents i.e. toluene and chloroform on the addition reaction of acrylic acid onto ELNR [84]. The addition reaction performed in chloroform was found to be slightly better than using toluene. The detection of the addition of the acrylic acid was the absorption band in FTIR spectroscopy at  $1408\text{ cm}^{-1}$  representing the acrylate function. Another technique carried out was the use of potentiometric titration to measure the unreacted acrylic acid in the reaction system. Duangthong S also investigated the effect of acrylic acid

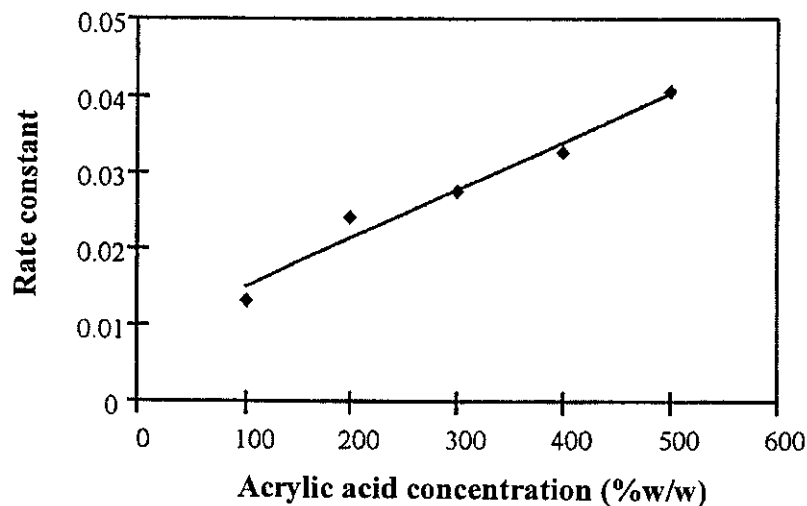


**Figure 3.22** Plot of pseudo first order rate constant ( $k'$ ) obtained from acrylation reaction with various amounts of acrylic acid concentration [84]

concentration on the addition reaction. He used various amount of acrylic acid from 1 to 5 fold weight by weight of ELNR solution (50% DRC). The kinetic rate constant ( $k'$ ) of the addition reaction was found to be increased with the increase of acrylic acid concentration (see Figure 3.22).

## 5. Photoinduced polymerization or crosslinking reaction

The polymerization or crosslinking reaction by the aid of light has been considered a particularly rapid and low cost method. The process can be normally performed in solution or solventless system. However, the materials used have to be composed of the photosensitive or photopolymerizable molecules using suitable radiation energy such as visible, ultraviolet (UV), electron or laser beam. The photoinduced reaction is a method to convert liquid monomers into solid form or to induce formation of three-dimensional structure in polymeric materials. Therefore, several parameters have to be known for the study of the photoreaction.

### 5.1 UV sources

UV-radiation is a useful energy increasingly used for the study of polymers. Its applications have widespread range from printed circuits to decorative coatings. The

radiation is in the wavelength range from 450 nm up to 1 nm, which is a part of the spectrum of the electro-magnetic radiation. The UV-range is classified into 5 sections.

1. UV-V 450 up to 390 nm
2. UV-A 390 up to 325 nm
3. UV-B 325 up to 280 nm
4. UV-C 280 up to 180 nm
5. V-UV 180 up to 1 nm

In commercial applications, UV-A, UV-B and UV-C are 3 ranges of ultraviolet light the most commonly used [85,86]. The UV-A, which is high wavelength, can penetrate through the volume of resin until the curing is completed. The favorable use is in the photopolymerization of vinyl monomers. The UV-B and UV-C show lower wavelength than UV-A, they can penetrate beyond a few microns from the surface of the polymeric resin. The V-UV is not useful for curing system while the UV-V wavelength is near visible light, which is suitable for special works such as dry major color ink. Generally, energy emitted from high-pressure mercury lamp contains 25-30% of UV light, 5-10% of visible light and 60-65% of IR light [85]. It is therefore necessary to take into consideration of the apparatus used to have an IR filter to absorb the emission of IR light. The IR emission may cause the heating in the sample and subsequent deflection of the pan from the baseline.

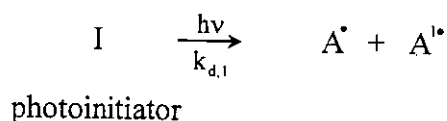
## 5.2 UV irradiation polymerization mechanism

Bulk polymerization of photopolymerizable monomer or photoreaction of photosensitive polymer under UV irradiation generally proceeds by free radical initiated mechanism. If the system composes of multifunctional monomers or polymers containing multifunctional groups, the three-dimensional or crosslinking structures are formed. Basically, the UV light can induce active species from the monomers to start up the polymerization reaction. However, the monomers employed cannot produce sufficiently high yield of active species, therefore photosensitive initiator is practically added to initiate the photopolymerization. The reaction mechanism includes 3 sequential stages as initiation, propagation and termination [87-89].

### 5.2.1 Initiation stage

In this stage, an initiator (I) usually called photoinitiator is decomposed into two equal or unequal primary radicals. The active fraction will react with unsaturated molecules to form primary active propagating species that undergo propagation reaction.

**Initiation stage:**



-  $k_{d,1}$  = rate constant for decomposition

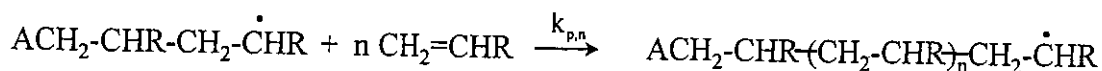
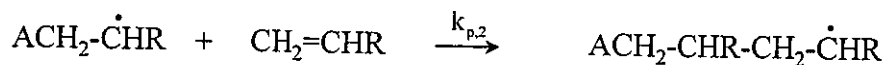


-  $k_{p,1}$  = rate constant for primary radical-unsaturated molecular reaction

### 5.2.2 Propagation stage

The active propagation species will further react with another polymerizable molecule, generating a growing linear polymer chain. If the system contains various kinds of polymerizable molecules such as functionalized active mono-, di- and multifunctional monomers or functionalized active oligomers, three-dimensional network structures are produced.

**Propagation stage:**



-  $k_{p,2/n}$  = rate constant for propagation

### 5.2.3 Termination stage

In the bulk polymerization, the termination of macroradical species is resulted when radical coil or oligomeric radical can contact with another radical coil. Then the

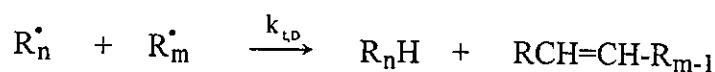
chemical reaction by recombination or disproportionation between two active species is performed. However, in the system of crosslinking reaction, the termination reaction of oligomeric radicals shows less effective in high reaction conversion as high viscosity system may inhibit the encountering of the active species. The reaction is stopped by frozen radical coils in solidification form of the polymeric network.

**Termination stage:**

(i) Combination reaction



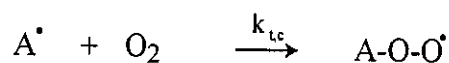
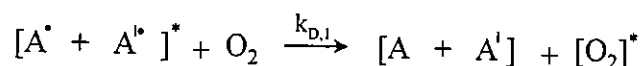
(ii) Disproportionation reaction



-  $k_t$  = rate constant for termination

If the photoreaction is operated under atmospheric pressure in open-air system, a side reaction named oxygen inhibition is usually involved. The oxygen can retard or completely inhibit the reaction by acting in the excited stage of the initiation process. It will transfer the energy or reacting with alkyl active radicals in propagation stage and acts as a radical scavenger to yield peroxide radical. The radical will not react with the monomer in the system as shown below.

**Oxygen inhibition:**



### 5.3 Photoinitiator

Photoinitiator is a compound that absorbs light at a certain wavelength in the ultraviolet or visible region and undergoes fragmentation, leading to species able to initiate polymerization. There are a number of photoinitiators available in the market depending on the molecular transformations involved under UV exposure [87,90,91]. Some examples are showed in Figure 3.23.

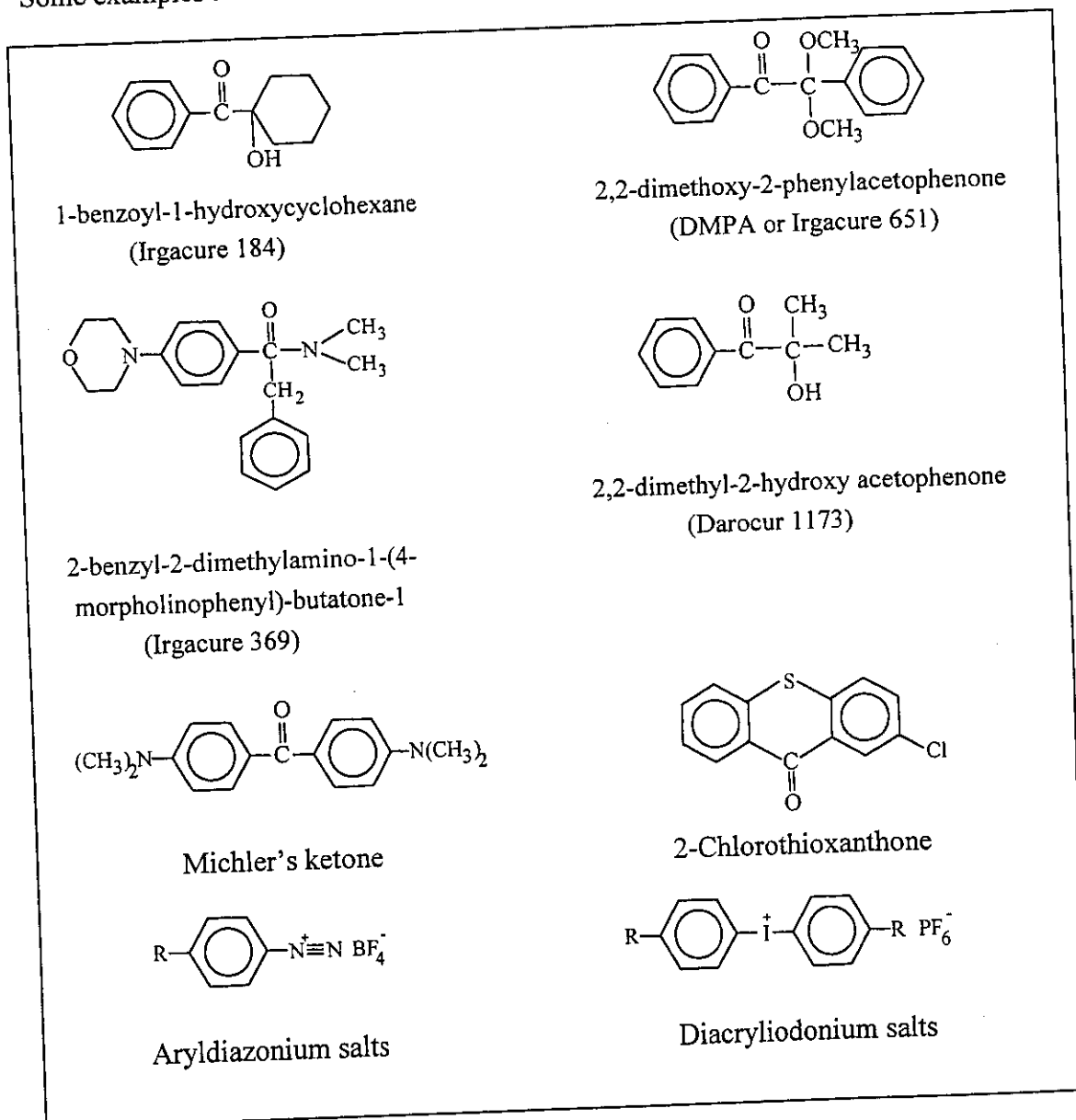


Figure 3.23 Examples of photoinitiators

### 5.3.1 Free radical initiator

In most photocuring system, photoinitiators generating reactive radical species are the most interesting for commercial applications. The fragmentation of the molecules to form radical species can be occurred by three different pathways as followed:

#### a) Radical formation by homolytic cleavage

The mechanism of radical formation by homolytic cleavage is usually applied for aromatic carbonyl compounds such as benzoin, benzene alkyl ether, hydroxyalkyl ketones, dialkoxyacetophenones and benzoylphosphine oxides. The compound undergoes a Norrish type I fragmentation which causes the bond scission ( $\alpha$ -cleavage) when it is exposed to UV light. This process will lead to the formation of benzoyl and ketal radicals (Figure 3.24). These radicals will further initiate chain polymerization or crosslinking reaction.

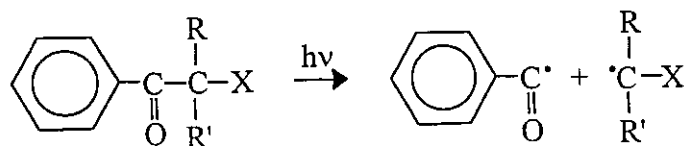


**Figure 3.24** Homolytic cleavage reaction of radical photoinitiator under UV irradiation [87]

#### b) Radical generation by hydrogen abstraction

The radical generation by hydrogen abstraction fits to photochemical reaction of aromatic ketone such as benzophenone that is one of the best known in this category. Upon UV irradiation, the benzophenone is excited to an excited state, and then it transfers the energy to H-donor molecules. A radical is introduced to H-donor molecules by hydrogen abstraction of excited benzophenone, then a ketyl and alkyl radical are formed, both of which can initiate propagating reactions (Figure 3.25). However, ketyl radical is disappearing mainly by a radical coupling process more than propagating process. Then, the radical polymerization is performing mainly from the last radical.

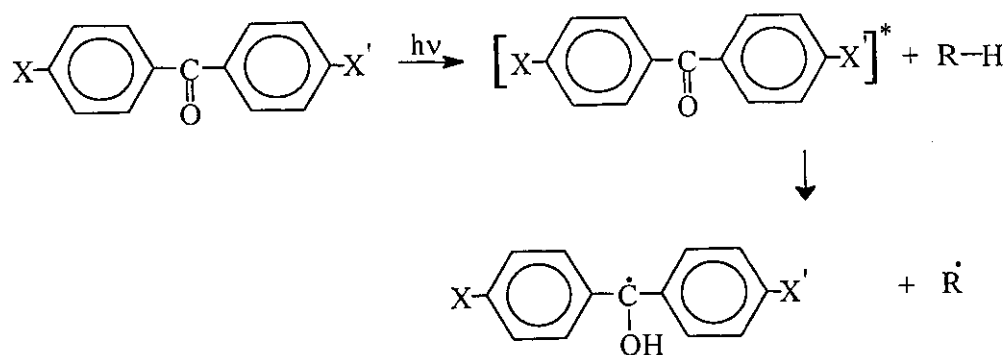


**Figure 3.25** Hydrogen abstraction reaction of radical photoinitiator under UV irradiation [87]

### c) Radical decomposition by electron transfer process

A combination of an amine and aromatic ketone under specific irradiation will result in electron transfer process, leading to formation of radical species. The wavelength involved in this type of initiator is greater than 400 nm. The radical generation mechanism is shown in Figure 3.26. The amine radical intermediate is occurred by proton transfer from the amine to the aromatic ketone. This radical formed will then initiate the polymerization.

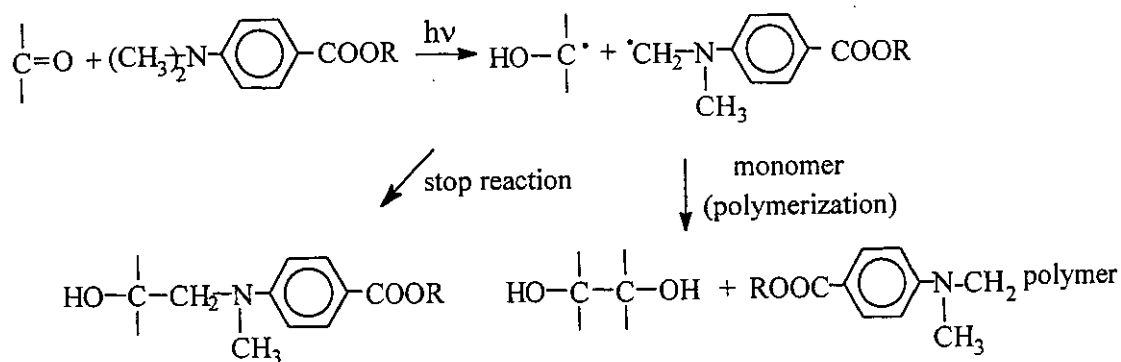


**Figure 3.26** Electron transfer reaction of radical photoinitiator under UV irradiation [87]

### 5.3.2 Cationic photoinitiator

Cationic photoinitiator is an initiator, which generates reactive cationic species under UV irradiation. It is mostly used for the formation of materials incorporating epoxidized units. The most active cationic initiator is Lewis acids ( $\text{BF}_3$ ,  $\text{AsF}_5$ ,  $\text{PF}_5$ , etc)

or photonic acid. In some cases, co-catalysts can be added to accelerate the formation of reactive species. Figure 3.26 showed the formation of free Lewis acid,  $\text{BF}_3$  under UV exposure of cationic initiator. Generally, the rate of initiation by cationic photoinitiator is lower than by radical photoinitiator.

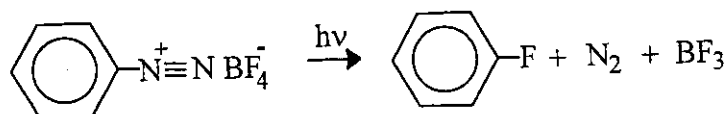


**Figure 3.26** Reaction of cationic photoinitiator under UV irradiation

#### 5.4 Functionalized oligomers or prepolymers

Materials that can undergo polymerization reaction upon UV irradiation normally contain photopolymerizable moieties such as cinnamate, methacrylate and acrylate functional groups. If polyfunctional groups are attached to the polymeric chains, crosslinking reaction can be occurred. Among the three photoactive groups, the acrylate function is the most sensitive to UV irradiation and is found in the market as epoxy acrylates resin, urethane acrylates resin and polyester acrylates resin [90,92]. The mechanical properties of the UV cured polymers depend on the functionality and chemical structure of the bases polymers. The epoxy acrylates produce stiff and hard materials while the UV cured materials from urethane acrylates and polyester acrylates lead to elastic materials. The former groups are suitable for surface coating of rigid substrates and the later is considered to be suitable for application on flexible supports. Functionalizations of synthetic and natural rubber for the application upon UV curing process are another possibility to find new flexible and elastic materials. The cured products should exhibit excellent elasticity and high impact resistance due to elastomeric character of the rubber and crosslinking network from UV curing.

Xuan HL and Decker C had studied photocrosslinking of acrylated natural rubber and acrylated liquid natural rubber with 3% w/w of photoinitiator [63,93]. After UV irradiation, acrylated rubber showed insoluble character in organic solvent, high flexibility, excellent impact resistance and fair hardness. These properties depended on the amount of acrylated units on the rubber chain and the UV exposure time. They found that the hardness of the final product increased with the increase of the degree

of acrylation and exposure time. The formation of the gel content was also observed and followed the same influence of acrylation content and exposure time.

Duangthong S had prepared photocrosslinkable rubber containing different level of acrylate function from ELNR [84]. He found that higher amount of acrylate function resulted in increasing the rate of photocrosslinking reaction.

### 5.5 Reactive diluents

Generally, photosensitive oligomers are very viscous materials, reactive diluents are required to modify and control the viscosity and reactivity of the required system for specific applications [89,90,94]. They are usually reactive monomers that may affect both the polymerization rate and the properties of the final product obtained. Some examples are shown in Figure 3.28. Moore JE described photocalorimetric technique to study extents and rates of polymerization of various mono-, di- and polyfunctional acrylate and methacrylate monomers [95]. Diacrylate (HDDA, DMGDA, DEGDA and TEGDA) gave the highest conversion because of Tromsdorff acceleration comparing with monoacrylate. More sterically hindered, polyols, tri- and tetracrylate gave the lowest conversion. The same trend is observed for methacrylate monomers that high steric hindrance exhibited both lower extents of conversion and rate of polymerization than acrylate monomers.

Allen PEM et al. studied the influence of the length of soft oxyethylene units of dimethacrylates,  $\text{CH}_2=\text{C}(\text{CH}_3)\text{CO}(\text{OCH}_2\text{CH}_2)_x\text{OCOC}(\text{CH}_3)=\text{CH}_2$ , on the final properties of UV-cured products [96]. They found that the increase of length of oxyethylene units (x) caused the increase of the flexibility of network and the decrease of the crosslink density of the cured product. The number of length of x between 1-4 gave the rigid glasses product obtained, while x between 4-9 showed leatherly properties. For  $x > 9$ , the cured products exhibited soft rubbery properties. Hossain MS et al. [92] characterized UV cured films obtained from urethane acrylate oligomer in the presence of various types of monomers. The highest hardness is obtained with the films of trifunctional monomer, TMPTA because of more crosslinking density with the oligomer backbone compared to mono- and difunctional monomer. Among the two difunctional monomers (TPGDA and HDDA), HDDA showed more hardness of UV

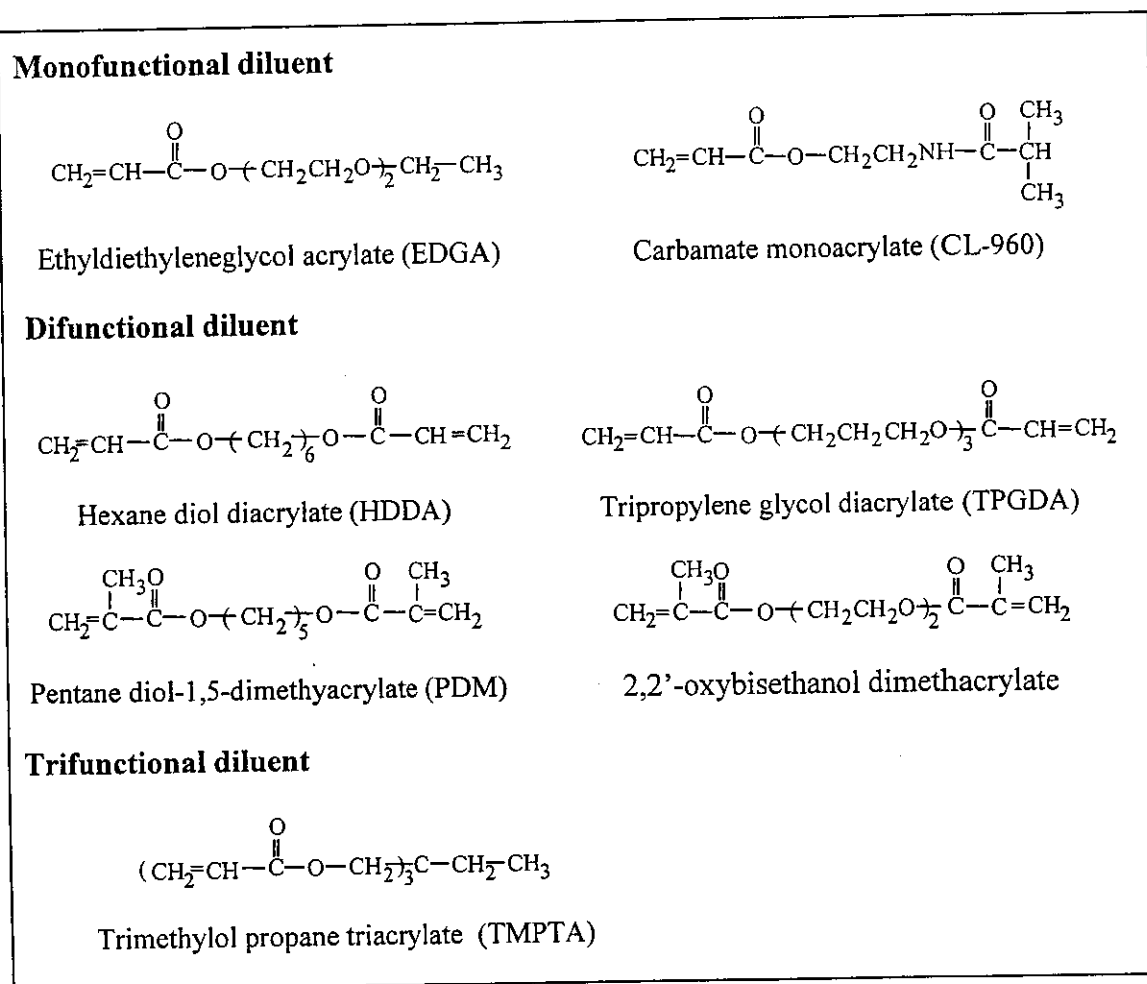


**Figure 3.28** Examples of reactive diluents

cured film than TPGDA, while TPGDA has produced film of higher tensile strength than HDDA.

Hai L et al. studied the effects of some mono-, di- and tri-acrylate diluents upon UV curable coating of epoxy acrylate [97]. They indicated that the gelation extent increased with increasing the functionality of monomer i.e. mono- < di- < tri-acrylate. An exception was found in the case of tripropylene glycol diacrylate (TPGDA), which produced faster rate of gelation than trimethyl propane triacrylate (TMPTA). Therefore, the assorted diluents for photopolymerization depend not only on the functionality of the monomer, but also on its chemical structure.

Although, reactive diluents have more powerful on improvement of properties of the cured film according to the various dense of network structure. Acrylate monomer was claimed to be dermal irritants because of their low volatility [98].

Moreover, reactive monomers have high odour, toxicity and may cause carcinogenic [94]. The low viscosity oligomers are developed to reduce the use of monomers by copolymerization of the oligomer and the monomers. Decker C et al. also studied the UV irradiation of copolymerization of acrylated rubber and diacrylate and triacrylate monomers [83]. They found that addition of 50 phr HDDA and TMPTA to acrylated rubber led to sharp increase in the polymerization rate. The 70% of conversion was occurred after 0.1 second of light exposure. Moreover, they proposed the polymerization of acrylated rubber and 50 phr of HDDA under sunlight. A half of acrylated double bond was found to be polymerized after 2 minute exposure time. This is probably due to the inhibition effect of atmospheric oxygen, which becomes important in radical polymerization at low light intensity.

Duangthong S studied the photocrosslink reaction and physical properties of acrylated epoxidized liquid rubber (AELNR) in the presence of various types and amounts of initiator (Irgacure 184 and Darocur 1173) and monomers (HDDA and TPGDA) [84]. He reported that the AELNR in the presence of 60 phr of HDDA and 20 phr of Irgacure 184 exhibited the fastest curing rate and hardest cured film under 2 seconds of UV irradiation. In addition, the AELNR with 22.5 phr of HDDA and 22.5 phr of TPGDA in the presence of 20 phr of Irgacure 184 gave the highest flexibility and good adhesion measured on iron and aluminum plates.

## **5.6 Analytical method for studying the photopolymerization**

Photopolymerization considered in this section is the process carried out under ultraviolet irradiation. The process is ultrafast which can be in the order of second. Several techniques can be used to follow the progress of the reaction as well as the kinetic investigations such as real-time infrared (RTIR), real-time ultraviolet spectroscopy and photocalorimetry.

### **5.6.1 Infrared spectroscopic method**

The photoreaction of materials containing acrylate function can be possibly followed by the use of infrared spectroscopic technique as the acrylate group has a characteristic absorption band at  $810\text{ cm}^{-1}$ . The reduction of the signal at this wave number signifies the reaction of the acrylic function, which the double bond is

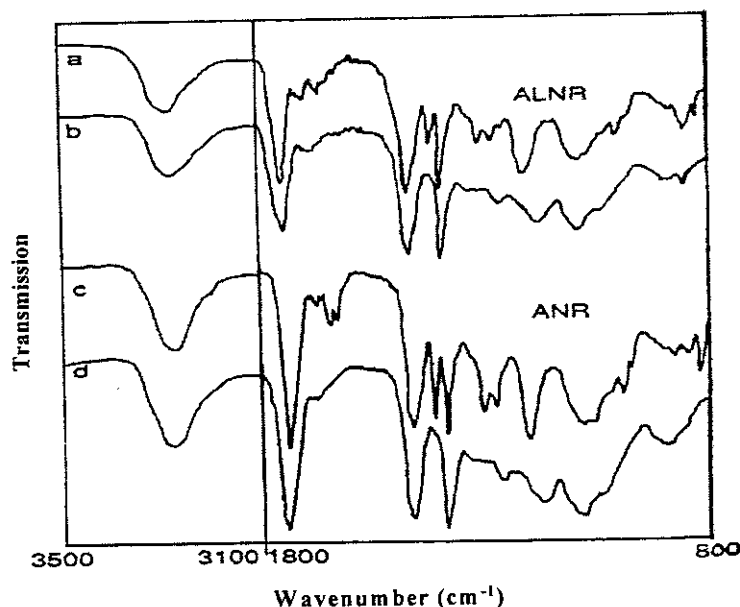


**Figure 3.29** Infrared spectra of ALNR and ANR before (a,c) and after (b,d) UV curing, exposure time 30 second, film thickness 10  $\mu\text{m}$ . [63]

progressively disappeared. Real-time infrared spectroscopy (RTIR) can be directly used to record conversion versus time in millisecond timescale.

Moussa K and Decker C used IR spectroscopy to follow the polymerization of acrylic monomer under UV irradiation [99]. The extent of polymerization process was evaluated quantitatively from the decrease of the signal at 810  $\text{cm}^{-1}$ . Xuan HL and Decker C studied the cure kinetics of acrylated NR in the presence of a radical photoinitiator under UV irradiation [63]. They monitored the progress of the reaction by following the disappearance of IR absorption band of the crosslinked product at 810  $\text{cm}^{-1}$ . Decker C et al. had also investigated the photoreaction of epoxidized NR in the presence of cationic photoinitiator [93]. The spectrophotometer was operated in the absorbance mode and the detective wavelength set is either at 810  $\text{cm}^{-1}$  and 1408  $\text{cm}^{-1}$  for the acrylic monomer or at 877  $\text{cm}^{-1}$  for the epoxidized units. The degree of conversion was calculated from the ratio of the absorbance of irradiated sample at the considered wavenumber to the absorbance of the unexposed sample. Figure 3.29 showed infrared spectra of acrylated liquid natural rubber (ALNR) and acrylated natural rubber (ANR) films before and after UV exposure. It can be seen that the

absorption band characteristic of acrylate function at  $810\text{ cm}^{-1}$  and  $1408\text{ cm}^{-1}$  have been reduced after 30 second of irradiation.

The real time fourier transform (RT / FTIR) technique is an interesting new IR technique. This method concedes the cure reaction to be continuously and rapidly monitored, in real time, at the molecular level without significant post-cure errors. The sensitivity of IR technique allows the detection of very small structure changes in the components of an adhesive formulation. It can therefore produce quantitative information regarding the cure kinetic parameters such as photosensitivities of the initiators, resins, or stabilizers. The induction period or post cure, as well as the amount of residual monomers in polymers network can also be easily detected. This technique is much used to study changes occurring at or near the surface, substrate interfaces and at various depths in the film. However, this method cannot illustrate internal behavior of the cured polymer such as the change of heat of polymerization. Yang DB had studied anionic reaction of ethyl cyanoacrylate and hydrosilation reaction (addition reaction) using RT/FT-IR technique [100]. In anionic polymerization, the effect of concentration of photoinitiator and inhibitor were investigated. The change of C=C stretching of the ethyl cyanoacrylate during the polymerization at  $1617\text{ cm}^{-1}$  was monitored. The kinetic studies of hydrosilation was monitored by disappearance of Si-H (silicone hydride) stretching bond located at  $2169\text{ cm}^{-1}$ . The collected 204 spectra per minute of RT/FTIR were very fast and appropriated for kinetic analysis.

### 5.6.2 Ultraviolet spectroscopic method

Real-time ultraviolet (RT/UV) spectroscopy can be used to follow continuously the disappearance of the photoinitiator in curable system under intense UV exposure. Ultraviolet technique permits the photoinitiator loss profile to be directly recorded in a time scale of 1 second or more. The kinetic profiles are corrected for any shift in the baseline, which might have occurred due to the formation of photoproducts absorbing at that wavelength as shown in Figure 3.30 [101]. The problem of this method is to select the correct wavelength for maximum absorption of photoinitiator. The system having direct contact with  $\text{O}_2$  upon UV-exposure may cause inhibition of the photoreaction. Besides, other compounds in the photocuring

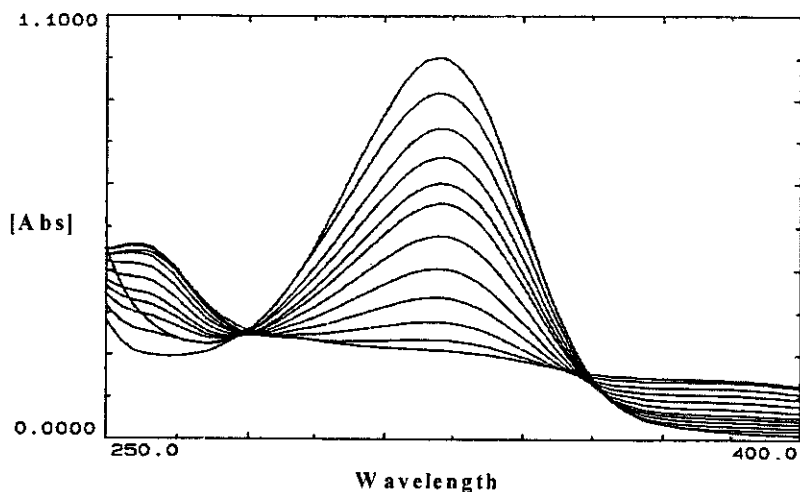


**Figure 3.30** UV absorption spectrum of a TPGDA film containing 2% Irgacure 369, initially (top) and after various exposure times: 0.5, 1, 1.5, 2, 2.5, 3.5, 5, 7, 10, 15, 25 second, light intensity:  $110 \text{ mW cm}^{-2}$  [101]

formulations such as diluents or resins should not participate in the region of the detection.

Decker C had studied the photolysis kinetic of radical initiator, during the polymerization of di- and tri-acrylated monomers under UV irradiation via RT/UV spectroscopy [101]. The polymerization rate of the acrylated monomer was relatively detected from the decrease of photoinitiator absorption at the wavelength set. Decker C also studied the photocopolymerization of triacrylated monomer in poly(methyl methacrylate) matrix in the presence of photoinitiator to form semi-interpenetrating polymer networks by using RT/UV technique [101]. The RT/UV method can also be used to follow the photopolymerization of epoxy monomer by detection of the decay rate of the cationic photoinitiator [101].

### 5.6.3 Calorimetric method

Differential scanning calorimetry (DSC), referred to heat capacity of a sample versus temperature or time, compared with reference sample, is a technique to analyze data according to heating profile of the sample as real time of melting or polymerization. For photocalorimetry experiments, the standard DSC has slightly

modified. The sample chamber of modified DSC has been changed as including a quartz window to allow UV irradiation to the sample. Modified DSC that adapted with irradiation part named double beam photocalorimetry (DPA) will give direct information on a photoreactive material. The heat of polymerization and the percent conversion can be directly calculated from the exothermic thermogram. Therefore, characteristics of different formulations of samples before and after exposure to UV light can be investigated. The photocalorimetry has been comprehensively used to explore the kinetics of photopolymerization because it can be obtained direct information of the changeable polymerization upon UV exposure, the availability of accuracy, controllable the effect of oxygen, requirement of small amount of sample, good temperature control and very good simulation of real commercial irradiation techniques.

Wight FR and Hicks GW had extended the Perkin-Elmer DPA-DSC 1B to study various formulations of photocurable resins [102]. They can estimate initiator efficiencies, optimization of curing parameters (initiator concentration, lamp design) and the sensitivity of prepolymers to oxygen and wavelength by this technique. In 1989, Abadie MJM and Appelt BK applied DSC analysis successfully to study dental composites [103]. However, they can only analyze the samples in a discontinuous mode. Scranton AB et al. reported the copolymerization of ethylene glycol monomethacrylates with small amounts of dimethacrylate crosslinking agents via Perkin-Elmer DSC-4, the amount of the gel effect was found to depend on the crosslinker concentration, dilution and pendent chain length [104]. Poly(ethylene glycol) diacrylates polymerization was investigated by Kurdiker DL and Peppas NA who showed that an increase in the monomer chain length caused an increase in conversion due to the increase in the mobility of the pendent double bonds [105]. Bosch P et al. used both calorimetric analysis and electron spin resonance (ESR) to study the photopolymerization of di- and tri-functional (meth)acrylic monomers in the styrene-butadiene-styrene polymeric matrix [106]. Kinetics of the photopolymerization reaction had also been followed by the calorimetry while the ESR was used to determine the structure and concentration of radicals in the reaction.

In recent years, self-designed equipment of combining a DSC with irradiation unit has been developed under the name DPA-DSC 7. The light is focused into the

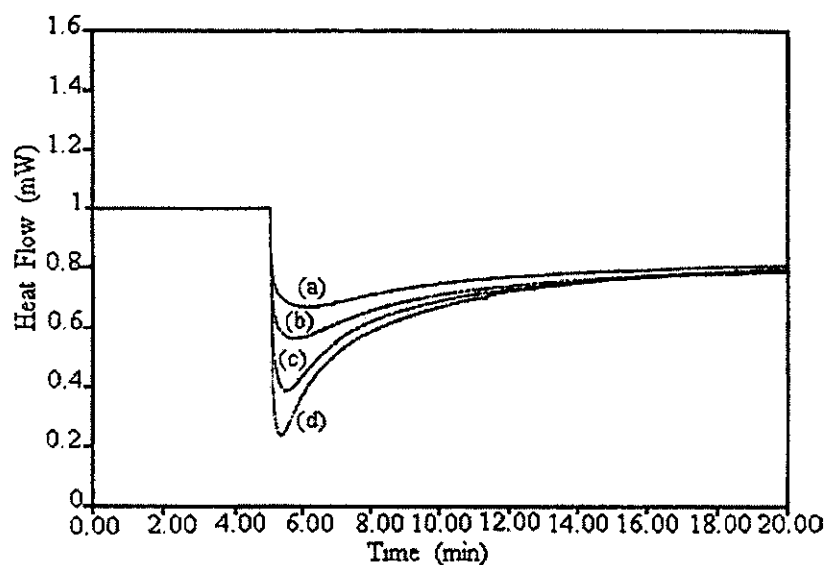


**Figure 3.31** Photocrosslinking exothermic thermogram of AELNR 1 with various amount of diacrylate monomer and photoinitiator; (a) A1H30T20I05, (b) A1H20T30D05, (c) A1H20T20I10 and (d) A1H20T20D15 [84]

DSC via deflecting mirror that control the balance of the intensity between the sample and reference sides, minimizing any error heating and homogeneous reaction would be obtained.

Anseth KS et al. used Perkin-Elmer DPA-DSC7 studied reaction behavior, kinetic constants and kinetic evidence of reaction diffusion during the photopolymerization of multi (metha)acrylate monomers [107,108].

The use of this equipment for kinetic study of the photocrosslinkable of acrylated epoxidized liquid natural rubber (AELNR) with photoinitiators and reactive diluents were also reported by Duangthong S [84]. Figure 3.31 showed the exothermic thermogram of photocrosslinking reaction of AELNR with various amounts of diacrylate monomers and initiator concentration. The thermogram showed that the onset of autoacceleration of reaction decreased as initiator concentration increased. Lecamp L et al. researched the influence of photoinitiator concentration, temperature and light intensity of a dimethacrylate oligomer with radical photoinitiator by employing DSC 7 photocalorimeter [109,110]. They used the results obtained to analyze the kinetic of photoinitiated polymerization which can be characterized either by an autocatalytic model or by a mechanistic model in 1999.

## CHAPTER IV

### MATERIALS AND METHODS

#### 1. Materials and Instruments

1. Natural rubber latex (60% DRC) was supplied by Bangkok Rubber Company, Thailand.
2. Proteinase B KP 3939 was supplied by Kao Co. Ltd., Thailand.
3. Sodium dodecyl sulfate (SDS) (>98% GC grade) was used as purchased from Fluka.
4. Poly(ethylene oxide fatty alcohol)hexadecylether (Teric) was supplied by East Asiatic Company, Thailand.
5. Nonyl phenol ethoxylated (Sinnopal NP 307) was supplied by Cognis Company.
6. Potassium persulfate (>99%) was used as purchased from Fluka.
7. Propanal (98%) was used as purchased from Fluka.
8. Tri-sodium phosphate (tert) dodecahydrate was used as purchased from Fluka.
9. Formic acid (98-100% analytical grade) was used as purchased from Merck.
10. Hydrogen peroxide (35% standard grade) was used as purchased from Ajax Chemicals.
11. 3-Chloroperbenzoic acid was used as purchased from Fluka.
12. Periodic acid (99% analytical grade) was used as purchased from Acros Organics.
13. 4-Methyl-4-octene was supplied by laboratory of Chimie et Physique des Materiaux Polymères, l'Université du Maine, Le Mans, France.
14. Synthetic liquid rubber (LIR-30) was supplied by Kuraray Company, Japan

15. Acrylic acid (99.5% pure and stabilized with 180-220 ppm hydroquinone monomethylether) was used as purchased from Acros Organics.
16. Irgacure 184 and Darocur 1173 were supplied by Ciba-Geigy (Thailand) Co.Ltd.
17. 1,6 Hexanediol diacrylate (HDDA) and tripropylene glycol diacrylate (TPGDA) were supplied by Sartomer Co.Ltd. and used without further purification.
18. Sodium hydroxide (NaOH) was used as purchased from J.T.Baker.
19. Potassium carbonate ( $K_2CO_3$ ) was used as purchased from Fisher Scientific.
20. Sodium bicarbonate ( $NaHCO_3$ ) was used as purchased from BDH.
21. Acetone, methanol, chloroform, dichloromethane and toluene are commercial grade and were purified by distillation before utilization.
22. Tetrahydrofuran (99.9% A.C.S. Reagent) was used as purchased from J.T.Baker.
23. Deuteriochloroform (99.5% analytical grade) was used as purchased from Fluka.
24. Ultracentrifuge machine (H 600 centrifuge).
25. Fourier transform infrared spectrometer (PERKIN ELMER, PE 2000).
26. NMR spectrometer (Bruker AM 400 spectroscopy 300 MHz).
27. Supercritical fluid chromatography (SFC 3000 series), Carlo Erba Instruments.
28. Processor viscosity system (PVS1, LAUDA).
27. Gel permeation chromatography (waters<sup>TM</sup> 150-CV plus).
28. Double beam photocalorimeter accessory (DPA 7, Perkin-Elmer) and differential scanning calorimeter (DSC 7, Perkin-Elmer).
29. Gas chromatography-mass spectrometer (GC-MS)

## 2. Preparation of Purified Natural Rubber

0.04% w/v Proteolytic enzyme (proteinase B KP 3939) was added to high ammonia natural rubber latex (60% dry rubber content, DRC) which was diluted to 30% DRC and stabilized with 1.0% w/v surfactant (sodium dodecyl sulfate (SDS), Sinnopal NP 307 or Teric). The mixture was stirred in a glass reactor at 37°C for 24 hours. It was filtered through 200 meshes sieve before centrifugation in ultracentrifuge machine for 30 min. at 13,000 rpm. The cream fraction was separated from the liquid residue and redispersed in 1.0% w/v aqueous solution of surfactant. The redispersed rubber was further centrifuged at the same condition as before. The purified natural rubber (PNR) obtained was finally kept in 0.5% w/v aqueous solution of surfactant in dark bottle. DRC of the PNR latex obtained was determined from the weight of the latex and the dry coagulum which was obtained from coagulation by acetic acid (99%).

The PNR after drying under vacuum is characterized by FTIR and  $^1\text{H}$  NMR spectroscopy. Nitrogen content of the NR and PNR was measured by micro-Kjeldahl method. The intrinsic viscosity,  $[\eta]$  was determined by PVS1 viscometer.

## 3. Degradation of Purified Natural Rubber Latex by Using Potassium Persulfate and Propanal

200 ml of PNR latex (25% DRC) stabilized by 0.5 phr of surfactant was diluted with 300 ml of distilled water. The latex was combined with various amounts of potassium persulfate ( $\text{K}_2\text{S}_2\text{O}_8$ ), propanal and sodium phosphate ( $\text{Na}_3\text{PO}_4$ ). The mixture was poured in one-liter glass reactor equipped with a condenser and a controlled speed stirrer of 400 rpm. The reaction was carried out at 60-80°C during 30 hours. Various degradation conditions were carried out as shown in Table 4.1. During the progress of the reaction, the latex was sampling and precipitated in methanol, then purified by dissolution and reprecipitation using the couple of toluene/methanol. After drying under reduced pressure, the liquid purified natural rubber (LPNR) obtained was transparent viscous liquid. The structure of LPNR was characterized by FTIR and  $^1\text{H}$  NMR spectroscopy. The molecular weight of the dried rubber was determined by viscometer and gel permeation chromatography (GPC).

**Table 4.1** Reagents used in the preparation of liquid purified natural rubber (LPNR)

Samples	% DRC		K <sub>2</sub> S <sub>2</sub> O <sub>8</sub> (phr)	Propanal (phr)	Na <sub>3</sub> PO <sub>4</sub> (phr)	Surfactant	O <sub>2</sub>	Temperature °C
	PNR	NR						
LNR 1	-	5	1	32	0.34	SDS	-	70
L 1	5	-	1	32	0.34	SDS	-	70
L 2	5	-	2	32	0.34	SDS	-	70
L 3	5	-	3	32	0.34	SDS	-	70
L 4	5	-	1	16	0.34	SDS	-	70
L 5	5	-	1	64	0.34	SDS	-	70
L 6	5	-	1	32	0.20	SDS	-	70
L 7	5	-	1	32	0.25	SDS	-	70
L 8	5	-	1	32	0.30	SDS	-	70
L 9	5	-	1	32	0.38	SDS	-	70
L 10	5	-	1	32	0.34	SDS	-	60
L 11	5	-	1	32	0.34	SDS	-	80
L 12	5	-	2	32	0.34	SDS	-	60
L 13	5	-	2	32	0.34	SDS	-	80
L 14	10	-	2	32	0.34	SDS	-	70
L 15	15	-	2	32	0.34	SDS	-	70
L 16	5	-	1	32	0.20	SDS	O <sub>2</sub>	70
L 17	10	-	1	16	0.20	SDS	-	70
L 18	10	-	1	16	0.20	SDS	O <sub>2</sub>	70
L 19	5	-	2	32	0.34	Sinnopal	-	70
L 20	5	-	2	32	0.34	Teric	-	70

#### 4. Epoxidation Reaction of Liquid Purified Natural Rubber

Epoxidation of LPNR was performed by two methods; in latex phase using in-situ performic acid and in organic media, using m-chloroperbenzoic acid.

##### 4.1 By in-situ performic acid

LPNR in latex form was stabilized by stirring with desired amount of surfactant (the same surfactant previously used in the preparation of PNR) at room temperature

in one liter glass reactor. The stabilized latex was heated to 50°C, then all the desired amount of formic acid was slowly dropped. After 15 min., required amount of hydrogen peroxide was slowly added. The epoxidation reaction was allowed to take place at 50°C during a certain period. The epoxidation conditions are presented in Table 4.2 and 4.3. The epoxidized rubber was achieved by precipitation in methanol. The purification was done by redissolving the rubber in toluene, then reprecipitation in methanol. The viscous product obtained after drying under vacuum at room temperature was transparent with light yellow color. The extent of epoxidation and structural characterization were analyzed by <sup>1</sup>H NMR, <sup>13</sup>C NMR and FTIR spectroscopy. The intrinsic viscosity was measured by PVS1 viscometer.

**Table 4.2** Main feeding compositions of reagents used in the preparation of epoxidized liquid natural rubber (ELPNR)

Formulation	Composition number		
	ELS	ELT	ELD
10% DRC of LPNR latex, ml	200	200	200
Isoprene unit, mol/L	1.47	1.47	1.47
H <sub>2</sub> O <sub>2</sub> /isoprene unit, mole/mole	0.3-1.2	0.3-1.2	0.3-0.6
HCOOH/ isoprene unit, mole/mole	0.15-0.50	0.15-0.50	0.15-0.50
Surfactant	Sinnopal	Teric	SDS
Reaction temperature (°C)	50	50	50
Reaction time (hrs.)	30	30	30
Starting [η] of LPNR	0.39	0.35	0.20

**Table 4.3** Detailed compositions of each main feeding compositions (ELS (a-h), ELT (b,d-i) and ELD (a-g))

Formulation	Composition number								
	a	b	c	d	e	f	g	h	i
H <sub>2</sub> O <sub>2</sub> /isoprene unit, mole/mole	0.3	0.3	0.3	0.3	0.6	0.6	0.6	1.2	1.2
HCOOH/ isoprene unit, mole/mole	0.15	0.15	0.15	0.25	0.15	0.25	0.5	0.25	0.5
Surfactant, phr	0.5	1.5	3	1.5	1.5	1.5	1.5	1.5	1.5

#### 4.2 By m-chloroperbenzoic acid

10 g of LPNR dissolved in 50 ml of toluene was poured in a round bottom flask. The system was cooled to 0°C and stirred magnetically. The calculated amount of m-chloroperbenzoic acid dissolved in toluene was slowly added. After 2 hours, the rubber solution was precipitated in methanol. The epoxidized rubber obtained was purified by twice precipitation using the couple of toluene/methanol for elimination of m-chlorobenzoic acid. After drying in vacuum until constant weight, the epoxidized rubber was analysed by <sup>1</sup>H NMR and FTIR spectroscopy. The [η] was measured by viscometer.

### 5. Degradation Reaction of Epoxidized Purified Natural Rubber by Using Periodic Acid

In this section, epoxidized purified natural rubber (EPNR) was prepared prior to the degradation by using periodic acid (H<sub>5</sub>IO<sub>6</sub>).

32 ml of PNR latex (25% DRC) was diluted by 8 ml of distilled water. The latex was stabilized by 4 phr of Sinnopal NP 307 as a non-ionic surfactant at room temperature (RT) before pouring into 250 ml glass reactor equipped with a controlled speed stirrer of 300 rpm. The latex was heated up to 60°C before adding the calculated amount of formic acid. The latex was further stirred for 15 minutes, and then the desired amount of hydrogen peroxide was slowly dropped. The reaction was allowed to stir during 24 hours. The latex was sampling for characterization and determination of epoxide content after precipitation in methanol, then purification by using the couple of dichloromethane and methanol.

The EPNR latex was cooled down to 30°C. Then a required amount of H<sub>5</sub>IO<sub>6</sub> aqueous solution was slowly added. The degradation conditions are shown in Table 4.4. The degraded rubber was sampling, then precipitated in methanol. The liquid epoxidized purified natural rubber (LEPNR) obtained was purified by reprecipitation using the couple of dichloromethane/ methanol, and dried under vacuum until constant weight. The structural characterizations were carried out using <sup>1</sup>H NMR, <sup>13</sup>C NMR and FTIR spectroscopy. The intrinsic viscosity and molecular weight were determined by PVS1 viscometer and GPC.

The degradation of natural rubber such as NR and PNR by  $H_5IO_6$  was also investigated in the same procedure. Various degradation conditions are shown in Table 4.4.

**Table 4.4** Degradation conditions of rubber latex with periodic acid carried out at 30°C

	Type of rubber latex	Epoxide content (%)	$H_5IO_6$ /epoxide unit (mole/mole)	$H_5IO_6$ /isoprene unit (mole/mole)	$H_2O_2$ /isoprene unit, (mole/mole)	Rx. Time (hours)
LE 1	EPNR	20	0.24	0.07	-	30
LE 2	EPNR	20	0.51	0.13	-	30
LE 3	EPNR	20	1.13	0.26	-	21
LE 4	EPNR	5	4.06	0.21	-	21
LE 5	NR	-	-	0.20	-	30
LE 6	PNR	-	-	0.20	-	30
LE 7	PNR	-	-	0.20	0.3	30

## 6. Addition Reaction of Acrylic Acid onto Epoxidized Molecules

The addition conditions of acrylic acid onto epoxidized molecules are shown in Table 4.5.

### 6.1 Addition reaction of acrylic acid onto 4,5-epoxy-4-methyloctane (EMO)

4,5-epoxy-4-methyloctane was prepared by the reaction of 0.1 mole of 4-methyl-4-octene (5 g in 100 ml of dichloromethane) with 0.15 mole of m-chloroperbenzoic acid (8.2 g in 100 ml of dichloromethane) at 0°C during 2 hours. Unreacted solid by-product was separated by filtration. The filtrate was purified by washing with 0.05 M aqueous solution of NaOH for removing unreacted peracid and then with distilled water. The organic phase was separated and dried on  $K_2CO_3$ . The dichloromethane was removed using rotary evaporator. The 4,5-epoxy-4-methyloctane was purified by distillation under reduced pressure. (4-methyl-4-octene,  $E_{b760 \text{ mmHg}} = 141-142^\circ\text{C}$ ; 4,5-epoxy-4-methyloctane,  $E_{b760 \text{ mmHg}} = 164-165^\circ\text{C}$ ) [3].

1.47 g of 4,5-epoxy-4-methyloctane was dissolved with toluene (10 ml) and poured into 100 ml glass reactor. The mixture was heated to 70°C before slow addition

of acrylic acid (10 fold per mole of epoxidized unit, 11 ml). During stirring at 70°C, the mixture was sampling (1.5 ml) at different intervals of time. The sample was cooled down to room temperature and diluted with 10 ml of toluene. The solution sample was poured in a vessel containing an excess amount of NaHCO<sub>3</sub> wetted by a few drop of water, for removal of unreacted acrylic acid. The unreacted acrylic acid reacted with NaHCO<sub>3</sub> resulted in generation of bubble CO<sub>2</sub>, then salt and acrylated product solution were obtained. After leaving the solution mixture staying overnight, the solution was retreated with the NaHCO<sub>3</sub>. The toluene was later evaporated, then the acrylated model was finally kept in a refrigerator. The characteristic analysis of the epoxidized and acrylated products were reported by SFC, FTIR, <sup>1</sup>H NMR and <sup>13</sup>C NMR spectroscopy.

## **6.2 Addition reaction of acrylic acid onto epoxidized liquid synthetic rubber**

Epoxidized liquid synthetic rubber (ELIR) was prepared by the reaction of liquid synthetic rubber (LIR 30, 2.75g in 100 ml of dichloromethane) with m-chloroperbenzoic acid (1.82 g in 100 ml of dichloromethane) at 0°C during 5 hours. The epoxidized rubber obtained was purified by twice reprecipitation using the couple of dichloromethane/methanol for elimination of m-chlorobenzoic acid. After drying under reduced pressure, the rubber was analysed by FTIR, <sup>1</sup>H NMR, <sup>13</sup>C NMR spectroscopy.

The ELIR (2g, 17% oxirane ring) was then dissolved in 20 ml of toluene and stirred until homogenous solution. The solution was poured into 100 ml glass reactor and heated up to 70°C. Acrylic acid (10 fold per mole of epoxidized unit, 2.7 ml) was slowly added. The mixture at various times was sampling and precipitated in methanol. The acrylated rubber was dissolved and reprecipitated in dichloromethane/methanol. After drying under vacuum, the transparent acrylated liquid rubber was obtained. The acrylated rubbers were characterized by FTIR, <sup>1</sup>H NMR, <sup>13</sup>C NMR spectroscopy.

### **6.3 Addition reaction of acrylic acid onto epoxidized liquid purified natural rubber**

Two different sources of epoxidized rubber were used in this section; ELPNR and LEPNR. Epoxidized rubber solution obtained was prepared by dissolution of dry epoxidized rubber in toluene and by transfer of epoxidized rubber molecules from latex phase to toluene phase.

By dissolution of dry epoxidized rubber in toluene, the epoxidized rubber solution (5 g of rubber in 25 g of toluene) was poured into 100 ml glass reactor. The solution was heated and stirred magnetically to the desired temperature (60-70°C). The calculated amount of acrylic acid was slowly added. The reaction was carried out during 34-72 hours. The solution at various reaction times was sampling and precipitated in methanol. The acrylated rubber was purified by dissolution and reprecipitation twice by using the couple of dichloromethane/methanol, and dried under vacuum. The transparent acrylated liquid rubber was obtained. The structural and content of acrylate function on rubber molecules were characterized by FTIR, <sup>1</sup>H NMR and <sup>13</sup>C NMR spectroscopy.

By transfer technique, 200 ml of toluene was added into 50 ml of epoxidized latex (20% DRC of LEPNR latex in 1.5 phr of Sinnopal NP 307) in a one liter reactor. Then, an appropriate amount of methanol was added under stirring until the clear solution of aqueous phase was observed. Then, the mixture was left at room temperature without stirring. At the end point, the system became 3 phases, the upper phase was methanol because of the lowest density as 0.79. The middle phase was the mixture of toluene and rubber particles. And the lower was aqueous phase. After staying overnight, the lower phase was pulled out and the upper phase was left in the reactor, which was composed of methanol, toluene and rubber particles was heated up to 75°C and left stirring continuously during 3 hours for removing of methanol and increasing the dry rubber content. The solution was sampling for determination of DRC and chemical characterization. The temperature of the solution was decreased to 70°C and the calculated amount of acrylic acid (10 fold of epoxide units) was added. The acrylation reaction was studied by sampling of the reaction mixture at various times. The acrylated product was analyzed after twice precipitation using the couple of

dichloromethane/methanol. Appendices...showed the photograph of phase transfer of 10% DRC of ELPNR from latex phase to toluene phase, and then addition of acrylic acid.

**Table 4.5** Summary of different conditions of addition reaction of acrylic acid onto epoxidized molecules

Sample	Type of epoxidized rubber	Epoxide content (%)	Methodology of preparation of acrylated materials			
			Coagulation or transfer process	Temp. (°C)	Fold of acrylic acid (per mole of epoxide content)	Reaction time (hours)
Amodel 1	EMO	93	-	70	10	48
ALIR 1	ELIR	17	Coag.	70	10	70
ALPNR 1	LEPNR	19	Transf.	60	10	34
ALPNR 2	LEPNR	19	Transf.	70	10	48
ALPNR 3	ELPNR	26	Coag.	70	10	72
ALPNR 4	ELPNR	26	Coag.	70	10 <sup>a</sup>	70
ALPNR 5	LEPNR	17	Coag.	70	2	72
ALPNR 6	LEPNR	17	Coag.	70	10	34

a: acrylic acid was distilled before use

## 7. Analysis

### 7.1 Chemical structure characterization

The chemical structures of the NR and modified NR including epoxidized and acrylated NR were characterized by the following techniques.

#### 7.1.1 By infrared spectroscopy

The rubber samples were dissolved in dichloromethane before casting as a thin film directly on NaCl cell. The FTIR spectra of the dried films were recorded on Perkin Elmer System 2000 FTIR spectrophotometer in the range of 4000-600  $\text{cm}^{-1}$ , using 16 scans.

### **7.1.2 By $^1\text{H}$ NMR and $^{13}\text{C}$ NMR spectroscopy**

The rubber samples were dissolved in  $\text{CDCl}_3$  for analysis. The  $^1\text{H}$  NMR and  $^{13}\text{C}$  NMR spectra were recorded on 300 MHz Bruker AM 400 spectroscopy operating at 300 MHz, using tetramethylsilane as an internal standard.

## **7.2 Separation characterization technique**

### **7.2.1 By supercritical fluid chromatography (SFC)**

Supercritical fluid chromatography is an instrument used for separation of small molecules i.e. 4,5-epoxy-4-methyloctane, acrylic acid and acrylated model molecules.

1  $\mu\text{l}$  of mixture solution (0.01 g of the sample mixture in 1 ml of dichloromethane) was injected into the tubular capillary column coated with 0.4  $\mu\text{m}$  film of diphenyldimethylpolysiloxane and detection by FID 40 flame ionization detector. The data were recorded on SFC 3000 series chromatography, Carlo Erba Instruments.

### **7.2.2 By Gas chromatography-mass spectrometer (GC-MS)**

## **7.3 Determination of nitrogen content by micro-Kjeldahl method**

The nitrogen content is considered to be related to protein content in natural rubber was determined by micro-Kjeldahl method, following to the standard of ASTM 03533-82 [111].

First, digestion step, 0.1 g of NR sample was combined with 0.65 g of catalyst mixture and 2.5 ml of sulfuric acid in Kjeldahl flask. The catalyst mixture is composed of 7.5 g of anhydrous  $\text{K}_2\text{SO}_4$ , 1 g of  $\text{CuSO}_4 \cdot 5\text{H}_2\text{O}$  and 0.5 g of Se powder. The sample mixture was digested at  $370^\circ\text{C}$  until the solution became a clean green color solution. In the case of PNR, which has low nitrogen content, higher amount of rubber and

ingredient were required i.e. 0.15 g, 0.8 g and 4.5 ml for PNR, catalyst mixture and sulfuric acid, respectively.

Second, distillation step, 10 ml of boric acid combined with 2 drops of indicator solution (0.05 g of methyl red and 0.025 g of methylene blue dissolved in 50 ml of ethanol) were poured into receiving conical flask which was then placed at the end of the condenser. The digested sample was poured into a distillation vessel, after that 10 ml of NaOH (67% w/v) was added. After 8 minutes of distillation, the sample solution was titrated with standardized 0.1 N H<sub>2</sub>SO<sub>4</sub>. The nitrogen content was calculated using eq. (4.1).

$$\% \text{ Nitrogen content} = \frac{[(V_1 - V_2)N \times 0.014 \times 100]}{W} \quad (4.1)$$

V<sub>1</sub> and V<sub>2</sub> : volume of H<sub>2</sub>SO<sub>4</sub> required for titration of rubber sample and blank, respectively

N : concentration of H<sub>2</sub>SO<sub>4</sub> (normality)

W : weight of sample (g)

0.014 : millimoles mass of nitrogen

#### 7.4 Determination of epoxide content

The epoxide content of the epoxidized rubbers can be calculated from the spectra of <sup>1</sup>H NMR and <sup>13</sup>C NMR spectroscopy.

##### 7.4.1 By <sup>1</sup>H NMR spectroscopy

By using the integrated areas of the signal from <sup>1</sup>H NMR at 2.7 ppm (A<sub>2.7</sub>), representing the proton adjacent to epoxide ring and 5.1 ppm (A<sub>5.1</sub>), representing the proton adjacent to C=C, the epoxide content of the epoxidized rubber can be calculated from eq. (4.2) [51,64,70,112,113].

$$\text{Epoxide content (\%)} = \left( \frac{A_{2.7}}{A_{2.7} + A_{5.1}} \right) \times 100 \quad (4.2)$$

### 7.4.2 By $^{13}\text{C}$ NMR spectroscopy

The integration areas of signal from  $^{13}\text{C}$  NMR at 64.5 ppm ( $A_{64.5}$ ), representing the oxirane carbon and 124.4, 125.0 and 125.7 ppm ( $A_{124.4,125.0,125.7}$ ), representing the olefinic carbon were also used to calculate the epoxide content of the epoxidized rubber as shown in eq. (4.3) [51,64,112,113].

$$\text{Epoxide content (\%)} = \left( \frac{A_{64.5}}{A_{64.5} + A_{124.4,125.0,125.7}} \right) \times 100 \quad (4.3)$$

### 7.5 Determination of acrylate content

On the addition of acrylic acid to epoxidized molecule, three main characteristic signals of acrylate function at 5.08, 6.04 and 6.36 ppm were observed [114]. Beside acrylate function, secondary reactions were also noticed. Therefore, acrylate content of the modified rubber is calculated from the integration area of  $A_{(5.80+6.04+6.36)/3}$ , representing the proton adjacent to C=C of acrylate function,  $A_{2.7}$ , representing the residual proton adjacent to C-O-C of oxirane ring,  $A_x$ , representing the proton from the secondary products and  $A_{5.1}$ , representing the proton adjacent to C=C of isoprene function as shown in eq. (4.4)

$$\text{Acrylate content (\%)} = \left( \frac{A_{(5.80+6.04+6.36)/3}}{A_{(5.80+6.04+6.36)/3} + A_{2.7} + A_x + A_{5.1}} \right) \times 100 \quad (4.4)$$

### 7.6 Molecular weight determination

The molecular weight of NR and modified NRs were analysed as intrinsic viscosity using viscometry and average molecular weight using gel permeation chromatography (GPC).

#### 7.6.1 By viscometry

0.1 - 0.2 g/dl of the rubber dissolved in toluene was prepared for the analysis in Processor viscosity system (PVS1, LAUDA). The rubber solution was filtered through sintered glass funnel (0.16-0.40  $\mu\text{m}$ ) before the analysis. The flow time of the pure

solution and polymer solution were recorded at 30°C. An average of 5 concentration values was used for calculation of intrinsic viscosity,  $[\eta]$  as shown in eq. (4.5).

$$[\eta] = (\eta_{sp}/C)_{c=0} = (\ln \eta_{rel}/C)_{c=0} \quad (4.5)$$

### 7.6.2 By gel permeation chromatography

Gel permeation chromatography is the technique for measurement of the average molecular weight and molecular weight distribution of polymers. 0.2% w/v of rubber dissolved in tetrahydrofuran (THF) was prepared and the molecular weight averages data were recorded at 30°C on the gel permeation chromatography (waters<sup>TM</sup> 150-CV plus) equipped with refractometer and capillary viscometer detectors. Polystyrene gels were used as standard calibrators.

## 8. Photocrosslinking Reaction of Acrylated Elastomers

The modified rubbers containing the acrylate functions were exposed to UV light for the study of photocrosslinking reaction in photocalorimetry. The detail of instrument and preparation of samples for analysis are listed below.

### 8.1 Operating apparatus

Double beam photocalorimeter accessory, DPA 7 connected with Perkin Elmer DSC 7 was used to study photoreaction of the modified rubbers. This apparatus consists of the optical part and analytical part. The optical parts have the DPA 7 accessory, power supply and purge box. DPA 7 accessory includes the 100 w/2 Hg - lamp HBO, condenser, transfer optic which exposes full wavelength at  $\lambda$  set 285-440 nm, water filter that serves for removal of the infrared radiation, light shutter system, beam splitter which deflects beam light to two deflecting mirror before going into the DSC holder.

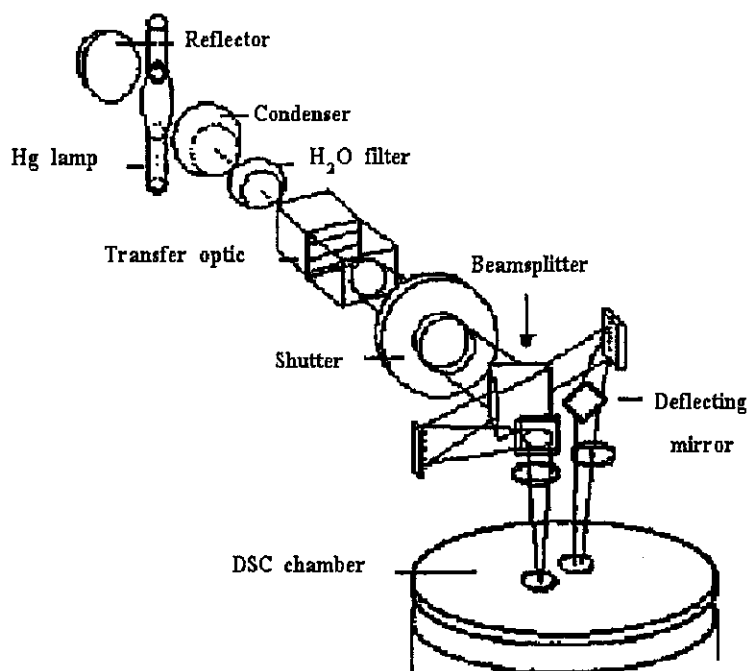
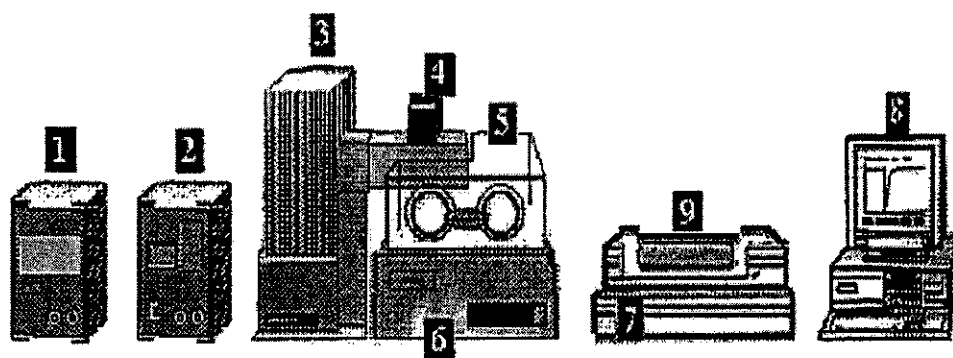


**Figure 4.1** DPA 7 optical part

The analytical parts consist of the DSC 7 Perkin-Elmer, instrument controller (TAC), computer and printer.



- |                 |                   |                               |
|-----------------|-------------------|-------------------------------|
| 1. Cooler       | 4. Transfer optic | 7. Instrument controller, TAC |
| 2. Power supply | 5. Purge box      | 8. Computer                   |
| 3. Lamp housing | 6. DSC 7          | 9. Printer                    |

**Figure 4.2** Schematic illustration of DPA-DSC 7 instrument used for photoreaction

## 8.2 Preparation of samples for the study of photoreaction

0.1 g of rubber was mixed with 1 ml of reactive diluent solution (0.5-3 g of diluents in 100 ml of chloroform) and 0.05-0.5 ml of photoinitiator solution (0.12 g of photoinitiator in 10 ml of chloroform) in a small dark bottle. After drying under reduced pressure at room temperature about 3-6 hrs, 1 mg of the sample mixture was placed in an aluminum DPA pan covered with quartz window. The sample cell was flushed with nitrogen for 5 min before exposure to UV light because of oxygen is a well-known inhibitor of free radical polymerization. The photocrosslinking was allowed to proceed at various isothermal temperatures (30-90°C). Calculated polymerization data from the exothermic thermogram shown in Figure 4.3 after baseline correction was obtained. Three types of rubber i.e. LPNR, ELPNR and ALNR were used for the study of photocrosslinking by photocalorimeter. 1,6 hexanediol diacrylate (HDDA) and tripropyleneglycol diacrylate (TPGDA) were reactive diluents used to control viscosity and properties of the final products. Irgacure 184 and Daracur 1173 were two photoinitiators used in the study as they can produce clear coating. Various formulations studied are listed in Table 4.6.

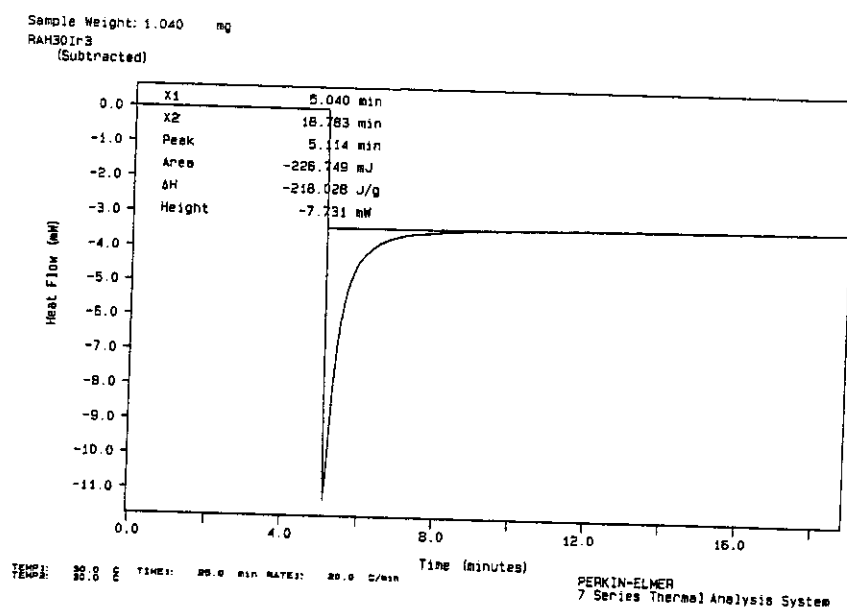


**Figure 4.3** Thermogram of exothermic peak of photopolymerization of acrylated liquid rubber with HDDA and Irgacure184 at isothermal temperature of 30°C

**Table 4.6** Formulations for photocrosslinking study

Sample Codes	Rubber	HDDA	TPGDA	Acrylic acid	Irgacure 184 per total solid content	Darocur 1173 per total solid content
A1H20I.5	100	20	-	-	0.5	-
A1H20I1	100	20	-	-	1	-
A1H20I3	100	20	-	-	3	-
A1H20I5	100	20	-	-	5	-
A1H20D.5	100	20	-	-	-	0.5
A1H20D1	100	20	-	-	-	2
A1H20D3	100	20	-	-	-	3
A1H20D5	100	20	-	-	-	5
A1T20I.5	100	-	20	-	0.5	-
A1T20I1	100	-	20	-	1	-
A1T20I3	100	-	20	-	3	-
A1T20I5	100	-	20	-	5	-
A1T20D.5	100	-	20	-	-	0.5
A1T20D1	100	-	20	-	-	1
A1T20D3	100	-	20	-	-	3
A1T20D5	100	-	20	-	-	5
A1H5I3	100	5	-	-	3	-
A1H10I3	100	10	-	-	3	-
A1H30I3	100	30	-	-	3	-
A1H5D3	100	5	-	-	-	3
A1H10D3	100	10	-	-	-	3
A1H30D3	100	30	-	-	-	3
A1T5I3	100	-	5	-	3	-
A1T10I3	100	-	10	-	3	-
A1T30I3	100	-	30	-	3	-
A1T5D3	100	-	5	-	-	3
A1T10D3	100	-	10	-	-	3
A1T30D3	100	-	30	-	-	3
A2H20I.5	100	20	-	-	0.5	-
A2H20I1	100	20	-	-	1	-
A2H20I3	100	20	-	-	3	-
A2H20I5	100	20	-	-	5	-
A2H20D.5	100	20	-	-	-	0.5

Sample Codes	Rubber	HDDA	TPGDA	Acrylic acid	Irgacure 184 per total solid content	Darocur 1173 per total solid content
A2H20D1	100	20	-	-	-	2
A2H20D3	100	20	-	-	-	3
A2H20D5	100	20	-	-	-	5
A2T20I.5	100	-	20	-	0.5	-
A2T20I1	100	-	20	-	1	-
A2T20I3	100	-	20	-	3	-
A2T20I5	100	-	20	-	5	-
A2T20D.5	100	-	20	-	-	0.5
A2T20D1	100	-	20	-	-	1
A2T20D3	100	-	20	-	-	3
A2T20D5	100	-	20	-	-	5
A3H20I3(30)	100	20	-	-	3	-
A3H20I3(45)	100	20	-	-	3	-
A3H20I3(60)	100	20	-	-	3	-
A3H20I3(75)	100	20	-	-	3	-
A3H20I3(90)	100	20	-	-	3	-
A3H20D3(30)	100	20	-	-	-	3
A3H20D3(45)	100	20	-	-	-	3
A3H20D3(60)	100	20	-	-	-	3
A3H20D3(75)	100	20	-	-	-	3
A3H20D3(90)	100	20	-	-	-	3
A3T20I3(30)	100	-	20	-	3	-
A3T20I3(45)	100	-	20	-	3	-
A3T20I3(60)	100	-	20	-	3	-
A3T20I3(75)	100	-	20	-	3	-
A3T20I3(90)	100	-	20	-	3	-
A3T20D3(30)	100	-	20	-	-	3
A3T20D3(45)	100	-	20	-	-	3
A3T20D3(60)	100	-	20	-	-	3
A3T20D3(75)	100	-	20	-	-	3
A3T20D3(90)	100	-	20	-	-	3
LH20I.5	100	20	-	-	0.5	-
LH20I1	100	20	-	-	1	-
LH20I3	100	20	-	-	3	-
LH20I5	100	20	-	-	5	-

Sample Codes	Rubber	HDDA	TPGDA	Acrylic acid	Irgacure 184 per total solid content	Darocur 1173 per total solid content
LH20D.5	100	20	-	-	-	0.5
LH20D1	100	20	-	-	-	2
LH20D3	100	20	-	-	-	3
LH20D5	100	20	-	-	-	5
LT20I.5	100	-	20	-	0.5	-
LT20I1	100	-	20	-	1	-
LT20I3	100	-	20	-	3	-
LT20I5	100	-	20	-	5	-
LT20D.5	100	-	20	-	-	0.5
LT20D1	100	-	20	-	-	1
LT20D3	100	-	20	-	-	3
LT20D5	100	-	20	-	-	5
LH10a10I1	100	10	-	10	1	-
LH10a10D1	100	10	-	10	-	1
LT10a10I1	100	-	10	10	1	-
LT10a10D1	100	-	10	10	-	1
LH5a15I1	100	5	-	15	1	-
LH5a15D1	100	5	-	15	-	1
LT5a15I1	100	-	5	15	1	-
LT5a15D1	100	-	5	15	-	1
EH20I.5	100	20	-	-	0.5	-
EH20I1	100	20	-	-	1	-
EH20I3	100	20	-	-	3	-
EH20I5	100	20	-	-	5	-
EH20D.5	100	20	-	-	-	0.5
EH20D1	100	20	-	-	-	2
EH20D3	100	20	-	-	-	3
EH20D5	100	20	-	-	-	5
ET20I.5	100	-	20	-	0.5	-
ET20I1	100	-	20	-	1	-
ET20I3	100	-	20	-	3	-
ET20I5	100	-	20	-	5	-
ET20D.5	100	-	20	-	-	0.5
ET20D1	100	-	20	-	-	1
ET20D3	100	-	20	-	-	3

Sample Codes	Rubber	HDDA	TPGDA	Acrylic acid	Irgacure 184 per total solid content	Darocur 1173 per total solid content
ET20D5	100	-	20	-	-	5
EH10a10I1	100	10	-	10	1	-
EH10a10D1	100	10	-	10	-	1
ET10a10I1	100	-	10	10	1	-
Ea10T10D1	100	-	10	10	-	1
EH5a15I1	100	5	-	15	1	-
EH5a15D1	100	5	-	15	-	1
ET5a15I1	100	-	5	15	1	-
ET5a15D1	100	-	5	15	-	1

A1 = acrylated liquid natural rubber - 1, containing 11.3 % acrylate content,

$$[\eta] = 0.22 \text{ and } \bar{M}_v = 25,500$$

A2 = acrylated liquid natural rubber - 2, containing 5.0 % acrylate content,

$$[\eta] = 0.23 \text{ and } \bar{M}_v = 26,900$$

A3 = acrylated liquid natural rubber - 3, containing 9.9 % acrylate content,

$$[\eta] = 0.31 \text{ and } \bar{M}_v = 38,000$$

L = liquid purified natural rubber,  $[\eta] = 0.252$  and  $\bar{M}_v = 29,800$

E = epoxidized liquid natural rubber, containing 14.4 % epoxidation content,

$$[\eta] = 0.27 \text{ and } \bar{M}_v = 32,400$$

## CHAPTER V

### RESULTS AND DISCUSSION

#### 1. Purified Natural Rubber

High ammonia natural rubber (HANR) latex obtained from *Hevea brasiliensis* was used in this study. The HANR concentrated by centrifugation technique consists of about 2% w/v of non-rubber constituent including mainly lipids and proteins. It has been reported that the extraction and isolation of proteins and some non-rubber constituents from rubber particles can be done by enzymatic treatment and surfactant washing [1-3]. Proteinase B KP 3939 and sodium dodecyl sulphate (SDS) are the enzyme and surfactant, used respectively to extract proteins from HANR in this study. After treatment of HANR with proteinase B KP 3939 and SDS during 24 hours at room temperature, the rubber fraction was isolated by ultracentrifugation. For this, the water-soluble proteins, the extracted proteins from rubber particles and some non-rubber components should be eliminated as ~~having been~~ mentioned by Hasma H [22] and Ichikawa N et al. [33]. The presence of proteins in natural rubber (NR) is usually reported in term of nitrogen content (%N) [19,33,38]. It was found in this study that the nitrogen content by micro-Kjeldahl technique of the HANR was reduced from 0.4% to 0.03%. The rubber cream fraction obtained in the first treatment can be redispersed into latex form by the help of surfactants either ionic or non ionic character. In our study, SDS (anionic surfactant), Teric and Sinnopal NR 307 (both non-ionic surfactants) were used. It was found that the use of SDS surfactant provided better redispersion of the latex than ~~in the case of~~ Teric and Sinnopal. When the redispersed latex was taken to another centrifugation, the nitrogen content was found to be slightly lower (0.02-0.03%).

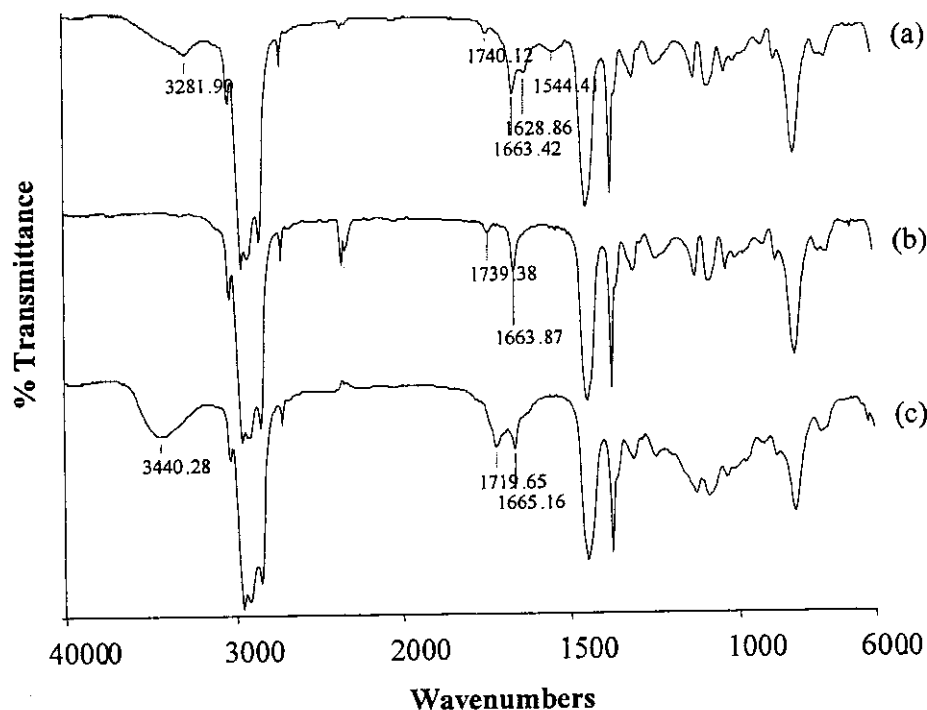


**Figure 5.1** Infrared spectra of (a) Natural rubber (NR), (b) Purified natural rubber (PNR) and (c) Liquid purified natural rubber (LPNR)

The IR spectra of the NR and the purified natural rubber (PNR) are presented in Figure 5.1. It was clearly found that the characteristic amide signals at  $3282\text{ cm}^{-1}$  (N-H stretching),  $1629\text{ cm}^{-1}$  (amide I vibration) and  $1544\text{ cm}^{-1}$  (amide II vibration) were disappeared. This can be used to confirm the reduction of proteins from HANR, similar to several reports in the literature [36-39]. The PNR showed small signal at about  $1740\text{ cm}^{-1}$  which can be attributed to some abnormal groups such as carbonyl functions as reported by Lu FJ and Hsu SL [36].

The intrinsic viscosity,  $[\eta]$  of PNR was found decreasing after the treatment with proteinase enzyme and twice centrifugation. The  $[\eta]$  of NR was 5.88 and that of PNR was found to be 4.31. However, the chemical structure of cis-1,4-polyisoprene was not destroyed by the enzymatic treatment process. The  $^1\text{H}$  NMR spectrum of the PNR shows the same characteristic signal of proton adjacent to C=C at 5.14 ppm as the original NR as well as the signal of the methyl group adjacent to C=C of cis-structure at 1.67 ppm and the signal of methylene proton of the saturated hydrocarbon at 2.03 ppm (see Figure 5.2). No extra signals are detected around 9-10 ppm.

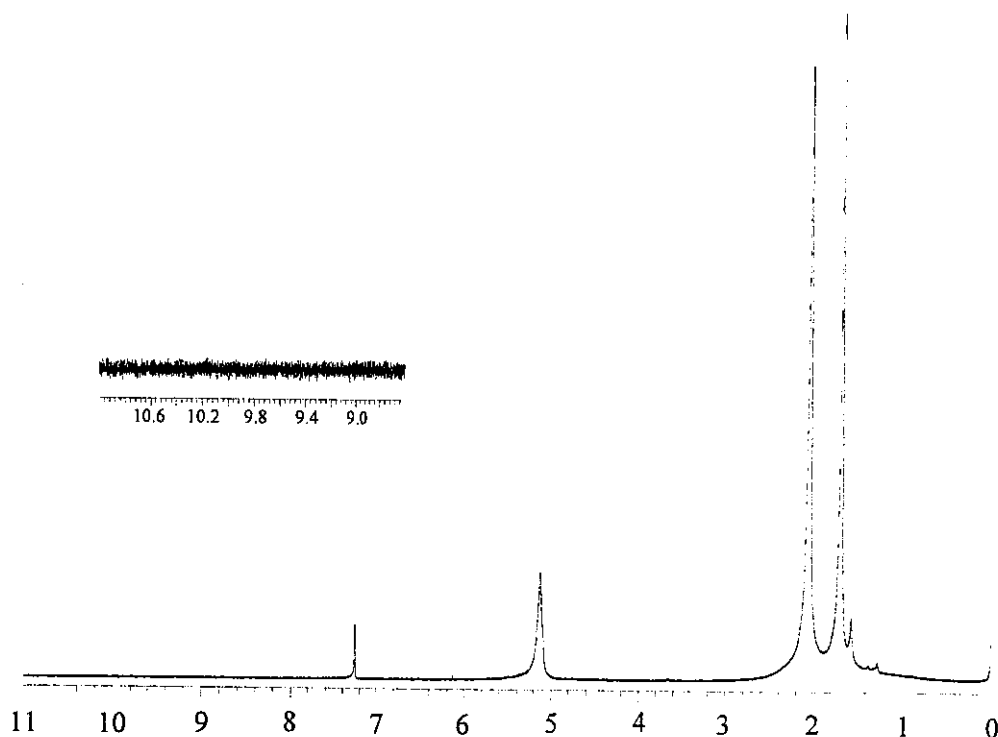
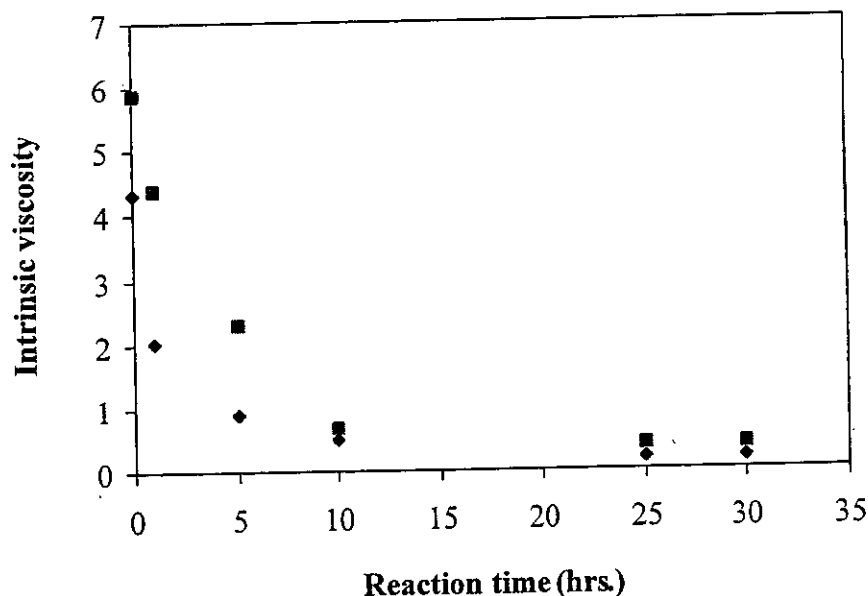


Figure 5.2  $^1\text{H}$  NMR spectrum of PNR

## 2. Degradation of Purified Natural Rubber by Using Potassium Persulfate and Propanal

It has been reported in several papers that degradation of NR can be occurred if reactive radicals have been <sup>created</sup> introduced to the rubber chain through chemical treatment. Pautrat R [45] used phenylhydrazine and oxygen to degrade NR while Tangpakdee J et al [46] had employed potassium persulfate ( $\text{K}_2\text{S}_2\text{O}_8$ ) in combination with various types of carbonyl compounds for the degradation of PNR. In this presented work, the oxidative degradation of PNR in latex form was studied by using  $\text{K}_2\text{S}_2\text{O}_8$  as a radical initiator in conjunction with a small carbonyl compound (propanal). The degradation reaction of NR was also carried out and firstly compared with the degraded PNR. In both cases, the reaction was performed by using 5% DRC of the latex, 1 phr of  $\text{K}_2\text{S}_2\text{O}_8$ , 32 phr of propanal and 0.34 phr of  $\text{Na}_3\text{PO}_4$  at  $70^\circ\text{C}$ . It was found that intrinsic viscosities,  $[\eta]$  of both cases were exponentially reduced according to the increased reaction time as shown in Figure 5.3. This can be postulated that  $\text{K}_2\text{S}_2\text{O}_8$  should induce radical species on the rubber chain, leading later to chain degradation. The

*the formation*



**Figure 5.3** Plots of intrinsic viscosity,  $[\eta]$ , of LPNR and LNR prepared by using 1 phr of  $K_2S_2O_8$ , 32 phr of propanal and 0.34 phr of  $Na_3PO_4$  at  $70^\circ C$ ; (◆) 5 % DRC of PNR latex (■) 5 % DRC of NR latex

decreasing rate of the  $[\eta]$  of PNR seems to be better than the NR. This may be due to the presence of non-rubber constituents in NR such as tocotrienol, which may act as antioxidants might retard the oxidative degradation [21]. The presence of some microgels in NR or higher value of  $[\eta]$  of NR than PNR may also slower rate of degradation of NR than PNR [19]. The kinetic rate constants of the degraded PNR and NR were investigated in later section. The  $[\eta]$ s of degraded rubber obtained from PNR and NR <sup>after</sup> at 25 hours of reaction were 0.19 and 0.41 respectively. The resulting degraded rubber from PNR is a colorless viscous liquid while the one from NR has a brown color. The color might come from the presence of  $\beta$ -carotenoid pigments and polyphenol oxidase or oxidation of non-rubber constituents in the NR. It can be concluded in this stage that color less liquid rubber can be prepared from oxidative degradation of the PNR.

## 2.1 Proposed reaction mechanism

The degraded rubbers obtained from both NR and PNR showed similar characteristic signals in IR,  $^1\text{H}$  NMR and  $^{13}\text{C}$  NMR spectroscopies. The comparison of IR spectrum of NR, PNR and liquid purified natural rubber (LPNR) are shown in Figure 5.1. It can be clearly seen that the LPNR consisted of extra peaks at  $1720\text{ cm}^{-1}$  and  $3440\text{ cm}^{-1}$ , which can be attributed to the signals of carbonyl and hydroxyl groups, respectively. In  $^1\text{H}$  NMR shown in Figure 5.4, the LPNR shows main characteristic signals as those of the NR and PNR at 5.14 ppm, attributed to proton adjacent to  $\text{C}=\text{C}$ , at 1.67 ppm which belongs to methyl group adjacent to  $\text{C}=\text{C}$  of cis-structure and the signal of methylene proton of the saturated hydrocarbon at 2.03 ppm. The small extra-signal of proton was found in the case of LPNR at 9.4 ppm, which can be attributed to the proton of aldehyde function. The spectrum in  $^{13}\text{C}$  NMR of LPNR is shown in Figure 5.5.

*suggested*  
The mechanism of the degradation of PNR using  $\text{K}_2\text{S}_2\text{O}_8$  and propanal is proposed in Figure 5.6. The persulfate radicals ( $\text{SO}_4^{\cdot-}$ ) generated from the decomposition of  $\text{K}_2\text{S}_2\text{O}_8$  abstract hydrogen atoms *from* the polymer chain preferably *at m* allylic positions, forming macroradicals (I). The radical then reacted with oxygen presented in the system, followed by proton transfer from another rubber chain, resulting in the formation of alkyl hydroperoxide (Ia). Then, the decomposition of the compound Ia will lead to an alkoxy radical (Ib) and a hydroxyl radical ( $\text{OH}^{\cdot}$ ). The degradation of the rubber molecule containing unstable alkoxy radical Ib was thermodynamically performed to a more stable molecule IIIa and macroradical Ic. The alkyl radical fraction (Ic) will then be terminated by hydroxyl radical presented in the system to form the molecular structure IIIb or recombine with another macroradical which might result in increasing the size of the rubber molecule. However, the inhibition of recombination of macroradicals was successfully performed to a certain extent by the aid of propanal, resulting in the proposed molecular structure IIIc. Meanwhile, it can not be omitted the formation of the molecular structure II from the reaction of any macroradical with a hydroxyl radical. Therefore, at least four types of molecular structures (II, IIIa, IIIb and IIIc) should be formed during oxidative degradation of the PNR by  $\text{K}_2\text{S}_2\text{O}_8$  and propanal. By calculating the chemical shifts of

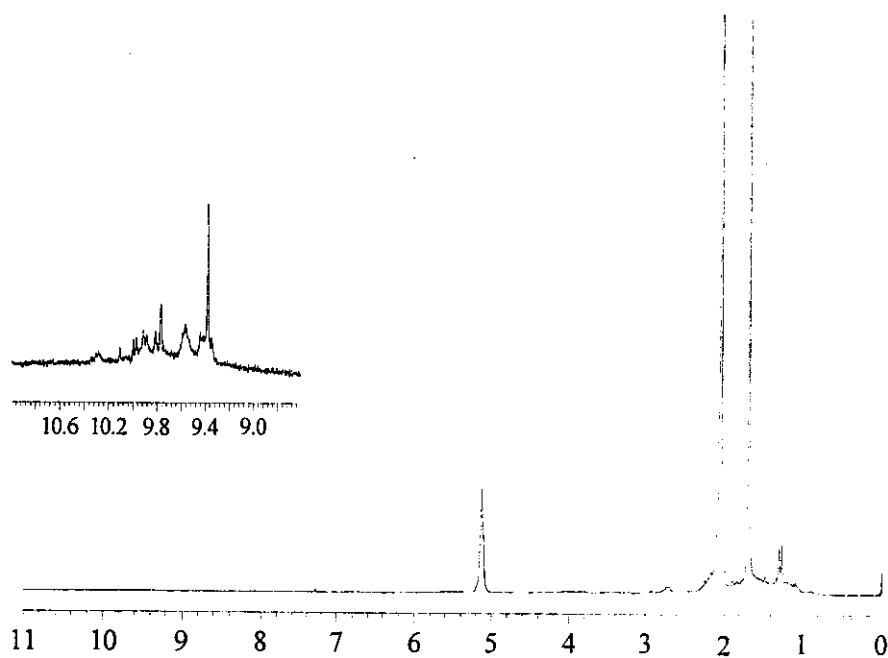


Figure 5.4  $^1\text{H}$  NMR spectrum of LPNR

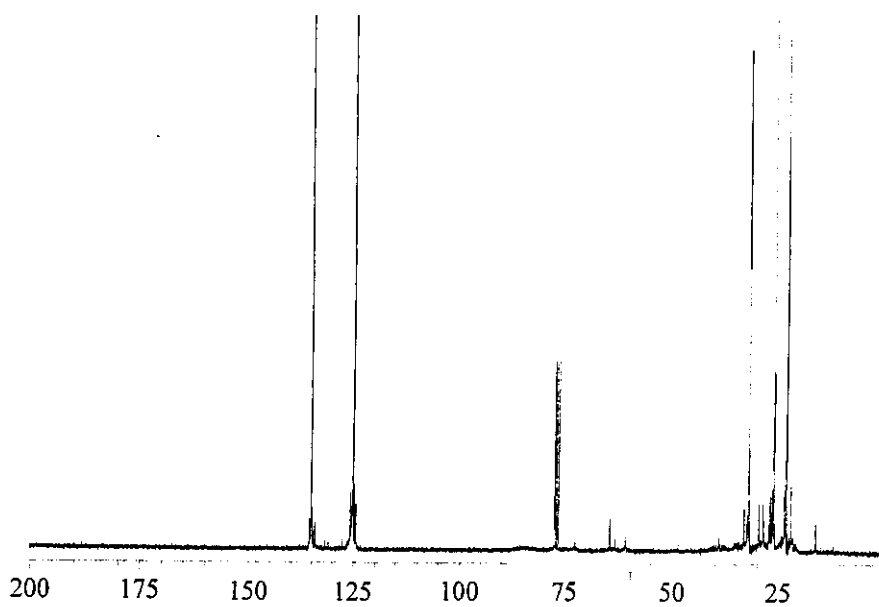


Figure 5.5  $^{13}\text{C}$  NMR spectrum of LPNR

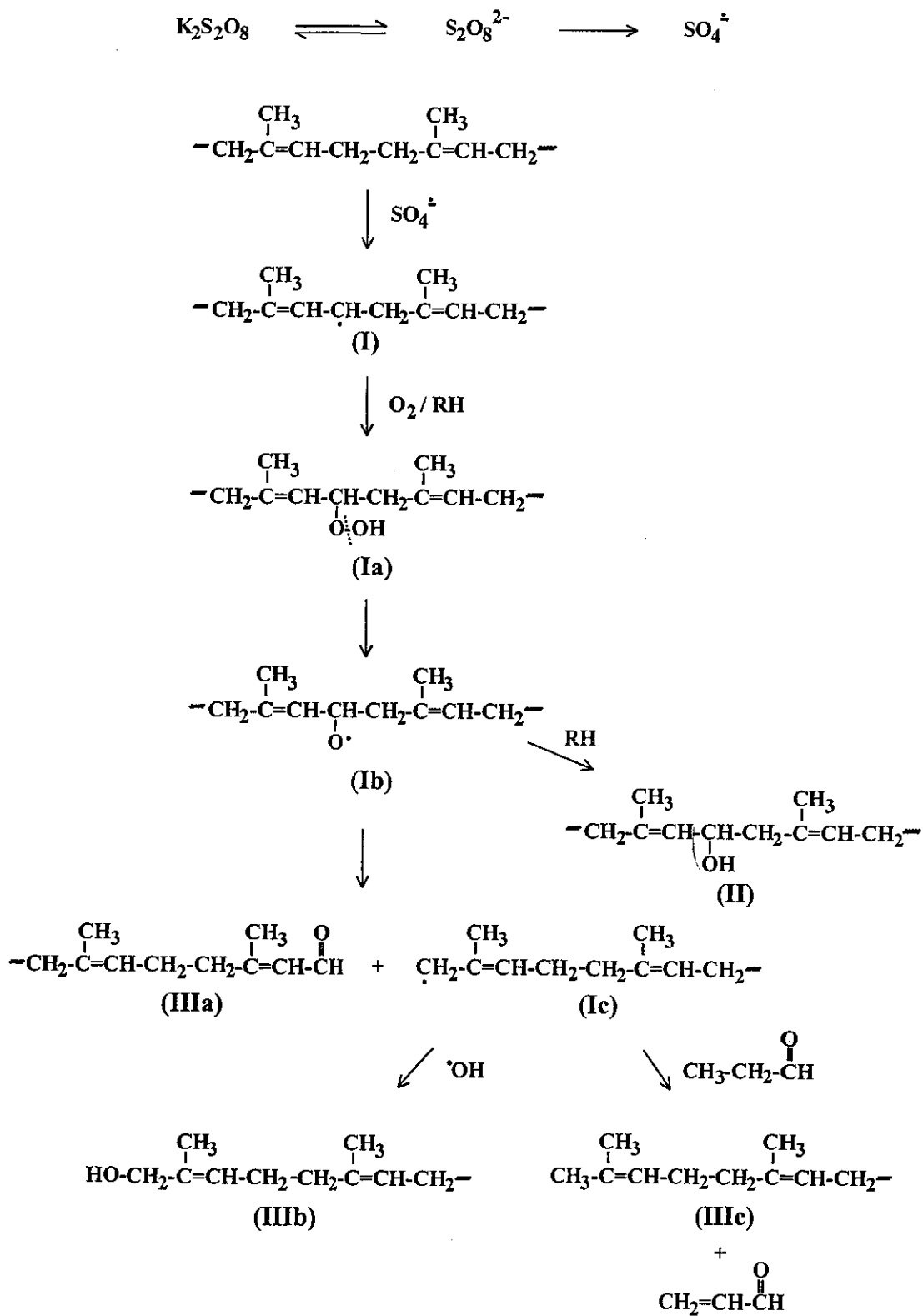
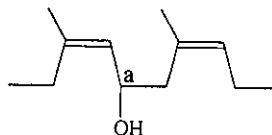
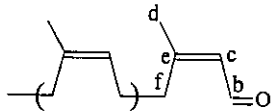
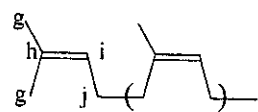
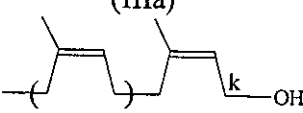
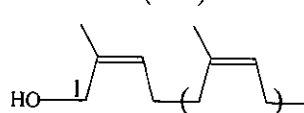


Figure 5.6 Proposed mechanism of degradation reaction of purified natural rubber

**Table 5.1** Calculated [115] and observed chemical shifts in  $^{13}\text{C}$  NMR spectrum of proposed chemical structure of the LPNR obtained

<b>Proposed chemical Structure of LPNR</b>	 <p style="text-align: center;">(II)</p>											
	 <p style="text-align: center;">(IIIa)</p>						 <p style="text-align: center;">(IIIc)</p>					
	 <p style="text-align: center;">(IIIb')</p>						 <p style="text-align: center;">(IIIb)</p>					
	Carbons	a	b	c	d	e	f	g	h	i	j	k
$\delta$ (ppm) (Calculated)	72.4	189.7	128.1	19.3	162.1	36.5	22.4	131.4	124.1	26.5	60.7	63.5
$\delta$ (ppm) (Observed)	72.7	188.1	127.6	19.2	162.4	35.0	22.2	131.6	124.4	26.5	60.7	63.2

main carbons of the repeating unit of the above proposed structures, the results found were successfully fitted with the signals observed from  $^{13}\text{C}$  NMR as shown in Table 5.1. However, the molecular structure IIIb and IIIb' can be both occurred depending on which side of the repeating unit is broken. The  $^{13}\text{C}$  NMR spectrum of LPNR shows clearly the signal of carbon bonded to the hydroxyl group which was observed in IR spectrum.

## 2.2 Parameters effecting the degradation reaction

Various parameters effecting the chain degradation of PNR <sup>was</sup> ~~have been~~ studied i.e. amount of  $\text{K}_2\text{S}_2\text{O}_8$  and propanal, reaction temperature, dry rubber content (DRC), the presence of tri-sodium phosphate ( $\text{Na}_3\text{PO}_4$ ) and oxygen.

### 2.2.1 Effect of concentration of $\text{K}_2\text{S}_2\text{O}_8$

As shown in the former section that radical initiator is the principal reagent to cause the chain scission as the macroradicals have been prior generated from the

Why?

reaction of persulfate radical ( $\text{SO}_4^{\cdot-}$ ) with the rubber chain. The degradation of PNR using various amounts of  $\text{K}_2\text{S}_2\text{O}_8$  (1, 2 and 3 phr) at  $70^\circ\text{C}$  was therefore investigated. Generally, higher amount of radical initiators may result in better degradation process as more sites for the formation of hydroperoxides can be produced. However, very high radical initiators may result in formation very high amount of radical polymeric species (I and Ic in Figure 5.6), which might lead to the increase of the possibility of chain recombination reaction. Plots of  $[\eta]$  at various reaction times of the degradation of PNR at different amount of  $\text{K}_2\text{S}_2\text{O}_8$  are shown in Figure 5.7. It seems likely that increasing the amount of  $\text{K}_2\text{S}_2\text{O}_8$  from 1 phr to 2 phr resulted in better lowering of the  $[\eta]$  of the PNR. However, increasing the amount of  $\text{K}_2\text{S}_2\text{O}_8$  to 3 phr did not accelerate further the degradation reaction. It was found that using 2 phr of  $\text{K}_2\text{S}_2\text{O}_8$  gave lowest  $[\eta]$  of 0.27 after 10 hours, while 1 phr and 3 phr gave 0.51 and 0.36, respectively, as shown in Table 5.2. The  $[\eta]$ s of the LPNR after 25 hours of the reactions, using 1 phr, 2 phr and 3 phr of the initiators were 0.19, 0.18 and 0.21, respectively. At longer reaction time, higher  $[\eta]$  was obtained in the case of 3 phr of  $\text{K}_2\text{S}_2\text{O}_8$  than the use of 2 phr. These results correlate well with the fact that very high amount of radical initiator will lead to very high amount of macroradicals (I) which will increase the potential of intermolecular chain recombination during the degradation process.

**Table 5.2** Results of intrinsic viscosity,  $[\eta]$  and kinetic rate constant ( $k$ ) obtained from degradation of NR and PNR latex at  $70^\circ\text{C}$

Samples	DRC (%)		$\text{K}_2\text{S}_2\text{O}_8$ (phr)			Propanal (phr)			$[\eta]$ after 10 hrs.	$[\eta]$ after 25 hrs.	$k \times 10^{-2}$ ( $\text{sec}^{-1}$ )
	NR	PNR									
LNR 1	5	-	1	-	-	-	32	-	0.70	0.41	3.57
L 1	-	5	1	-	-	-	32	-	0.51	0.19	7.34
L 2	-	5	-	2	-	-	32	-	0.32	0.18	8.10
L 3	-	5	-	-	3	-	32	-	0.36	0.21	7.01
L 4	-	5	1	-	-	16	-	-	0.79	0.36	4.07
L 1	-	5	1	-	-	-	32	-	0.51	0.19	7.34
L 5	-	5	1	-	-	-	-	64	0.52	0.20	7.11

### 2.2.2 Effect of concentration of propanal

OK ( It has generally been known that the macroradical formed on the polymeric chain in any circumstance is active and it will react with oxygen if there are some, leading to chain degradation or the extension of the molecular chain via intermolecular recombination. It was found in the case of degradation of PNR by using only  $K_2S_2O_8$  without the addition of propanal that some gel formation was detected at a few hours of reaction time.

( Addition of various amounts of propanal as 16, 32 and 64 phr for the system of 1 phr of  $K_2S_2O_8$  and 0.34 phr of  $Na_3PO_4$  <sup>was</sup> ~~were~~ investigated. The results of the degradation are shown in Figure 5.8 and Table 5.2. It was found that after 10 hours of reaction at  $70^\circ C$ , the  $[\eta]$ s of the degraded rubbers using 16, 32 and 64 phr of propanal were 0.79, 0.51 and 0.52, respectively. The results of 25 hours of reaction time are also presented in Table 5.2. These results indicated that the propanal plays some role on the oxidative degradation reaction. It can be postulated that during the degradation was proceeding, the propanal may act as a radical scavenger by transferring a proton to terminate the macroradical generated, particularly the molecular structure Ic as proposed in Figure 5.6, inhibiting the intermolecular recombination. However, the excess amount of the propanal (64 phr) may not be necessary as the self aldol-condensation of the propanal may be occurred rather than the reaction with the rubber molecule Ic.

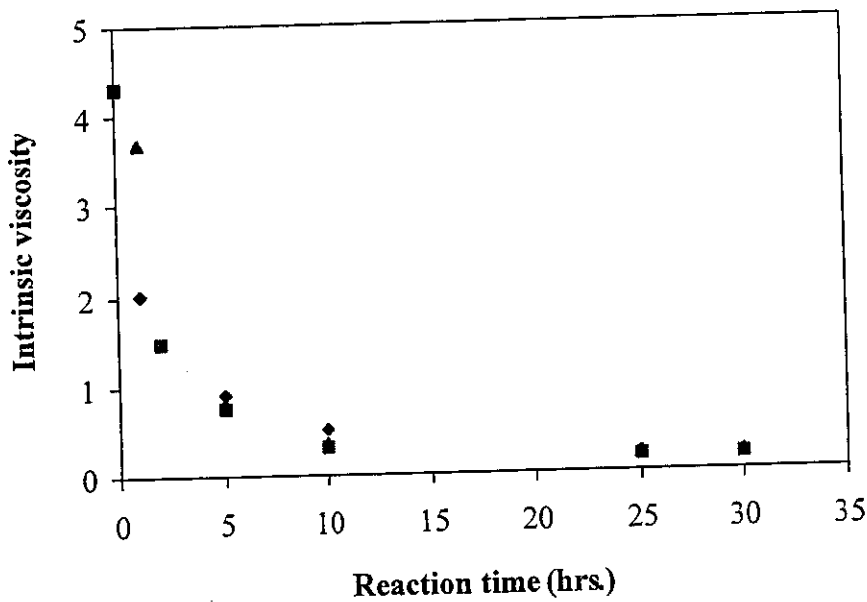


**Figure 5.7** Plots of intrinsic viscosity,  $[\eta]$ , of LPNR prepared from 5 % DRC of PNR latex, 32 phr of propanal and 0.34 phr of  $\text{Na}_3\text{PO}_4$  at  $70^\circ\text{C}$ ; ( $\blacklozenge$ ) 1 phr of  $\text{K}_2\text{S}_2\text{O}_8$  ( $\blacksquare$ ) 2 phr of  $\text{K}_2\text{S}_2\text{O}_8$  and ( $\blacktriangle$ ) 3 phr of  $\text{K}_2\text{S}_2\text{O}_8$

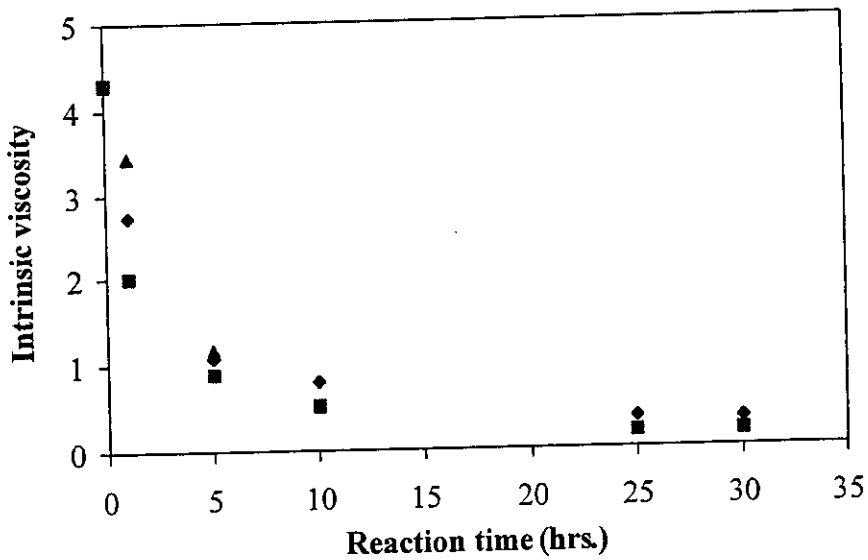


**Figure 5.8** Plots of intrinsic viscosity,  $[\eta]$ , of LPNR prepared from 5 % DRC of PNR latex, 1 phr of  $\text{K}_2\text{S}_2\text{O}_8$  and 0.34 phr of  $\text{Na}_3\text{PO}_4$  at  $70^\circ\text{C}$ ; ( $\blacklozenge$ ) 16 phr of propanal ( $\blacksquare$ ) 32 phr of propanal and ( $\blacktriangle$ ) 64 phr of propanal

### 2.2.3 Effect of Na<sub>3</sub>PO<sub>4</sub>

In our system, Na<sub>3</sub>PO<sub>4</sub> was used as a pH-controlling reagent. It was reported that at pH lower than 8.5, the decomposition of the K<sub>2</sub>S<sub>2</sub>O<sub>8</sub> was less efficient [18]. Various amounts of Na<sub>3</sub>PO<sub>4</sub> were used to make the degradation condition being pH of about 10. It was found that the use of 0.20, 0.25, 0.3, 0.34, and 0.38 phr of Na<sub>3</sub>PO<sub>4</sub> in the system of 5% DRC of PNR latex, 1 phr of K<sub>2</sub>S<sub>2</sub>O<sub>8</sub> and 32 phr of propanal gave the [η]s of the degraded rubbers after 10 hours of 0.67, 0.54, 0.53, 0.51 and 0.99 respectively. The [η]s of the LPNR after 25 hours of the reactions are shown in Table 5.3. It was found that the increased amount of Na<sub>3</sub>PO<sub>4</sub> (0.20, 0.25, 0.3 and 0.34 phr) resulted in better degradation reaction. However, very high amount of Na<sub>3</sub>PO<sub>4</sub> (0.38 phr) may interfere the decomposition of initiator or the degradation process as the [η] was only decreased to 0.99. Therefore, 0.34 phr of Na<sub>3</sub>PO<sub>4</sub> was found to be the most suitable for the PNR degradation in our system.

**Table 5.3** Results of intrinsic viscosity, [η] and kinetic rate constant (k) obtained from degradation of PNR latex using various amounts of Na<sub>3</sub>PO<sub>4</sub> at 70°C

Samples	DRC (%)	K <sub>2</sub> S <sub>2</sub> O <sub>8</sub> (phr)	Propanal (phr)	Na <sub>3</sub> PO <sub>4</sub> (phr)	[η] after 10 hrs.	[η] after 25 hrs.	k x 10 <sup>-2</sup> (sec <sup>-1</sup> )
L 6	5	1	32	0.20	0.67	-	3.39
L 7	5	1	32	0.25	0.54	0.35	4.99
L 8	5	1	32	0.30	0.53	0.32	5.01
L 1	5	1	32	0.34	0.51	0.19	7.34
L 9	5	1	32	0.38	0.99	0.38	3.85

### 2.2.4 Effect of reaction temperature

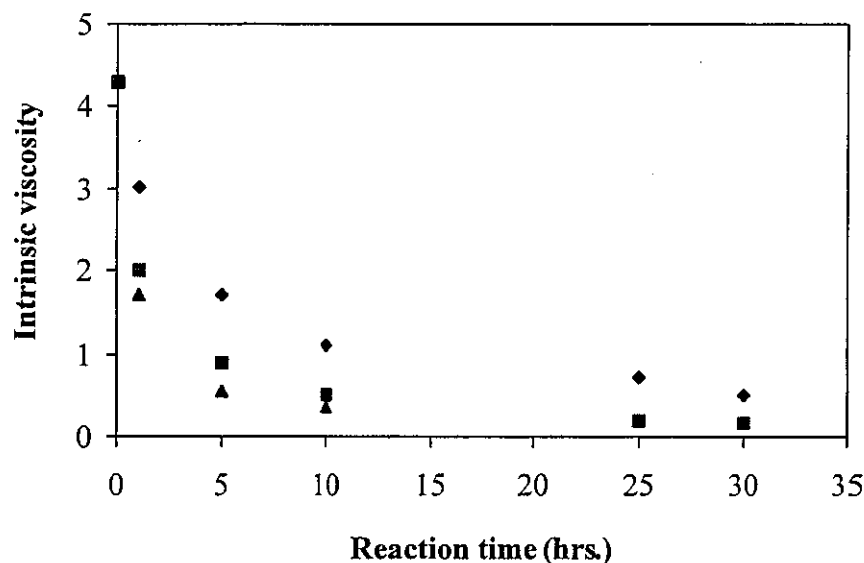
The reaction temperature has an influence on the efficiency of the decomposition of the radical initiator as well as the molecular motion in general. The decomposition temperature of K<sub>2</sub>S<sub>2</sub>O<sub>8</sub> is about 50-90 °C that can show the difference of decomposition rate [116]. The degradation of 5% DRC of PNR latex using 1 phr of K<sub>2</sub>S<sub>2</sub>O<sub>8</sub>, 32 phr of propanal and 0.34 phr of Na<sub>3</sub>PO<sub>4</sub> was compared at 60, 70 and 80°C. The plots of [η] at various reaction times at three different temperatures are shown in

Figure 5.9. It is not surprising to find that the rate of degradation is more important at higher temperature.

Table 5.4 also pointed out the  $[\eta]$  values during 10 and 25 hrs of reaction times at 60, 70 and 80°C. It was found that during the degradation of 10 hours, the  $[\eta]$ s were 1.11, 0.51 and 0.36 at 60, 70 and 80°C, respectively. It is seen that higher temperature resulted in better lowering of the  $[\eta]$ , i.e. lower molecular weight can be obtained. This may be due to the increased temperature resulted in increasing the rate of dissociation of the  $K_2S_2O_8$  as well as the molecular motion of the rubber chain which will increase the collision efficiency of the reagents and the rubber molecules. Consequently, the degradation rate will be increased. At longer reaction time (25 hours), lower  $[\eta]$ s can be further obtained. However, if the reaction carried out by using higher amount of initiator (2 phr), the  $[\eta]$ s values after 10 and 25 hours at 80°C were higher than the reaction at 70°C. At higher temperature, the rate of formation of the active radicals was increased as well as the rate of intermolecular recombination of the macroradicals. Higher amount of initiator i.e. higher amount of macroradical generated will increase the possibility of chain recombination at higher temperature. It is therefore necessary to balance the reaction temperature and the amount of the initiator i.e. the radical species, for the degradation of PNR.

**Table 5.4** Results of intrinsic viscosity,  $[\eta]$  and kinetic rate constant (k) obtained from degradation of PNR latex at different amount of  $K_2S_2O_8$  and various reaction temperatures

Samples	DRC (%)	$K_2S_2O_8$ (phr)	Propanal (phr)	Temperature (°C)			$[\eta]$ after 10 hrs.	$[\eta]$ after 25 hrs.	$k \times 10^{-2}$ (sec <sup>-1</sup> )
L 10	5	1	32	60	-	-	1.11	0.71	2.38
L 1	5	1	32	-	70	-	0.51	0.19	7.34
L 11	5	1	32	-	-	80	0.36	0.19	11.33
L 12	5	2	32	60	-	-	1.32	0.42	3.61
L 2	5	2	32	-	70	-	0.32	0.18	8.10
L 13	5	2	32	-	-	80	0.58	0.27	5.49



**Figure 5.9** Plots of intrinsic viscosity,  $[\eta]$ , of LPNR prepared from 5 % DRC of PNR latex, 1 phr of  $K_2S_2O_8$ , 32 phr of propanal and 0.34 phr of  $Na_3PO_4$  at various reaction time; (◆) 60°C (■) 70°C and (▲) 80°C

### 2.2.5 Effect of dry rubber content (DRC)

It was found in section 2.2.3 that increasing reaction temperature resulted in facilitating the molecular collision for the degradation reaction. Increasing concentration of the reaction medium should give similar consequence. The rubber concentration of 5, 10 and 15% DRC of PNR latex were therefore handled for the study of degradation reaction using 2 phr of  $K_2S_2O_8$ , 32 phr of propanal and 0.34 phr of  $Na_3PO_4$  at 70°C. The plots of  $[\eta]$  of the different conditions at various reaction times are presented in Figure 5.10. It was found that after 25 hours of reaction, the  $[\eta]$ s obtained from utilization of 5, 10 and 15% DRC of PNR latex were 0.18, 0.23 and 0.42 respectively (see Table 5.5). These results are not unexpected as increasing of dry rubber content may result in an increase the possibility of recombination of polymeric radical species, generated during the degradation. Therefore, better degradation can be achieved at lower concentration of rubber used.

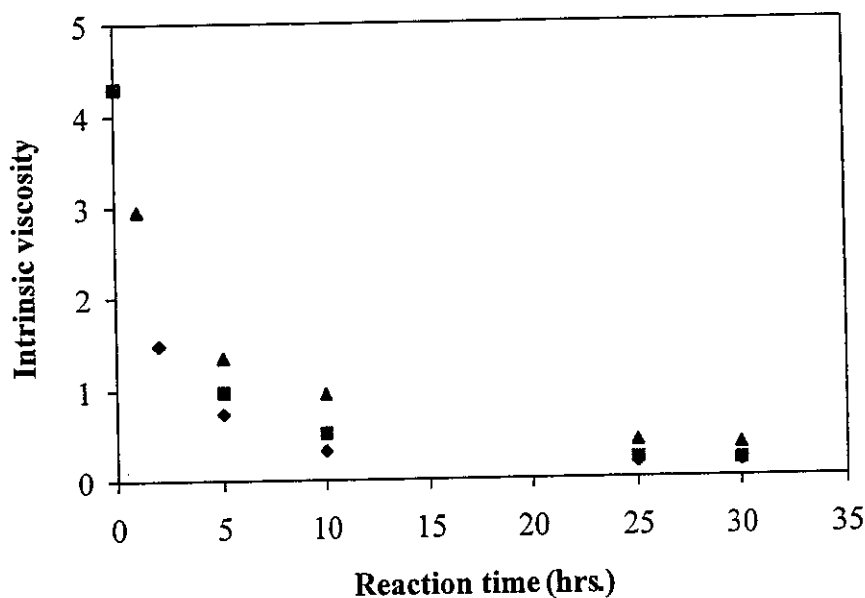


**Figure 5.10** Plots of intrinsic viscosity,  $[\eta]$ , of LPNR prepared from PNR latex, 32 phr of propanal and 0.34 phr of  $\text{Na}_3\text{PO}_4$  at  $70^\circ\text{C}$ ; (♦) 5 % DRC (■) 10 % DRC and (▲) 15 % DRC

**Table 5.5** Results of intrinsic viscosity,  $[\eta]$  and kinetic rate constant ( $k$ ) obtained from degradation of different rubber concentrations of PNR latex, carried at  $70^\circ\text{C}$

Samples	DRC (%)	$\text{K}_2\text{S}_2\text{O}_8$ (phr)	Propanal (phr)	$[\eta]$ after 10 hrs.	$[\eta]$ after 25 hrs.	$k \times 10^{-2}$ ( $\text{sec}^{-1}$ )
L 2	5	2	32	0.32	0.18	8.10
L 14	10	2	32	0.52	0.23	6.57
L 15	15	2	32	0.96	0.42	3.50

### 2.2.6 Effect of oxygen

Generally, polyisoprenic rubber is prone to be degraded by using chemical reagent or high temperature ( $>100^\circ\text{C}$ ) in the presence of oxygen. [50] The oxygen plays an important role by reacting with the radical generated by initiator or temperature, leading to chain scission. The amount of oxygen under promotion of chemical initiator may therefore have influence on the amounts of reactive radicals

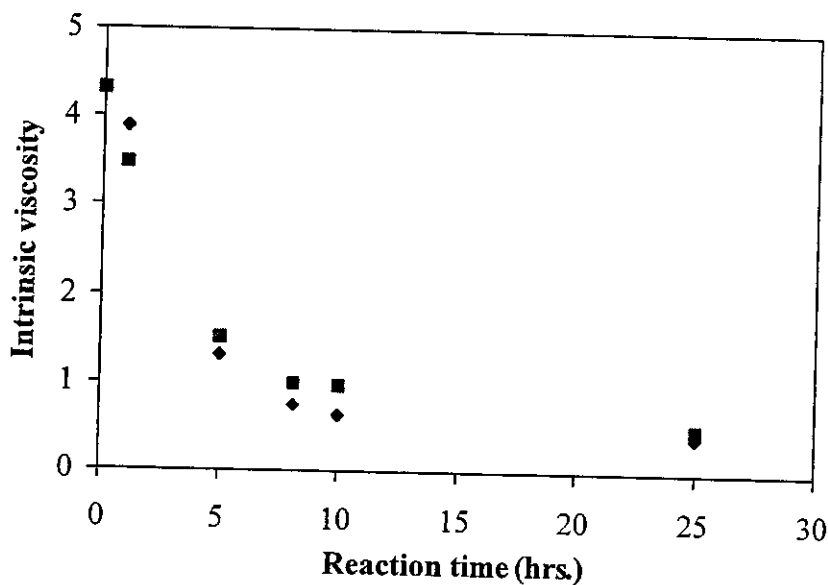


**Figure 5.11** Plots of intrinsic viscosity,  $[\eta]$ , of LPNR prepared from 5 % DRC of PNR latex, 1 phr of  $K_2S_2O_8$ , 32 phr of propanal and 0.25 phr of  $Na_3PO_4$  at  $70^\circ C$ ; (◆) non using  $O_2$  (■) using  $O_2$

**Table 5.6** Results of intrinsic viscosity,  $[\eta]$  and kinetic rate constant (k) obtained from degradation of PNR latex at  $70^\circ C$

Samples	DRC (%)		$K_2S_2O_8$ (phr)	Propanal (phr)	$O_2$	$[\eta]$ after 10 hrs.	$[\eta]$ after 25 hrs.
L 7	5	-	1	32	normal	0.54	0.35
L 16	5	-	1	32	excess	0.64	0.42
L 17	-	10	1	32	normal	0.63	0.42
L 18	-	10	1	32	excess	0.98	0.50

formed before leading to chain scission [50-54]. Addition of excess oxygen by pumping 10 mmHg air into the reaction of 5 and 10% DRC of PNR latex in the presence of 1 phr of  $K_2S_2O_8$  and 32 phr of propanal at  $70^\circ C$  were compared with the reaction at normal atmospheric oxygen and the results are shown in Table 5.6. It was found that after 10 hours of reaction, the  $[\eta]$  of 5% DRC using excess air was 0.64 while the reaction carried out at normal condition, the  $[\eta]$  was 0.54. The results of 5% DRC were shown in Figure 5.11. It can be seen that an excessive amount of  $O_2$  does

not help in enhancement of degradation reaction under the aid of  $K_2S_2O_8$ /propanal system.

### 2.2.7 Effect of surfactant

The main role of surfactant is to retain the polymer or rubber particles in colloidal forms. It stays normally at the surface of the rubber particles. Therefore, further chemical reaction of the rubber particles often depends also on the types of surfactant presented [70,74,78]. In our system, the deproteinization step may destroy natural surfactant of the rubber latex, therefore additional synthetic surfactant is needed. Sodium dodecyl sulphate (SDS), which is an anionic surfactant has been widely used to stabilize natural rubber latex. However, the anionic nature of SDS may effect on further modification. Nonionic surfactant such as nonyl phenol ethoxylated (Sinnopal NP 307) and poly(ethylene oxide fatty alcohol)hexadecylether (Teric) were used to compare with SDS for the degradation of 5% DRC of PNR latex, 2 phr of  $K_2S_2O_8$ , 32 phr of propanal and 0.34 phr of  $Na_3PO_4$  at  $70^\circ C$ . The results demonstrated that the use of SDS as anionic surfactant gave better degradation reaction than the Sinnopal NP 307 and Teric. The  $[\eta]$ s of the degraded rubbers by using SDS, Sinnopal NP 307 and Teric after 25 hours were 0.18, 0.42 and 0.38, respectively (as shown in Table 5.7 and Figure 5.12). This may be explained that the degradation reaction is effective in basic medium, the hydrophilic character ( $OSO_3^-$ ) of the decomposed initiator is more stable and active to the ionic surface than nonionic surface of the rubber particles. However, the advantage of nonionic surfactant is to improve the stability of colloidal particles in wider range of pH than anionic surfactant [40].

**Table 5.7** Results of intrinsic viscosity,  $[\eta]$  and kinetic rate constant (k) obtained from degradation of PNR latex at  $70^\circ C$

Samples	DRC (%)	$K_2S_2O_8$ (phr)	Propanal (phr)	Surfactant	$[\eta]$ after 10 hrs.	$[\eta]$ after 25 hrs.	$k \times 10^{-2}$ ( $sec^{-1}$ )
L 2	5	2	32	SDS	0.32	0.18	8.10
L 19	5	2	32	Sinnopal	0.88	0.42	2.36
L 20	5	2	32	Teric	0.83	0.38	2.77

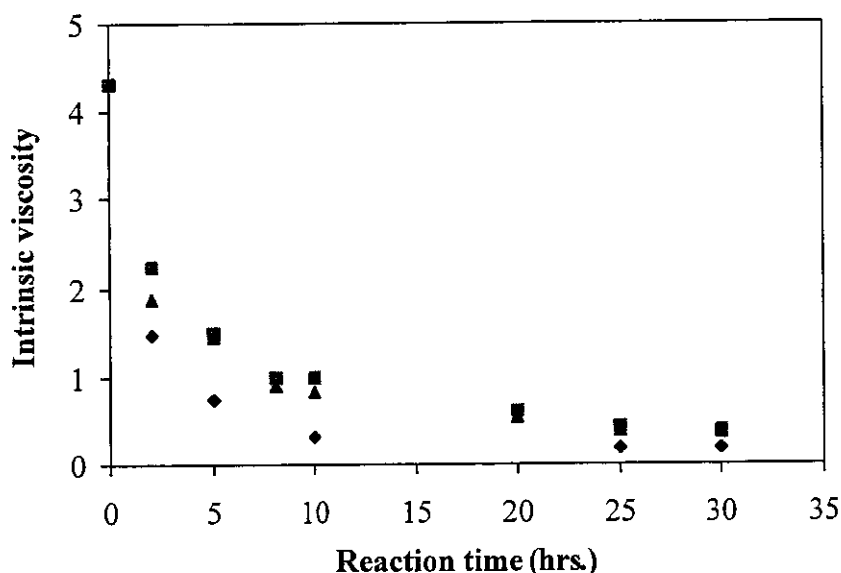


**Figure 5.12** Plots of intrinsic viscosity,  $[\eta]$ , of LPNR prepared from 5 % DRC of PNR, 1 phr of  $K_2S_2O_8$ , 32 phr of propanal and 0.34 hr of  $Na_3PO_4$  at  $70^\circ C$ ; (♦) SDS as surfactant (■) Sinnopal NP 307 as surfactant (▲) Teric as surfactant

### 2.3 Kinetics study of degradation reaction

If the chain degradation occurred in a polymer molecule and in random manner. The fraction of bonds broken ( $\alpha$ ) can be derived by eq. (5.1).

$$\alpha = \frac{1}{\overline{DP}_n(t)} - \frac{1}{\overline{DP}_n(0)} = kt \tag{5.1}$$

The kinetic rate constant ( $k$ ) of natural rubber degradation can be calculated where  $\overline{DP}_n(0)$  and  $\overline{DP}_n(t)$  are the number average degrees of polymerization at the beginning time ( $t = 0$ ) and time  $t$  respectively [117, 118]. To investigate the kinetic of degradation of the PNR, the relationship between  $[\eta]$  and viscosity average molecular weight ( $\overline{M}_v$ ) via Mark-Houwink equation in eq. (5.2) is involved. In our system, the  $K$  and  $a$  values were evaluated by using eight samples of different molecular weights of degraded PNR (LPNR) prepared. The  $[\eta]$  was achieved by viscometer and  $\overline{M}_v$  was measured by gel permeation chromatography (GPC). The results were shown in



*on was perform their calibration?*

*|| ?*

Appendix B (Table B-1). The K and a values of the Mark-Houwink equation were evaluated from the plot of the  $\ln [\eta]$  and  $\ln \bar{M}_v$  as shown in Figure 5.13. The  $K = 3.46 \times 10^{-5}$  and  $a = 0.863$  were obtained. These values are also similar to the work reported by Angulo-Sanchez [119]. These K and a values were further used for transformation of the  $[\eta]$  of other degraded rubber samples from various conditions into  $\bar{M}_v$ .

$$[\eta] = K \bar{M}_v^a \quad (5.2)$$

The  $\bar{M}_v$  can also be expressed as in eq. (5.3). It has been reported in the literature that the  $\bar{M}_v$  and weight average molecular weight ( $\bar{M}_w$ ) are related to some extent [120,121]. For  $a = 1$ ,  $\bar{M}_v$  is identical to  $\bar{M}_w$  (shown in eq. (5.4)).

$$\bar{M}_v = \left( \frac{\sum NiMi^{1+a}}{\sum NiMi} \right)^{1/a} \quad (5.3)$$

$$\text{if } a = 1, \quad \bar{M}_v = \frac{\sum NiMi^2}{\sum NiMi} = \bar{M}_w \quad (5.4)$$

It was found in our case that plots of  $\ln \bar{M}_v$  and  $\ln \bar{M}_w$  (measured by GPC) in Figure 5.14 shows a straight line. The relationship of  $\bar{M}_v$  and  $\bar{M}_w$  is therefore expressed as in eq. (5.5). This relationship was then used as a calibration curve for liquid rubber at various conditions studied.

$$\bar{M}_v = 1.77 \times 10^{-2} \bar{M}_w^{1.28} \quad (5.5)$$

The values of weight average degree of polymerization ( $\overline{DP}_w$ ) and number average degree of polymerization ( $\overline{DP}_n$ ) were estimated from the values of  $\bar{M}_w$  and  $\bar{M}_n$  determined by GPC (shown in Appendix). The plots of  $\overline{DP}_w$  versus  $\overline{DP}_n$  shows a straight line of the slope value of 6.27 (shown in eq. (5.6)).

$$\overline{DP}_w = 6.27 \overline{DP}_n \quad (5.6)$$

By using equation (5.2), (5.5) and (5.6), the values of  $[\eta]$  obtained from

How is it determined?

A non-de  
maneu' play  
stature

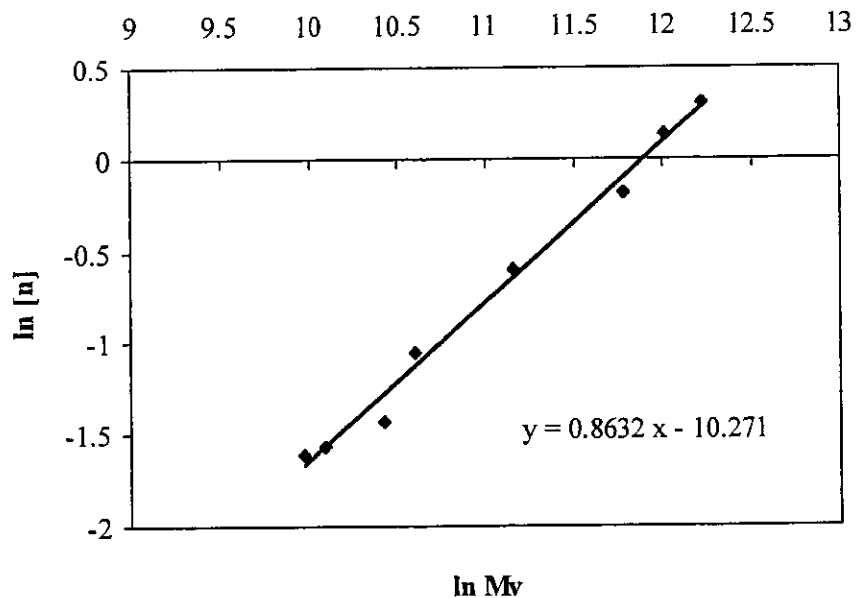


**Figure 5.13** Relationship between  $\ln[\eta]$  and  $\ln \bar{M}_v$  of LPNR

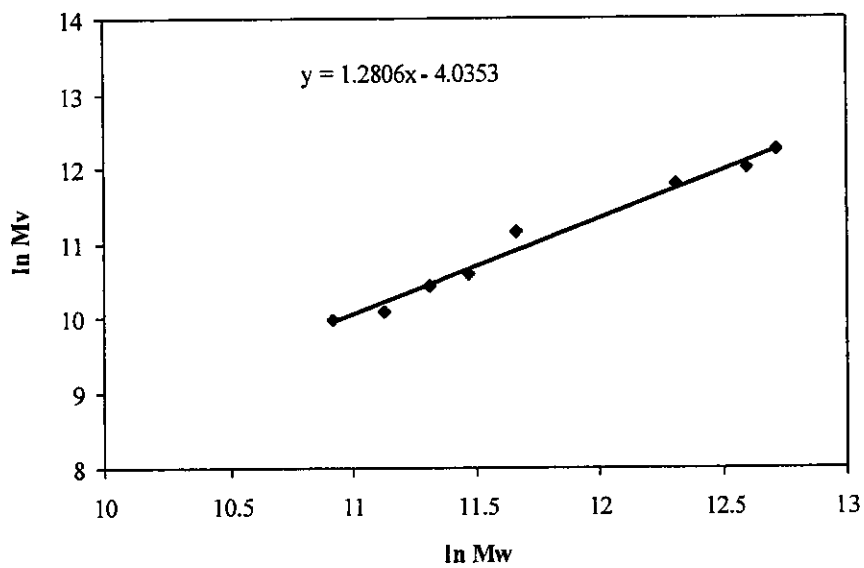


**Figure 5.14** Relationship between  $\ln \bar{M}_v$  and  $\ln \bar{M}_w$  of LPNR

various conditions can be transformed into the values of  $\overline{DP}_n$ . Therefore, the kinetic rate constant ( $k$ ) of the degradation reaction can be evaluated from the slope of the plot of  $\frac{1}{\overline{DP}_{n(t)}} - \frac{1}{\overline{DP}_{n(0)}}$  at various reaction times. Figure 5.15 showed the plots of

$\frac{1}{\overline{DP}_{n(t)}} - \frac{1}{\overline{DP}_{n(0)}}$  versus time of the degradation of PNR and NR, using 5% DRC of

latex, 1 phr of  $K_2S_2O_8$ , 32 phr of propanal and 0.34 phr of  $Na_3PO_4$  at  $70^\circ C$ . The  $k$  values of the degradation of purified and unpurified natural rubber were found to be  $7.34 \times 10^{-2}$  and  $3.57 \times 10^{-2} \text{ sec}^{-1}$ , respectively. These results showed that in the same chemical degradation method, the PNR presented higher rate constant than the NR. It can be concluded that the non-rubber presented in NR can retard the chemical degradation reaction using  $K_2S_2O_8$ /propanal system.

The  $K_2S_2O_8$  is the starting reagent that provides active sites on the rubber chain. Increasing amount of  $K_2S_2O_8$  from 1 to 2 phr with 5% DRC of PNR latex, 32 phr of propanal at  $70^\circ C$ , the  $k$  values of the chain degradation were increased and found to be  $7.34 \times 10^{-2}$  and  $8.10 \times 10^{-2} \text{ sec}^{-1}$ , respectively. However, the excess amount of active sites may increase the competition between chain recombination and chain degradation, it was found that the use of 3 phr of  $K_2S_2O_8$ , the  $k$  value of chain degradation was reduced to  $7.01 \times 10^{-2} \text{ sec}^{-1}$  as shown in Table 5.2.

The propanal is another reagent found in section 2.2.2 that has an influence on the degradation reaction. Increasing the amount of propanal is helping in better inhibition of recombination of macroradicals. The use of 16 and 32 phr of propanal with 5% DRC of PNR latex, 1 phr of  $K_2S_2O_8$  at  $70^\circ C$  led to the  $k$  values of  $4.07 \times 10^{-2}$  and  $7.34 \times 10^{-2} \text{ sec}^{-1}$ , respectively. However, the excess amount of propanal is not necessary to the degradation reaction. The  $k$  value of the degradation by using 64 phr of propanal was found to be  $7.11 \times 10^{-2} \text{ sec}^{-1}$  that is a similar value as in the case of using of 32 phr of propanal (Figure 5.16).

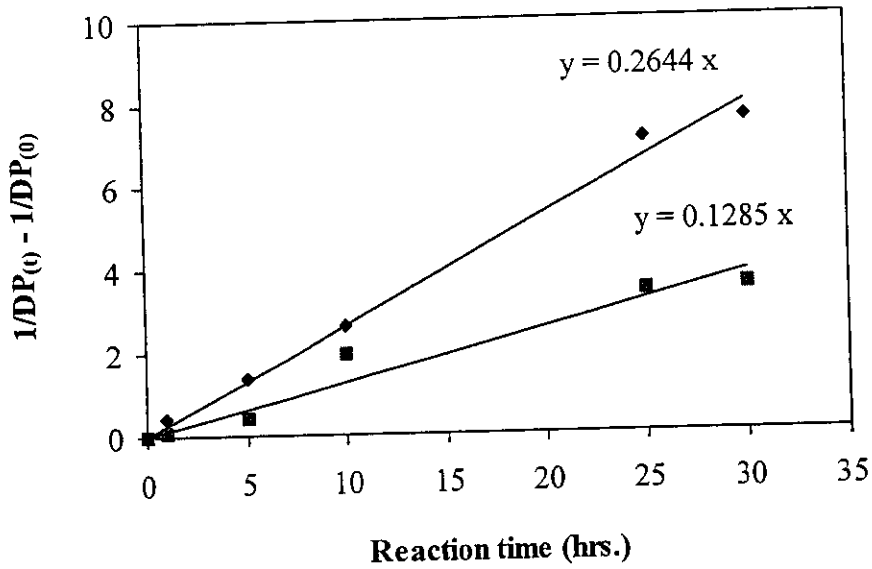


**Figure 5.15** Plots of  $1/DP(t) - 1/DP(0)$  vs. time of LPNR prepared from 1 phr of  $K_2S_2O_8$ , 32 phr of propanal and 0.34 phr of  $Na_3PO_4$  at various reaction times; ( $\diamond$ ) 5 % DRC of PNR latex, ( $\blacksquare$ ) 5 %DRC of NR latex

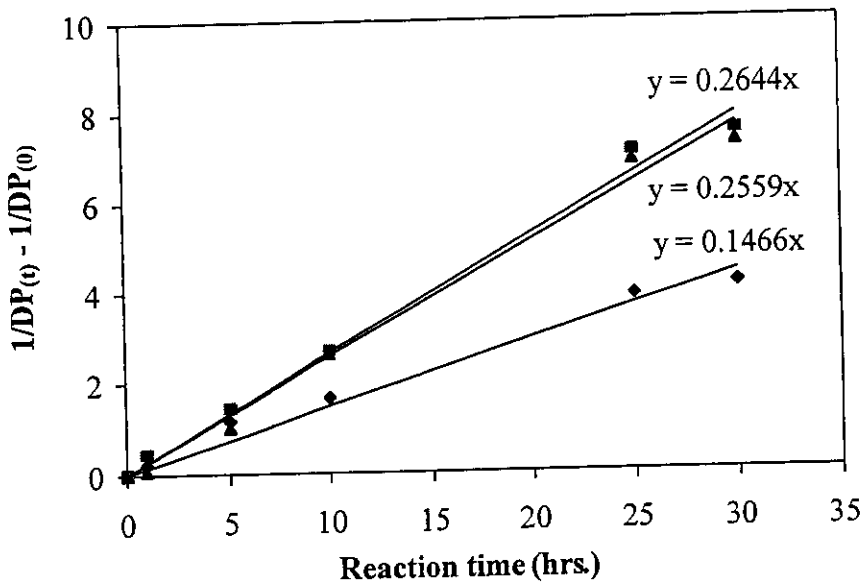


**Figure 5.16** Plots of  $1/DP(t) - 1/DP(0)$  vs. time of LPNR prepared from 5 % DRC of PNR latex, 2 phr of  $K_2S_2O_8$ , and 0.34 phr of  $Na_3PO_4$  at  $70^\circ C$  various amount of propanal; ( $\diamond$ ) 16 phr, ( $\blacksquare$ ) 32 phr and ( $\blacktriangle$ ) 64 phr

In the case of effect of dry rubber content on the degradation reaction, the kinetic study also showed that at lower concentration of the rubber, the  $k$  value is greater than at higher rubber concentration. The  $k$  values of 5, 10 and 15% DRC of PNR latex were found to be  $8.10 \times 10^{-2}$ ,  $6.57 \times 10^{-2}$  and  $3.50 \times 10^{-2} \text{ sec}^{-1}$ , respectively.

The kinetic rate constants of the degradation of the PNR using different types of surfactant can be also used to confirm the influence of the surfactant on the degradation reaction. For 5% DRC of PNR latex combined with 2 phr of  $\text{K}_2\text{S}_2\text{O}_8$  and 32 phr of propanal at  $70^\circ\text{C}$  stabilized with anionic surfactant, SDS the  $k$  value was found higher than the use of nonionic surfactants (Sinnopal NP 307 and Teric). It was found to be  $8.10 \times 10^{-2}$ ,  $2.36 \times 10^{-2}$  and  $2.77 \times 10^{-2} \text{ sec}^{-1}$  for SDS, Sinnopal NP 307 and Teric respectively. It can be concluded that the negative charge of SDS may help the degradation reaction in the system of  $\text{K}_2\text{S}_2\text{O}_8$  and propanal than the Sinnopal NP 307 and Teric which have not a negative charge.

To evaluate the activation energy of the degradation reaction, the kinetics of degradation of PNR at 60, 70 and  $80^\circ\text{C}$ , using 5% DRC of PNR latex, 1 phr of  $\text{K}_2\text{S}_2\text{O}_8$ , 32 phr of propanal, 0.34 phr of  $\text{Na}_3\text{PO}_4$ , were investigated. The  $k$  values of the reactions at 60, 70 and  $80^\circ\text{C}$  were found to be  $2.38 \times 10^{-2}$ ,  $7.34 \times 10^{-2}$  and  $11.33 \times 10^{-2} \text{ sec}^{-1}$ , respectively (as shown in Figure 5.17). The highest rate constant is found at  $80^\circ\text{C}$ . The activation energy for cleavage of carbon-carbon single bond of rubber molecule can be calculated from Arrhenius equation in eq. (5.7).

$$k = Ae^{-E_a/RT} \quad (5.7)$$

The plot of  $\ln k$  versus reciprocal of different temperatures gave the activation energy value of  $76.56 \text{ kJ mol}^{-1}$  (Figure 5.18). This value is actually less than the activation energy ( $108.0 \text{ kJ mol}^{-1}$ ) needed to break down the isoprene unit of natural rubber carried in cyclohexane at  $60\text{-}100^\circ\text{C}$  [111]. This result showed that the chemical degradation of PNR in this work is much faster than the thermal degradation of natural rubber.

*polyisoprene*

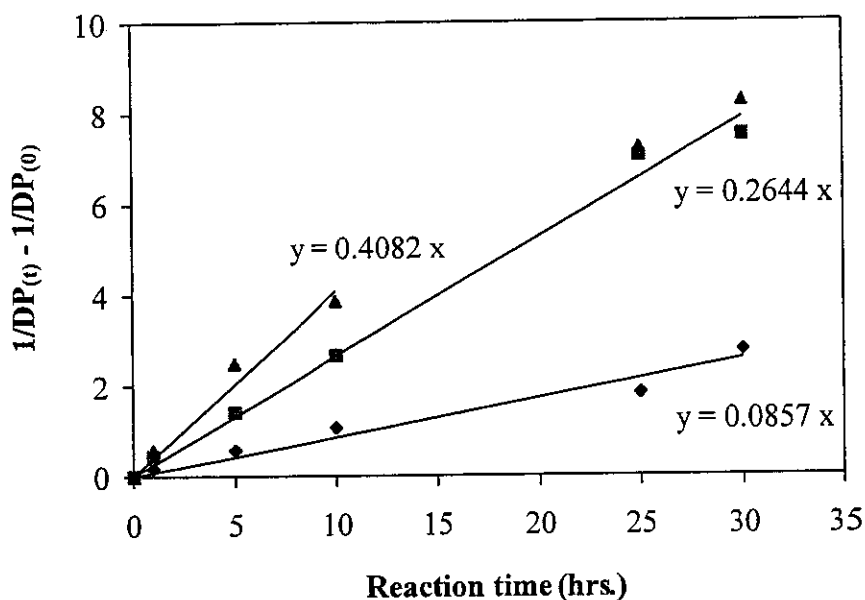


**Figure 5.17** Plots of  $1/DP(t) - 1/DP(0)$  vs. time of LPNR prepared from 5 % DRC of PNR latex, 1 phr of  $K_2S_2O_8$ , 32 phr of propanal and 0.34 phr of  $Na_3PO_4$  at various reaction temperature; (♦) 60°C, (■) 70°C and (▲) 80°C

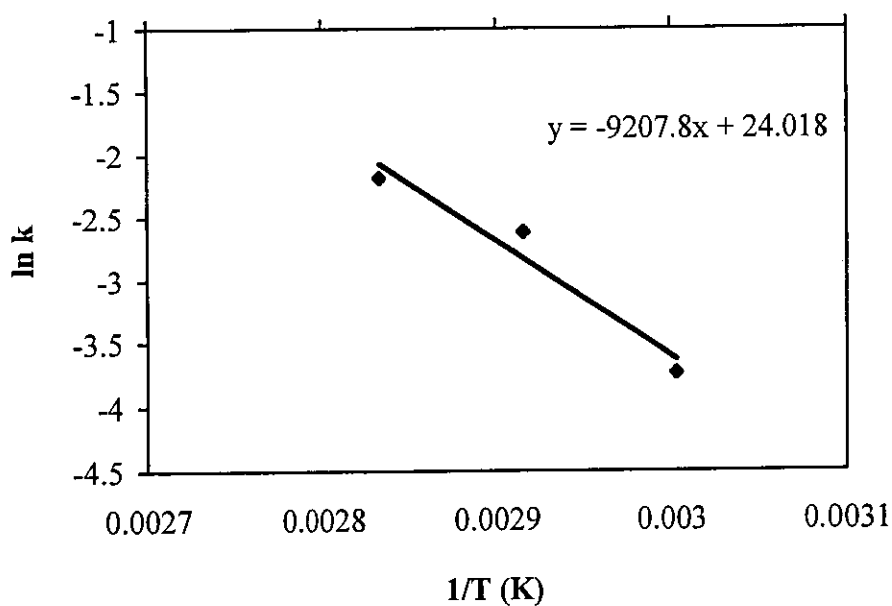


**Figure 5.18** Plots of  $\ln k$  and  $1/T$  (K) from degradation of PNR latex

### 3. Epoxidation of Liquid Purified Natural Rubber

Epoxidation of liquid purified natural rubber (LPNR) was carried out <sup>now</sup> by 2 methods, in organic phase using m-chloroperbenzoic acid and in latex phase using in-situ performic acid generated from hydrogen peroxide and formic acid.

#### 3.1 Epoxidation by using m-chloroperbenzoic acid

The epoxidation of LPNR by using m-chloroperbenzoic acid (MCPBA) was carried out at low temperature (0°C) in toluene. The desired amount of epoxide content depended mainly on the amount of MCPBA used. The acid by-product is eliminated by twice precipitation of the resulting product in methanol. The infrared spectrum of the epoxidized rubber obtained is shown in Figure 5.19. The appearance of the characteristic signals at 1250 and 872 cm<sup>-1</sup>, assigned to the epoxide whole ring stretching and the epoxide half ring stretching, respectively confirms the occurrence of epoxidation reaction. The decrease of absorption band at 837 cm<sup>-1</sup> (CH adjacent to C=C) compared to the signal at 1375 cm<sup>-1</sup> (CH<sub>3</sub> bending) of the isoprene repeating unit was also observed. These results are in accordance with several reports [12,65,71,73,112].

<sup>13</sup>C NMR spectrum in Figure 5.20 of the partially epoxidized rubber showed the presence of characteristic signals of olefinic quarternary carbon and methine carbon at 134-135 ppm and 124-125 ppm. The signals of oxirane tertiary carbon and secondary carbon were appeared at 60.81 ppm and 64.50 ppm, respectively. This observation is similar to the work reported by Bradbury JH and Perera CS [64]. The analysis by <sup>1</sup>H NMR of the partially epoxidized product in Figure 5.21 showed the presence of the characteristic signals corresponding to methine proton of isoprene unit and oxirane unit at 5.12 ppm and 2.69 ppm, respectively. The methyl proton adjacent to the C=C was positioned at 1.67 ppm while the methyl proton adjacent to the oxirane ring was appeared at 1.26 ppm. The signals at 2.09 and 2.16 ppm were the methylene proton of the isoprene unit and epoxidized unit, respectively. There are not other signals indicating chemical structure of secondary reactions such as epoxide ring opening at 3.40 ppm (proton adjacent to hydroxyl group) and 3.90 ppm (proton at furan ring) as reported in the literature of the epoxidation with peracetic acid [72]. The

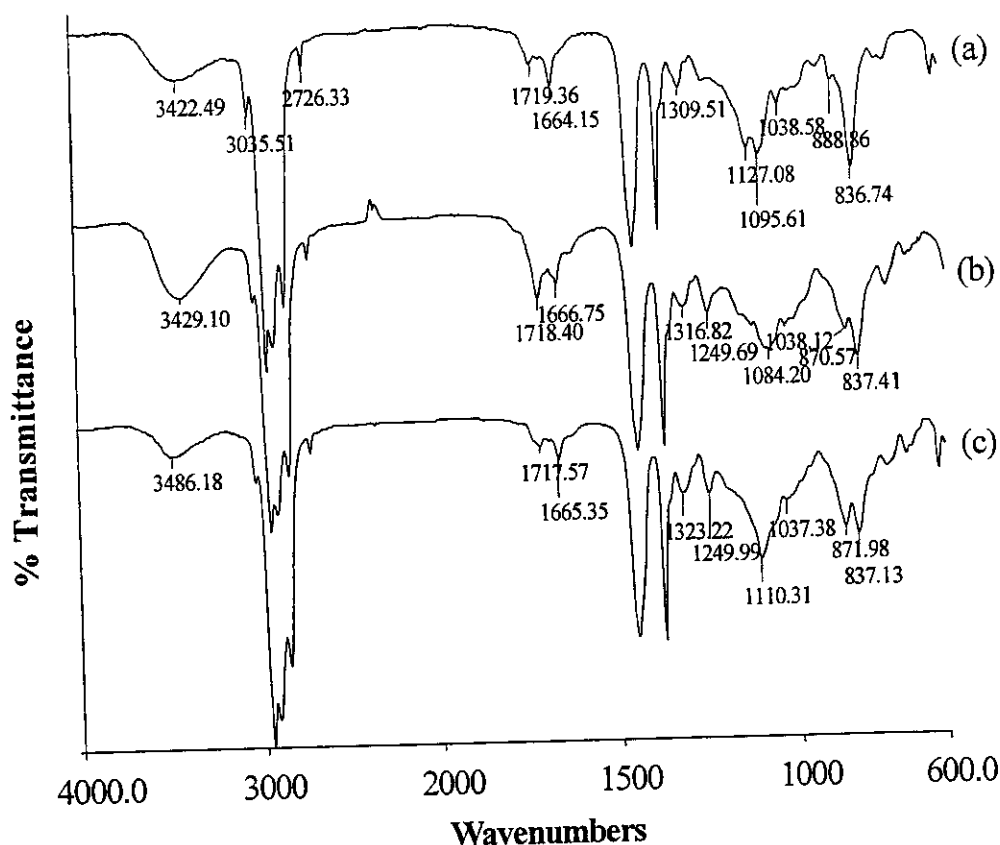


**Figure 5.19** Infrared spectra of (a) Liquid purified natural rubber, (b) Epoxidized liquid purified natural rubber (using LPNR reacting with H<sub>2</sub>O<sub>2</sub>/HCOOH) and (c) Epoxidized liquid purified natural rubber (using LPNR reacting with m-chloroperbenzoic acid)

epoxidation level can be successfully calculated from the integration area of the signal of proton adjacent to the C=C and the proton adjacent to the oxirane ring, as shown in chapter 4 (section 7.4)

By this procedure, desired amount of epoxide group on the rubber chain can be conveniently achieved. However, this method is carried out in organic solvent and the MCPBA has relatively high cost.



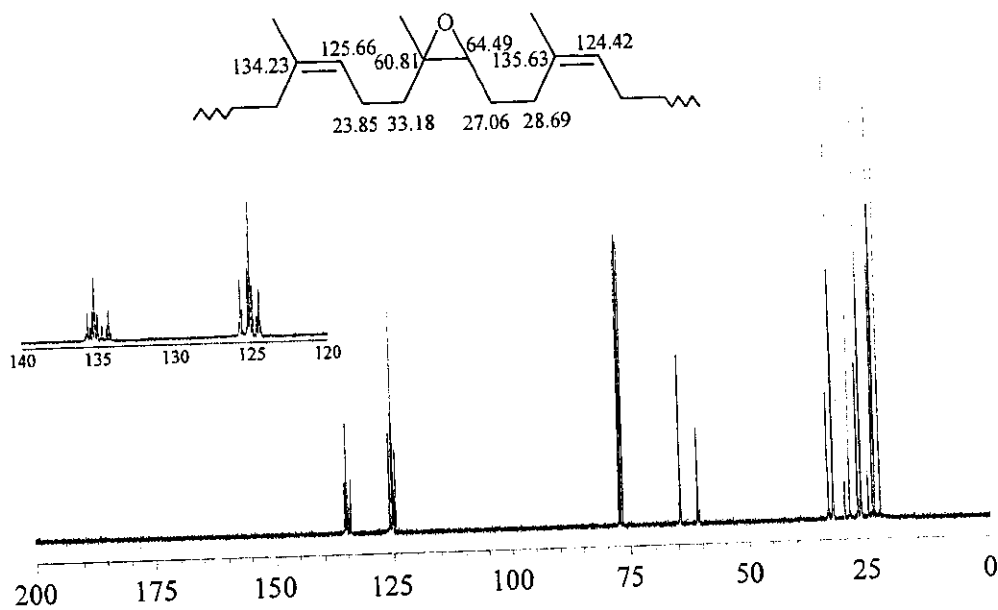


Figure 5.20  $^{13}\text{C}$  NMR spectrum of partially epoxidized liquid purified natural rubber (ELPNR) prepared by using m-chloroperbenzoic acid

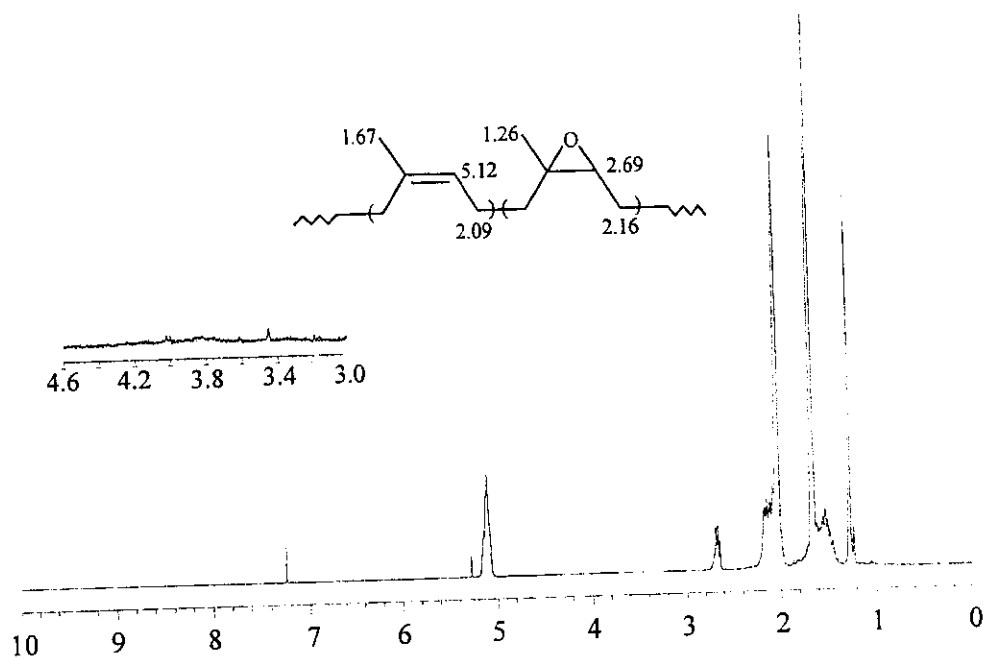


Figure 5.21  $^1\text{H}$  NMR spectrum of partially epoxidized liquid purified natural rubber (ELPNR) prepared by using m-chloroperbenzoic acid

### 3.2 Epoxidation by using in-situ performic acid

The preparation of LPNR in section 2 was carried out in latex phase. Therefore, epoxidising agents such as peracetic and performic acids could be used. As the epoxidation was going to be carried out in the environment of acidity, surfactants such as SDS (anionic surfactant), nonionic surfactants (Sinnopal NP 307 and Teric) have to be added to keep the stability of the NR latex intact. In this study, the epoxidation of the LPNR latex was performed by addition of hydrogen peroxide (H<sub>2</sub>O<sub>2</sub>) and formic acid (HCOOH). The schematic diagram of the epoxidation is shown in Figure 5.22. The pH of the reaction medium was found to be about 2.3-2.7. The epoxidation was successfully <sup>performed</sup> ~~occurred~~ as it <sup>was</sup> ~~has been~~ reported <sup>in the literature</sup> that the formation of in-situ <sup>used</sup> performic acid for epoxidation can be <sup>produce of</sup> ~~successfully occurred~~ in the acidic medium (pH=2.2-3) [55,74,79]. The epoxidized <sup>rubber</sup> ~~product~~ obtained was precipitated twice in methanol in order to remove the contamination of the formic acid formed. It was reported in <sup>previous papers</sup> ~~many literatures~~ that epoxidation of NR in latex phase was often accompanied by secondary reactions and several parameters can have influence on the epoxidation level differently from the epoxidation in organic phase.

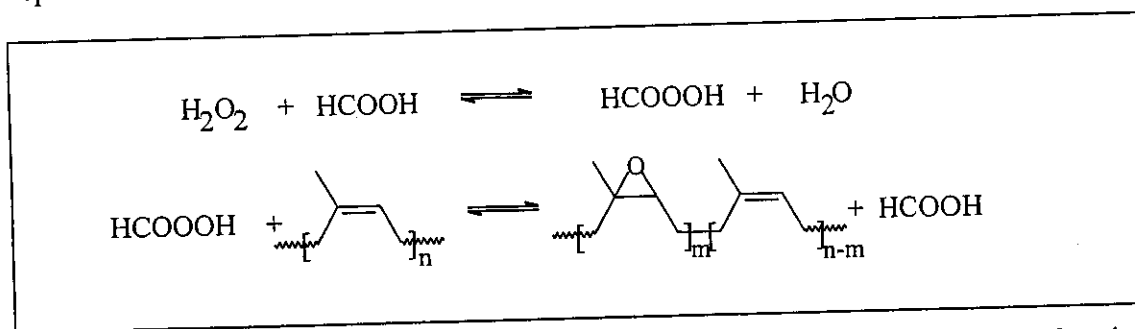


Figure 5.22 Epoxidation reaction of natural rubber by using *in-situ* performic acid

#### 3.2.1 Chemical structure of epoxidized product

The IR spectra of the LPNR, the epoxidized rubber obtained by using 0.3 mole/mole of H<sub>2</sub>O<sub>2</sub> /isoprene unit and 0.15 mole/mole of HCOOH/isoprene unit, and the epoxidized product obtained by using MCPBA were compared in Figure 5.19. The appearance of the absorption bands corresponding to epoxidized unit at 1250 cm<sup>-1</sup> (epoxide whole ring stretching) and 870 cm<sup>-1</sup> (epoxide half ring stretching) of the epoxidized rubber obtained from performic acid are similar to the product obtained by

using MCPBA. It is clearly seen in Figure 5.19 that the epoxidized product obtained from performic acid contained two strong signals at 1718  $\text{cm}^{-1}$  assigned to C=O stretching and 3429  $\text{cm}^{-1}$  assigned to OH stretching. These peaks are coincided to secondary reactions as reported in many literatures i.e. epoxide ring opening by hydrolysis or by addition of the formic acid residual to the epoxide ring [65,71,73].

<sup>1</sup>H NMR spectrum of the epoxidized rubber in this case showed several characteristic signals at 5.12 ppm (olefinic methine proton), 2.69 ppm (oxirane methine proton), 1.67 ppm (olefinic methyl proton), 1.26 ppm (oxirane methyl proton), 2.09 ppm (methylene proton of isoprene unit) and 2.16 ppm (methylene proton of oxirane unit) respectively. There are also the extra signals at 3.40, 3.90 and 8.00 ppm which might belong to secondary reactions shown in Figure 5.23. Proposed chemical structures of the epoxidized unit and secondary products are shown in Figure 5.24.

The epoxidation was carried out in aqueous phase, the epoxide ring can be possibly hydrolysed into vic-diol structure. The formic acid residual can also cause epoxide ring opening reaction, leading to formyl ester adduct as well as the formation of hydrofuran (THF) and intermolecular ether formation. The signal at 3.40 ppm can be attributed to the signal of proton adjacent to hydroxyl group of hydrolysed epoxide 1,2 diols unit, ether linkage structure and formyl adduct. The proton at furan ring can be responsible for the signal of proton at 3.90 ppm. The signal of proton adjacent to carbonyl group of formyl adduct is positioned at 8 ppm. In the case of using non-ionic surfactant, there is an appearance of another signal at 9.4 ppm. This can be assumed to be the signal of proton of  $\alpha,\beta$  unsaturated aldehyde structure.

The determination of epoxidation level is generally calculated by using the signal of proton adjacent to C=C at 5.14 ppm and the signal of proton adjacent to the epoxide ring as in the former case (section 3.1) by omitting the presence of secondary structures as reported by many authors. However, in this study, the percentage of the epoxidized unit and its secondary reactions were also compared in various conditions of the reaction.

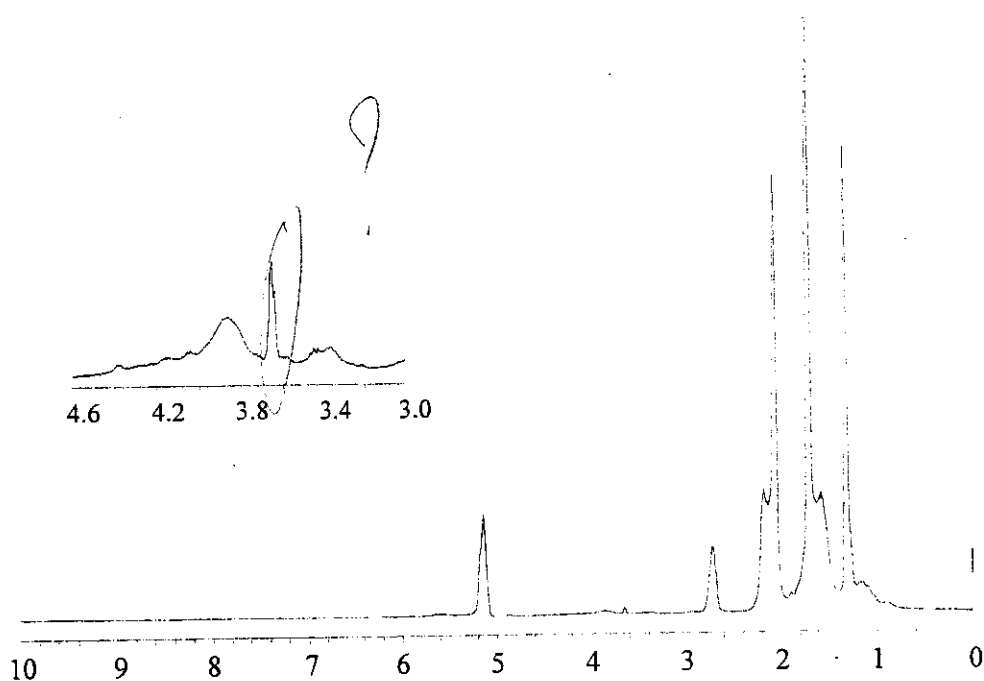


**Figure 5.23**  $^1\text{H}$  NMR spectrum of partially epoxidized liquid purified natural rubber (ELPNR) prepared by using LPNR(Sinnopal) and 1.2 mole/mole of  $\text{H}_2\text{O}_2$  per isoprene unit and 0.25 mole/mole of  $\text{HCOOH}$  per isoprene unit

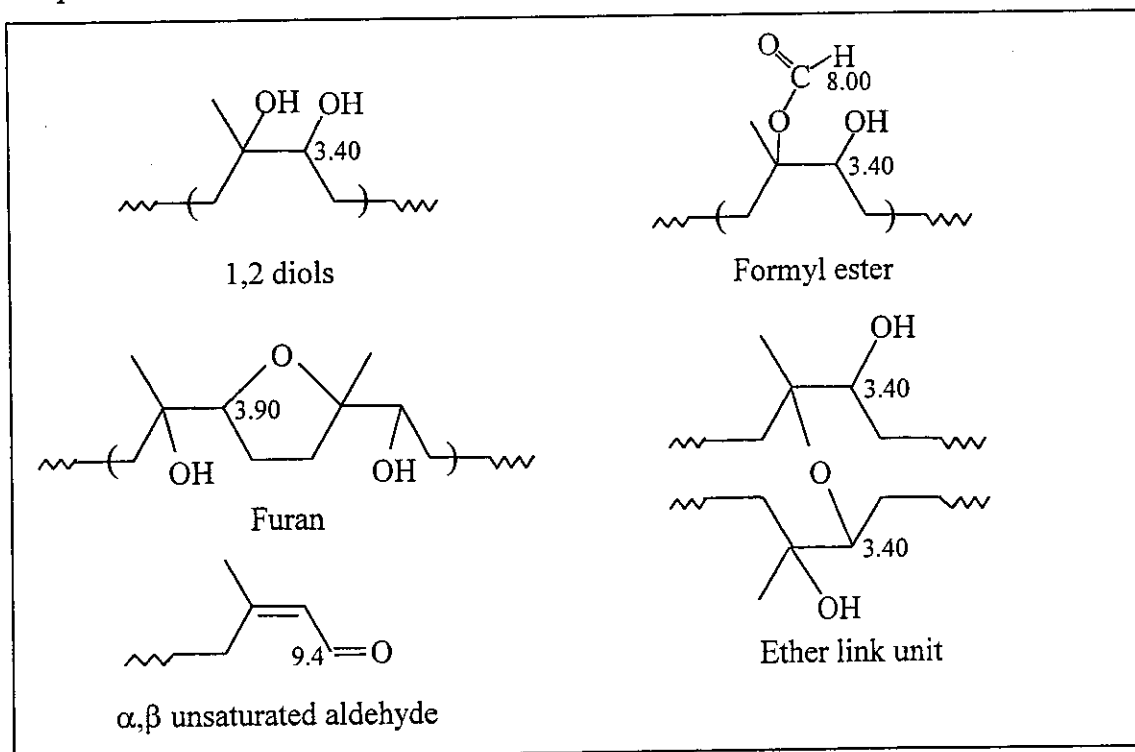


**Figure 5.24**  $^1\text{H}$  NMR positions of proposed secondary structures obtained from epoxidation reaction of LPNR latex by using *in-situ* performic acid

### 3.2.2 Parameters effecting epoxidation reaction

Various parameters <sup>a</sup> effecting the preparation of epoxidized liquid purified rubber in latex phase such as types of surfactant, amount of H<sub>2</sub>O<sub>2</sub> and HCOOH were investigated.

#### 3.2.2.1 Effect of surfactant

Generally, epoxidation reaction is preferably occurred in acidic medium as it involves reagents generating acidic molecules [74,79]. The performance of epoxidation of rubber hydrocarbon in colloidal (latex) medium may depend on surfactant surrounding the rubber particles. Most of the works dealing the epoxidation of natural rubber latex was performed with the latex stabilized with non-ionic surfactant [73,74,77,79,80]. Very few works <sup>was</sup> had done in ionic surfactants. Gan LH and Ng SC studied the epoxidation reaction of natural rubber latex in cationic surfactant [70]. The results showed that positive charge of cationic micelles help reducing the ring opened products by inhibiting the reaction between regenerated formic acid and the oxirane unit. In <sup>the present</sup> ~~our~~ reaction, the use of non-ionic surfactants (Sinnopal NP 307 and Teric), an anionic surfactant (SDS) were investigated and compared in terms of epoxidation level and the occurrence of secondary reactions.

The progress of epoxidation at various reaction times was <sup>followed</sup> ~~detected~~ by <sup>1</sup>H NMR. Two important signals at 2.7 and 5.1 ppm, corresponding to the signal of the proton adjacent to epoxide ring and C=C respectively were used to determine the epoxidation level by omitting the occurrence of secondary reaction. <sup>3</sup> The % <sup>epoxidized unit</sup> epoxide content equals to  $(A_{2.7}/(A_{2.7}+A_{5.1})) \times 100$ . The intrinsic viscosities of the epoxidized products at various reaction times were also measured. Figure 5.25 showed <sup>5</sup> the results of epoxide contents and the intrinsic viscosities at various reaction times of 10% DRC of LPNR latex stabilized with 1.5 phr of different surfactants (Sinnopal NP 307, Teric and SDS), using 0.3 mole/mole (0.44 mol.l<sup>-1</sup>) of H<sub>2</sub>O<sub>2</sub> per isoprene unit and 0.15 mole/mole (0.22 mol.l<sup>-1</sup>) of HCOOH per isoprene unit, carried out at 50°C.

It can be seen that both non-ionic surfactants showed the same trend of epoxide content and the change of intrinsic viscosity values. The epoxide content increased rapidly at the beginning of the reaction time. After 10 hours up to 34 hours,

slight increase of epoxidation level was observed. However, when the reaction was left to be continued until 48 hours, the epoxidation level became decreasing. The intrinsic viscosities in both cases were decreased at longer reaction time. This may be due to the increase of epoxide unit on the molecular chain resulted in the change of hydrodynamic volume of ELPNR comparing to the starting LPNR in toluene solution or the chain degradation may be also occurred. The later assumption was supported by the presence of signal of proton at 9.4 ppm in  $^1\text{H}$  NMR that may be assigned to proton of  $\alpha,\beta$  unsaturated aldehyde. The aldehyde structure may come from the chain degradation occurring by the presence of high amount of hydrogen peroxide added for the epoxidation.

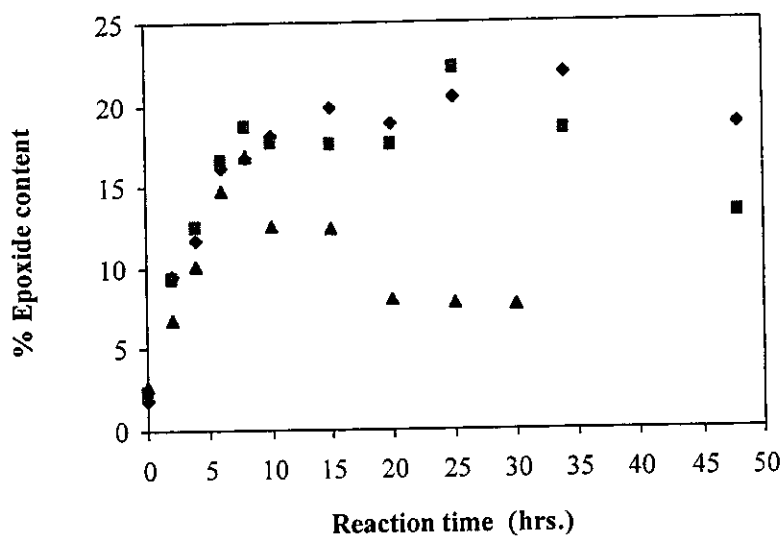
It clear  
point to  
change of  
hydrodynamic

In the case of the epoxidation carried out by using SDS as a surfactant, the epoxidation level was found lower than the use of non-ionic surfactant at the same reaction time. It can be noticed that after 15 hours of reaction time, the epoxidation level was found decreasing. In contrast to other cases, it was found that the intrinsic viscosity of the epoxidized product increased at longer reaction time. This may be postulated that slightly crosslinked structure might be occurred as the rubber is still soluble in toluene.

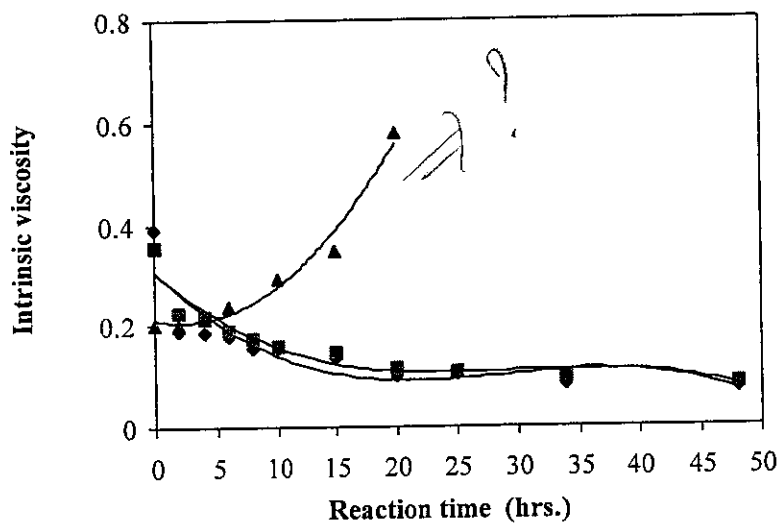
(A)  
# epoxidation  
NR data  
stabilized by  
DS  
in solution  
from

OK

The investigation of the epoxidized products and the secondary structures of ~~the~~ <sup>of resulting</sup> reaction carried out by using Sinnopal NP 307 and SDS surfactants were ~~carried~~ <sup>made</sup> ~~out.~~ The signal of proton corresponding to the 1,2-diol structure and the ether was found to be appeared at the same position in  $^1\text{H}$  NMR (3.4 ppm) so it is not possible to differentiate these two structures. However, the amount of formate adduct can be calculated from the signal of proton at 8 ppm, therefore by subtraction of this signal from the intensity at 3.4 ppm, the amount of diol/ether unit can be achieved. Figure 5.26 showed the progress of oxirane function and secondary products (diol/ether structure, hydrofuran and formate adduct) at various reaction times. The results showed that about maximum of 8% of hydrofuran formation was found both in the case of using Sinnopal and SDS. Very tiny amount of formate adduct was observed at various reaction times. The different amounts of diol/ether were noticed for the epoxidation in different surfactants. The maximum of 1 % of diol/ether structure was

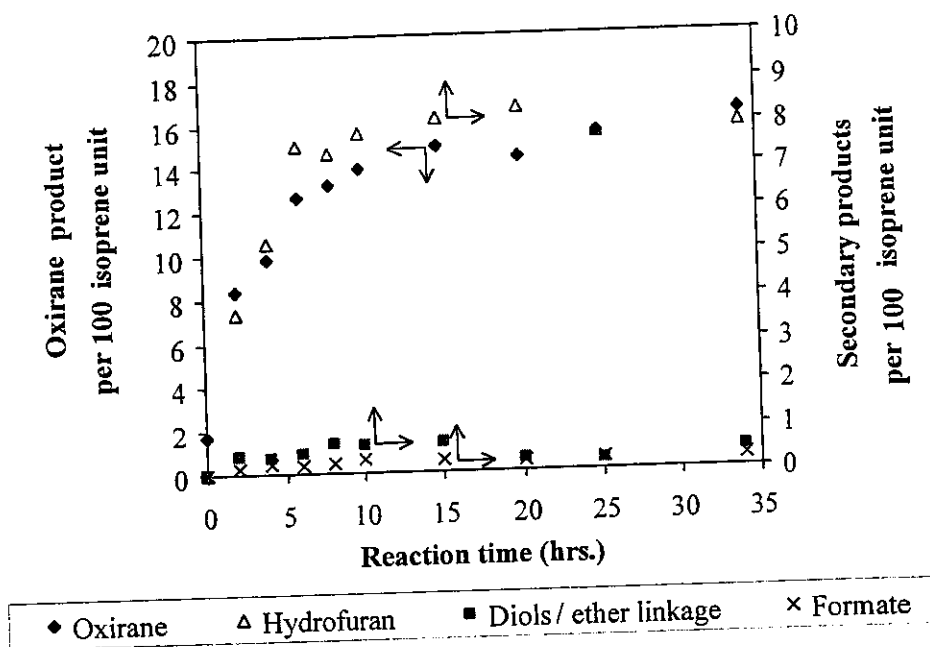


(A)

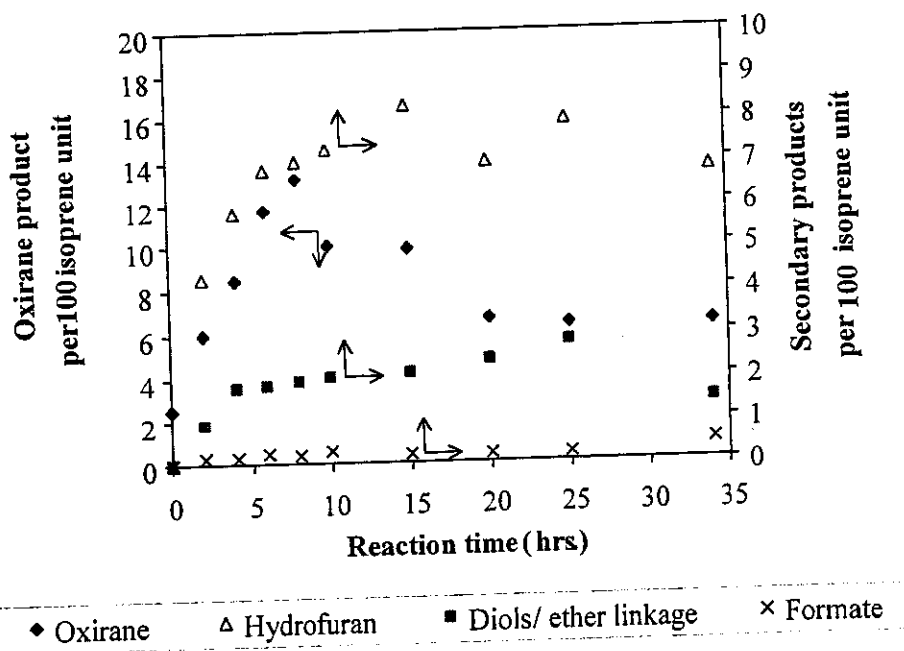


(B)

**Figure 5.25** Plot of (A) Epoxide content (%) and (B) Intrinsic viscosity at various reaction times of epoxidation of LPNR latex with 0.3 mole/mole of  $H_2O_2$  and 0.15 mole/mole of  $HCOOH$ , using different surfactants; ( $\blacklozenge$ ) Sinnopal NP 307, ( $\blacksquare$ ) Teric and ( $\blacktriangle$ ) SDS



(A)



(B)

**Figure 5.26** Plots of amounts of oxirane, hydrofuran, diols/ether linkage and formate structures found in epoxidation of LPNR latex by using 0.3 mole/mole of  $[H_2O_2]$  and 0.15 mole/mole of  $[HCOOH]$  in different surfactants; (A) Epoxidized liquid purified natural rubber (Sinnopal) and (B) Epoxidized liquid purified natural rubber (SDS)

found in the case of using Sinnopal while the presence of SDS resulted in about 3% of diol/ether structure. This can be used to support the increase of the intrinsic viscosity of the modified product found in the condition of using SDS surfactant as the presence of intermolecular ether linkage may lead to increasing the molecular weight of the resulting product.

OK // The use of non-ionic surfactant resulted in higher epoxidation level and less amount of secondary reactions than that of anionic surfactant. This may be due to the different behaviors in stabilization of the colloidal rubber particles. The anionic surfactant (SDS) stabilizes the colloidal particles by electrostatic repulsion of negative charges. These ionic species at the surface of the rubber particles may be favor to the opposite charges of the rebuilt formic acid after releasing the active oxygen to the isoprene unit. The formic acid may be able to stay close to the rubber particles, therefore the secondary reactions can be easily occurred. In the case of non-ionic surfactant which stabilized the colloidal particles by steric repulsion theory, there is not the ionic interaction of the surface of rubber particle and the formic acid presented in the system. The secondary reactions due to the formic acid may not be significant [55,65,72,73,76,80].

By varying the amounts of surfactant, Bac NV and coworker found that it affected the pH of the system, which affected further to the formation of epoxidized rubber [74]. Therefore, the amount of surfactant is considered to be one of the important parameter to control the pH and stability of the natural rubber latex. Stephanie MH studied the effect of amount of Sinnopal NP 307 on the epoxidation reaction of natural rubber and synthetic rubber [78]. The results showed that 2 to 5 phr of Sinnopal NP 307 presented the same rate and yield of epoxide content on NR. The rate of epoxidation was retarded when the surfactant was increased to 8 and 12 phr. In our work, various amounts of surfactants (0.5, 1.5 and 3 phr) were studied for the system of 10% DRC of LPNR latex, 0.3 mole/mole of  $H_2O_2$  and 0.15 mole/mole of  $HCOOH$ . Results of the use of two types of surfactants (Sinnopal NP 307 and Teric) are shown in Table 5.8. It was found that the rate of epoxidation and yield of oxirane units were increased at higher amounts of surfactants. However, too high quantity of surfactant (3 phr), the rate and yield of epoxidation reaction were retarded. It may be

Part of the reaction  
Why?

**Table 5.8** Maximum epoxide content (%), kinetic rate constant (k) and intrinsic viscosity,  $[\eta]$  of epoxidation reaction of 10% DRC of LPNR latex stabilized with Sinnopal NP 307 (LPNR-S), Teric (LPNR-T) or SDS (LPNR-D) at 50°C using performic acid by varying types and amount of surfactant

Sample	H <sub>2</sub> O <sub>2</sub> /IP <sup>a</sup> (mole/mole)	HCOOH/IP <sup>a</sup> (mole/mole)	Surfactant (phr)	Max. epoxide content (%)	k x 10 <sup>-5</sup> (sec <sup>-1</sup> )	$[\eta]$ after 20 hrs.
LPNR-S	-	-	0.5	2	-	0.39
ELSa	0.3	0.15	0.5	14	3.19	0.18
ELSc	0.3	0.15	1.5	22	6.01	0.10
ELSc	0.3	0.15	3.0	17	4.09	0.15
LPNR-T	-	-	0.5	2	-	0.35
ELTb	0.3	0.15	1.5	22	6.35	0.12
LPNR-D	-	-	0.5	3	-	0.20
ELDa	0.3	0.15	0.5	14	2.67	-
ELDb	0.3	0.15	1.5	17	5.12	0.58
ELDc	0.3	0.15	3.0	11	2.32	-

a : isoprene unit

due to the fact that increasing the quantity of the surfactant will lead to the increase of concentration of the hydrophilic part of the nonionic surfactant (ethylene oxide) on the surface of the rubber particles or the increase of repulsion of negative charge in the case of anionic surfactant, which reduced the ability of peracid to go inside the rubber particle. Therefore, this will lead to the reduction of the rate as well as yield of the epoxidation reaction.

### 3.2.2 Effect of hydrogen peroxide

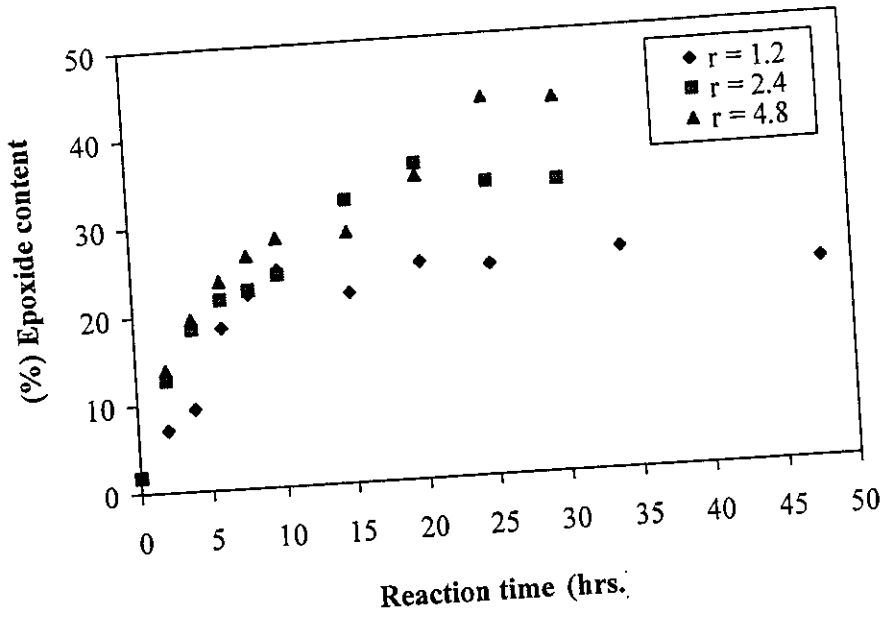
The epoxidation of LPNR using various amounts of H<sub>2</sub>O<sub>2</sub> (0.3, 0.6 and 1.2 mole/mole of H<sub>2</sub>O<sub>2</sub>/isoprene unit) with constant value at 0.25 mole/mole of HCOOH/isoprene unit, or the mole ratio (r) of [H<sub>2</sub>O<sub>2</sub>]/[HCOOH] equals to 1.2, 2.4 and 4.8 respectively were investigated. The results of epoxide contents at various reaction times of different types of surfactants used are shown in Figure 5.27. Generally, H<sub>2</sub>O<sub>2</sub> is the key reagent that controls the amount of epoxidation as the oxirane unit is occurred while the exhaustion of H<sub>2</sub>O<sub>2</sub> is preceded but the HCOOH is renewable.

Higher amount of  $H_2O_2$  may result in formation of higher amount of peracid, then higher amount of epoxide content can be formed. It was found in the case of using LPNR(Sinnopal) and LPNR(Teric) that epoxide content was increased with increasing the amount of  $H_2O_2$ . However, the epoxide content obtained did not relate directly to the amount of  $H_2O_2$  added as  $H_2O_2$  may be partially decomposed into water and oxygen molecule. Figure 5.27 showed also that at various amounts of  $H_2O_2$  used, the epoxidation levels in the case of non-ionic surfactants (Sinnopal and Teric) are higher than the use of anionic surfactant (SDS).

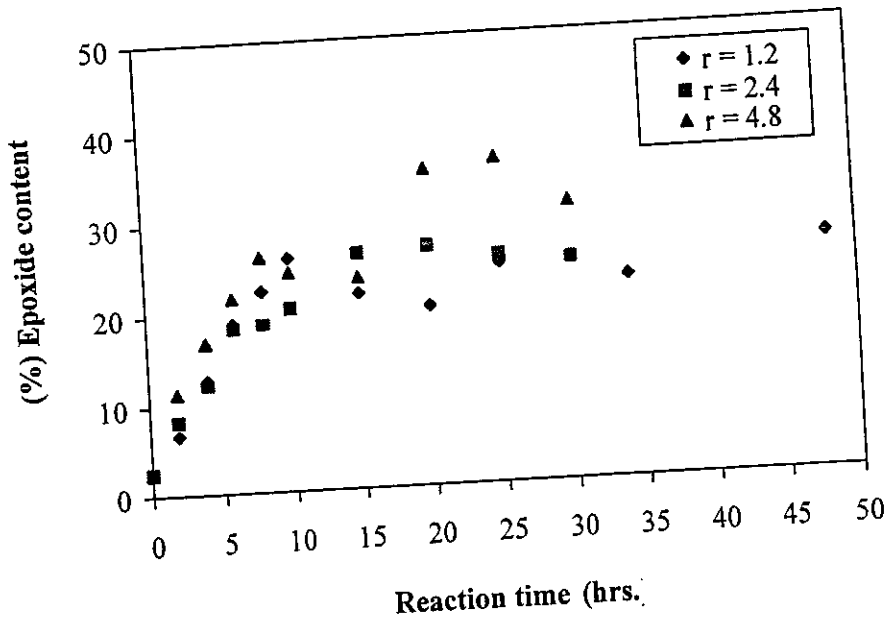
At the same amount of  $H_2O_2$  used (0.6 mole/mole of  $H_2O_2$ /isoprene unit) at different types of surfactants, the best result of epoxidation level was obtained in the case of Sinnopal surfactant. The rate of epoxidation reaction was found to be increased with increasing the amount of  $H_2O_2$ . The maximum of epoxide content and yield in different conditions are presented in Table 5.9. The epoxidation level of about 40% was achieved when 1.2 mole/mole of  $H_2O_2$ /isoprene unit was used at 25 hours of reaction time at  $50^\circ C$ .

The effect of the amount of  $H_2O_2$  on the secondary reactions of the epoxidation was also investigated. It was found in Figure 5.28 that the secondary reactions in the case of LPNR(Sinnopal) depend on the amount of  $H_2O_2$ . Increasing of  $H_2O_2$  from 0.3 to 1.2 mole/mole of isoprene unit resulted in increasing the amount of diol/ether structures, the formation of hydrofuran and the formate adduct. The diols/ether, hydrofuran and formate adduct were found to be 0.2, 7.1, 0.2 % respectively in the case of using 0.3 mole/mole of  $H_2O_2$ /isoprene unit at 25 hours of reaction time. While using of 1.2 mole/mole of  $H_2O_2$ /isoprene unit, diol/ether structures were increased to be 1.7% and the other by products were not increased.

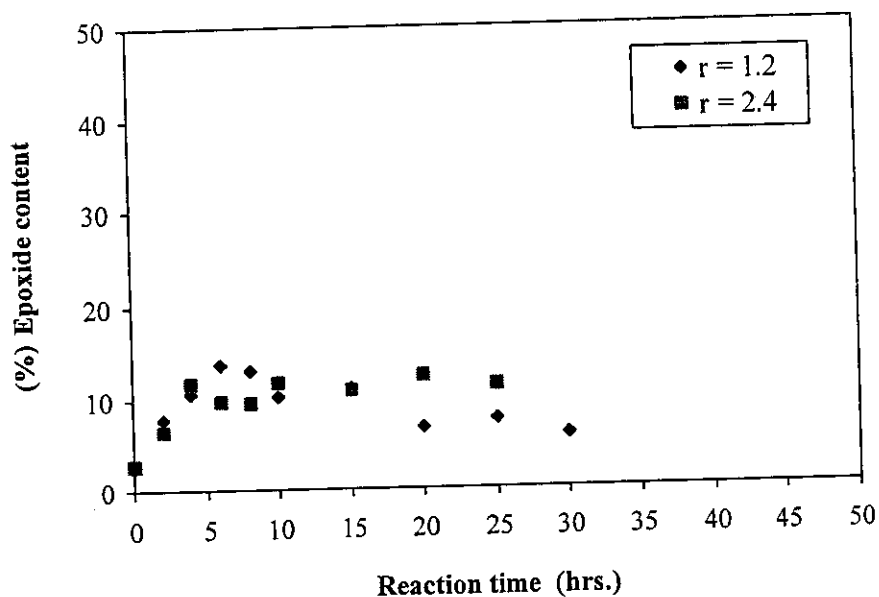
Similar results were obtained in the case of using 0.3 and 0.6 mole/mole of  $H_2O_2$ /isoprene unit for the epoxidation of LPNR(SDS) that increasing the amount of  $H_2O_2$  resulted in increasing the formation of diol/ether and hydrofuran structures and formyl adduct as shown in Figure 5.29. The epoxide content (%) by using 0.3 and 0.6 mole/mole of  $H_2O_2$ /isoprene unit were found to be 8% and 11% after 25 hours. The secondary products corresponding to diols/ether and hydrofuran structures as well as the formate adduct were 2.8, 6.2, 0.2 %, respectively for the use of 0.3 mole/mole of



(A)



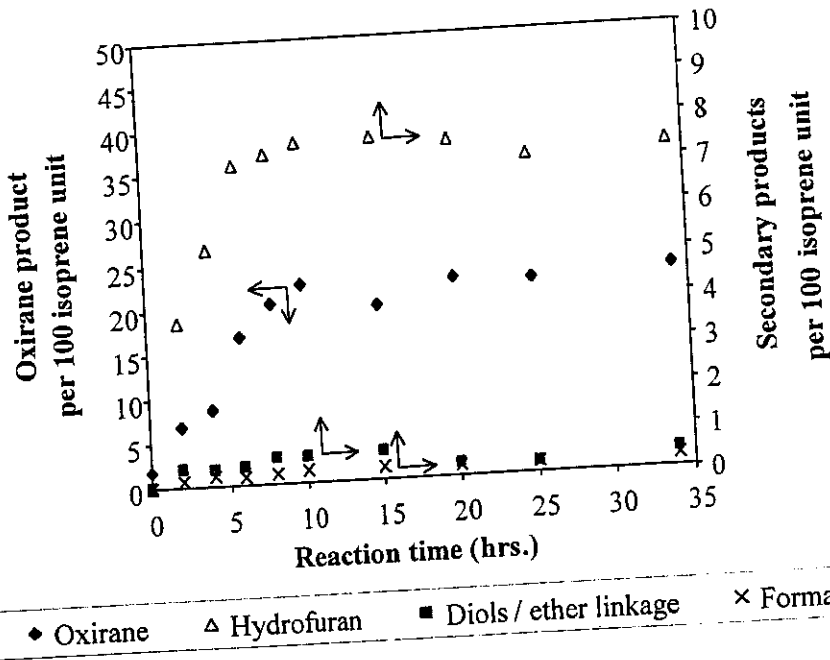
(B)



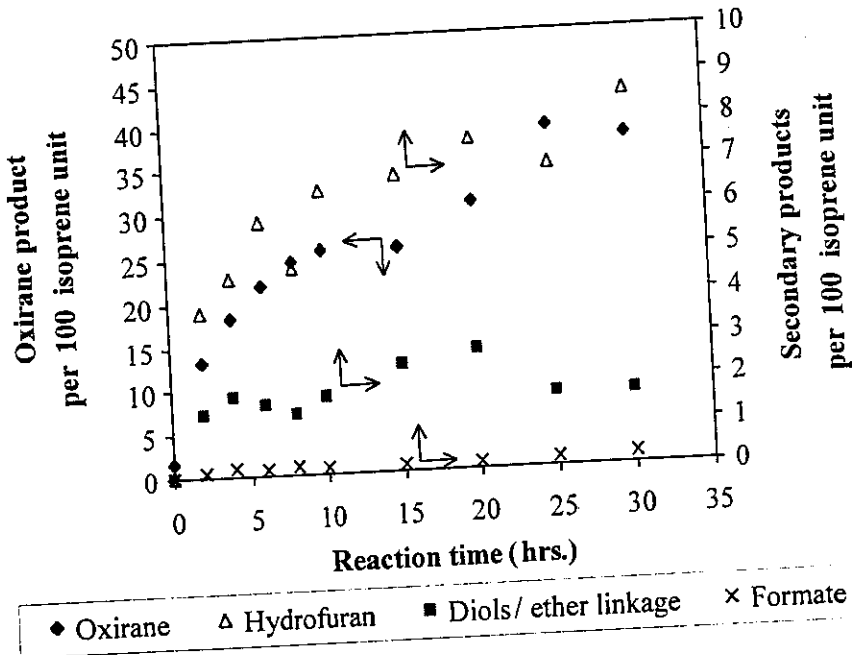
(C)

**Figure 5.27** Results of epoxide content (%) at various reaction times of different ratio of  $[H_2O_2]/[HCOOH]$ , ( $r$ ), as 1.2, 2.4 and 4.8 at constant value of  $[HCOOH]$  as 0.25 mole/mole of isoprene unit; (A) Epoxidized liquid rubber (Sinnopal), (B) Epoxidized liquid purified natural rubber (Teric) and (C) Epoxidized liquid purified natural rubber (SDS)

$H_2O_2$ /isoprene unit and 5.3, 9.1, 0.7 %, respectively for the used of 0.6 mole/mole of  $H_2O_2$ /isoprene unit after 25 hours of epoxidation reaction. The increase of ether linkage values was postulated to be responsible for the increase of molecular weight of the rubber. It will result in retardation of the epoxidation reaction on the rubber chain, leading to low epoxide content.

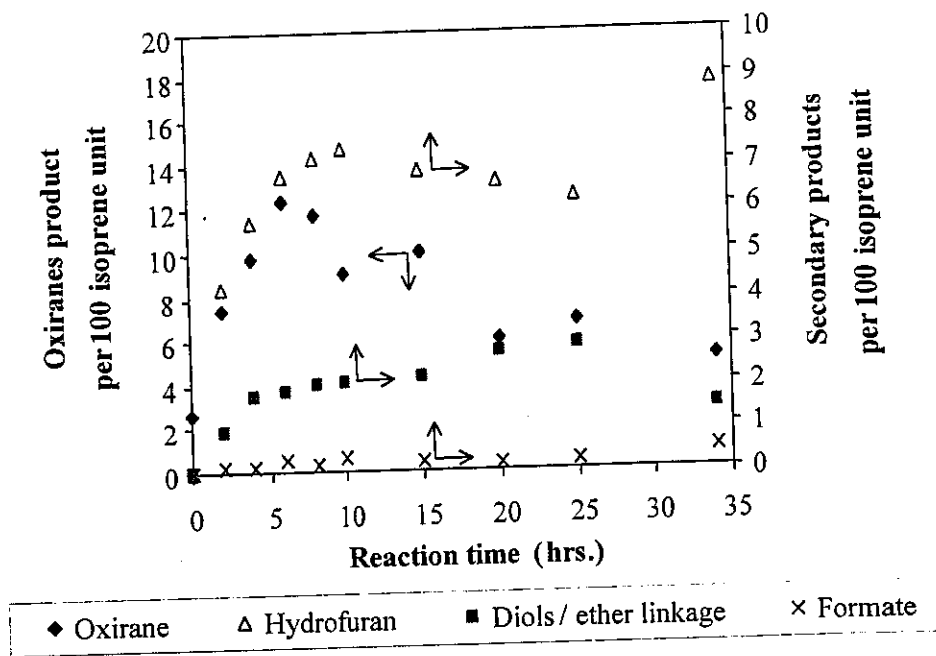


(A)

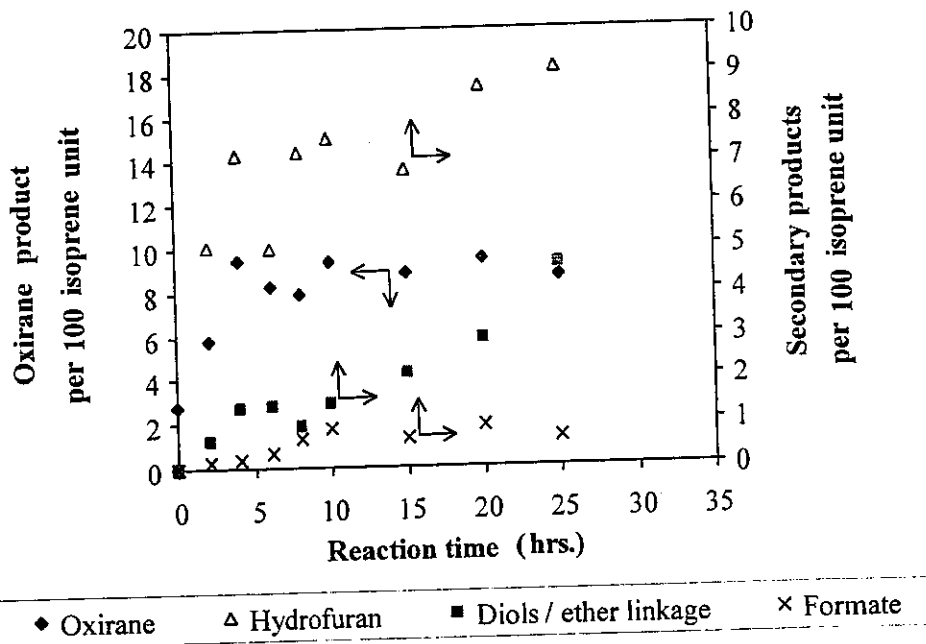


(B)

**Figure 5.28** Plots of amounts of oxirane, hydrofuran, diols/ether linkage and formate structures found in epoxidation of LPNR(Sinnopal) using constant [HCOOH] of 0.25 mole/mole of isoprene unit with different amount of H<sub>2</sub>O<sub>2</sub>; (A) 0.3 mole/mole of H<sub>2</sub>O<sub>2</sub>/isoprene unit and (B) 1.2 mole/mole of H<sub>2</sub>O<sub>2</sub>/isoprene unit



(A)



(B)

**Figure 5.29** Plots of amounts of oxirane, hydrofuran, diols/ether linkage and formate structures found in epoxidation of LPNR(SDS) using constant [HCOOH] of 0.25 mole/mole of isoprene unit with different amount of H<sub>2</sub>O<sub>2</sub>; (A) 0.3 mole/mole of H<sub>2</sub>O<sub>2</sub>/isoprene unit and (B) 0.6 mole/mole of H<sub>2</sub>O<sub>2</sub>/isoprene unit

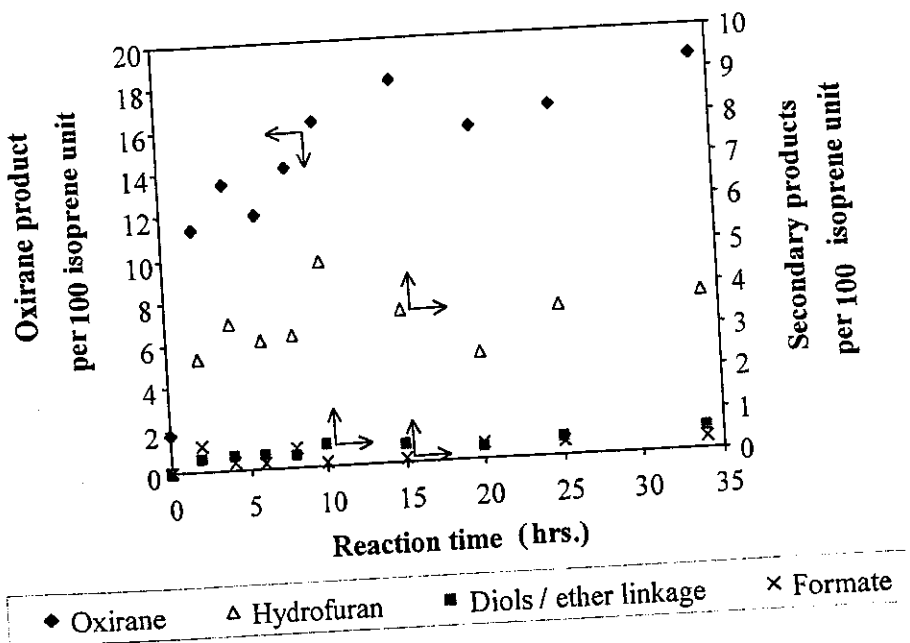
**Table 5.9** Maximum epoxide content (%), yield (%) and kinetic rate constant (k) of epoxidation reaction of 10% DRC of LPNR latex stabilized by Sinnopal NP 307 (LPNR-S), Teric (LPNR-T) or SDS (LPNR-D) at 50°C using various amounts of hydrogen peroxide and fixed amount of formic acid

Sample	H <sub>2</sub> O <sub>2</sub> /IP <sup>a</sup> (mole/mole)	HCOOH/IP <sup>a</sup> (mole/mole)	Max. epoxide content (%)	Yield (%)	k x 10 <sup>-5</sup> (sec <sup>-1</sup> )
LPNR-S	-	-	2	-	-
ELSd	0.30	0.25	25	83	4.41
ELSf	0.60	0.25	36	60	2.19
ELSh	1.20	0.25	43	36	1.35
LPNR-T	-	-	2	-	-
ELTd	0.30	0.25	26	87	4.60
ELTf	0.60	0.25	27	45	1.63
ELTh	1.20	0.25	36	30	1.23
LPNR-D	-	-	3	-	-
ELDd	0.30	0.25	14	47	3.03
ELDf	0.60	0.25	12	20	0.76

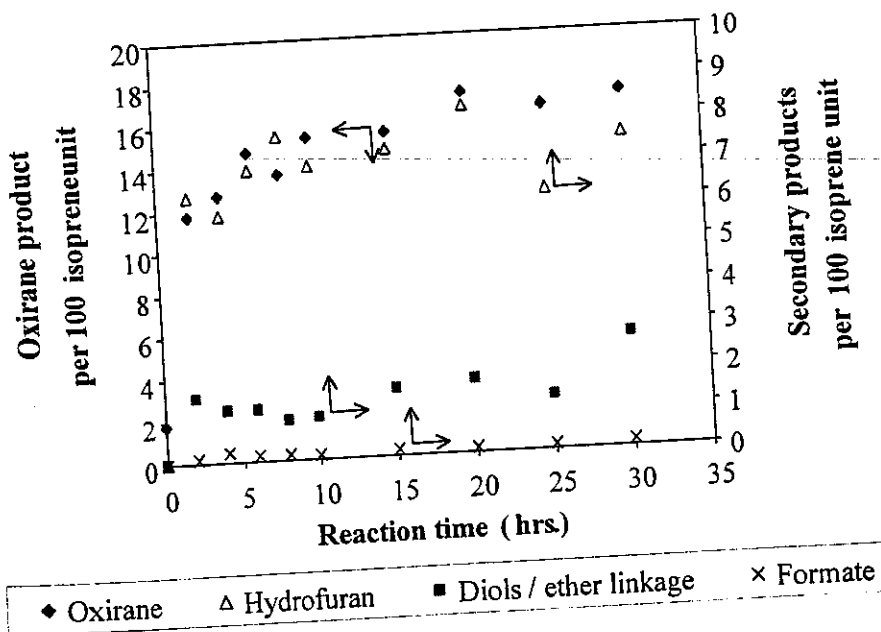
a : isoprene unit

### 3.2.3 Effect of formic acid

Various amounts of formic acid (0.15, 0.25 and 0.50 mole/mole of HCOOH/isoprene unit) at constant amount of hydrogen peroxide (0.6 mole/mole) were used to investigate the effect of the formic acid on the epoxidation of LPNR latex (10 %DRC) using different surfactants (Sinnopal, Teric and SDS). The results are shown in Figure 5.30 and 5.31 and Table 5.10. It was found that in the system of using Sinnopal as a surfactant, the epoxide content increase with increasing the amount of formic acid (0.15 to 0.25 mole/mole). However, using vary high amount of formic acid (0.50 mole/mole), the epoxide content was less than at lower amount of the formic acid. This may be explained by using the results in Figure 5.30 that at high concentration of formic acid resulted in higher amount of secondary reactions particularly the formation of diol/ether structures than in the case of using less quantity of formic acid. The secondary products corresponding to diols/ether and hydrofuran structures as well as the formate adduct were 0.4, 3.6, 0.3 %, respectively for the use

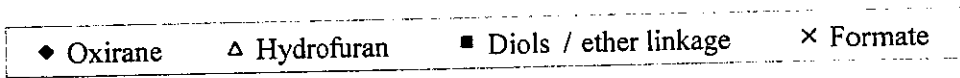
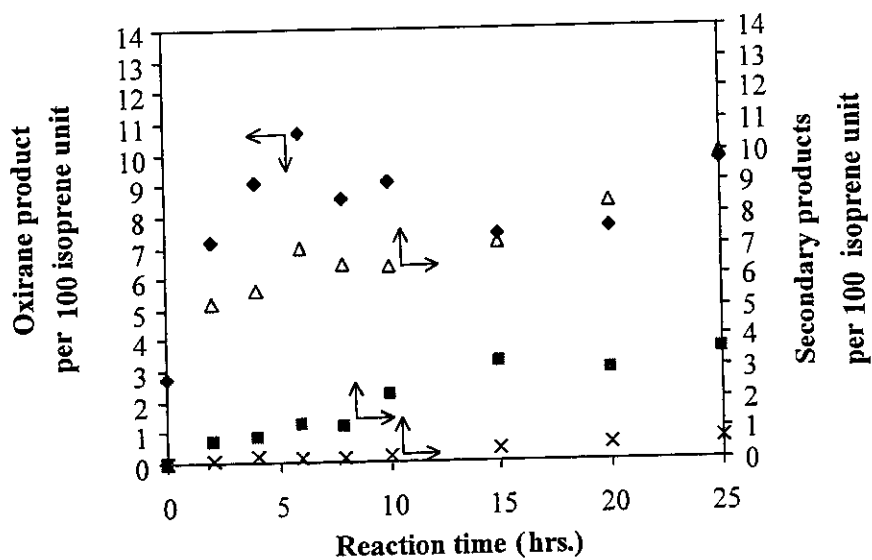


(A)

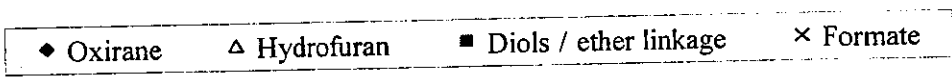
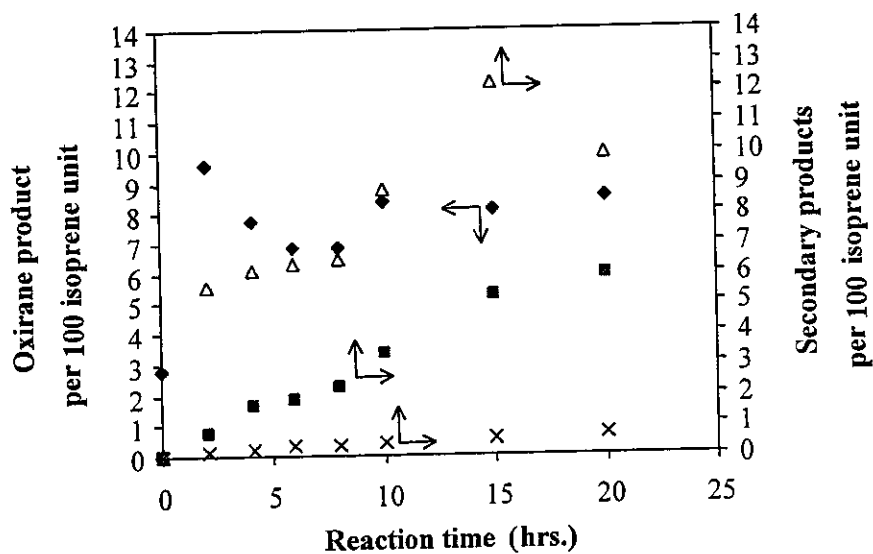


(B)

**Figure 5.30** Plots of amounts of oxirane, hydrofuran, diols/ether linkage and formate structures found in epoxidation of LPNR(Sinnopal) using constant  $[H_2O_2]$  of 0.6 mole/mole of isoprene unit with different amount of  $HCOOH$ ; (A) 0.15 mole/mole of  $HCOOH$ /isoprene unit and (B) 0.5 mole/mole of  $HCOOH$ /isoprene unit



(A)



(B)

**Figure 5.31** Plots of amounts of oxirane, hydrofuran, diols/ether linkage and formate structures found in epoxidation of LPNR(SDS) using constant  $[H_2O_2]$  of 0.6 mole/mole of isoprene unit with different amount of HCOOH; (A) 0.15 mole/mole of HCOOH/isoprene unit and (B) 0.5 mole/mole of HCOOH/isoprene unit

Chor. Wayakron Phetphaisit

of 0.15 mole/mole of HCOOH/isoprene unit and 1.3, 6.2, 0.1%, respectively for the used of 0.50 mole/mole of HCOOH/isoprene unit after 25 hours of epoxidation reaction. These secondary reactions are assumed to interfere the epoxidation reaction.

For the epoxidation reaction onto LPNR(Teric), the results showed little difference from the reaction with LPNR(Sinnopal) that the epoxide content kept increasing with increasing the amount of formic acid (0.15 to 0.50 mole/mole). In the case of using SDS as a surfactant in the epoxidation, it was found that increasing the amount of formic acid did not result in better epoxidation. The maximum epoxidation level was about 12%. The secondary reactions were found increasing at longer reaction time as shown in Figure 5.31. Increasing the amount of formic acid resulted in increasing the amount of secondary reactions. The secondary products corresponding to diols/ether and hydrofuran structures as well as the formate adduct were 2.9, 8.4, 0.6 %, respectively for the use of 0.15 mole/mole of HCOOH/isoprene unit and 5.9, 9.9, 0.7%, respectively for the used of 0.50 mole/mole of HCOOH/isoprene unit after 20 hours of epoxidation reaction. It can be noticed that the occurrence of diol/ether structures was higher in the system of LPNR latex stabilized with anionic surfactant than stabilized with non-ionic surfactant.

Table 5.11 showed the amount of oxirane unit and secondary products comparing with 100 units of isoprene, intrinsic viscosity and gel content in various epoxidation conditions of LPNR(SDS). It can be seen that amount of H<sub>2</sub>O<sub>2</sub> and HCOOH have strong effect on the occurrence of secondary products. In addition, the increase of intrinsic viscosity and gel content were found to be related to the increase amount of secondary products especially ether structure in the system of anionic surfactant.

**Table 5.10** Maximum epoxide content (%), Yield (%) and kinetic rate constant (k) of epoxidation reaction of 10% DRC of LPNR latex stabilized with Sinnopal NP 307 (LPNR-S), Teric (LPNR-T) or SDS (LPNR-D) at 50°C, using various amounts of formic acid

Samples	H <sub>2</sub> O <sub>2</sub> /IP (mole/mole)	HCOOH/IP (mole/mole)	Max. epoxide content (%)	Yield (%)	k x 10 <sup>-5</sup> (sec <sup>-1</sup> )
LPNR-S	-	-	2	-	-
ELSe	0.60	0.15	24	40	2.77
ELSp	0.60	0.25	36	60	2.19
ELSp	0.60	0.50	24	40	1.01
LPNR-T	-	-	2	-	-
ELTe	0.60	0.15	25	42	2.98
ELTf	0.60	0.25	27	45	1.63
ELTg	0.60	0.50	36	60	1.01
LPNR-D	-	-	3	-	-
ELDe	0.60	0.15	13	22	2.32
ELDf	0.60	0.25	12	20	0.76
ELDg	0.60	0.50	12	20	0.48

**Table 5.11** The amount of oxirane unit, secondary products per 100 isoprene unit, intrinsic viscosity, [η] and gel content found in epoxidized LPNR latex stabilized with SDS (LPNR-D) after 20 hours of epoxidation reaction.

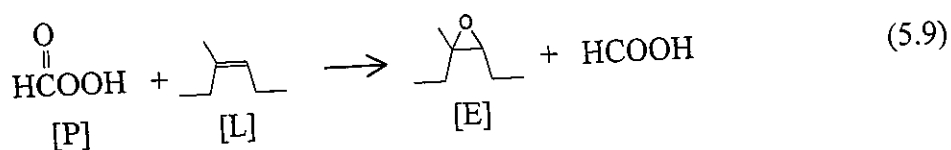
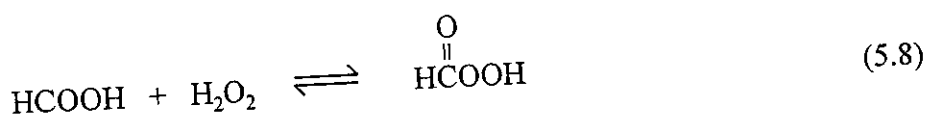
Samples	H <sub>2</sub> O <sub>2</sub> (mole/mole)	HCOOH (mole/mole)	Product per 100 isoprene units				Epoxide content (%)	[η]	Gel content (%)
			Oxiranes	Hydroxyl/ether linkage	Hydrofuran	Formate			
LPNR-D	-	-	2.65	a	a	a	2.7	0.2	a
ELDb	0.3	0.15	6.67	2.36	6.69	0.17	7.2	0.6	a
ELDd	0.3	0.25	6.03	2.88	7.79	0.27	6.0	0.8	a
ELDe	0.6	0.15	7.60	3.56	8.38	0.55	8.4	b	21.6
ELDf	0.6	0.25	9.48	5.25	8.65	0.61	10.6	b	34.7
ELDg	0.6	0.50	8.50	5.91	9.94	0.65	9.3	b	40.5

a : was not detected;

b : can not be measured

### 3.3 Kinetics study of epoxidation reaction

The kinetics of epoxidation reaction of LPNR and PNR latex with performic acid were studied. Eq. (5.8) represents the formation of performic acid from the reaction of hydrogen peroxide and formic acid. The performic acid will later react with C=C of isoprene unit, forming the epoxidized compound and regenerated formic acid as shown in eq. (5.9).



The rate of epoxidation is considered to be controlled by the formation of the performic acid. In our system, the amount of  $\text{H}_2\text{O}_2$  was not added in excess compared to the isoprene unit. The concentration of formic acid,  $[\text{HCOOH}]$  is assumed to remain constant throughout the reaction period which is due to the fact that the formic acid is rebuilt after epoxidation reaction.[70,77] The kinetic rate of epoxidation is shown in eq. (5.10).

$$R_p = \frac{d[\text{E}]}{dt} = k([\text{H}_2\text{O}_2]_0 - [\text{E}])[\text{HCOOH}]_0 \quad (5.10)$$

$$\text{Then } \frac{d[\text{E}]}{([\text{H}_2\text{O}_2]_0 - [\text{E}])} = k[\text{HCOOH}]_0 dt \quad (5.11)$$

Integration of eq. (5.11) and where  $k'$  is  $k[\text{HCOOH}]_0$ , then

$$\ln\left(\frac{([\text{H}_2\text{O}_2]_0 - [\text{E}]_0)}{([\text{H}_2\text{O}_2]_0 - [\text{E}]_t)}\right) = k't \quad (5.12)$$

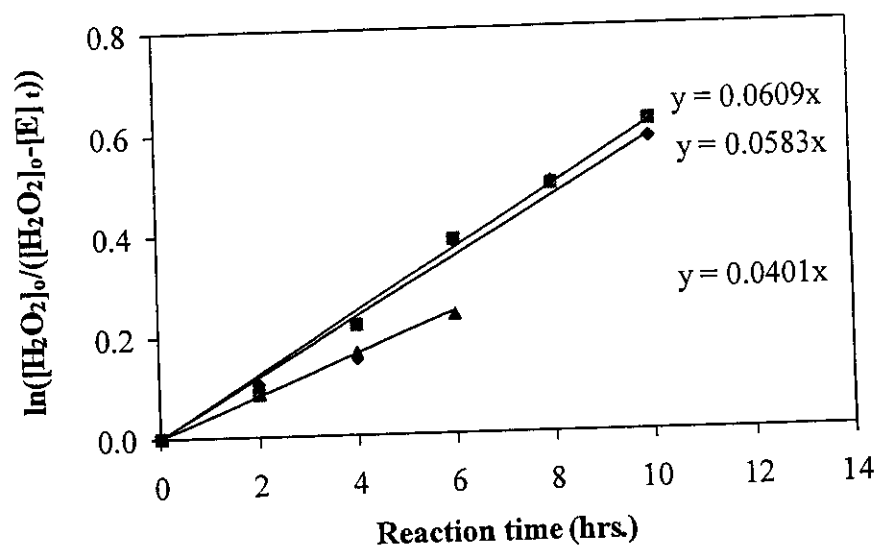
The kinetic rate constant ( $k'$ ) can be measured where,  $[\text{H}_2\text{O}_2]_0$  is the initial concentration of  $\text{H}_2\text{O}_2$ ,  $[\text{E}]_0$  is concentration of epoxidized unit at initial reaction time,  $t = t_0$ ,  $[\text{E}]_t$  is concentration ( $\text{mol.l}^{-1}$ ) of epoxide content at various reaction time,  $t = t$ , in mole fraction.

Therefore, the kinetic rate constant ( $k'$ ) of epoxidation reaction can be estimated from eq. (5.12) from the slope of the plot of  $\ln([\text{H}_2\text{O}_2]_0 - [\text{E}]_0) / ([\text{H}_2\text{O}_2]_0 - [\text{E}]_t)$  at various reaction times. The concentration of epoxidized unit,  $[\text{E}]$  can be calculated from  $^1\text{H}$  NMR. Generally, kinetic rate constant is used to predict how quickly a reaction is occurred before approaching an equilibrium. Therefore, the formation of oxiranes ring between 0 to 10 hours was considered for calculation of the kinetic rate constant. The real kinetic rate constant ( $k$ ) of epoxidation can be achieved by division of  $k'$  by  $[\text{HCOOH}]_0$ .

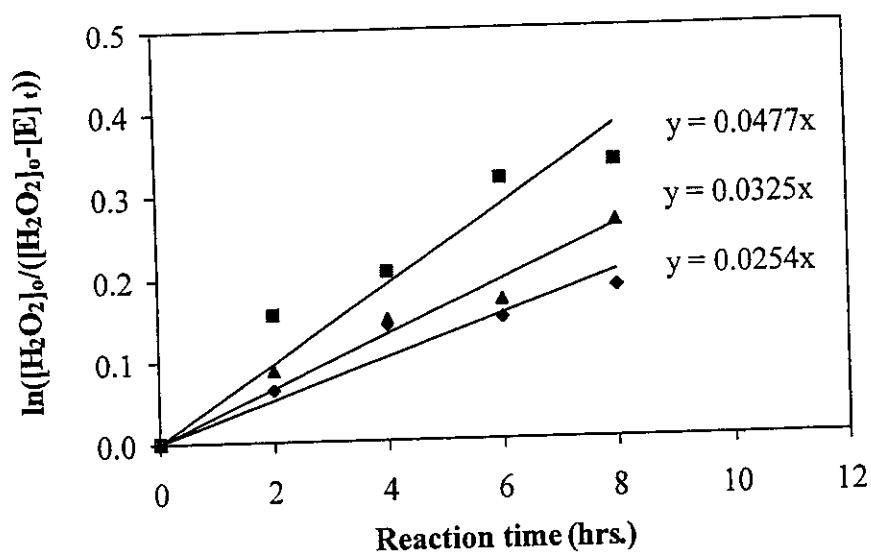
$$k = k' / [\text{HCOOH}]_0 \quad (5.13)$$

Figure 5.32 showed the plots of  $\ln([\text{H}_2\text{O}_2]_0 - [\text{E}]_0) / ([\text{H}_2\text{O}_2]_0 - [\text{E}]_t)$  versus time of epoxidation of 10% DRC of LPNR latex, using different types of surfactant; Sinnopal, Teric and SDS, with 0.3 mole/mole ( $0.441 \text{ mol.l}^{-1}$ ) of  $\text{H}_2\text{O}_2$ /isoprene unit and 0.25 mole/mole ( $0.368 \text{ mol.l}^{-1}$ ) of  $\text{HCOOH}$ /isoprene unit at  $50^\circ\text{C}$ . The  $k$  values of the formation of oxirane ring using Sinnopal, Teric and SDS were found to be  $4.60 \times 10^{-5}$ ,  $4.41 \times 10^{-5}$  and  $3.03 \times 10^{-5} \text{ sec}^{-1}$ , respectively. The results showed that the rate of epoxidation reaction in nonionic surfactant is higher than using the anionic surfactant. This can be explained as mentioned earlier that the negative charge of anionic surfactant may bring the rebuilt formic acid come close to the rubber particles that caused the ring opened products more easily than the rubber particles surrounded by non-ionic surfactants. The increase of rate of secondary reactions will decrease the rate of epoxidation reaction of the system.

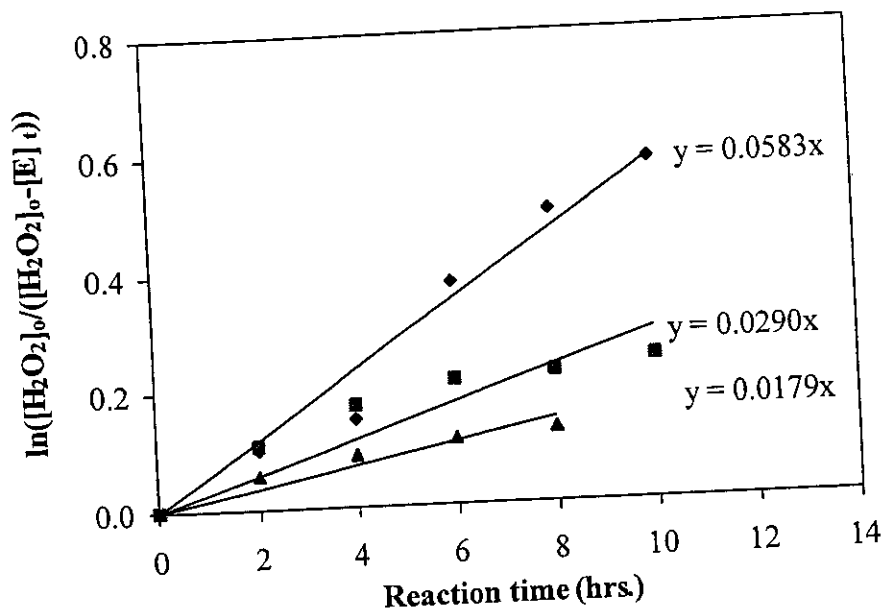
For the explanation of the effect of amounts of surfactant on the rate of the formation of epoxide function, the epoxidation of 10% DRC of LPNR latex stabilized with 0.5, 1.5 and 3 phr of Sinnopal by using 0.3 mole/mole ( $0.441 \text{ mol.l}^{-1}$ ) of  $\text{H}_2\text{O}_2$  and 0.15 mole/mole ( $0.221 \text{ mol.l}^{-1}$ ) of  $\text{HCOOH}$  at  $50^\circ\text{C}$  were investigated. Figure 5.33 showed the plots of  $\ln([\text{H}_2\text{O}_2]_0 - [\text{E}]_0) / ([\text{H}_2\text{O}_2]_0 - [\text{E}]_t)$  versus reaction time at various amounts of Sinnopal (0.5, 1.5 and 3 phr). The  $k$  values of the system were found to be  $3.20 \times 10^{-5}$ ,  $6.01 \times 10^{-5}$  and  $4.09 \times 10^{-5} \text{ sec}^{-1}$ , respectively. It may be postulated that 1.5 phr of Sinnopal NP 307 is the suitable amount of surfactant for stability of LPNR latex for the epoxidation reaction. Using 3 phr of surfactant did not effect on increasing the reaction rate. This may be possible that high amount of surfactant may cover the



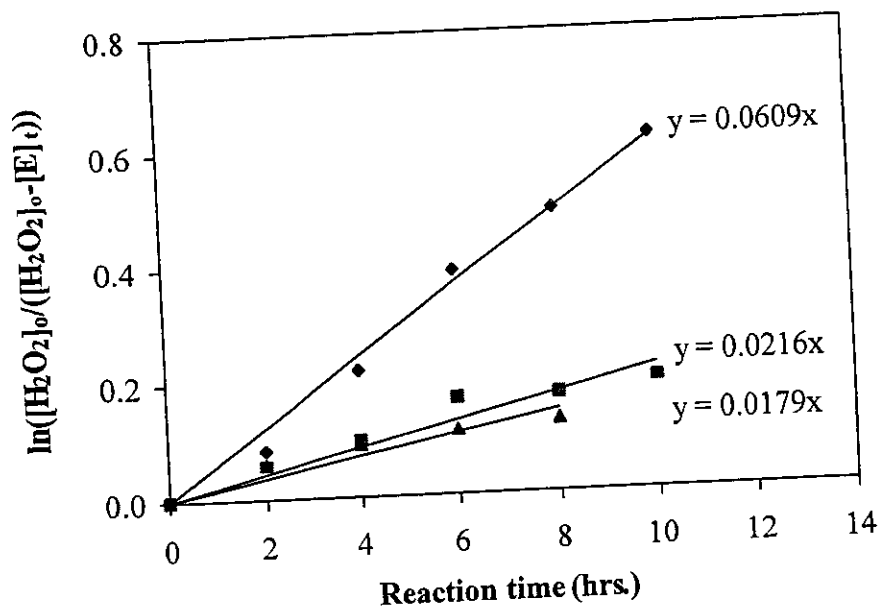
**Figure 5.32** Plots of  $\ln ([H_2O_2]_0/([H_2O_2]_t-[E]_t))$  at various reaction times of epoxidation, prepared from 10 % DRC of LPNR latex, 0.3 mole/mole ( $0.441 \text{ mol.l}^{-1}$ ) of  $H_2O_2$  and 0.25 mole/mole ( $0.368 \text{ mol.l}^{-1}$ ) of  $HCOOH$ , using various types of surfactant; (◆) 1.5 phr of Sinnopal NP 307, (■) 1.5 phr of Teric and (▲) 1.5 phr of SDS



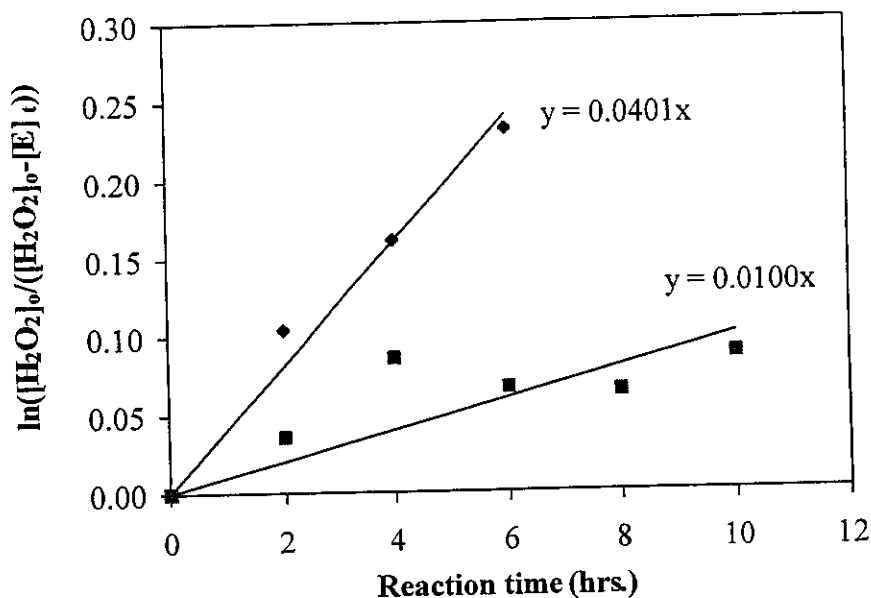
**Figure 5.33** Plots of  $\ln ([H_2O_2]_0/([H_2O_2]_t-[E]_t))$  at various reaction times of epoxidation, prepared from 10 % DRC of LPNR latex, 0.3 mole/mole ( $0.441 \text{ mol.l}^{-1}$ ) of  $H_2O_2$  and 0.15 mole/mole ( $0.221 \text{ mol.l}^{-1}$ ) of  $HCOOH$ , using various amounts of Sinnopal NP 307; (◆) 0.5 phr, (■) 1.5 phr and (▲) 3 phr



(A)



(B)



(C)

**Figure 5.34** Plots of  $\ln ([H_2O_2]_o/([H_2O_2]_o-[E]_t))$  at various reaction times of epoxidation, prepared from 10% DRC of LPNR latex, 0.25 mole/mole ( $0.368 \text{ mol.l}^{-1}$ ) of HCOOH at various amount of  $H_2O_2$ ; ( $\blacklozenge$ ) 0.3 mole/mole of isoprene unit, ( $\blacksquare$ ) 0.6 mole/mole of isoprene unit and ( $\blacktriangle$ ) 1.2 mole/mole of isoprene unit and various types of surfactant; (A) Sinnopal NP 307, (B) Teric and (C) SDS

rubber particles into two layers, leading to reduction of the ability of performic acid to go to contact with the rubber particle, then the rate of epoxidation reaction was decreased.

Figure 5.34 showed the effect of  $[H_2O_2]$  on kinetic rate constant of epoxidation reaction of LPNR stabilized with Sinnopal NP 307, Teric and SDS. The results showed the same trend that kinetic rate constant on the formation of oxirane structure decreased with increasing very high amount of  $[H_2O_2]$ . Then, the kinetic rate constants were found to be decreased with increasing the  $[H_2O_2]$ . The kinetic rate constant on the effect of various amounts of HCOOH were also found to be the same trend that the kinetic rate constants decreased with increasing of HCOOH (see Table 5.10). The increase of HCOOH caused the increase of the secondary reactions.

### 3.4 Degradation of Epoxidized Purified Natural Rubber by Using Periodic Acid

Generally, epoxidation is a well-known method to introduce polar functional group onto polydiene but does not necessarily result in much lowering the molecular weight of the starting material. Degradation of epoxidized polymer is going to be considered as the second stage modification to get the desired low molecular weight material containing epoxide functions. Periodic acid had been reported to be used for the degradation of natural rubber, epoxidized rubber and copolymer of styrene-butadiene [58,59]. In our study, degradation of epoxidized purified natural rubber (EPNR) was carried out by using this chemical.

#### 3.4.1 Preparation of epoxidized natural rubber

The epoxidized purified natural rubber (EPNR) in this study was prepared by epoxidation of PNR in latex phase using in-situ performic acid generated from hydrogen peroxide and formic acid, similar to the epoxidation of LPNR latex in section 3.2. As it has been shown previously that Sinnopal is an effective non-ionic surfactant for epoxidation of the LPNR latex, therefore Sinnopal was selected for epoxidation of PNR latex. Various amounts of Sinnopal (2, 3 and 4 phr) were added to the PNR latex for investigation of the epoxidation reaction. The studied condition was the use of 20%DRC of PNR latex with 30% H<sub>2</sub>O<sub>2</sub> and 30% HCOOH at 60°C during 24 hours. Infrared and <sup>1</sup>H NMR spectroscopies were used to analyse the epoxidized product. The IR spectrum of the EPNR is presented in Figure 5.35. The characteristic signals of epoxide ring on EPNR were found at 1250 and 870 cm<sup>-1</sup> which are similar to those of the ELPNR in previous section.

The signals in <sup>1</sup>HNMR of proton adjacent to epoxide ring and C=C of isoprene unit of EPNR were observed at 2.69 and 5.12 ppm, respectively. No signal of proton corresponding to side reactions such as epoxide ring opening unit was detected. This may be proposed to be due to the high molecular weight of the PNR that the very small quantity of the side reactions occurred in ELPNR might not be noticed. The epoxide content of the EPNR was calculated by using the signal in <sup>1</sup>HNMR as in the case of ELPNR in the former section. The rate of epoxidation of PNR by using

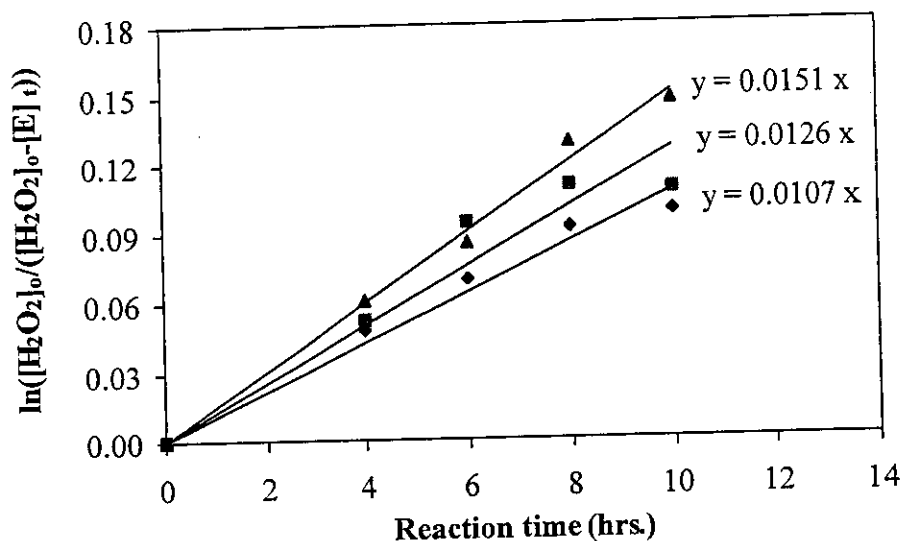


**Figure 5.35** Plots of  $\ln ([\text{H}_2\text{O}_2]_o/([\text{H}_2\text{O}_2]_o-[\text{E}]_t))$  at various reaction times of EPNR prepared from 20 % DRC of PNR latex, 0.3 M/M (0.882 mol.l<sup>-1</sup>) of H<sub>2</sub>O<sub>2</sub> and 0.3 M/M (0.882 mol.l<sup>-1</sup>) at various amounts of Sinnopal NP 307; (♦) 2 phr, (■) 3 phr and (▲) 4 phr

different amounts of Sinnopal was investigated. Figure 5.35 shows the plots of  $\ln ([\text{H}_2\text{O}_2]_o/([\text{H}_2\text{O}_2]_o-[\text{E}]_t))$  at various reaction times of epoxidation of PNR using different amount of surfactant. It was found that using 4 phr of Sinnopal gave the highest kinetic rate constant ( $4.76 \times 10^{-6} \text{ sec}^{-1}$ ) on epoxidation reaction. While using of 2 and 3 phr of Sinnopal, the kinetic rate constant were  $3.37 \times 10^{-6} \text{ sec}^{-1}$  and  $3.97 \times 10^{-6} \text{ sec}^{-1}$ , respectively. The epoxide contents found for the reactions using 2, 3 and 4 phr of Sinnopal after 24 hours of epoxidation were 15.3, 17.6 and 21.6%, respectively.

Comparison of the use of the amount of surfactant used for epoxidation of LPNR and PNR, it was found that the best quantity is 1.5 phr and 4 phr, respectively. The PNR requires more surfactant than the LPNR. It may be due to the high molecular weight of PNR therefore high values of hydrophobic interaction are generated between hydrocarbon molecules and high values of van der Waals attraction is also concerned. The kinetic rate constant on the formation of oxiranes function on LPNR using performic acid was found to be higher than that of epoxidation of PNR. The higher molecular weight of PNR than the LPNR may be responsible of this event and the

formation of oxirane ring from the epoxidation reaction was produced at the surface of colloidal particle before go inside the rubber particle [69].

### 3.4.2 Degradation reaction

The EPNR prepared in the former section was in latex phase, it was then treated with periodic acid ( $H_5IO_6$ ) at  $30^\circ C$ . The resulting degraded product was purified by using the couple of dichloromethane and methanol. Chemical structure of the liquid epoxidized purified natural rubber (LEPNR) was analyzed by FTIR,  $^1H$  NMR and  $^{13}C$  NMR spectroscopies. The decrease of the molecular weight of the rubber was observed by measurement of its molecular weight by using viscosimetry and GPC. The degradation was carried out at different reaction times and various conditions (see Table 4.4, Chapter IV).

Infrared spectra in Figure 5.36 of the EPNR starting material and the LENR are compared. It was found that the LEPNR contained the signal at  $870\text{ cm}^{-1}$  and  $1249\text{ cm}^{-1}$  similar to the signal of the EPNR. These signals can be assigned to the characteristic of epoxide structure. Moreover, the spectrum of the LEPNR showed the appearance of the new characteristic band of carbonyl function ( $C=O$ ) at  $1721\text{ cm}^{-1}$  and hydroxyl function (OH stretching) at  $3460\text{ cm}^{-1}$ .

The  $^1H$  NMR spectrum of LEPNR in Figure 5.37 exhibited the signal corresponding to the epoxide structure on the liquid rubber chain at 2.7 ppm (oxirane methine proton) in addition to the signal of proton adjacent to  $C=C$  of isoprene unit at 5.14 ppm. The signals of methyl group and methylene proton adjacent to oxirane ring were observed at 1.26 ppm and 2.16 ppm, respectively. The appearance of extra signals at 2.1, 2.15-2.6 and 9.8 ppm can be assigned to the signals of three types of proton adjacent to carbonyl functions;  $CH_3-C=O$ ,  $-CH_2-C=O$  and  $H-C=O$ , respectively. These signals confirmed the presence of strong peak of carbonyl group found in IR spectrum of the LEPNR obtained. It can be proposed in this step that the chemical structure of the LEPNR composed of  $C=C$  of the isoprene unit, epoxidized structure, ketone and aldehyde functional groups. Therefore, three different structures are proposed in Table 5.12.

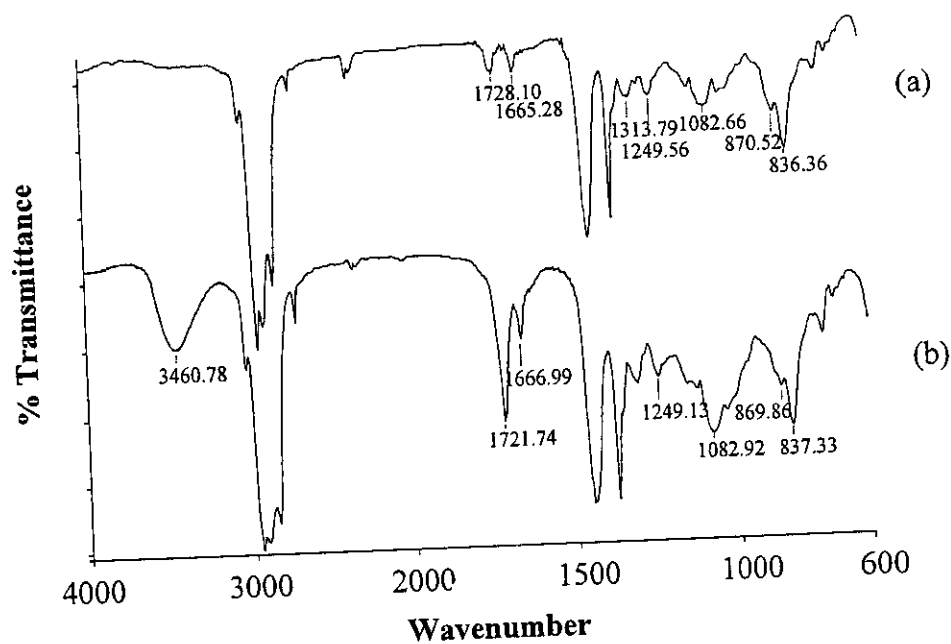


Figure 5.36 FTIR spectra of (a) Epoxidized purified natural rubber (EPNR) and (b) Liquid epoxidized purified natural rubber (LEPNR)

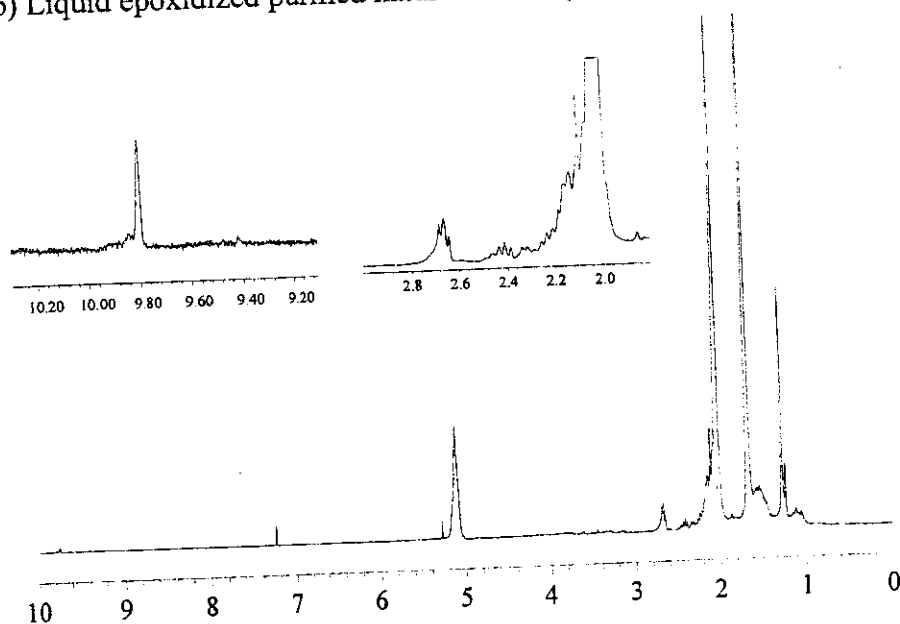


Figure 5.37  $^1\text{H}$  NMR spectra of liquid epoxidized purified natural rubber (LEPNR) obtained by using 1.13 mol/mol of  $\text{H}_5\text{IO}_6$ /epoxide unit and 0.26 mol/mol of  $\text{H}_5\text{IO}_6$ /isoprene unit after 21 hours

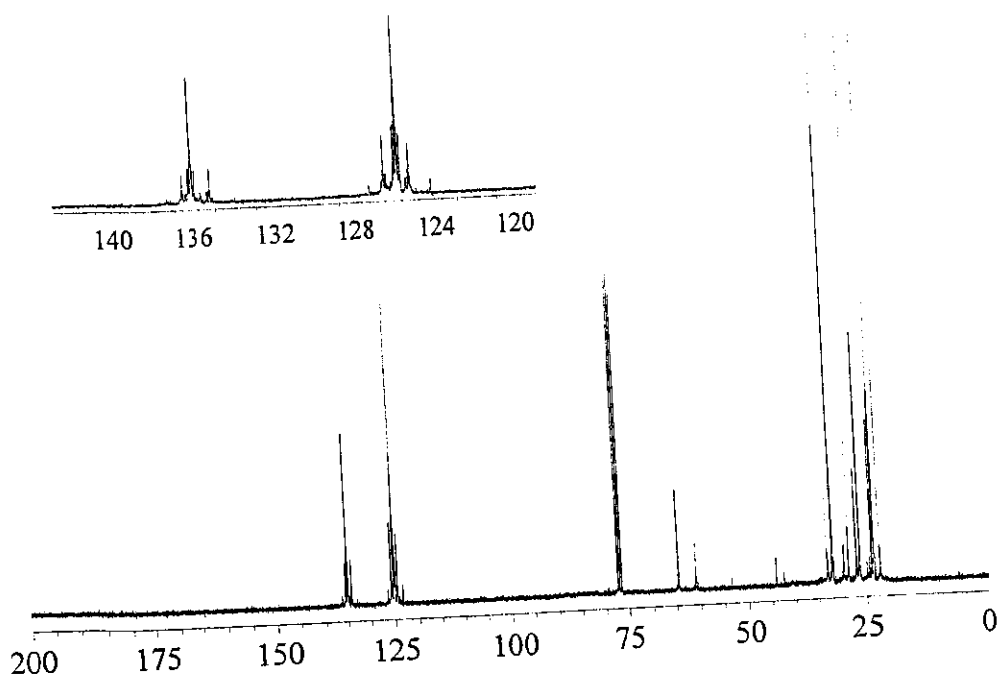


Figure 5.38  $^{13}\text{C}$  NMR spectra of LEPNR by using 1.13 mol/mol of  $\text{H}_5\text{IO}_6$ /epoxide unit and 0.26 mol/mol of  $\text{H}_5\text{IO}_6$ /isoprene unit after 21 hours

Table 5.12 Calculated [ ] and observed characteristic signal of LEPNR by  $^{13}\text{C}$  NMR spectroscopy

Position	$\delta$ (ppm)		Position	$\delta$ (ppm)	
	Calculated	Observed		Calculated	Observed
a	135.2	135.2	i	123.0	123.3
b	125.0	125.0	j	23.33	23.4
c	61.2	60.8	k	136.0	136.4
d	64.9	64.5	l	202.0	202.1
e	29.6	29.7	m	42.2	42.3
f	208.1	208.7	n	32.9	33.1
g	43.5	43.9	o	132.3	133.0
h	25.6	24.7	p	125.7	125.7

The LEPNR was also analyzed by  $^{13}\text{C}$  NMR spectroscopy (Figure 5.38). The chemical shift assignments calculated of the proposed structures of the degraded rubber and found in  $^{13}\text{C}$  NMR spectrum of the degraded rubber are compared in Table 5.12. It can be seen that the proposed chemical structures of the LEPNR fit well with the results observed in  $^{13}\text{C}$  NMR. It can be confirmed that the degradation of EPNR by using periodic acid resulted in the degraded rubber containing epoxide functional group, ketone and aldehyde functions.

The molecular weight of the degraded rubber was significantly reduced depending on the reaction time and the amount of periodic acid used as shown in Table 5.13. The amount of the epoxide group presented in the LEPNR was calculated by using the signal of proton at 5.1 and 2.7 ppm as in section 3.1. It was found in Table 5.13 that the epoxide content of the LEPNR obtained is approximately the same as the amount of epoxide group of the EPNR starting material at various reaction times.

### 3.4.3 Parameters affecting the degradation reaction

The degradation of the epoxidized rubber by periodic acid is complicated in terms of its mechanism. It is therefore necessary to investigate different parameters that can influence on the degradation reaction such as the amount of periodic acid, epoxide content as well as different types of rubber.

#### 3.4.3.1 Amount of periodic acid

The degradation of EPNR composed of 20% of oxiranes units was investigated by using various amounts of periodic acid ( $\text{H}_5\text{IO}_6$ ) (0.24, 0.51 and 1.13 mole/mole of  $\text{H}_5\text{IO}_6$ /epoxide unit) at  $30^\circ\text{C}$ . It was found in each degraded sample the presence of the absorption peak in infrared spectrum of oxirane function and carbonyl function ( $\text{C}=\text{O}$ ) at  $870\text{ cm}^{-1}$  and  $1720\text{ cm}^{-1}$ . It was found that at longer reaction time, the degradation was continuously occurred as lower molecular weight of the rubber was obtained as shown in Table 5.14. The increase of the signal of carbonyl at  $1720\text{ cm}^{-1}$  at longer reaction time may be due to the increasing of the number of bond scission which led to the formation of the ketone and aldehyde at the chain ends. The better the degradation reaction, the higher the ratio of the carbonyl function compared to the  $\text{C}=\text{C}$  of isoprene

unit. It was also found that at longer reaction time, the intensity of the signal at  $3460\text{ cm}^{-1}$  (hydroxyl group) was also increased. This can be postulated that the treatment of EPNR with periodic acid might cause the oxidation of the rubber chain, leading to hydroxyl function before the periodic acid further oxidizes the vic-diols into degraded rubber containing aldehyde and ketone at chain ends.

The intensity ratio of the signal of  $\text{C}=\text{O}$  at  $1720\text{ cm}^{-1}$ , comparing to the signal of methyl group adjacent to  $\text{C}=\text{C}$  at  $1374\text{ cm}^{-1}$  were found increasing when higher amount of  $\text{H}_5\text{IO}_6$  (0.24, 0.51 and 1.13 mole/mole of  $\text{H}_5\text{IO}_6/\text{epoxide unit}$ ) were used (Figure 5.39). These results are expected as increasing the amount of the periodic acid, the numbers of bond broken of the molecular chain has to be increased, leading to increasing the intensity of the carbonyl function at the chain end.

It was found in all cases that at various reaction times, the amount of the epoxide content determined by  $^1\text{H NMR}$  is approximately the same as the starting material. It seems likely that the degradation was not occurred at the epoxide function but more probably at the  $\text{C}=\text{C}$  of the isoprenic fraction which was prior oxidized to vic-diols structure. Figure 5.39 shows  $^1\text{H NMR}$  spectra of EPNR and LEPNR obtained from degradation reaction using 0.51 and 1.13 mole/mole of  $\text{H}_5\text{IO}_6/\text{epoxide unit}$ . The signal of proton adjacent to the epoxide ring before and after degradation was not changed and it appeared at 2.7 ppm.

The use of small amount of the periodic acid (0.24 mole/mole of  $\text{H}_5\text{IO}_6/\text{epoxide unit}$ ) did not give a significant degradation reaction of the EPNR. The molecular weight of the degraded rubber seemed to be very high and it was not possible to get a clear soluble solution of the degraded rubber. Therefore, the molecular weights of the samples were not determined. Table 5.13 and 5.14 presented the results of molecular weight ( $\overline{M}_w$  and  $\overline{M}_n$ ) of the degraded rubbers obtained by using 0.51 and 1.13 mole/mole of  $\text{H}_5\text{IO}_6/\text{epoxide unit}$ , respectively. The epoxide content at various reaction times was also calculated and presented in the Table 5.13 and 5.14. The reduction of the molecular weight of the rubber chain can be considered in term of the fraction of the molecular bonds broken ( $\alpha$ ) which can be determined by using eq. (5.1) (see section 2.3 in Chapter V).

$$\alpha = \frac{1}{\overline{DP}_{n(t)}} - \frac{1}{\overline{DP}_{n(0)}} = kt \quad (5.1)$$

The molecular weights of the EPNR analysed by GPC showed that the rate of degradation of the EPNR by using 1.13 mole/mole of  $H_5IO_6$ /epoxide unit was faster than the use of 0.51 mole/mole of  $H_5IO_6$ /epoxide unit. The molecular weight of the EPNR in the former case was significantly decreased after 10 minutes of the reaction. The degradation reaction was continuously preceded and reached approximately constant values after 12 hours. The liquid rubbers obtained in both cases were colorless and transparent product with approximately the same  $\overline{M}_n$  of 5000. When the reaction was allowed to continue to 21 and 30 hours, there were not significant decreased of the molecular weight. However, it was noticed only in infrared spectrum that the intensity of the signal of the carbonyl group was increasing. This may be assumed that the periodic acid may play a role as an oxidizing agent to transform probably the hydroxyl to ketone or the aldehyde to carboxylic acid.

It was found that the polydispersity index (I) found in the beginning of the reaction is large and the value became small at longer reaction time. This can be postulated that the degradation reaction is a random process, leading to variety of the molecular size. At longer reaction time, the more the chains were cleaved, the smaller the molecular chain were obtained, therefore important fractions of the polymer chain become similar in size.

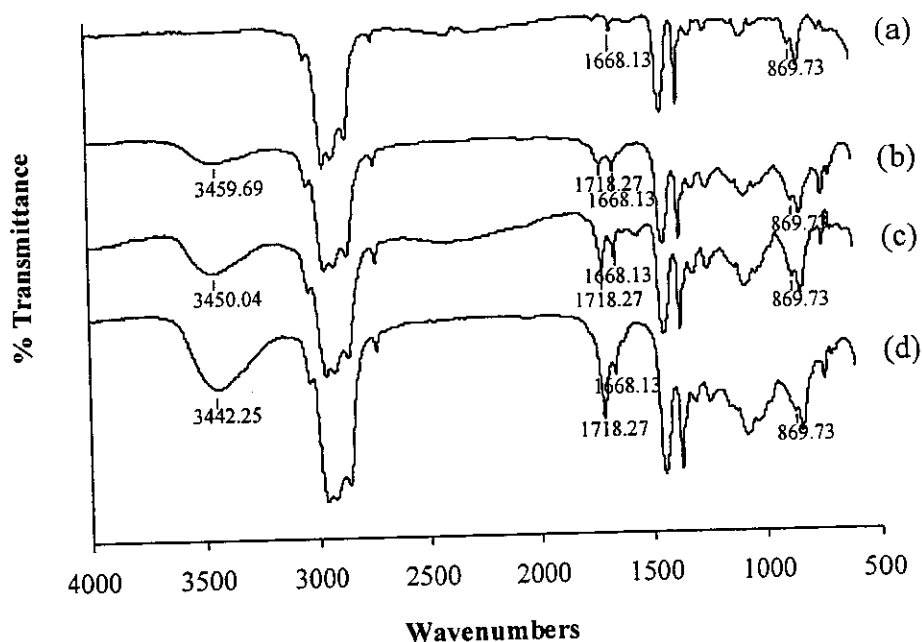


**Figure 5.39** FTIR spectra of degraded rubbers by using various amounts of  $H_5IO_6$  (a) EPNR, (b) LEPNR (using 0.24 mole/mole of  $H_5IO_6$ /epoxide unit), (c) LEPNR (using 0.51 mole/mole of  $H_5IO_6$ /epoxide unit) and (d) LEPNR (using 1.13 mole/mole of  $H_5IO_6$ /epoxide unit)

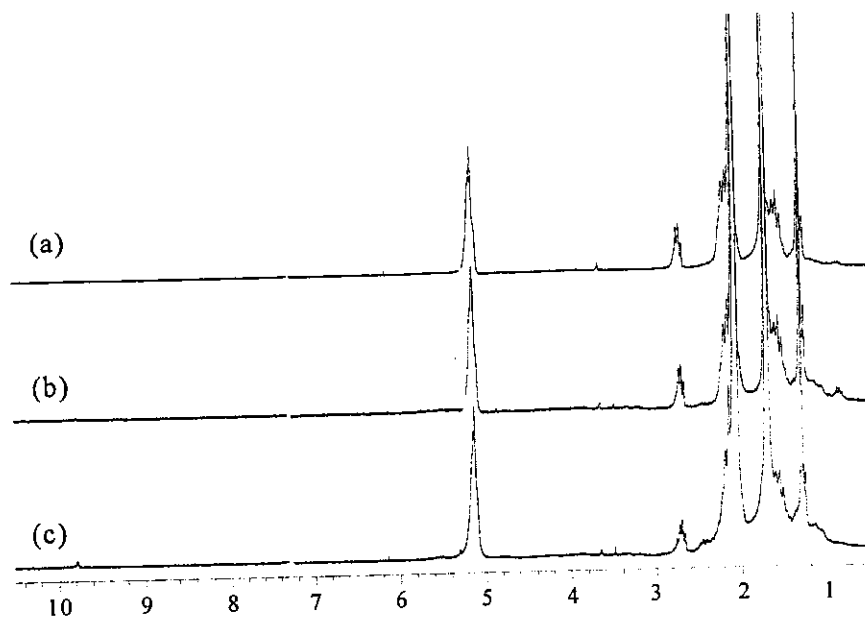


**Figure 5.40** <sup>1</sup>H NMR spectra of degraded rubbers obtained by using various amounts of  $H_5IO_6$  (a) EPNR, (b) LEPNR (using 0.51 mole/mole of  $H_5IO_6$ /epoxide unit) and (c) LEPNR (using 1.13 mole/mole of  $H_5IO_6$ /epoxide unit)

**Table 5.13** Results of degradation of EPNR (20.4% epoxide content), using 0.51 mole/mole of  $H_5IO_6$ /epoxide unit, at various reaction times

Reaction time (hours)	0.51 mol/mol of $H_5IO_6$ /epoxide unit or 0.13 mol/mol of $H_5IO_6$ /isoprene unit				
	Epoxide content (%)	$\bar{M}_w \times 10^4$	$\bar{M}_n \times 10^4$	$I^a$	$\alpha^b$ (%)
0	20.4	97.40 <sup>c</sup>	15.52 <sup>c</sup>	6.27 <sup>c</sup>	0
2	20.4	26.36	1.11	23.79	0.6
4	22.2	12.41	0.68	18.17	1.01
8	21.8	9.89	0.74	13.28	0.92
12	21.4	4.98	0.52	9.67	1.33
21	21.6	4.45	0.45	9.86	1.54
30	19.8	4.16	0.46	9	1.50

a = polydispersity index, b = fractions of bond broken, c = molecular weight measured of PNR

**Table 5.14** Results of epoxide content (%), average molecular weight ( $\bar{M}_w$  and  $\bar{M}_n$ ) polydispersity index (I) and fractions of bond broken ( $\alpha$ ) of degradation of EPNR (20.4% epoxide content), using 1.13 mole/mole of  $H_5IO_6$ /epoxide unit, at various reaction times

Reaction time (hours)	1.13 mol/mol of $H_5IO_6$ /epoxide unit or 0.26 mol/mol of $H_5IO_6$ /isoprene unit				
	Epoxide content (%)	$\bar{M}_w \times 10^4$	$\bar{M}_n \times 10^4$	I	$\alpha$ (%)
0	18.6	97.40 <sup>a</sup>	15.52 <sup>a</sup>	6.27	0
0.167	18.6	28.54	3.74	7.64	0.14
2	18.2	14.03	1.76	7.97	0.36
4	17.6	9.97	1.48	6.74	0.43
8	17.7	8.44	0.39	21.62	1.77
12	17.1	4.16	0.50	8.39	1.37
21	17.7	3.64	0.51	7.08	1.34

a = molecular weight measured of PNR

### 3.4.3.2 Amount of epoxide content of starting material

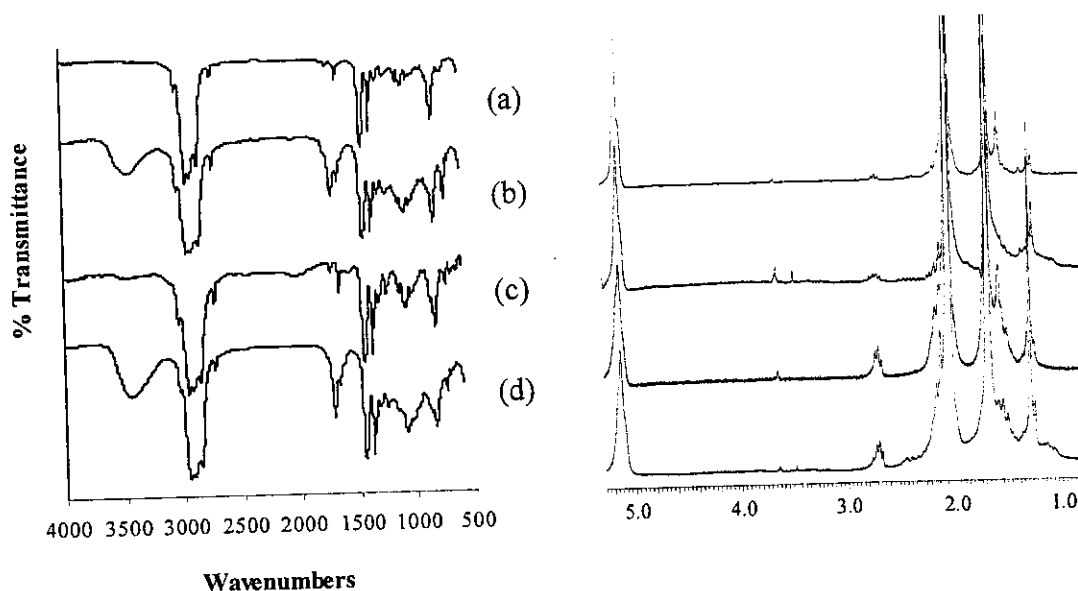
It was found in the former section that the epoxide content of the EPNR starting materials were almost unchanged at various reaction times of the degradation with periodic acid. Two different epoxide contents of EPNR (5% and 18%) were then used to compare the degradation reaction. The EPNR(5) and EPNR(18) containing 5% and 18% were treated with an excess amount of  $H_5IO_6$  i.e. 4.06 mole/mole of  $H_5IO_6$ /epoxide unit and 1.13 mole/mole of  $H_5IO_6$ /epoxide unit, respectively.

It was found in Table 5.15 that after 21 hours of reaction time, the  $\bar{M}_n$  of the degraded EPNR(5) obtained from using 4.03 mole/mole of  $H_5IO_6$ /epoxide is about 5000 which is similar to the molecular weight of the degraded EPNR(18) obtained from using 1.13 mole/mole of  $H_5IO_6$ /epoxide. The results found no significant change of the amount of the epoxide content in the both case. Moreover, the  $\alpha$  were found to be similar values i.e. 1.2 and 1.3 after 21 hours of degradation reaction of EPNR(5) and EPNR(18), respectively. These results may be used to support that the degradation by periodic acid did not occur at the epoxide function but it seems likely to be occurred at the C=C of the isoprene unit via an appropriate intermediate like vic-diols as reported in degradation of small vic-diols molecules.

**Table 5.15** Results of epoxide content (%), average molecular weight ( $\bar{M}_w$  and  $\bar{M}_n$ ) polydispersity index (I) and fractions of bond broken ( $\alpha$ ) of degradation of EPNR(5) (5% epoxide content) and EPNR(18) (18% epoxide content), using an excess of periodic acid at various reaction times

Reaction Time (hours)	EPNR(5) (4.06 mol/mol of $H_5IO_6$ /epoxide unit or 0.21 mol/mol of $H_5IO_6$ /isoprene unit)					EPNR(18) 1.13 mol/mol of $H_5IO_6$ /epoxide unit or 0.26 mol/mol of $H_5IO_6$ /isoprene unit				
	Epoxide content (%)	$\bar{M}_w \times 10^4$	$\bar{M}_n \times 10^4$	I	$\alpha$ (%)	Epoxide content (%)	$\bar{M}_w \times 10^4$	$\bar{M}_n \times 10^4$	I	$\alpha$ (%)
0	5	95.83 <sup>a</sup>	15.28 <sup>a</sup>	6.27	0	18.6	95.83 <sup>a</sup>	15.28 <sup>a</sup>	6.27	0
21	6	3.76	0.55	6.89	1.21	17.7	3.64	0.51	7.08	1.34

a = molecular weight measured of PNR



(A)

(B)

**Figure 5.41** (A) Infrared spectra and (B)  $^1\text{H}$  NMR spectra of different types of rubber; (a) EPNR (5% epoxide content), (b) LEPNR (degraded rubber containing 6% epoxide content), (c) EPNR (18.6% epoxide content) and (d) LEPNR (degraded rubber containing 17.7% epoxide content)

Figure 5.41 showed the comparison of FTIR and NMR spectra of starting epoxidized rubbers and its corresponding degraded rubber. The results show that the degraded rubber contained significant signal of carbonyl and hydroxyl groups at 1720 and  $3460\text{ cm}^{-1}$  in infrared spectrum both LEPNRs. While the  $^1\text{H}$  NMR revealed that the degraded rubbers contained the signal of the proton adjacent to epoxide function at  $2.7\text{ cm}^{-1}$  in similar quantity as the starting rubbers. The results are also found the different content of carbonyl function that the rubber contained higher amount of oxiranes unit on the rubber chain (EPNR(18)) showed the higher content of carbonyl function in the degraded product (LEPNR(18)).

### 3.4.3.3 Effect of type of rubber and chemical reagent

It seems that the degradation reaction by periodic acid did not occurred at the previous formed epoxide in the rubber chain. In this part, three types of rubber i.e. NR latex, PNR latex and EPNR latex were used to investigate the degradation characteristic of the periodic acid. Normally, the EPNR was prepared by in-situ

performic acid generated from hydrogen peroxide ( $H_2O_2$ ) and formic acid, it is proposed that the residual  $H_2O_2$  might effect on the degradation reaction. Therefore,  $H_2O_2$  was also added for studying the degradation of the rubbers. Table 5.16 to 5.19 showed the results of molecular weight of the different types of starting rubbers and their degraded forms at various reaction times and conditions.

The results found in Table 5.16 and 5.17 indicated that periodic acid could be used to break the rubber chain of NR and PNR. By using about 0.2 mole/mole of  $H_5IO_6$ /isoprene unit in both cases, the periodic acid could reduce the molecular weight of the rubbers to about 10,000 after 21 and 30 hours of reaction time for the PNR and NR respectively. The  $^1H$  NMR analysis of the degraded rubbers showed the presence of approximately 3% of epoxide content in both cases. It seems likely that the periodic acid can oxidize the rubber into epoxide functional group but at a very small quantity. It would rather oxidize the  $C=C$  into vic-diols which are responsible for the bond cleavage.

When the PNR was treated with periodic acid in the presence of  $H_2O_2$ , it was found in Table 5.18 that degradation of the PNR is faster than the reaction of periodic acid without the presence of  $H_2O_2$ , i.e. lower molecular weight of the rubber was obtained at the same reaction time. It can be proposed that the  $H_2O_2$  can be used to catalyst the oxidative chain degradation by periodic acid. However, it was found that the degraded rubbers from the addition of  $H_2O_2$  contained more epoxide content (about 6%) than the degradation of PNR without the  $H_2O_2$  (about 3% epoxide content). It has also been reported in the literature that the  $H_2O_2$  can be used to epoxidise  $\alpha,\beta$ -unsaturated ketone [122]. It may be proposed in this study that the epoxidation by  $H_2O_2$  may be occurred at the  $C=C$  unit adjacent only to the carbonyl function as a little bit higher amount of epoxide unit was found in the degraded rubber in the presence of  $H_2O_2$ .

Another experiment on the degradation of EPNR by using periodic acid was carried out to confirm the behavior of the oxidative degradation. It was found in Table 5.19 that increasing reaction time, the better the degradation was occurred. The percentage of epoxide content remains the same at various reaction times. The rate of

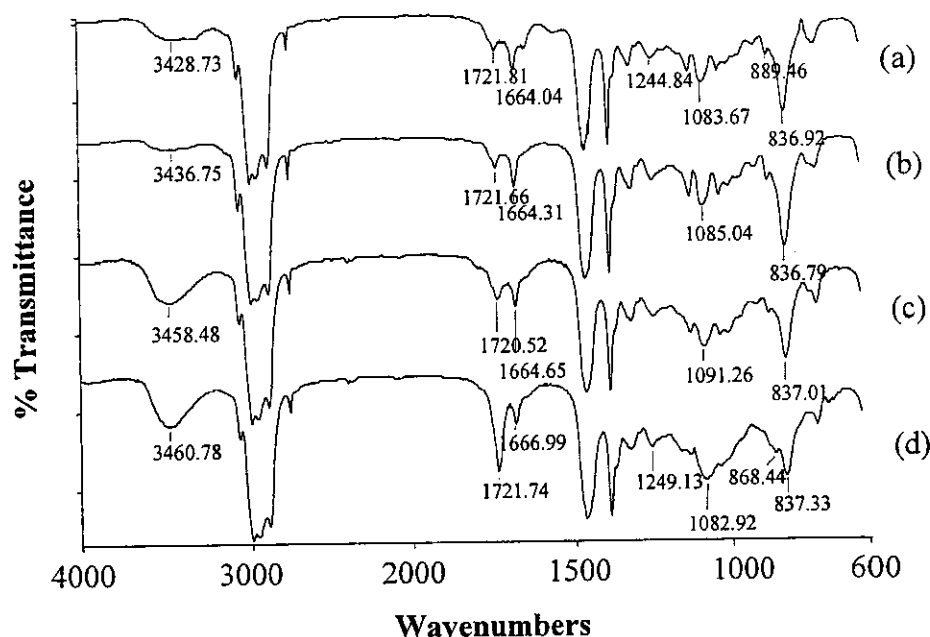


**Figure 5.42** Infrared spectra of degraded rubber after 21 hours of reaction time; (a) NR+H<sub>5</sub>IO<sub>6</sub>, (b) PNR+H<sub>5</sub>IO<sub>6</sub>, (c) PNR+H<sub>2</sub>O<sub>2</sub>+H<sub>5</sub>IO<sub>6</sub> and (d) EPNR+H<sub>5</sub>IO<sub>6</sub>

degradation by using periodic acid for the rubbers were found to be in the order of EPNR+H<sub>5</sub>IO<sub>6</sub> > PNR+H<sub>5</sub>IO<sub>6</sub>+H<sub>2</sub>O<sub>2</sub> > PNR+H<sub>5</sub>IO<sub>6</sub> > NR+H<sub>5</sub>IO<sub>6</sub>.

Infrared spectra in Figure 5.42 showed the appearance of the characteristic band of carbonyl function (1721 cm<sup>-1</sup>) and hydroxyl function (3450 cm<sup>-1</sup>) corresponding to the chain degradation of NR, PNR and EPNR latex. <sup>1</sup>H NMR spectra of degraded rubber by using NR + H<sub>5</sub>IO<sub>6</sub>, PNR + H<sub>5</sub>IO<sub>6</sub>, PNR + H<sub>5</sub>IO<sub>6</sub>+H<sub>2</sub>O<sub>2</sub> were shown in Figure 5.43. <sup>1</sup>H NMR spectra of degraded rubber by using ENR + H<sub>5</sub>IO<sub>6</sub> was noticed in Figure 5.37. It can be seen that using NR and PNR as starting rubbers, the signals corresponding to aldehyde function of the degraded rubbers were found at the same position (9.4 and 9.8 ppm). These signals were proposed to be related to α,β unsaturated aldehyde and aldehyde attached to methylene group, respectively. While using EPNR as starting rubber, the signal corresponding to degraded rubber was found only at 9.8 ppm. The addition of H<sub>2</sub>O<sub>2</sub> on the reaction of PNR with H<sub>5</sub>IO<sub>6</sub>, the lower molecular weight was obtained, comparing to NR and PNR treated with only H<sub>5</sub>IO<sub>6</sub>. Moreover, the α value of chain degradation by the help of H<sub>2</sub>O<sub>2</sub> was found to be increase and showed 2 times of α values of NR and PNR reacted with only H<sub>2</sub>O<sub>2</sub>

respectively. This may be postulated that the H<sub>2</sub>O<sub>2</sub> is a reagent for both degradation and epoxidation but at relatively low efficiency as has been reported in some literature.

**Table 5.16** Epoxide content (%), average molecular weight ( $\bar{M}_w$  and  $\bar{M}_n$ ) and fraction of bonds broken ( $\alpha$ ) of degradation of NR using H<sub>5</sub>IO<sub>6</sub>

Reaction Time (hours)	0.20 mol/mol of H <sub>5</sub> IO <sub>6</sub> /isoprene unit					
	Epoxide content (%)	$[\eta]$	$\bar{M}_v \times 10^4$	$\bar{M}_w \times 10^4$	$\bar{M}_n \times 10^4$	$\alpha$ (%)
0	0	5.88	117.94	129.49	20.62	0
8	0	0.59	8.03	15.87	2.53	0.24
12	0	0.43	5.59	11.75	1.90	0.32
21	2.62	0.33	3.97	9.16	1.46	0.44
30	2.60	0.22	2.50	6.38	1.02	0.64

\*  $\bar{M}_v$ ,  $\bar{M}_w$  and  $\bar{M}_n$  are calculated from  $[\eta]$  using  $K = 3.46 \times 10^{-5}$  and  $a = 0.863$  (see section 2.3, Chapter V)

**Table 5.17** Epoxide content (%), average molecular weight ( $\bar{M}_w$  and  $\bar{M}_n$ ) of degraded rubber and fraction of bonds broken ( $\alpha$ ) obtained from degradation of PNR using H<sub>5</sub>IO<sub>6</sub>

Reaction Time (hours)	0.20 mol/mol of H <sub>5</sub> IO <sub>6</sub> /isoprene unit					
	Epoxide content (%)	$[\eta]$	$\bar{M}_v \times 10^4$	$\bar{M}_w \times 10^4$	$\bar{M}_n \times 10^4$	$\alpha$ (%)
0	0	4.31	81.94	97.43	15.51	0
8	3.45	0.51	6.74	13.85	2.21	0.27
12	3.15	0.33	4.04	9.28	1.48	0.42
21	2.45	0.24	2.77	6.92	1.10	0.58
30	2.65	0.22	2.47	6.32	1.01	0.63

\*  $\bar{M}_v$ ,  $\bar{M}_w$  and  $\bar{M}_n$  are calculated from  $[\eta]$  using  $K = 3.46 \times 10^{-5}$  and  $a = 0.863$  (see section 2.3, Chapter V)

**Table 5.18** Epoxide content (%), average molecular weight ( $\bar{M}_w$  and  $\bar{M}_n$ ) of and fraction of bonds broken ( $\alpha$ ) obtained by degradation of PNR using  $H_5IO_6$  together and  $H_2O_2$

Reaction Time (hours)	0.20 mol/mol of $H_5IO_6$ /isoprene unit and 0.30 mol/mol of $H_2O_2$ /isoprene unit					
	Epoxide content (%)	$[\eta]$	$\bar{M}_v \times 10^4$	$\bar{M}_w \times 10^4$	$\bar{M}_n \times 10^4$	$\alpha$ (%)
0	0	4.31	81.94	97.43	15.51	0
2	0	0.45	5.74	12.21	1.94	0.57
4	5.86	0.37	4.62	10.31	1.64	0.97
8	5.48	0.27	3.14	7.62	1.21	0.89
12	7.06	0.19	2.16	5.69	0.91	1.29
21	6.7	0.15	1.58	4.45	0.71	1.49
30	5.76	0.13	1.33	3.89	0.62	1.45

\*  $\bar{M}_v$ ,  $\bar{M}_w$  and  $\bar{M}_n$  are calculated from  $[\eta]$  using  $K = 3.46 \times 10^{-5}$  and  $a = 0.863$  (see section 2.3, Chapter V)

**Table 5.19** Epoxide content (%), average molecular weight ( $\bar{M}_w$  and  $\bar{M}_n$ ) and fraction of bonds broken ( $\alpha$ ) obtained from degradation of EPNR using  $H_5IO_6$

Reaction Time (hours)	1.33 mol/mol of $H_5IO_6$ /epoxide unit and 0.245 mol/mol of $H_5IO_6$ /isoprene unit					
	Epoxide content (%)	$[\eta]$	$\bar{M}_v \times 10^4$	$\bar{M}_w \times 10^4$	$\bar{M}_n \times 10^4$	$\alpha$ (%)
0	18.94	4.31*	87.94	97.43	15.51	0
2	18.45	0.36	4.42	9.96	1.59	0.40
4	18.73	0.25	2.95	7.26	1.16	0.57
8	17.46	0.16	1.68	4.68	0.74	0.91
12	16.07	0.12	1.18	3.56	0.57	1.19
21	17.64	0.11	1.09	3.34	0.53	1.29

\*is the  $[\eta]$  and molecular weight calculated from PNR which was assumed that the  $[\eta]$  and molecular weight after epoxidation are constant comparing with PNR starting material

\*  $\bar{M}_v$ ,  $\bar{M}_w$  and  $\bar{M}_n$  are calculated from  $[\eta]$  using  $K = 3.46 \times 10^{-5}$  and  $a = 0.863$  (see section 2.3, Chapter V)

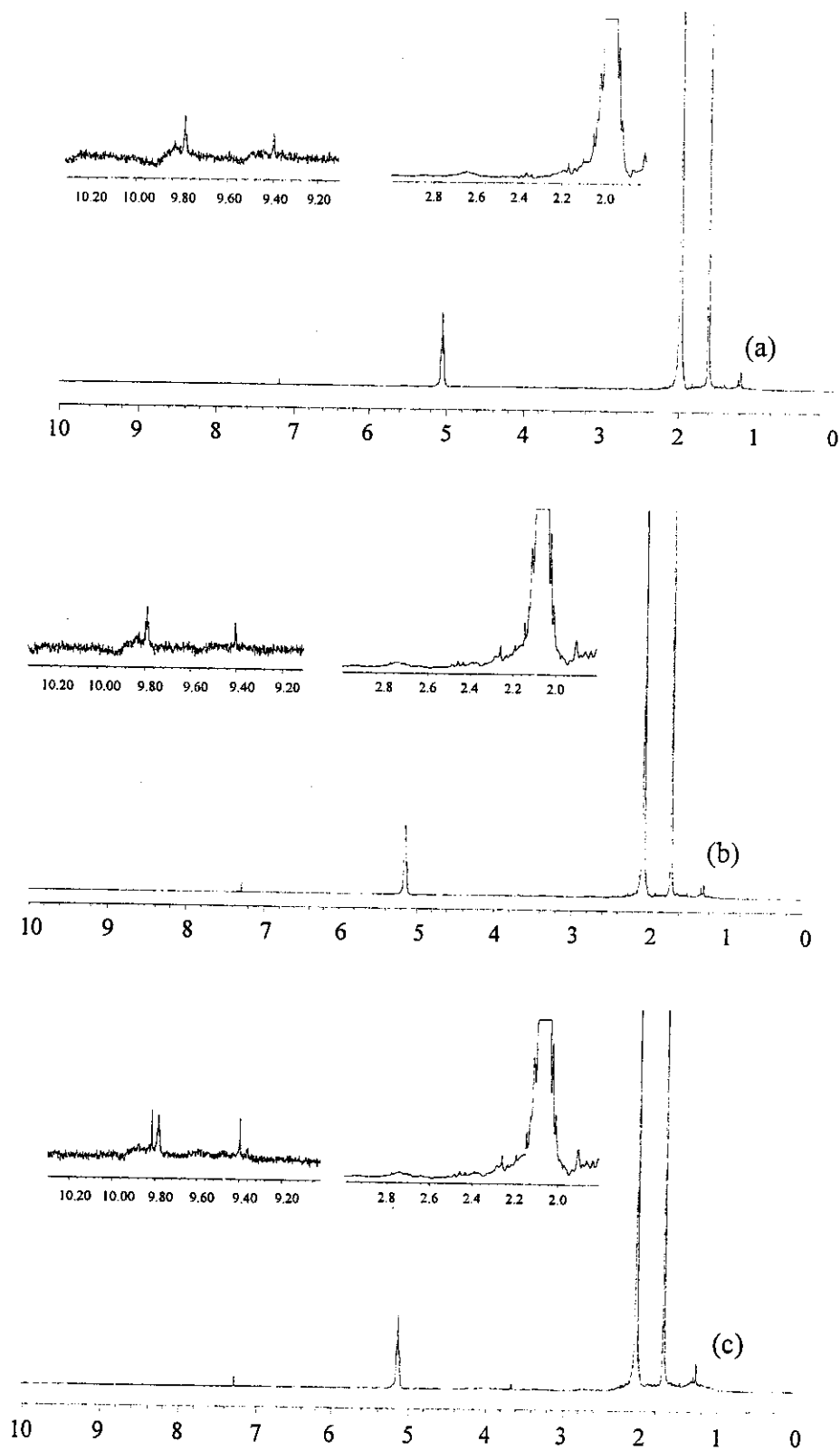


**Figure 5.43**  $^1\text{H}$  NMR spectra of (a) LNR ( $\text{NR}+\text{H}_5\text{IO}_6$ ), (b) LPNR ( $\text{PNR}+\text{H}_5\text{IO}_6$ ) and (c) LPNR ( $\text{PNR}+\text{H}_5\text{IO}_6+\text{H}_2\text{O}_2$ )

#### 3.4.3.4 Proposed degradation mechanism of rubber by periodic acid

Generally, periodic acid is effectively used to degrade organic compound containing vic-diol structure. However, it was found by Reyx D and Campistron I [47] that the molecular weights of the epoxidized polydienes such as synthetic and natural polyisoprene were reduced after the treatment with periodic acid. They found also the reduction of the epoxide group in the resulting product. These authors proposed that the epoxide rings in the epoxidized rubber were hydrolysed into vic-diols which were then followed by the conventional degradation reaction of the periodic acid. Gillier-Ritoit S et al. [60] studied the degradation of polyisoprene (PI) and the epoxidized polyisoprene (EPI) by the use of periodic acid in organic media. They proposed that in the case of the degradation of PI, the polymer chain was transformed into epoxidized compounds and vic-diol structures, then the epoxide was hydrolysed into vic-diols. All vic-diol structures were then degraded into smaller molecules. Mauler RS et al. found that the periodic acid can be used to degrade SBR with or without the presence of ultrasonic radiation. [58] The SBR did not contain any epoxidized fraction in the molecular chain. It seems likely that the periodic acid can break the C=C on the butadiene moiety in the molecular chain. The authors did not propose the reaction pathway. In our case, it was found in all the conditions used that the epoxide contents before and after degradation of epoxidized rubber were approximatedly the same. It seems likely that the existing epoxides did not involve in the degradation process. When the NR and PNR which did not contain the epoxide group were treated with periodic acid, the chain degradation was found to be effectively occurred but at a lower rate than the use of epoxidized rubber (EPNR). This may be proposed that the EPNR has higher polarity than the NR and PNR, therefore the interaction of the EPNR with the polar molecule like periodic acid is more compatible. As the reaction was carried out in aqueous solution, it can be proposed that the periodic acid acts as an oxidizing agent similar to potassium permanganate which oxidizes alkene compound into vic-diol. Then the carbon-carbon bond of the vic-diol was later cleaved by another molecule of periodic acid as shown in Figure 5.44. It may be also possible that the periodic acid oxidized the C=C unit into epoxide function but at a very low amount as there is not an increase of the epoxide content in any of the resulting product. The

OK

important

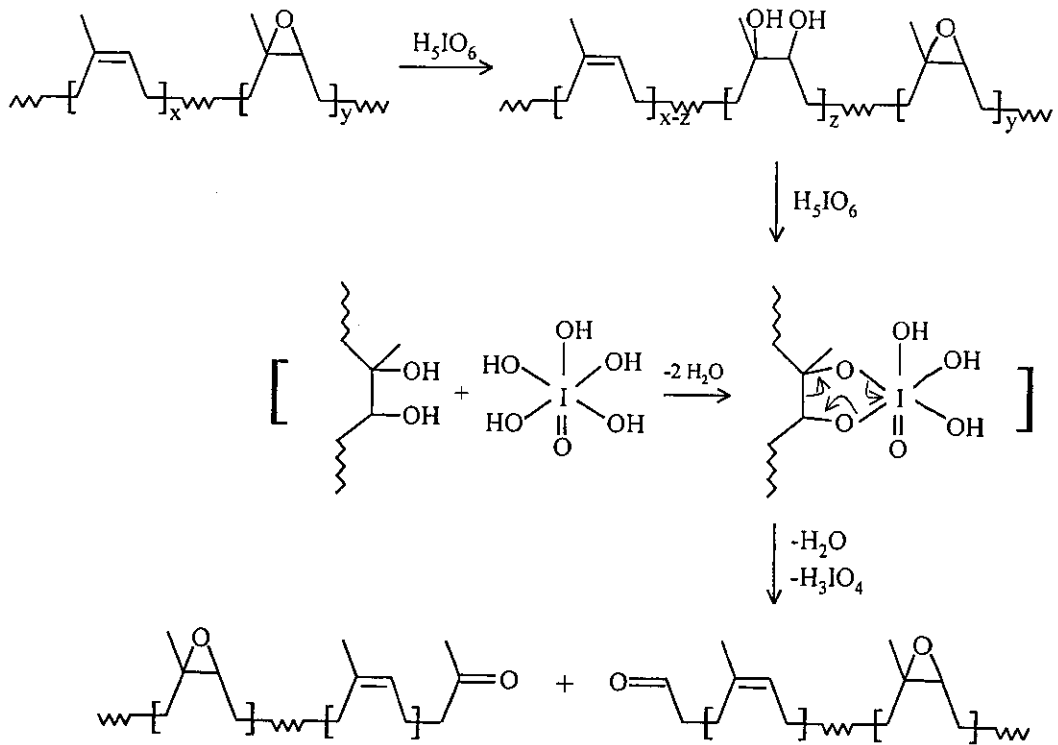


**Figure 5.44** Proposed degradation reaction pathway of epoxidized purified natural rubber (EPNR) by periodic acid

presence of the epoxide in the rubber chain may accerelate the degradation due to the increased polarity of the rubber.

#### 4. Addition of Acrylic Acid onto Epoxidized Molecules

The addition of acrylic acid onto oxirane ring is considered as a nucleophilic addition reaction. In our study, excess of acrylic acid was used, therefore the epoxide ring opening reaction can be occurred via self-acid catalyst system. 4,5-epoxy-4-methyloctane (EMO) was used as a model compound for studying the epoxide ring opening reaction by acrylic acid. Then, addition of acrylic acid onto epoxidized liquid synthetic rubber (EIR) and epoxidized liquid natural rubber were investigated.

##### 4.1 Addition of acrylic acid onto 4,5-epoxy-4-methyloctane

4,5-epoxy-4-methyloctane (EMO) was synthesized by the epoxidation of 4-methyl-4-octene with *m*-chloroperbenzoic acid (MCPBA) in dichloromethane at 0°C. The EMO obtained was characterized by using NMR spectroscopy and supercritical fluid chromatography (SFC). The characteristic signals of the EMO in <sup>1</sup>H NMR were observed at 2.68 ppm (proton adjacent to the epoxide), 1.24 and 1.28 ppm (cis- and trans-methyl protons attached to oxirane unit).

Then, the EMO dissolved in toluene was treated with an excess amount of acrylic acid (10 fold per mole of oxirane unit) at 70°C. The products obtained after 48 hours of reaction were analyzed by <sup>1</sup>H NMR, <sup>13</sup>C NMR, IR spectroscopies and SFC as well as gas chromatography-mass spectroscopy (GC-MS).

Generally, nucleophilic addition of unsymmetrical epoxide in acidic medium is occurred at the most substituted carbon atom of epoxide ring i.e. protonation reaction is occurred in the first step at the oxygen atom of the ring forming the intermediate I-1 as shown in Figure 5.45. Then, the protonated product (I-1) is converted into the most stable carbocationic intermediate (I-2) before the addition with a nucleophilic reagent or acrylate anion (<sup>-</sup>OOC-CH=CH<sub>2</sub>). Therefore, only one addition product should be obtained i.e. the compound (3).

However, in our system, the signals of <sup>1</sup>H NMR shown in Figure 5.46 revealed mixture products of the reaction. It was found that after 2 hours of acrylation reaction, the decrease of the characteristic signal of epoxide ring at 2.68 ppm was observed. While the signals of the mixture of the acrylate function at 6.14-6.20 ppm were detected as well as a weak signal at 6.03-6.14. Increasing of the reaction time to 5

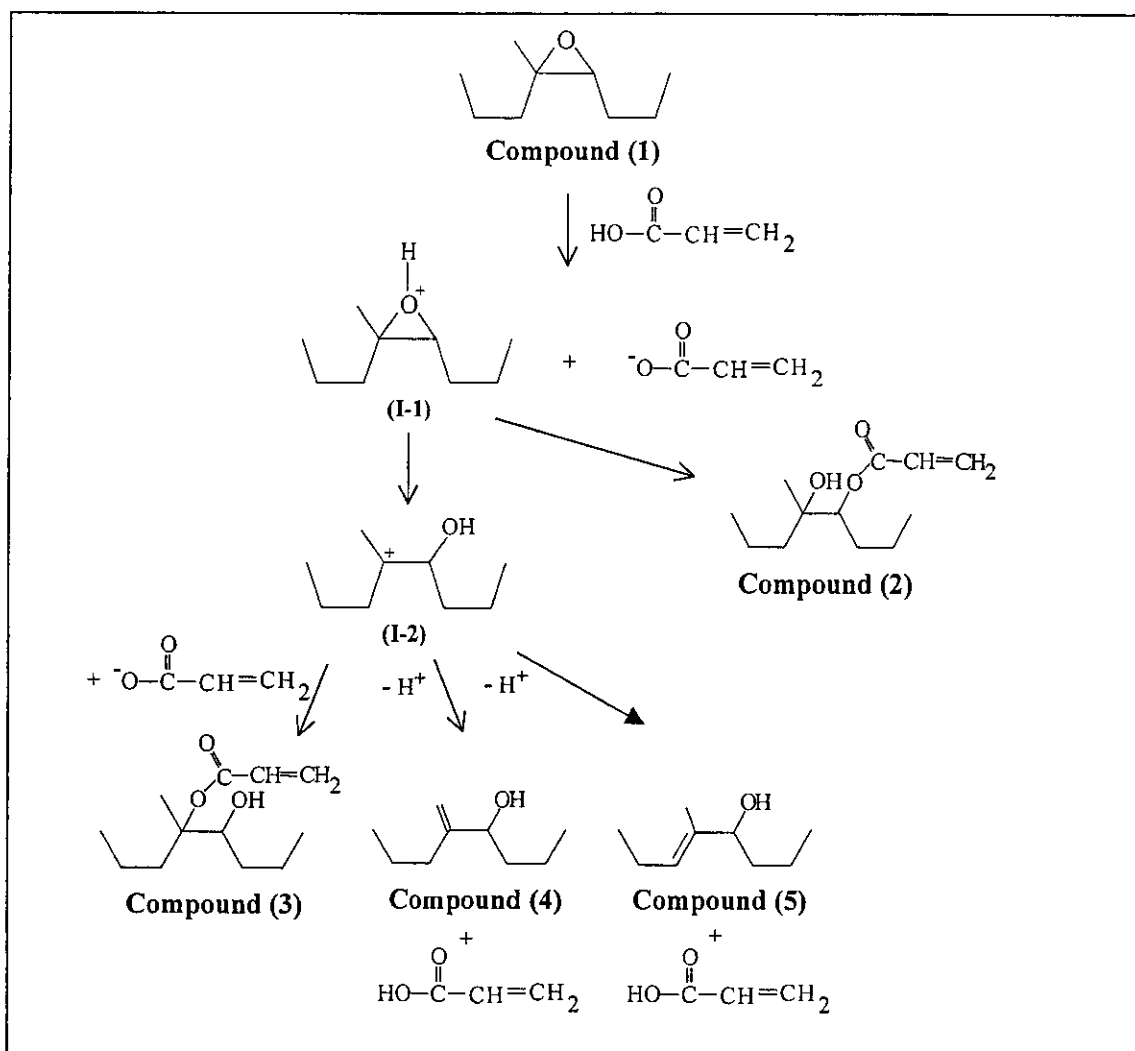


**Figure 5.45** Proposed the mechanism of addition reaction of excess acrylic acid onto 4,5-epoxy-4-methyloctane

hours, the intensity of the signal of the acrylated product at 6.06-6.13 ppm was higher, while the intensity of the signal at 6.14-6.20 ppm seems to be smaller. At 48 hours, the signal at 6.14-6.20 ppm was almost disappeared but the signal at 6.06-6.13 was significantly increased. It can be proposed that the signal at 6.06-6.13 was the main acrylated product or compound (3), and the signal at 6.14-6.21 ppm belongs to another possible acrylated product or compound (2). It was noticed that compound (2) was detected before the signal of the compound (3) at 2 hours. It can be postulated that the addition of the acrylic acid onto the protonated epoxide ring (I-1) forming the acrylated compound (2) is faster than the formation of the carbocationic intermediate (I-2). There were also two weak signals at 4.05 and 3.96 ppm, which can be assigned

to the methine proton adjacent to hydroxyl groups of compound (4) and (5) respectively. These two compounds can be possibly occurred by the loss of proton of carbon next to the carbocationic intermediate I-2, forming alkene function. The assignment of the signals of proton in  $^1\text{H}$  NMR spectrum of the EMO or compound (1), compounds (2)-(5) are presented in Figure 5.47.

The percentage of each compound in the mixtures at various reaction times can be signals in  $^1\text{H}$  NMR spectroscopy as shown in eq. (5.14)-(5.18).

$$\% \text{ Compound (1)} = \left( \frac{A_{2.68}}{A_x} \right) \times 100 \quad (5.14)$$

$$\% \text{ Compound (2)} = \left( \frac{A_{6.14}}{A_x} \right) \times 100 \quad (5.15)$$

$$\% \text{ Compound (3)} = \left( \frac{A_{6.06}}{A_x} \right) \times 100 \quad (5.16)$$

$$\% \text{ Compound (4)} = \left( \frac{A_{4.05}}{A_x} \right) \times 100 \quad (5.17)$$

$$\% \text{ Compound (5)} = \left( \frac{A_{3.96}}{A_x} \right) \times 100 \quad (5.18)$$

Where  $A_x$  = the integration area of proton from methyl proton at the two ends chain of the product obtained (the integration area at 0.82-1.01 divided by 6)

$A_{2.68}$  = the integration area of proton adjacent to oxirane unit

$A_{6.14}$  = the integration area of the proton adjacent to  $\text{C}=\text{C}$  of 4-methyl-5-acrylated-4-octanol (compound (2))

$A_{6.06}$  = the integration area of the proton adjacent to  $\text{C}=\text{C}$  of 5-methyl-5-acrylated-4-octanol (compound (3))

$A_{4.05}$  = integration area of the methine proton adjacent to alcohol of 2-propyl-1-hexene-3-ol (compound (4))

$A_{3.96}$  = integration area of the proton adjacent of alcohol of 5-methyl-5-octene-4-ol (compound (5))

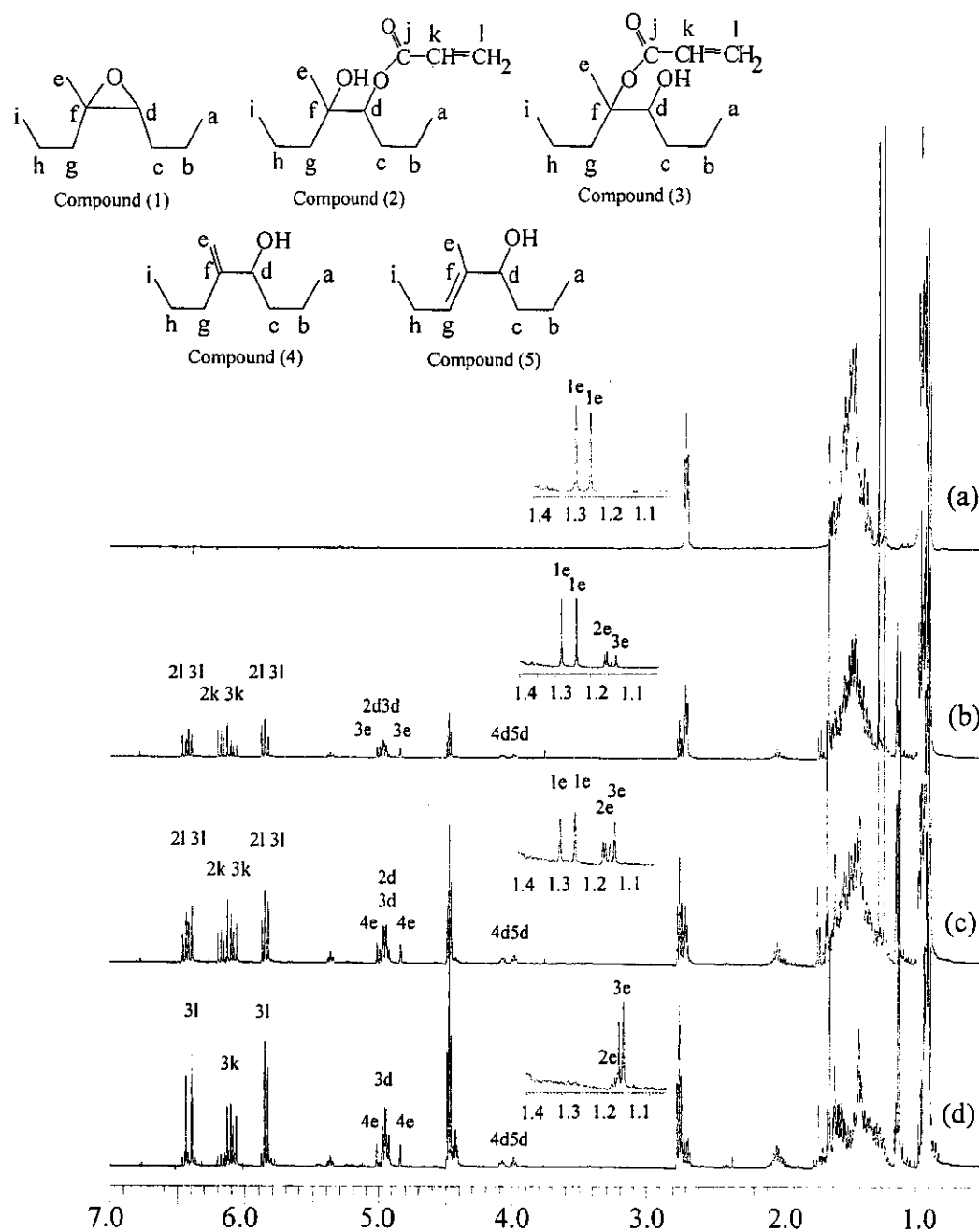


**Figure 5.46** <sup>1</sup>H NMR spectra of (a) 4,5-epoxy-4-methyloctane (EMO), (b) Mixture product obtained after 2 hours of acrylation reaction, (c) Mixture product obtained after 5 hours of acrylation reaction and (d) Mixture product obtained after 48 hours of acrylation reaction

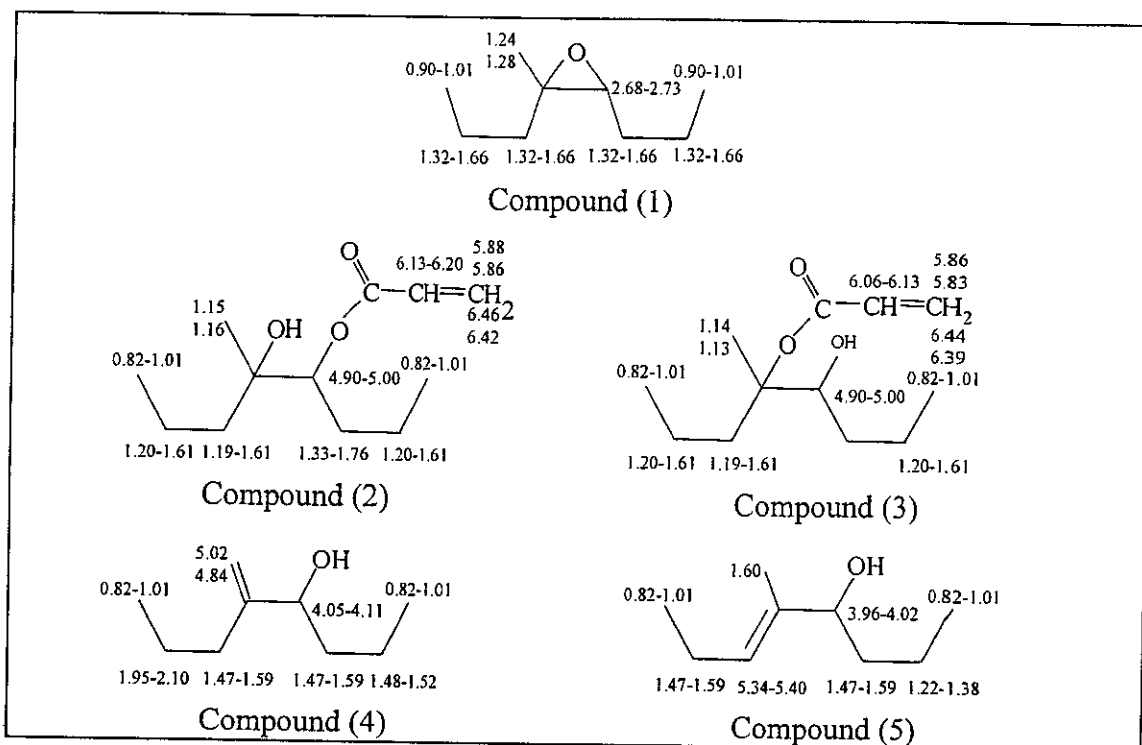


**Figure 5.47** Chemical shifts assignment in  $^1\text{H}$  NMR analysis of various chemical structures of mixture obtained from addition reaction of acrylic acid onto 4,5-epoxy-4-methyloctane

It was found that at 1 hour of acrylation reaction, the compound (2) was occurred 8 % while the compound (3) was occurred only 2%. After 2 hours of reaction, compound (2) and compound (3) were increased to 20% and 8%, respectively. 2-propyl-1-hexene-3-ol or compound (4) and 5-methyl-5-octene-4-ol or compound (5) were found at this reaction time to be 5% and 3%. After 5 hours of reaction, the compound (2) was decreased to 13% compound, while the compound (3), (4) and (5) were kept increasing to 30%, 7% and 7% compound, respectively. At longer reaction times (10 to 48 hours), the compound (2) was slowly decreased to 7 (10 hours of reaction) and to 5% (48 hours of reaction). The compound (3) was significantly increased from 44% to 67% at 10 and 48 hours of reaction, respectively. The compound (4) and (5) showed the change between 8 to 12% (between 10 to 48 hours of reaction), respectively. It was found the decrease of compound (2) and the increase of compound (3) at longer reaction time. The results of total combination of the amount of mixture products at various reaction times particularly at 48 hours were close to the starting epoxide content (93% oxirane units), it may be postulated that the

compound (2) may be partially transformed to compound (3) via intramolecular 5-membered ring transesterification reaction. The formation of the compound (2) more than the compound (3) at an early stage of reaction may be due to the addition of the nucleophile or acrylate anion to the less steric site of the intermediate I-1 is preferable.

Figure 5.48 showed the decreased of EMO and the progress of each resulting product obtained from acrylation reaction under self-acid catalyst. It was clearly seen that at longer reaction time, the compound (1) was decreased while the compound (2) + (3) were increased. At 48 hours of reaction time, the acrylated compound (2) + (3) were 72%, the compound (4) was 9% and the compound (5) was also 9%.

$^{13}\text{C}$  NMR spectra in Figure 5.49 showed the decrease of EMO by the observation of the change of the characteristic signal of oxirane carbon at  $\delta = 63.74$  and  $62.48$  ppm (cis- and trans- of quaternary carbon attached to epoxide function) and  $\delta = 59.73$  and  $59.65$  ppm (cis- and trans- of tertiary carbon attached to epoxide function) and the total disappearance of oxirane structure after 34 hours. The changes of acrylated compound (2) and (3) were observed at  $\delta = 130.05$  and  $130.03$  ppm (cis- and trans-carbon of  $=\text{CH}_2$  of compound (2)) and at  $\delta = 127.43$  ppm (carbon of  $\text{CH}=\text{}$  of compound (2)) and at  $\delta = 130.33$  and  $130.32$  (cis- and trans-carbon of  $=\text{CH}_2$  of compound (3)) and  $\delta = 126.96$  ppm (carbon of  $\text{CH}=\text{}$  of compound (3)), respectively. The characteristic signals detected by NMR spectroscopy corresponding to compound (1) to (5) were classified and shown in Figure 5.50. Similar results from  $^{13}\text{C}$  NMR spectrum were observed as from  $^1\text{H}$  NMR that at the beginning of acrylation reaction, compound (2) was occurred and progressively the compound (3) was appeared while the compound (2) was reduced.

Figure 5.51 showed the infrared spectrum of the products mixture after 48 hours of reaction. The spectrum showed the disappearance of the main absorption characteristic signal of epoxy group at  $1250\text{ cm}^{-1}$  (epoxy: whole ring stretching) and  $870\text{ cm}^{-1}$  (epoxy: half ring stretching) and the presence of the main absorption peak of acrylate group at  $1732\text{ cm}^{-1}$  (ester groups) and  $3500\text{ cm}^{-1}$  (OH groups). In addition, it appeared the new absorption peaks, which were directly related to the double bond of

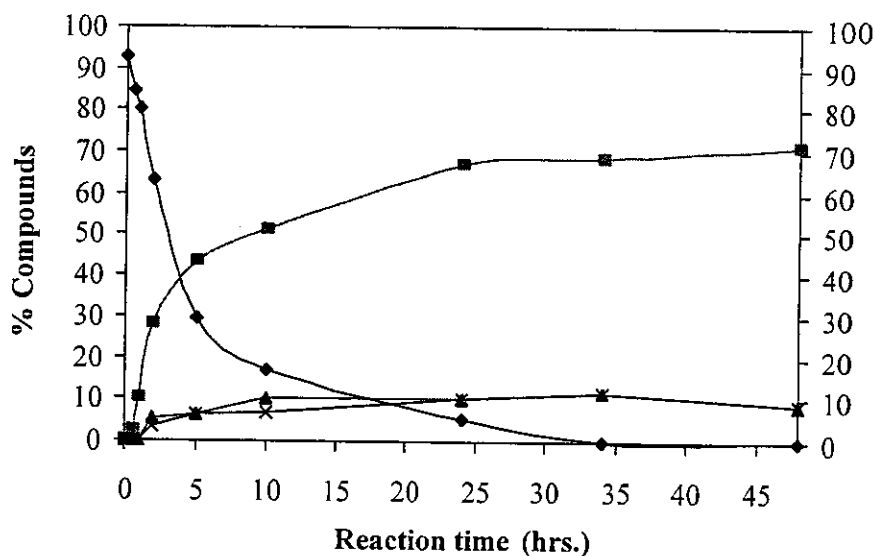


**Figure 5.48** Progression of products obtained from acrylation reaction onto 4,5-epoxy-4-methyloctane; (♦) Compound (1), (■) Compound (2) + (3), (▲) Compound (4) and (x) Compound (5)

acrylate function at  $1637\text{ cm}^{-1}$  and  $1620\text{ cm}^{-1}$  (C=C stretching),  $1409\text{ cm}^{-1}$  (=CH<sub>2</sub> deformation),  $1059\text{ cm}^{-1}$  (=CH<sub>2</sub> rocking),  $985\text{ cm}^{-1}$  (trans CH wagging) and  $810\text{ cm}^{-1}$  (=CH<sub>2</sub> twisting) [12].

The products mixture obtained from the acrylation reaction were analyzed by supercritical fluid chromatography (SFC). It was found by this technique that at an early stage of reaction time, five types of products were occurred in the mixture i.e. products compound (1), (2), (3), (4) and (5) (as shown in Appendix ). The SFC showed the characteristic signal corresponding to epoxidized unit (EMO) at  $16.53 \times 10^1$  minute. The acrylated compound (2) was detected at  $19.27 \times 10^1$  minute at the beginning of the reaction. At longer reaction time, the characteristic area of acrylated compound (2) was decreased, with an increase of characteristic area of acrylated compound (3) at  $22.50 \times 10^1$  minute. The alcohol compound (4) and (5) were observed at  $17.25 \times 10^1$  minute. No signal corresponding to acrylic acid was observed at  $15.27 \times 10^1$  minute in the resulting product.

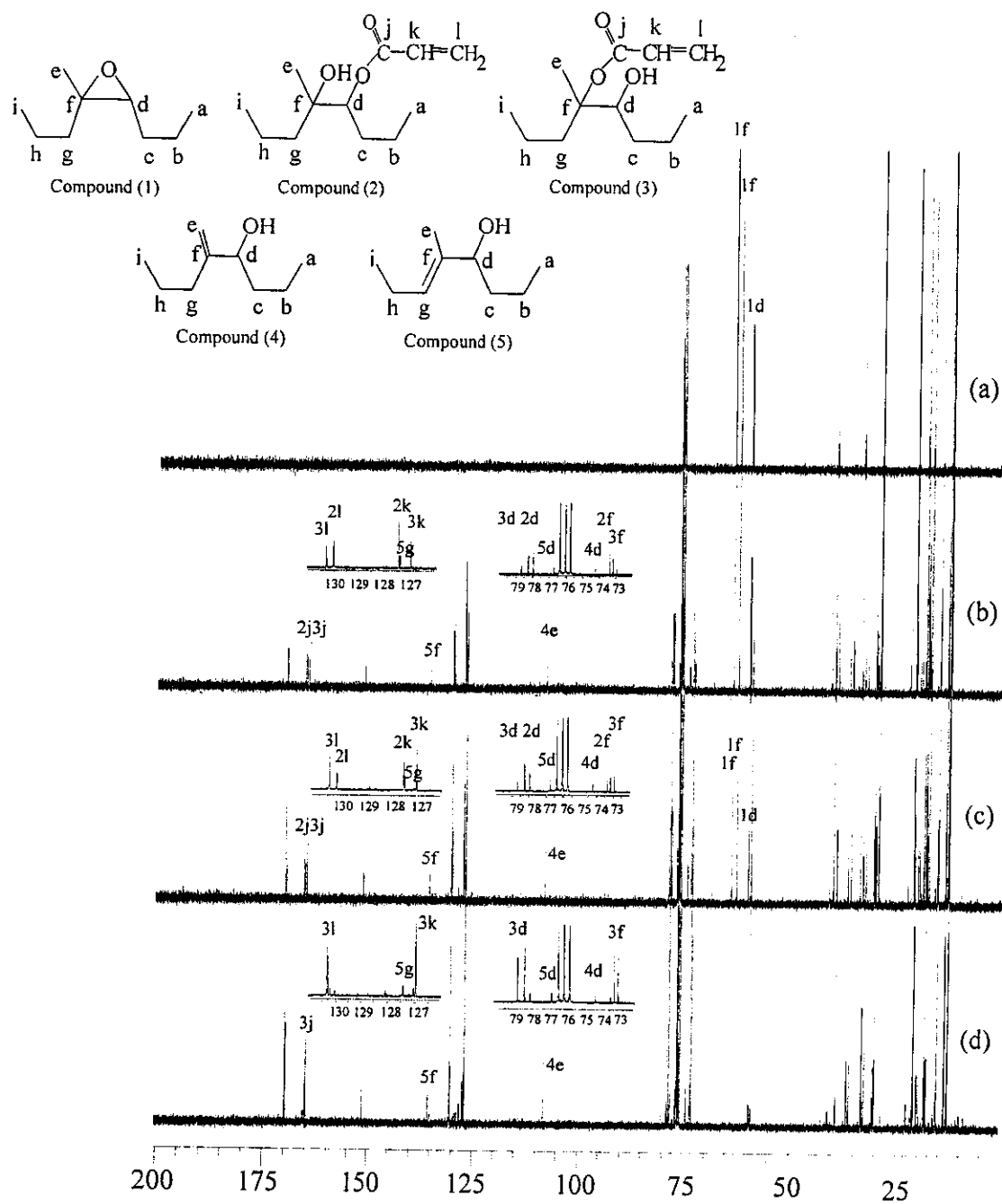


**Figure 5.49** <sup>13</sup>C NMR spectra of (a) 4,5-epoxy-4-methyloctane (EMO), (b) Mixture product obtained after 2 hours of acrylation reaction, (c) Mixture product obtained after 5 hours of acrylation reaction and (d) Mixture product obtained after 48 hours of acrylation reaction

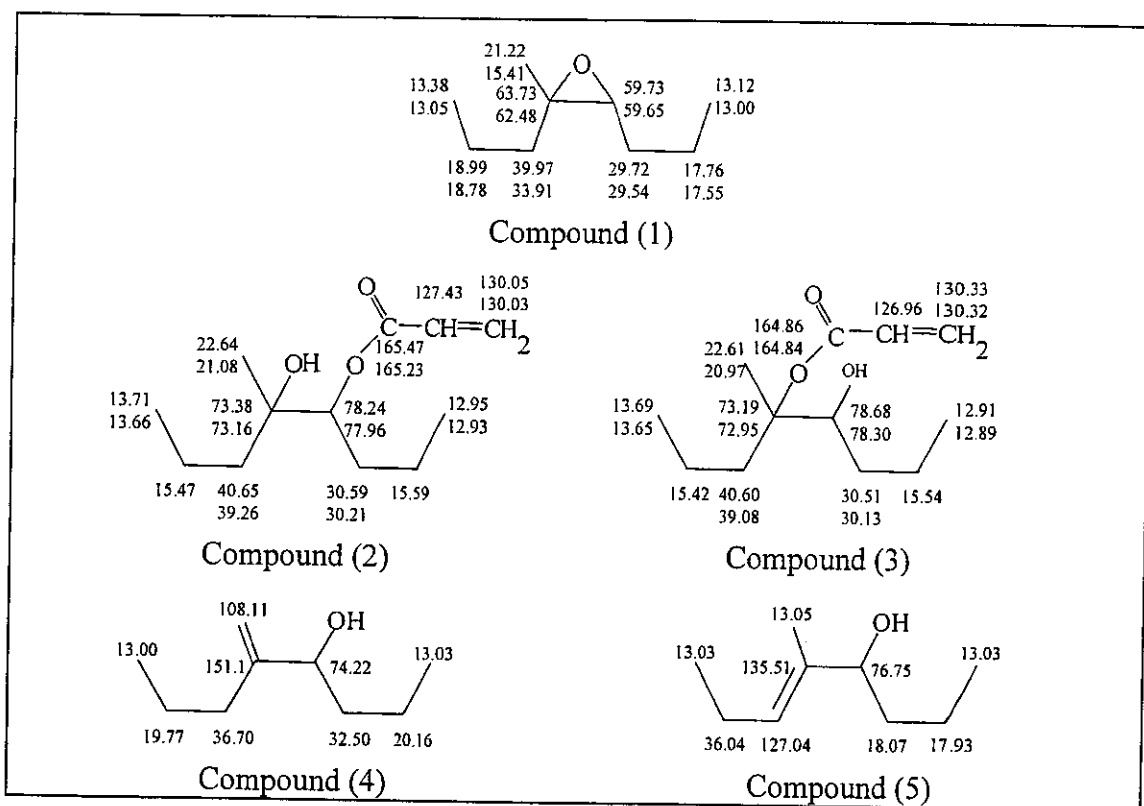


Figure 5.50 Structural analysis characterized by <sup>13</sup>C NMR spectroscopy

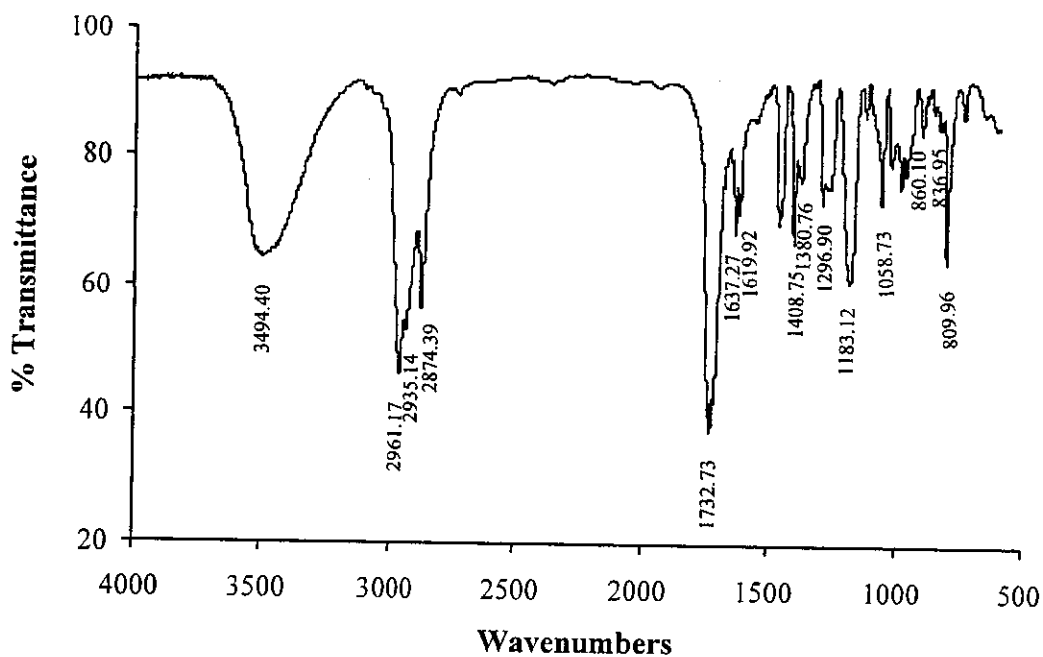


Figure 5.51 Infrared spectrum of products mixture obtained from acrylation reaction onto 4,5-epoxy-4-methyloctane after 48 hours

Gas chromatography-mass spectroscopy (GC-MS) had used to analyze the mixture of the acrylated products. The GC chromatogram of the product obtained at 10 hours of reaction showed 6 mains characteristic peaks which can be assigned to epoxide compound (cis- and trans-structures), compound (2), (3), (4) and (5). The cis- and trans-epoxidized compound (1) were separated at 6.5 and 6.9 minute, respectively. Compound (2), (3), (4) and (5) were assigned at 16.2, 22.0, 8.3 and 8.6 minute, respectively. At 48 hours of reaction, the characteristic peaks of cis- and trans- of compound (1) at 6.5 and 6.9 ppm were disappeared. The intensity of signal of 16.2 minute was decreased, while the peak intensity at 22.0 minute of compound (3) become very high which should be assigned as the main component of acrylated product. Compound (4) and (5) exhibited closely the same peak intensity at 10 and 48 hours of reaction time (as shown in Appendix ). The fraction of 6.5, 6.9, 8.3 and 8.6 minute were further analyzed by MS. The signal of  $m/z$  at 143 was detected. This may be corresponding to molecular weight of protonated of compound (1), (4) and (5) respectively. The other fraction at 16.2 and 22.0 minute exhibited the main signal of  $m/z$  at 197 and the weak signal at 215. These results were corresponding to molecular weight of protonated compound (2) and (3).

#### **4.2 Addition reaction of acrylic acid onto epoxidized liquid synthetic rubber**

Liquid synthetic rubber (LIR 30) containing 94 % of 1,4 polyisoprene units (64% cis- and 36% trans-structures) and 6% of 3,4 polyisoprene units was selected to prepare epoxidized liquid synthetic rubber (ELIR). The characteristic signals in  $^1\text{H}$  NMR of proton adjacent to  $\text{C}=\text{C}$  of 1,4-polyisoprene unit and 3,4-polyisoprene unit were observed at 5.11 and 4.65-4.75 ppm, respectively. The epoxidation of LIR was carried out by treating the LIR dissolved in dichloromethane with *m*-chloroperbenzoic acid at  $0^\circ\text{C}$ . The ELIR obtained showed the presence of extra signal in  $^1\text{H}$  NMR of proton adjacent to epoxide ring at 2.68 ppm. The signal of proton characteristic to 3,4-polyisoprene unit at 4.65-4.75 ppm was still relevant. It seems likely that the 3,4-polyisoprene unit was not epoxidized. The epoxidation level of the ELIR was determined by the integration area of signals at 2.68 ppm divided by the integration area of signal of 2.68+5.11+4.65+4.75 ppm. It was found that the ELIR contained

17% epoxide content. The Infrared spectrum of the ELIR revealed also the signal characteristic of epoxide ring at 1250 and 870  $\text{cm}^{-1}$ .

The acrylation reaction of ELIR was studied by using excess amount of acrylic acid (10 fold per mole of oxirane units). The infrared spectra of ELIR and the mixture products obtained after 72 hours of addition reaction were shown in Figure 5.52. The resulting product exhibited the same presentation of the decrease of oxirane characteristic signal at 1250  $\text{cm}^{-1}$  (epoxy: whole ring stretching) and 870  $\text{cm}^{-1}$  (epoxy: half ring stretching), compared to signal of methyl group of the isoprene unit at 1377  $\text{cm}^{-1}$ . The presence of new absorption band at 1727  $\text{cm}^{-1}$  can be assigned to the signal characteristic of carbonyl group of acrylate function. The signal at 3520  $\text{cm}^{-1}$  can be assigned to the signal of hydroxyl group. These two signals indicated the fixation of the acrylic acid onto the ELIR. The reduction of the signals at 1644  $\text{cm}^{-1}$  and 1621  $\text{cm}^{-1}$  ( $\text{C}=\text{C}$  stretching), 1405  $\text{cm}^{-1}$  ( $=\text{CH}_2$  deformation), 1057  $\text{cm}^{-1}$  ( $=\text{CH}_2$  rocking), 985  $\text{cm}^{-1}$  (trans CH wagging) and 810  $\text{cm}^{-1}$  ( $=\text{CH}_2$  twisting) compared to the signal of methyl group of isoprene unit at 1377  $\text{cm}^{-1}$  supported the occurrence of the acrylated EIR.

Figure 5.53 presented  $^1\text{H}$  NMR spectra of ELIR and the partially acrylated product after 72 hours of reaction times. Various chemical structures are proposed, I1, I2 and I3 represented the cis-1,4-, trans-1,4 and 3,4- polyisoprene units, respectively. The E1 and E2 represented the cis- and trans- epoxidized structures, respectively. The A1 and A2 represented two possible acrylated products and A3 and A4 represented two hydroxyl by-products. The spectra showed the presence of signals at 5.78-5.90, 6.01-6.24 and 6.34-6.49 ppm which can be assigned to three protons of acrylate function of the A1 and A2 structures, similar to compound (2) and (3) in section 5.1. The weak signal of secondary products i.e. two type of allyl alcohols (A3 and A4) at 4.00-4.10 and 3.92-3.99 ppm were also observed. Moreover, after long time of reaction (72 hours.), the spectra of the mixture still showed the presence of characteristic signal of oxirane units at 2.7 ppm (proton adjacent of oxirane units) and at 1.29 ppm (methyl proton adjacent of oxirane units). It will be seen that the epoxide ring of the ELIR was not totally opened by the acrylic acid after 72 hours in the condition used, as the signal of proton at 2.68 ppm is still relevant. It is proposed that

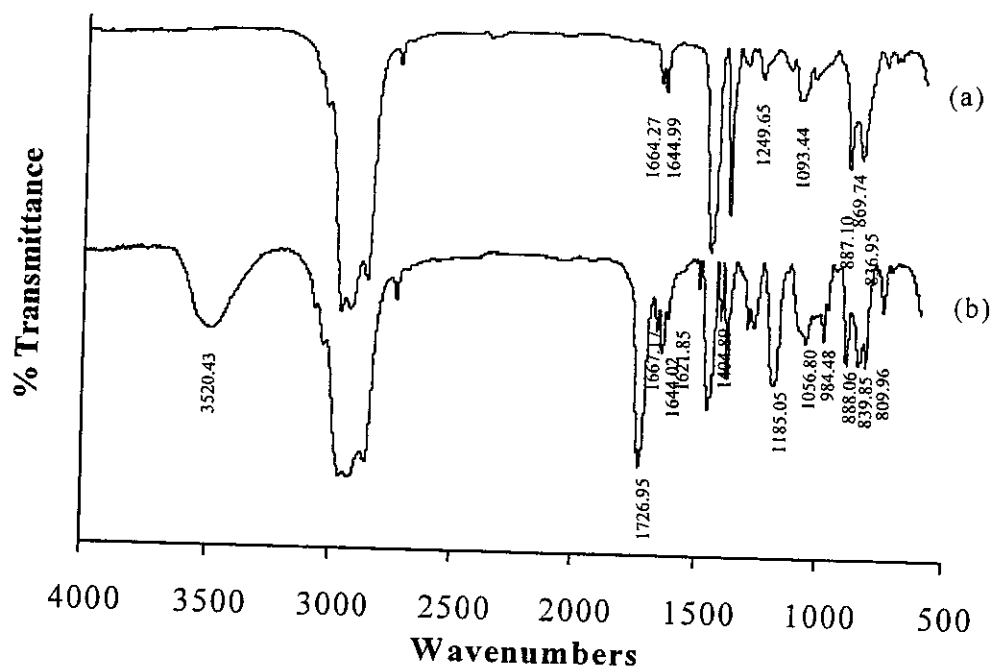


**Figure 5.52** Infrared spectra; (a) Epoxidized liquid synthetic rubber and (b) Acrylated liquid synthetic rubber

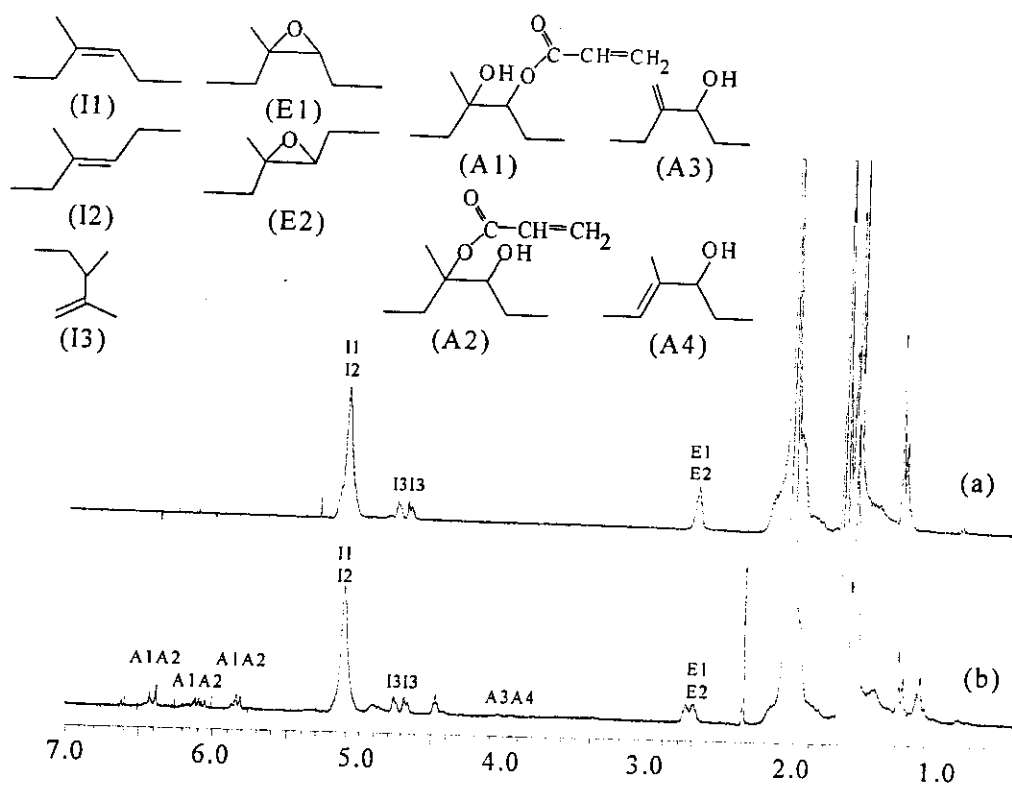


**Figure 5.53** <sup>1</sup>H NMR spectra; (a) Epoxidized liquid synthetic rubber and (b) Acrylated liquid synthetic rubber

the products obtained after the addition reaction of acrylic acid to high molecular weight elastomer (ELIR) are similar to the compound (1)-(5) in section 5.1.

Figure 5.54 showed the progress of acrylation reaction of the ELIR during 72 hours. It was found that the epoxide content (17 %) of the ELIR was reduced at longer reaction time while the percent of acrylated product was increased. The results exhibited the occurrence of about 6% acrylated structure or 35% yield from 17% epoxidized rubber or 100% yield of starting oxirane units. The two structures of alcohol by-products (A3 and A4) were found about 2 %. The  $^1\text{H}$  NMR also revealed the presence of 4% residual oxirane structure. Therefore, only about 12 % of epoxide units were transformed into the structures A1, A2, A3 and A4 including the residual epoxidized structure. Another 5% of the epoxidized units are transformed to unrecognized structures, possibly 5- and 7- cyclic structures. The chemical shift of proton adjacent to hydroxyl group of 5- and 7- cyclic ether were proposed to be occurred at 3.4 ppm similar to the signal found by Perera MCS et al. [72]. It can be noticed that the decrease of oxirane unit in this case is slower than in the case of the acrylation of EMO. The rate of addition reaction of acrylic acid onto the epoxide ring is slower than the addition onto EMO even though the reaction was carried out by using an excess acid system (10 fold per mole of oxirane units). This may be due to the very much higher molecular weight of ELIR than the EMO.

The percentage of different structural units presented in the molecular chain of the acrylated rubber can be calculated by using the signals in <sup>1</sup>H NMR spectrum and equations (5.19)-(5.22).

$$\% \text{ Epoxidized units} = \tag{5.19}$$

$$\left( \frac{A_{2.68}}{A_{2.68} + A_{5.11} + A_{(4.65+4.75)/2} + A_{(5.78+6.01+6.34)/3} + A_{4.00} + A_{3.92}} \right) \times 100$$

$$\% \text{ Acrylated units} = \tag{5.20}$$

$$\left( \frac{A_{(5.78+6.01+6.34)/3}}{A_{2.68} + A_{5.11} + A_{(4.65+4.75)/2} + A_{(5.78+6.01+6.34)/3} + A_{4.00} + A_{3.92}} \right) \times 100$$

$$\% \text{ Alcohol (A3) units} = \tag{5.21}$$

$$\left( \frac{A_{4.00}}{A_{2.68} + A_{5.11} + A_{(4.65+4.75)/2} + A_{(5.78+6.01+6.34)/3} + A_{4.00} + A_{3.92}} \right) \times 100$$

$$\tag{5.22}$$

$$\% \text{ Alcohol (A4) units} =$$

$$\left( \frac{A_{3.92}}{A_{2.68} + A_{5.11} + A_{(4.65+4.75)/2} + A_{(5.78+6.01+6.34)/3} + A_{4.00} + A_{3.92}} \right) \times 100$$

Where  $A_{2.68}$  = integration area of proton adjacent to oxirane unit

$A_{5.11}$  = integration area of proton adjacent to C=C of 1,4-polyisoprene unit

$A_{(4.65+4.75)/2}$  = integration area of proton adjacent to C=C of 3,4-polyisoprene unit ( $A_1 + A_2$ )

$A_{(5.78+6.01+6.34)/3}$  = integration area of proton adjacent to C=C of acrylated function

$A_{4.00}$  = integration area of proton adjacent to alcohol (A3)

$A_{3.92}$  = integration area of proton adjacent to alcohol (A4)

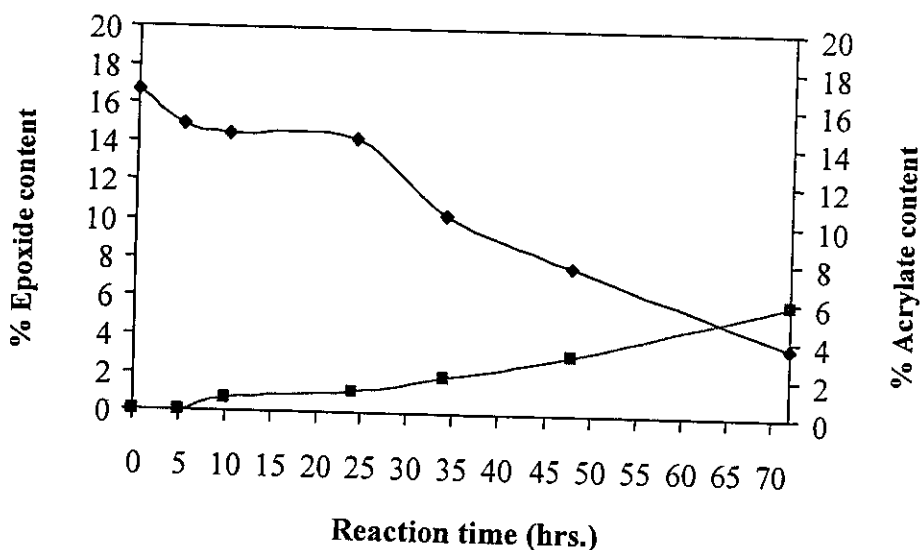


**Figure 5.54** Progression of acrylation reaction onto epoxidized liquid synthetic rubber; (◆) Epoxide content and (■) Acrylated content

#### 4.3 Addition reaction of acrylic acid onto epoxidized liquid purified natural rubber

Addition of acrylic acid onto epoxide unit of liquid purified natural rubber was carried out by using two types of rubbers; ELPNR and LEPNR. The ELPNR was the epoxidized rubber obtained from epoxidation of liquid natural rubber while the LEPNR was obtained from degradation of epoxidized natural rubber into low molecular weight. An excess amount of acrylic acid was used to react with the epoxidized rubbers. It was found that the acrylated rubbers obtained from both ELPNR and LEPNR showed the same characteristic signals in IR spectra and NMR spectra. Figure 5.55 showed the Infrared spectra of the epoxidized rubber and the acrylated product. The disappearance of characteristic absorption band of epoxide function at  $1250\text{ cm}^{-1}$  (epoxy: whole ring stretching) and  $870\text{ cm}^{-1}$  (epoxy: half ring stretching) as well as the appearance of new characteristic absorption band of acrylate function at  $1730\text{ cm}^{-1}$  (ester groups) and  $3500\text{ cm}^{-1}$  (OH groups) confirmed the acrylation reaction. The acrylated rubber also showed other characteristic signals at  $1640\text{ cm}^{-1}$  and  $1621\text{ cm}^{-1}$  corresponding to C=C stretching of isoprene unit and signals of C=C of acrylate function at  $1406\text{ cm}^{-1}$  ( $=\text{CH}_2$  deformation),  $1060\text{ cm}^{-1}$  ( $=\text{CH}_2$

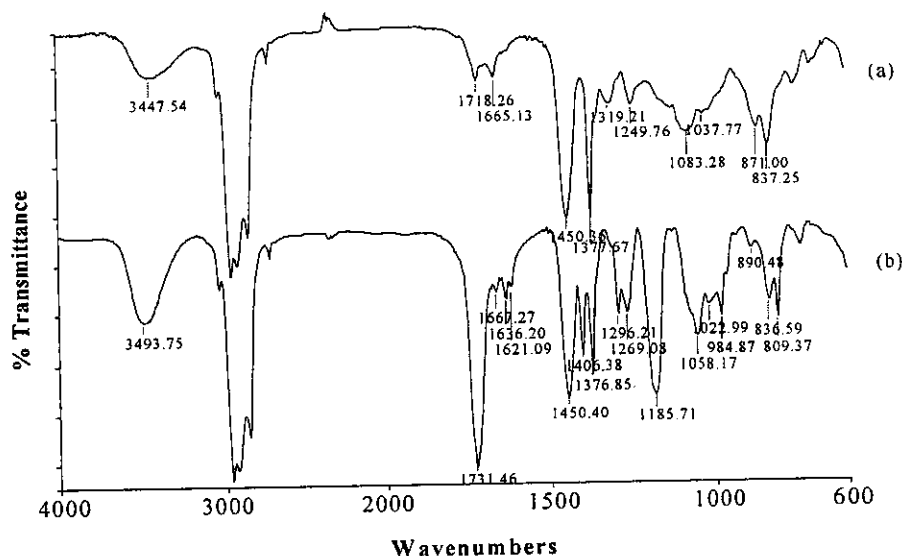
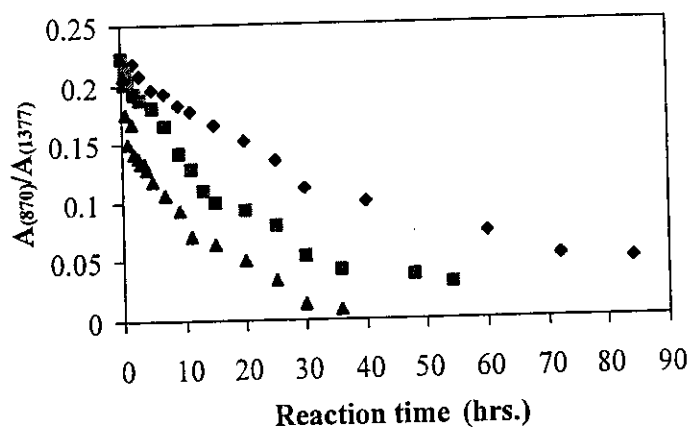


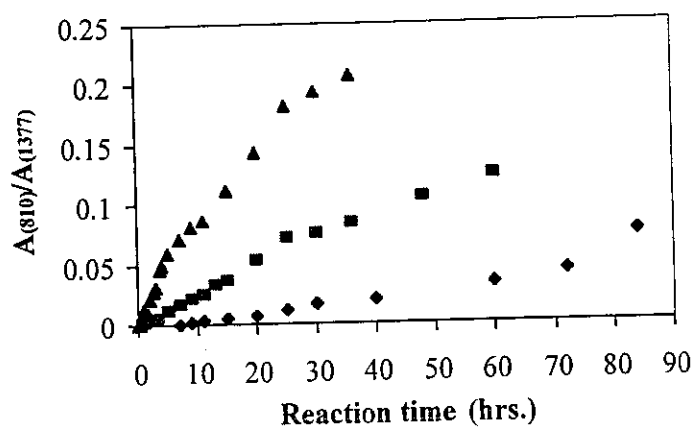
**Figure 5.55** Infrared spectra of (a) Epoxidized liquid purified natural rubber and (b) Acrylated liquid purified natural rubber

rocking),  $985\text{ cm}^{-1}$  (trans CH wagging) and  $810\text{ cm}^{-1}$  ( $=\text{CH}_2$  twisting). The methyl group of the isoprene unit was found at  $1377\text{ cm}^{-1}$ . The progress of addition reaction of acrylic acid can be followed by the ratio of the signal of epoxide ring at  $870\text{ cm}^{-1}$  to the signal of methyl group at  $1377\text{ cm}^{-1}$ , the ratio of signal at  $810\text{ cm}^{-1}$  ( $=\text{CH}_2$  twisting of acrylate function) and  $1377\text{ cm}^{-1}$  of the methyl group or the ratio of signal at  $1406\text{ cm}^{-1}$  ( $=\text{CH}_2$  deformation of the acrylate function) and  $1377\text{ cm}^{-1}$  of the methyl group.

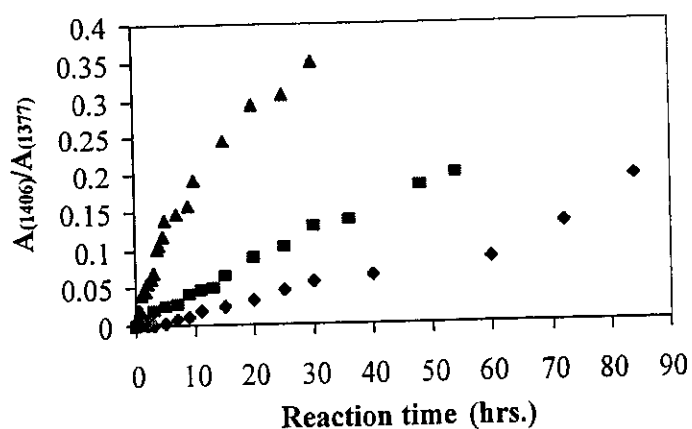
Figure 5.56 showed the progress at various reaction times of addition of excess amount of acrylic acid (10 fold per mole of oxirane unit) onto ELNR (28% oxirane units) at various temperatures ( $35$ ,  $50$  and  $70^\circ\text{C}$ ). The results exhibited the decrease of characteristic absorption band ratio of epoxide function ( $A_{871}/A_{1377}$ ) and increase of characteristic absorption band ratio of acrylate function ( $A_{1406}/A_{1377}$  and  $A_{810}/A_{1377}$ ). It can be seen that increasing reaction time, acrylation reaction is increasing. At  $70^\circ\text{C}$ , the epoxide ring opening reaction was completed before 40 hours. While at lower temperature, the epoxide ring is still present at 60 hours of reaction. It can be proposed that the rate of addition of acrylic acid onto the epoxide ring of the natural rubber depended on the reaction temperature. However, the disappearance of the epoxide ring



(A)



(B)



(C)

**Figure 5.56** Plots of absorption band ratio of signals in IR spectroscopy of acrylation reaction of epoxidized liquid natural rubber at various reaction temperatures i.e. ( $\blacklozenge$ ) 35 °C, ( $\blacksquare$ ) 50 °C and ( $\blacktriangle$ ) 70 °C; (A) Absorption band ratio of 870  $\text{cm}^{-1}$ / 1377  $\text{cm}^{-1}$ , (B) Absorption band ratio of 810  $\text{cm}^{-1}$ / 1377  $\text{cm}^{-1}$  and (C) Absorption band ratio of 1406  $\text{cm}^{-1}$ / 1377  $\text{cm}^{-1}$

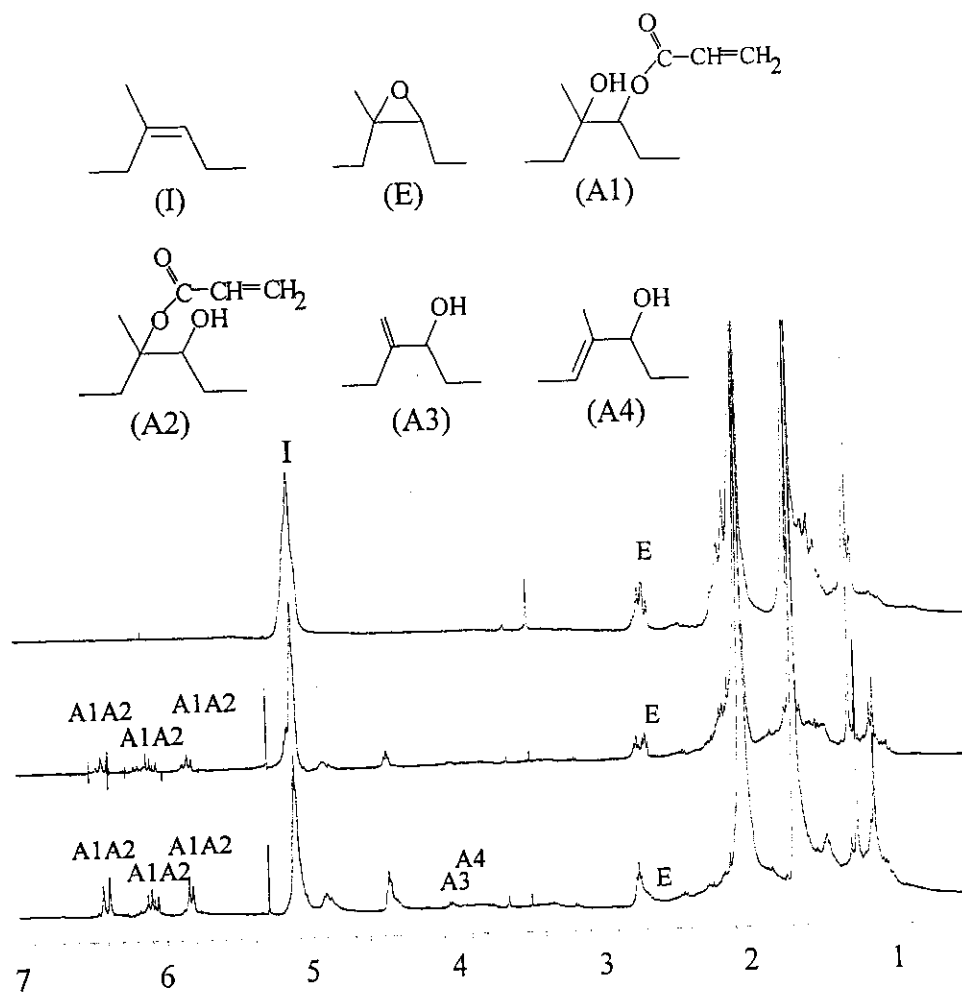


**Figure 5.57**  $^1\text{H}$  NMR spectra; (a) Liquid epoxidized liquid natural rubber, (b) Acrylated liquid natural rubber after 34 hours and (c) Acrylated liquid natural rubber after 70 hours

in Infrared spectrum can not be always used to represent the amount of the acrylic acid added onto the rubber as some side reactions can be occurred as shown in section 5.2 and 5.3.

$^1\text{H}$  NMR spectra of the acrylated products at 34 and 70 hours of reaction times are shown in Figure 5.57. Two types of acrylated rubbers (A1 and A2) seem to be occurred, due to the presence of the characteristic signals of three protons of acrylate function at 5.82-5.89, 6.05-6.21 and 6.37-6.48 ppm., similar to the signals of compounds (2) and (3) in section 5.1. The  $^1\text{H}$  NMR spectra also exhibited the formation of secondary products (allyl alcohol A3 and A4) because of the presence of

the signals at 3.92-4.00 and 3.82-3.91 ppm similar to the results obtained from acrylation of 4,5-epoxy-4-methyloctane and ELIR. Moreover, the spectra also reveal weak signal at 3.4 ppm which may be assigned to the formation of 5- and 7- cyclic ether [72].

The percentage of different structural units presented in the molecular chain of the acrylated natural rubber can be determined from the integration area of signals in  $^1\text{H}$  NMR analysis as shown in eq. (5.23)- (5.26).

$$\% \text{ Epoxidized units} = \quad (5.23)$$

$$\left( \frac{A_{2.68}}{A_{2.68} + A_{5.11} + A_{(5.82+6.05+6.37)/3} + A_{3.92} + A_{3.82}} \right) \times 100$$

$$\% \text{ Acrylated units} = \quad (5.24)$$

$$\left( \frac{A_{(5.82+6.05+6.37)/3}}{A_{2.68} + A_{5.11} + A_{(5.82+6.05+6.37)/3} + A_{3.92} + A_{3.82}} \right) \times 100$$

$$\% \text{ Alcohol (A3) units} = \quad (5.25)$$

$$\left( \frac{A_{3.92}}{A_{2.68} + A_{5.11} + A_{(5.82+6.05+6.37)/3} + A_{3.92} + A_{3.82}} \right) \times 100$$

$$\% \text{ Alcohol (A4) units} = \quad (5.26)$$

$$\left( \frac{A_{3.82}}{A_{2.68} + A_{5.11} + A_{(5.82+6.05+6.37)/3} + A_{3.92} + A_{3.82}} \right) \times 100$$

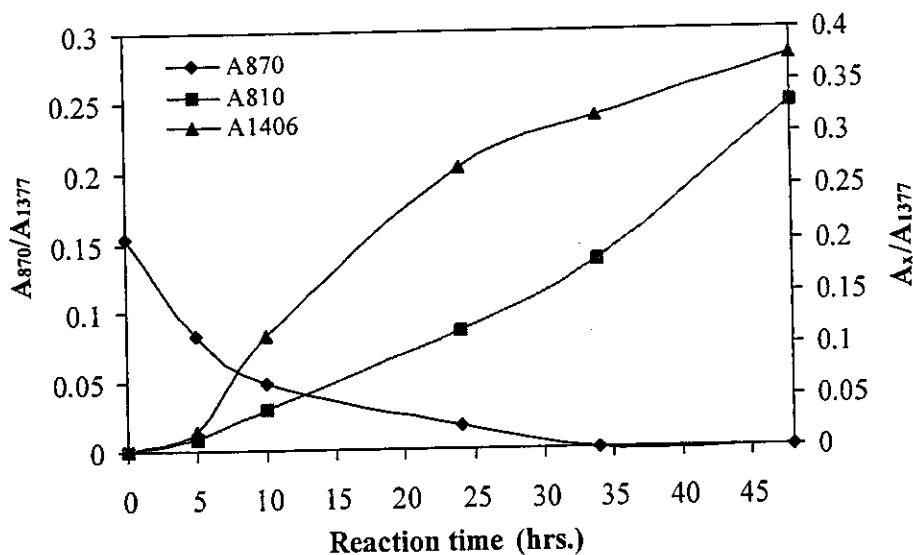
Where  $A_{2.68}$  = integration area of proton adjacent to oxirane unit

$A_{5.11}$  = integration area of proton adjacent to C=C of 1,4-polyisoprene unit

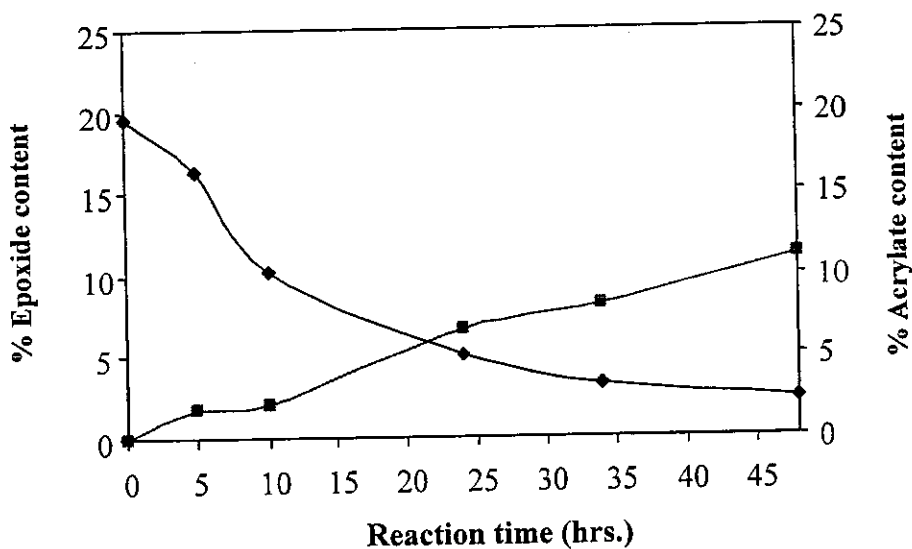
$A_{(5.82+6.05+6.37)/3}$  = integration area of the proton adjacent to C=C of acrylated function

$A_{3.92}$  = integration area of proton adjacent to alcohol (A4)

$A_{3.82}$  = integration area of proton adjacent to alcohol (A5)



(A)



(B)

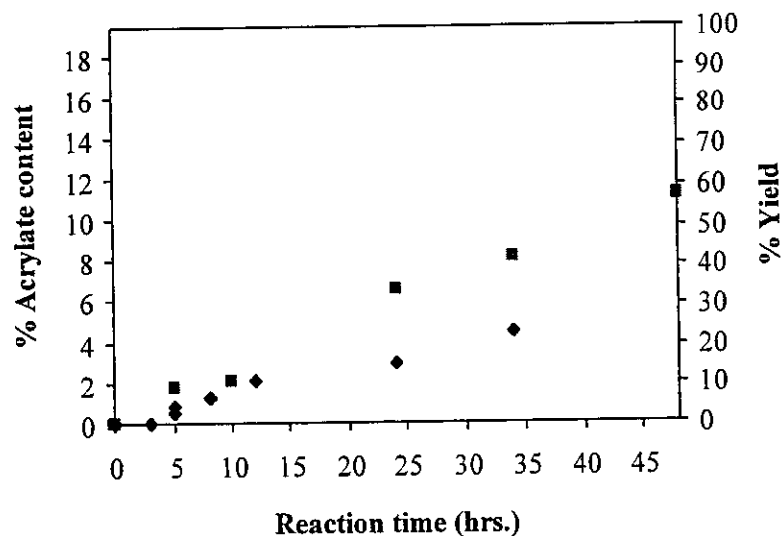
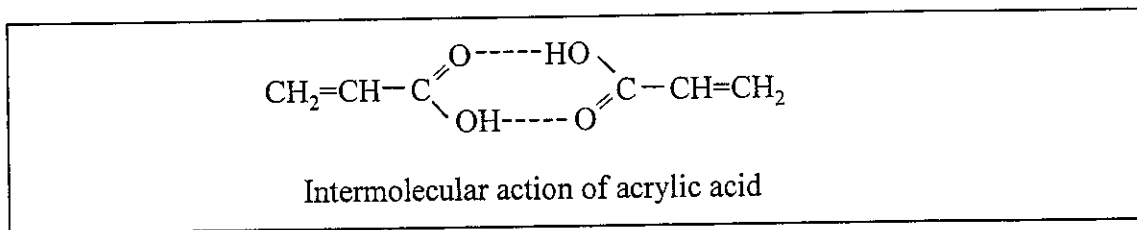
**Figure 5.58** (A) Absorption band ratio of signals from IR spectrum (B) % Epoxide content and % acrylate content determined from <sup>1</sup>H NMR of addition reaction of 10 fold per mole of acrylic acid onto LENR (19% epoxide compound) at 70°C

Figure 5.58 showed the comparison of the progress of addition reaction of 10 fold per mole of acrylic acid onto LENR (19% epoxide compound) at 70°C analyzed by IR and <sup>1</sup>H NMR spectroscopies. The results detected by IR spectroscopy showed the decrease of the ratio of oxirane units (A<sub>871</sub>/A<sub>1377</sub>) and the increase of ratio of

acrylate function ( $A_{1406}/A_{1377}$  and  $A_{809}/A_{1377}$ ) at various reaction times. The results in Infrared spectrum indicated the disappearance of the epoxide ring at 34 hours of reaction. The  $^1\text{H}$  NMR data showed the same trend that at longer reaction time, the signal of epoxide at 2.7 ppm was decreased and the signals of acrylate function at 5.82, 6.05 and 6.37 ppm were increased. It can be seen that starting with 19% epoxide content, only about 12 % of acrylate function was found on the rubber chain. The signal in  $^1\text{H}$  NMR also revealed about 2.3% of residual epoxide unit after 48 hours of reaction. However, the absorption band corresponding to epoxide structure was not detected by IR analysis. It seems likely that the decrease of oxirane unit is faster than the formation of acrylated product as detected by IR and  $^1\text{H}$  NMR analysis. This may support the proposed reaction mechanism of the addition of acrylic acid onto the epoxide unit through the formation of carbocation intermediate in Figure 5.43 before the addition of acrylate nucleophile ( $^-\text{OOC-CH=CH}_2$ ).

Figure 5.59 showed the % acrylate content determined by  $^1\text{H}$  NMR of addition reaction of 10 fold per mole of acrylic acid onto LENR (19% epoxide content) carried out at 60 and 70°C. The results revealed that higher acrylated product was obtained at higher temperature. These results supported the above data detected by IR analysis that increasing of reaction temperature increased the epoxide ring opening reaction by acrylic acid and then increasing the yield of acrylated product.

The effect of amount of acrylic acid in the preparation of acrylated rubber was studied with the ELNR containing 17% epoxide content by using 2 and 10 fold of mole of acrylic acid per mole of oxirane unit at 70°C. The results in Figure 5.60 showed that higher amount of acrylic acid used gave better addition reaction of acrylic acid onto the rubber, leading to higher % yield at shorter reaction time. These results are expected as the rate of addition of acrylic acid onto the epoxide ring depended on the free acid in the system. It is possible that the acrylic acid may loss the efficiency of nucleophilic character due to the formation of intermolecular H-bonding of two acrylic acid molecules. The higher the amount of acrylic acid, the better the addition reaction can be achieved.



**Figure 5.59** Results of acrylate content (%) and yield (%) determined from  $^1\text{H}$  NMR of addition reaction of acrylic acid onto epoxidized natural rubber at two different temperatures; (♦)  $60^\circ\text{C}$  and (■)  $70^\circ\text{C}$

Generally, acrylic acid (99.5% pure) is kept by addition of 180 to 220 ppm of p-methoxyphenol which is an inhibitor for homopolymerization of acrylic acid. Elimination of the inhibitor from the acrylic acid can be simply done by distillation under reduced pressure. Figure 5.61 compared the results obtained from the use of distilled and non-distilled acrylic acid for the addition reaction of the liquid rubber containing 26% epoxide content, carried out at  $70^\circ\text{C}$  using 10 fold per mole of epoxidized unit. The percents of acrylated compounds after 70 hours of reaction times were found to be 11% and 10% for the use of non-distilled acrylic acid and distilled acrylic acid, respectively. It can be said that the inhibitor in acrylic acid does not interfere the addition of acrylic acid onto the epoxidized rubber. Moreover, the stability of the rubber solution in the case of using distilled acrylic acid was poor. Therefore, it is not necessary to distill the acrylic acid before addition.

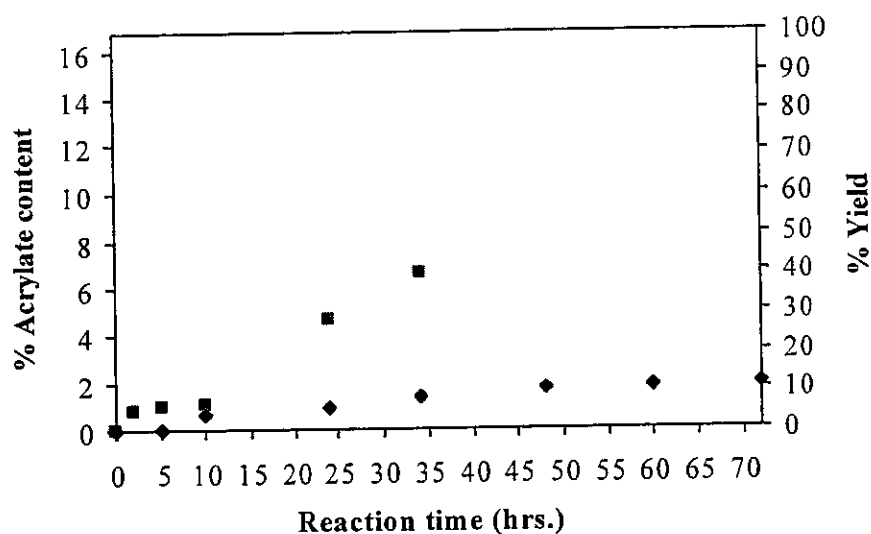


**Figure 5.60** Results of acrylate content (%) and yield (%) determined from  $^1\text{H}$  NMR of addition reaction acrylic acid with epoxidized natural rubber by using ( $\blacklozenge$ ) 2 fold of mold of acrylic acid per mole of oxirane units and ( $\blacksquare$ ) 10 fold of mold of acrylic acid per mole of oxirane units

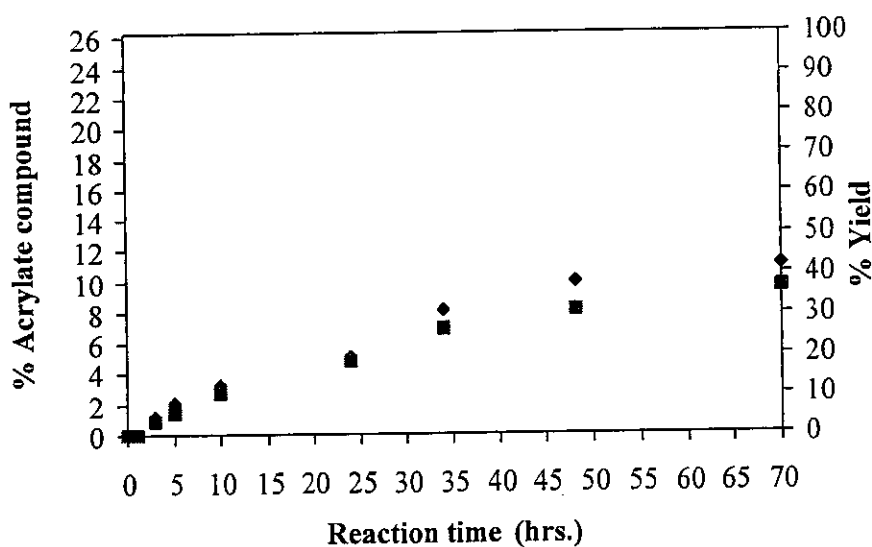


**Figure 5.61** Results of acrylate content (%) and yield (%) determined from  $^1\text{H}$  NMR of addition reaction of acrylic acid with epoxidized natural rubber by using ( $\blacklozenge$ ) Non-distillate acrylic acid and ( $\blacksquare$ ) Distillate acrylic acid

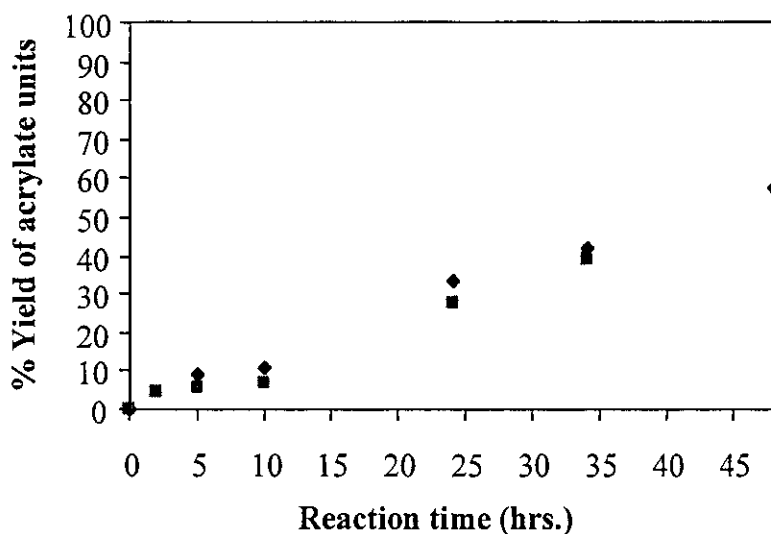
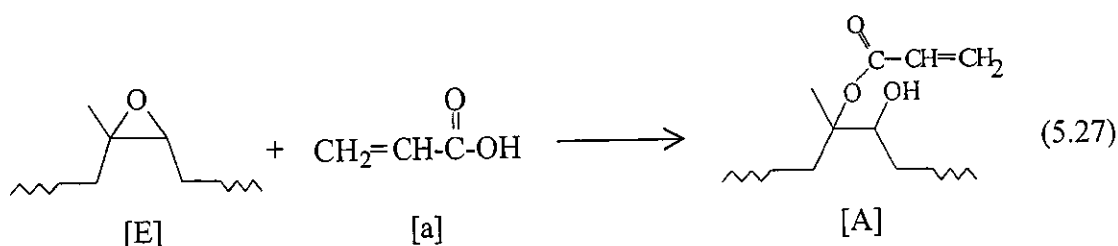


**Figure 5.62** Yield (%) of acrylated units after addition reaction of acrylic acid with epoxidized natural rubber by using (♦) Transfer technique and (■) Coagulation technique

The epoxidized rubber used for studying the acrylation can be obtained from two techniques i.e. coagulation and transfer techniques. The coagulation is the process used in the step of recovery of the rubber from the epoxidation reaction. The epoxidized rubber obtained from this process has to be dissolved in a solvent for further reaction. The transfer technique is carried out to recover directly the rubber obtained from the epoxidation in latex. The rubber is transferred from the aqueous phase to the organic phase. The later phase can be further used. Figure 5.62 showed the results of acrylation reaction of the systems using epoxidized rubbers obtained from coagulation and transfer techniques. It seems likely that no significant difference between these two systems was obtained. The acrylated rubber yields (%) after 34 hours of addition reaction time calculated from  $^1\text{H}$  NMR were 39% and 42% in the case of coagulation and transfer techniques respectively.

#### 4.4 Kinetic study of acrylation reaction

The kinetics of addition reaction of acrylic acid onto epoxidized molecules shown in eq. (5.27) was studied by using the results obtained from  $^1\text{H}$  NMR analysis.



The rate of addition reaction can be derived as in eq. (5.28).

$$\frac{-d[\text{E}]}{dt} = k[\text{E}][\text{a}] \quad (5.28)$$

Where [a] is the concentration of acrylic acid. In our system, an excess amount of acrylic acid (10 fold per mole of epoxide unit) was used, it can be therefore assumed that the amount of acrylic acid remains constant throughout the reaction period. It is assumed that the amount of the acrylated product obtained equals to the amount of the epoxide unit disappeared. Therefore, amount of residual epoxide unit at various reaction times can be represented as  $(1-[A])$  where [A] is the concentration of the acrylated product obtained.

$$\frac{-d(1-[A])}{dt} = k(1-[A]) \quad (5.29)$$

$$\frac{-d(1-[A])}{(1-[A])} = kdt \quad (5.30)$$

Integration of eq. (5.30), then

$$\ln\left(\frac{1-[A]_0}{1-[A]_t}\right) = kt \quad (5.31)$$

Where  $[A]_0$  is concentration ( $\text{mol.l}^{-1}$ ) of acrylated unit at initial reaction time,  $t = 0$  and  $[A]_t$  is concentration ( $\text{mol.l}^{-1}$ ) of acrylated unit at reaction time,  $t = t$  in mole fraction.

The kinetic rate constant ( $k$ ) of addition reaction can be calculated from the slope of the plot of  $\ln((1-[A]_0)/(1-[A]_t))$  at various reaction times of eq. (5.31). Figure 5.63 showed the plots of  $\ln((1-[A]_0)/(1-[A]_t))$  versus reaction time of addition of acrylic acid onto 4,5-epoxy-4-methyloctane. The  $k$  value, calculated from the slope

before approaching the equilibrium (upto 5 hours) was  $1.85 \times 10^{-5} \text{ sec}^{-1}$  as shown in Table 5.20.

Figure 5.64 showed the plots of  $\ln((1-[A]_o)/(1-[A]_t))$  at various reaction times of acrylation reaction of epoxidized synthetic liquid rubber (ELIR containing 17% epoxide content) and epoxidized liquid natural rubber (ELNR containing 17% epoxide content). It was found that the reaction with ELNR is faster than the ELIR and the  $k$  values were found to be  $7.89 \times 10^{-8}$  and  $2.47 \times 10^{-7} \text{ sec}^{-1}$ , respectively. This may be due to the presence of the trans-1,4 and 3,4- polyisoprene structural unit in ELIR that retard the addition reaction of acrylic acid. While the ELNR consisted only cis-1,4 polyisoprenic structures which might not effect much on the rate of the addition reaction.

The kinetic of the effect of the reaction temperatures on the addition of acrylic acid onto ELNR was studied and the results are shown in Figure 5.65. It was found that the reaction at  $70^\circ\text{C}$  is faster than at  $60^\circ\text{C}$  as the  $k$  values were  $3.22 \times 10^{-7} \text{ sec}^{-1}$  and  $1.68 \times 10^{-7} \text{ sec}^{-1}$ , respectively as shown in Table 5.20. This may be due to the fact that increasing the reaction temperature may enhance the movement of the reagents and the active sites to be encountered. It can be concluded that increasing of reaction temperature,  $60^\circ\text{C}$  to  $70^\circ\text{C}$ , rate of acrylation reaction onto epoxidized units is better, higher yield of acrylated product can be obtained. The activation energy of addition reaction was calculated from Arrhenius equation (see eq. (5.7)). The plot of  $\ln k$  versus reciprocal of different temperatures resulted in the activation energy values of  $61.99 \text{ kJ mol}^{-1}$  for the acrylation reaction of liquid epoxidized purified natural rubber.

The kinetic of the effect of amount of acrylic acid on acrylation reaction was also studied. The systems of using 2 fold and 10 fold of acrylic acid by mole per mole of oxirane unit with ELNR (17% epoxide content) were compared in Figure 5.66. The  $k$  values of  $0.47 \times 10^{-7} \text{ sec}^{-1}$  and  $2.81 \times 10^{-7} \text{ sec}^{-1}$  were found for the use of 2 fold and 10 fold of acrylic acid, respectively. The excess of amount of acrylic acid can act as self-acid catalyst for acrylation reaction, leading to the high rate of addition reaction and high content of acrylated product obtained.

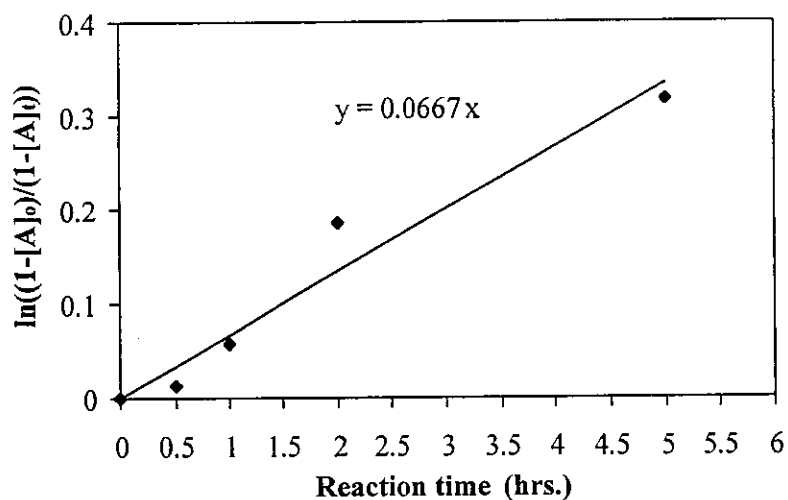


**Figure 5.63** Plot of  $\ln((1-[A]_0)/(1-[A]_t))$  versus reaction time of addition reaction of acrylic acid with 4,5-epoxy-4-methyloctane

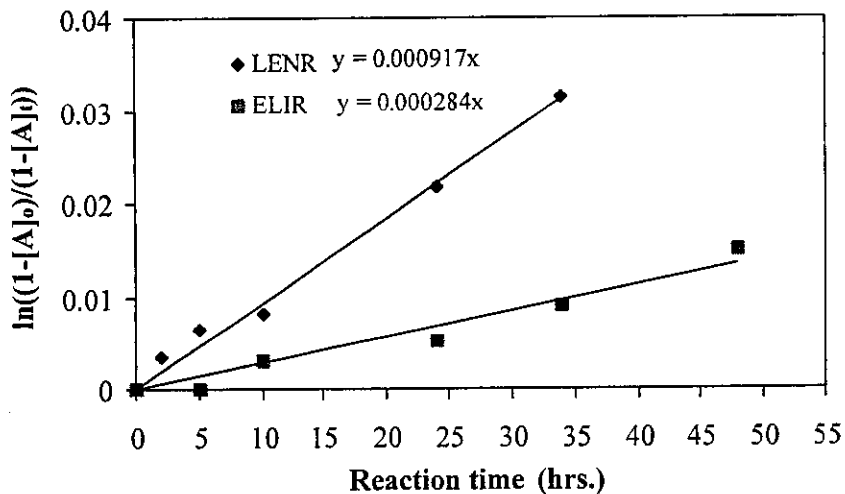


**Figure 5.64** Plot of  $\ln((1-[A]_0)/(1-[A]_t))$  versus reaction time of addition reaction of acrylic acid with epoxidized liquid rubber; ( $\blacklozenge$ ) Epoxidized liquid natural rubber and ( $\blacksquare$ ) Epoxidized liquid synthetic rubber

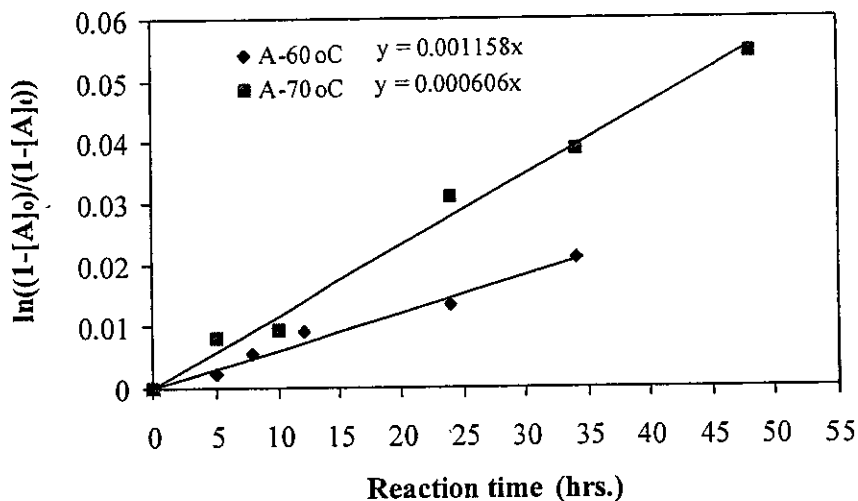


**Figure 5.65** Plot of  $\ln((1-[A]_0)/(1-[A]_t))$  versus reaction time of addition reaction of acrylic acid with Epoxidized liquid natural rubber at two different temperatures; (◆) 60°C and (■) 70°C

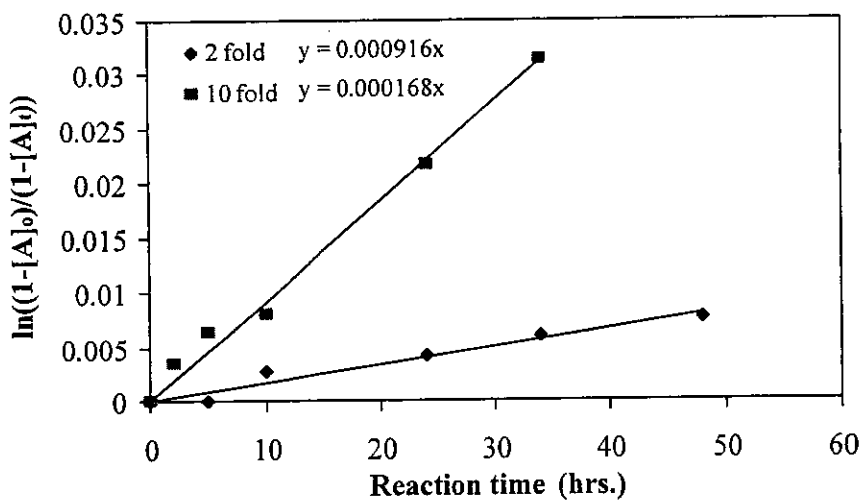


**Figure 5.66** Plot of  $\ln((1-[A]_0)/(1-[A]_t))$  versus reaction time of addition reaction of different amount of acrylic acid with Epoxidized liquid natural rubber; (◆) 2 fold per mole of oxirane unit and (■) 10 fold per mole of oxirane unit

**Table 5.20** Content (%), yield (%) and kinetic rate constant (k) on addition of acrylic acid onto epoxidized molecules

	Epoxide content of starting compound (%)	Non-dist. /dist. of acrylic acid	Temp.	Fold of acid (mole per mole of epoxide unit)	Time (hrs.)	Content (%)	Yield (%)	k (sec <sup>-1</sup> )
Amodel	93	Non-dist.	70	10	34	68.65	73.83	1.85 x 10 <sup>-5</sup>
					48	71.45	76.84	
ALIR 1	17	Non-dist.	70	10	34	1.88	11.28	7.89 x 10 <sup>-8</sup>
					48	3.12	18.72	
					72	5.89	35.33	
ALNR 1	19	Non-dist.	60	10	34	4.44	27.76	1.68 x 10 <sup>-7</sup>
ALNR 2	19	Non-dist.	70	10	34	8.18	41.93	3.22 x 10 <sup>-7</sup>
					48	11.18	57.30	
ALNR 3	26	Non-dist.	70	10	34	8.31	31.57	3.25 x 10 <sup>-7</sup>
					48	10.15	28.56	
					70	11.34	43.09	
ALNR 4	26	Dist.	70	10	34	7.06	26.82	2.81 x 10 <sup>-7</sup>
					48	8.26	31.38	
					70	9.85	37.42	
ALNR 5	17	Non-dist.	70	2	34	1.32	7.85	4.69 x 10 <sup>-8</sup>
					48	1.70	10.11	
					72	1.93	11.51	
ALNR 6	17	Non-dist.	70	10	34	6.62	39.48	2.54 x 10 <sup>-7</sup>

## 5. Study of Photocrosslinking Reaction

Introduction of acrylate groups into low molecular weight purified natural rubber is a method to transform the NR into a new material so called acrylated liquid purified natural rubber (ALPNR). The ALPNR is an attractive material as it is sensitive to ultraviolet radiation. Therefore, it can be cured by photoreaction process and the cured product or crosslinked product should possess the elastic character as well as good chemical resistance, hardness and adhesive strength. The ALPNR will extend the potential application for the natural rubber in the field of surface coating by ultraviolet irradiation.

Generally, surface coating materials (thermal or photocuring) are found in the form of compound formulations, containing various chemicals such as difunctional or multifunctional diluents to adjust the viscosity of the system as well as the properties of the final products. In photocuring materials, frequently a photoinitiator is added to accelerate the photocrosslinking reaction. The kinetic of photocrosslinking reaction of the ALPNR in the presence of initiators, diluents and temperature in this section was investigated by measuring the heat of polymerization ( $\Delta H$ ) using double beam photocalorimeter. The kinetic parameters of the reaction condition i.e. %conversion rate of photopolymerization ( $R_p$ ) and kinetic rate constant ( $k$ ) were studied for prediction and control of the anomalous behavior of materials.

### 5.1 Kinetic study of photocrosslinking reaction

The photopolymerization is generally a process that the carbon-carbon double bond ( $C=C$ ) of the monomer is polymerized under irradiation. It transformed the  $C=C$  into carbon-carbon single bond ( $C-C$ ) that makes the linkage between the monomer molecules. This is an exothermic process and the heat is released during the reaction. If the system contains multifunctional monomers, photocrosslinking is achieved. When the differential scanning calorimeter (DSC) equipped with ultraviolet light source, it can be used to measure the heat generated from the formation of chemical bonding from photopolymerization process. Double beam photocalorimeter accessory (DPA 7) is an accessory connected to the DSC-7 Perkin Elmer equipment. The acrylated rubber which is placed in the sample holder is irradiated by ultraviolet light, the heat evolved during irradiation of photosensitive materials can be detected.

Equation (5.32) represents a general equation of the transformation of a substance (A) to a new material (B) under UV irradiation. The heat generated can be detected in DSC mode.



Where A is the material before irradiation

B is the material after irradiation

$\Delta H$  is the heat released (J/g)

k is the Arrhenius rate constant

In the typical profile of thermogram of photopolymerization, heat flow versus time is recorded in an isothermal mode, which displays the polymerization exothermic peak during the reaction. Figure 5.67 showed exothermic diagram of photoreaction of acrylated rubber (ALPNR1) combined with 1,6 hexanediol diacrylate (20% by weight of rubber) and Darocur 1173 photoinitiator (1 % by weight of total solid content of rubber and diluent), carried out at 30°C. The formulation consisted of difunctional molecules (HDDA), therefore photocrosslinking was occurred. %Conversion of the photocrosslinking was calculated from the overall heat evolved over the reaction time t ( $\Delta H_t$ ) compared to the theoretical heat evolved as shown in eq.(5.33).

$$\text{Conversion (\%)} = \frac{\Delta H_t}{\Delta H_0^{\text{theor}}} \times 100 \quad (5.33)$$

Where  $\Delta H_t$  is the heat evolved at the irradiation time t

$\Delta H_0^{\text{theor}}$  is the theoretical heat evolved for complete photopolymerization

For the complete photoreaction, the heat of polymerization of the acrylate function can be calculated from the theoretical heat value of transformation of acrylate double bond (C=C) to single bond (C-C). It was reported in several papers that the theoretical heat value;  $\Delta H_0^{\text{theor}}$  of the acrylate function is 20.6 kcal.mol<sup>-1</sup> or 86.2 kJ.mol<sup>-1</sup>, while for acrylic acid, the value is 18.5 kcal.mol<sup>-1</sup> or 77.4 kJ.mol<sup>-1</sup> [108,108,124-126]. Therefore, the %conversion of photopolymerization reaction of the system containing acrylate functions can be obtained at various reaction times.

From eq. (5.32), the kinetic equation of the photopolymerization can be expressed in term of fraction of heat released as shown in eq. (5.34).

$$\frac{dH}{dt} = k(1-x)^n \quad (5.34)$$

$$\ln \frac{dH}{dt} = \ln k + n \ln (1-x) \quad (5.35)$$

Where  $dH/dt$  is the heat released obtained versus elapsed time of reaction.

$x$  is the mole fraction of heat released.

$n$  is the order of photopolymerization reaction.

$k$  is the kinetic rate constant

The  $k$  value of photopolymerization and order of reaction ( $n$ ) can be calculated from the slope and intercept of the plot of  $\ln(dH/dt)$  versus  $\ln(1-x)$ .

Generally, the rate of photopolymerization ( $R_p$ ) can be expressed as first order assumption according to Appelt BK and Abadie MJM [103], depending on the reactive monomer concentration as shown in eq. (5.36)

$$R_p = k [M]_0 \quad (5.36)$$

Where  $R_p$  is the rate of photopolymerization ( $\text{mol.l}^{-1}.\text{s}^{-1}$ )

$[M]_0$  is the initial active functional material concentration ( $\text{mol.l}^{-1}$ )

$k$  is the kinetic rate constant of photopolymerization ( $\text{min}^{-1}$ )

In our study, various types of acrylated rubbers were prepared. The study of photocrosslinking of the acrylated rubbers was expressed in terms of heat of polymerization and kinetic of the reaction.

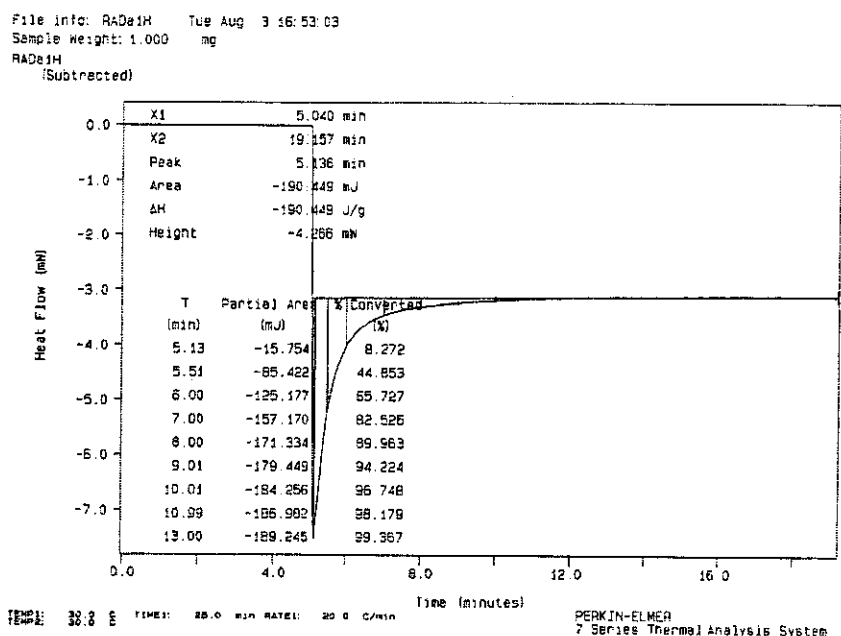
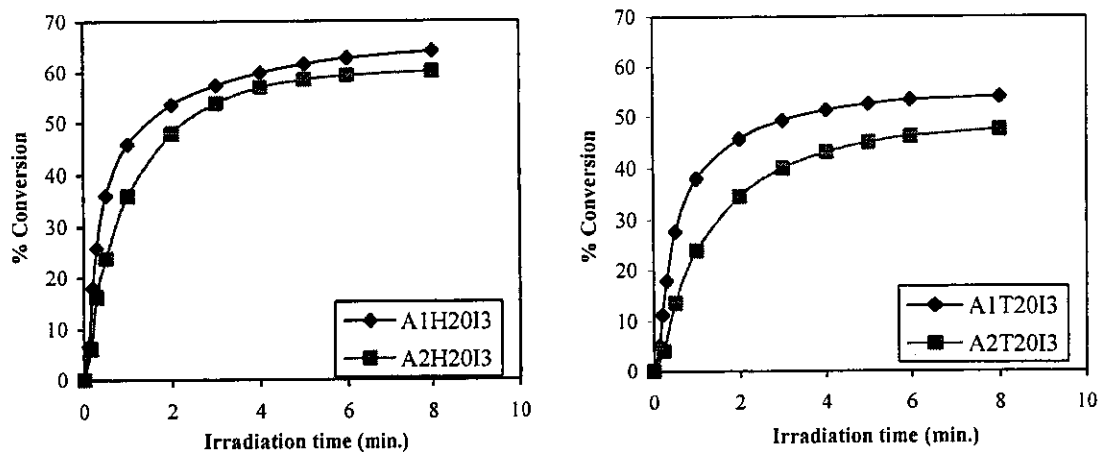


**Figure 5.67** Exothermic diagram of photopolymerization acrylated rubber (ALPNR1) combined with HDDA (20% by weight of rubber) and Darocur 1173 (1% by weight of total solid of rubber and diluent), carried out at 30°C

### 5.1.1 Heat of polymerization

Various compound formulations of acrylated rubbers in the presence of 1,6 hexanediol diacrylate (HDDA) or tripropylene glycol diacrylate (TPGDA) and photoinitiators (Irgacure 184) were used to study the kinetic of photopolymerization by using double beam photocalorimeter (DPA7). The heat of polymerization ( $\Delta H$ ) of the compound formulations at various irradiation times obtained from the DSC thermogram was used to calculate the %conversion according to eq. (5.33). Figure 5.68 shows plots %conversion of photocrosslinking of two types of acrylated rubbers; ALPNR1 (11% acrylate content) and ALPNR2 (5% acrylate content) in the presence of HDDA or TPGDA (rubber:diluent = 100:20) and Irgacure 184 (3% by weight of total solid of rubber and diluent). It can be seen that the %conversion of each compound formulation is less than 100%. This may be due to, at longer reaction time, the %conversion was increased, resulting in increasing the formation of crosslinked structure or gel structure therefore the rubbers became rigid, which led to the reduction of the mobility of the active molecules to be encountered by the propagating radicals. Therefore, a certain amount of the acrylate function was trapped in the rigid



(B)

(A)

**Figure 5.68** Plots of %conversion of photocrosslinking reaction versus irradiation time of ALPNR1 (11%acrylate function) and ALPNR2 (5%acrylate function), carried out at 30°C

(A) -◆- A1H20I3 (ALPNR1:HDDA:Irgacure = 100:20:3.6),

-■- A2H20I3 (ALPNR2:HDDA:Irgacure = 100:20:3.6)

(B) -◆- A1T20I3 (ALPNR1:TPGDA:Irgacure = 100:20:3.6),

-■- A2T20I3 (ALPNR2:TPGDA:Irgacure = 100:20:3.6)

crosslinked structure which prevented further polymerization. No more heat released can be detected.

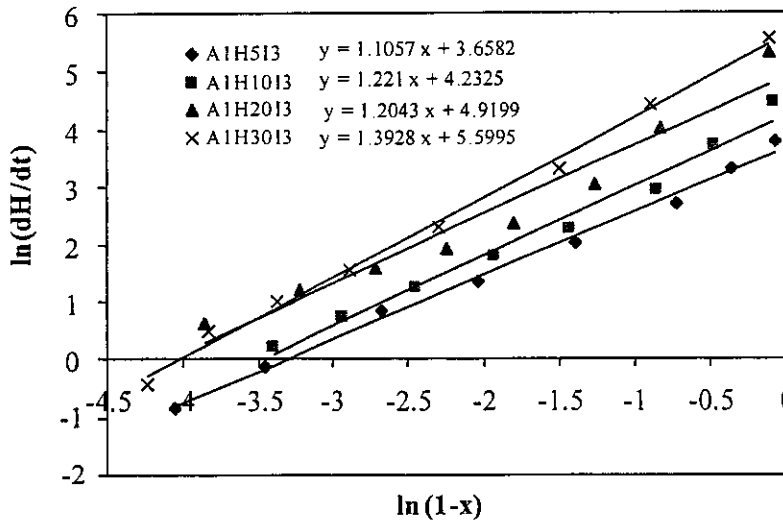
It was found in Figure 5.68 (A) that %conversion of A1H20I3 (ALPNR1:HDDA:Irgacure = 100:20:3.6) is higher than A2H20I3 (ALPNR2:HDDA: Irgacure = 100:20:3.6) at various reaction times. This can be explained that the ALPNR1 contained more acrylate functions than the ALPNR2, therefore there are more active sites on the molecular chain for reacting with the HDDA. For the compound formulations using TPGDA diluent, it was found in Figure 5.58 (B) that the %conversion obtained at various reaction times for A1T20I3 (ALPNR1:TPGDA: Irgacure= 100:20:3.6) is higher than for A2T20I3 (ALPNR2: TPGDA: Irgacure = 100:20:3.6). This may be due to the same reason that the ALPNR1 contained higher amount of acrylate function on the rubber molecules than ALPNR2, which help in better crosslinking reaction.

Comparing between the two types of diluents, it can be seen in Figure 5.58 (A) and (B) that %conversion in the compound formulation containing HDDA is higher than the use of TPGDA at the same irradiation time. The difunctional diluents are served as crosslinkers and the pendant propylene glycol chain length of TPGDA is longer than the ethylene glycol chain length of HDDA. Therefore, longer time is needed in the case of TPGDA for the arrival of the radical propagating species to form crosslinking structure with the rubber chain.

### 5.1.2 Kinetic of photopolymerization

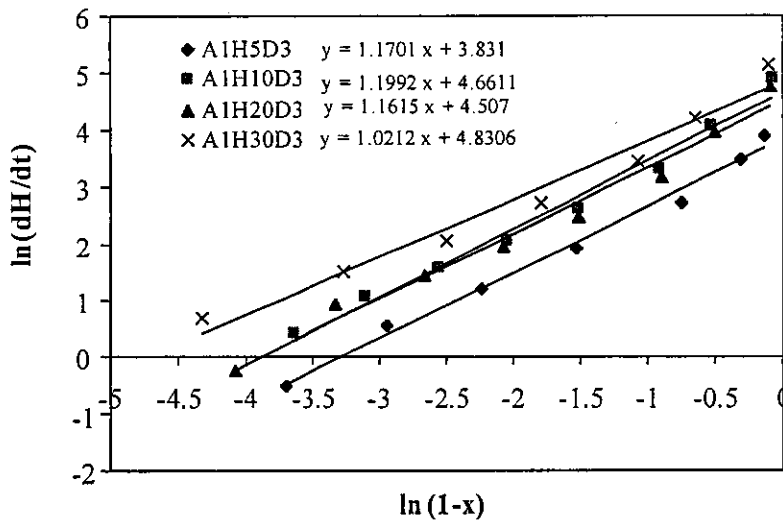
The kinetic of photopolymerization of acrylated rubbers is investigated by using the eq. (5.35). The rate constant ( $k$ ) of photopolymerization and order of reaction ( $n$ ) can be calculated from the slope and intercept of the plot of  $\ln(dH/dt)$  versus  $\ln(1-x)$ . Table 5.23 shows the results of  $k$  values of UV irradiation at 30°C of ALPNR1 (11% acrylate content), containing various amounts of reactive diluents (5, 10, 20 and 30 % by weight of rubber), combining with photoinitiators (3 % by weight of rubber and diluent of Irgacure 184 or Darocur 1173). It was found that increasing the amount of diluents,  $k$  is increased. This is in accordance with the report of Tsutsumi K et al. that the radical polymerization rate depends on the monomer concentration [127].

Figure 5.69-5.72 showed the plots of  $\ln(dH/dt)$  versus  $\ln(1-x)$  of various types of ALPNR1 compound formulations. Figure 5.69 shows the plots of  $\ln(dH/dt)$  versus  $\ln(1-x)$  of ALPNR1 using fixed amount of Irgacure and HDDA (5, 10, 20 and 30 % by weight of rubber). The  $k$  values of A1H5I3, A1H10I3, A1H20I3 and A1H30I3 were found to be 38.79, 68.89, 136.99 and 270.29  $\text{min}^{-1}$ , respectively. It was found that increasing the amount of HDDA, the  $k$  value is increased. This is not surprising as increasing the amount of crosslinking agent, the possibility of the propagating species to react with the diacrylate will also be increased, therefore, the rate of crosslinking formation is higher. Similar results were obtained when the Irgacure 184 was replaced by Darocur 1173 in the compound formulation as it was found that increasing the amount of HDDA, the kinetic rate constant is increased (Figure 5.70). The plots of  $\ln(dH/dt)$  versus  $\ln(1-x)$  of ALPNR1 containing of TPGDA (5, 10, 20 and 30 % by weight of rubber) and photoinitiators (3% by weight of rubber and diluent) were presented in Figures 5.71 and 5.72. The  $k$  values of each sample were showed in both cases that increasing the amount of the TPGDA, the  $k$  values are increased.



**Figure 5.69** Plot of  $\ln(dH/dt)$  versus  $\ln(1-x)$  of ALPNR1 combined with Irgacure 184 by various amount of HDDA, carried out at 30°C

- ◆- A1H5I3 (ALPNR1:HDDA:Irgacure = 100:5:3.15)
- A1H10I3 (ALPNR1:HDDA:Irgacure=100:10:3.3)
- ▲- A1H20I3 (ALPNR1:HDDA:Irgacure=100:20:3.6)
- x- A1H30I3 (ALPNR1:HDDA:Irgacure= 100:30:3.9)



**Figure 5.70** Plot of  $\ln(-dH/dt)$  versus  $\ln(1-x)$  of ALPNR1 combined with Darocur 1173 by various amount of HDDA, carried out at 30°C

- ◆- A1H5D3 (ALPNR1:HDDA:Darocue = 100:5:3.15)
- A1H10D3 (ALPNR1:HDDA:Darocue=100:10:3.3)
- ▲- A1H20D3 (ALPNR1:HDDA:Darocue=100:20:3.6)
- x- A1H30D3 (ALPNR1:HDDA:Darocue=100:30:3.9)

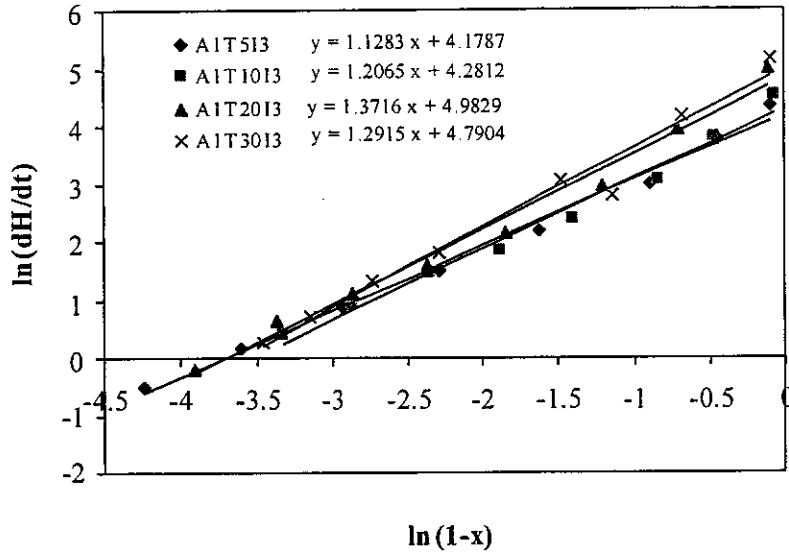


**Figure 5.71** Plot of  $\ln(-dH/dt)$  versus  $\ln(1-x)$  of ALPNR1 combined with Irgacure 184 by various amount of TPGDA, carried out at 30°C

- ♦-A1T5I3 (ALPNR1:TPGDA:Irgacure= 100:5:3.15)
- A1T10I3 (ALPNR1:TPGDA:Irgacure=100:10:3.3)
- ▲-A1T20I3 (ALPNR1:TPGDA:Irgacure=100:20:3.6)
- x-A1T30I3 (ALPNR1:TPGDA:Irgacure=100:30:3.9)

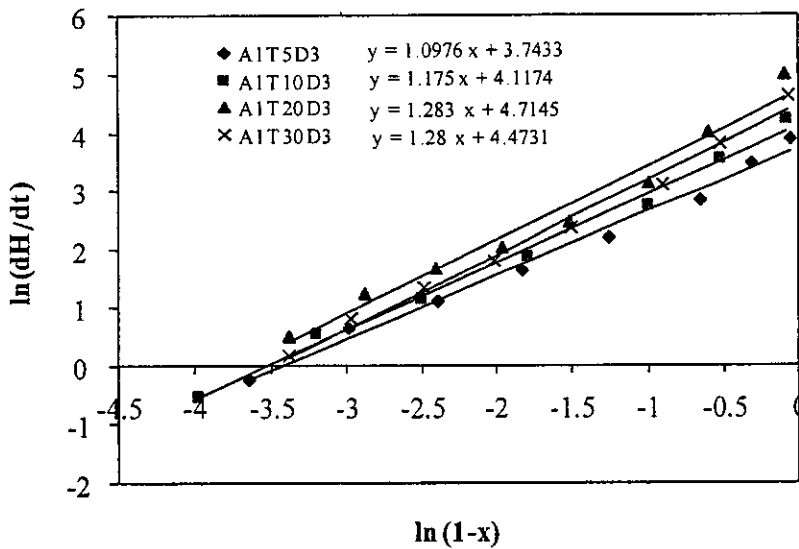


**Figure 5.72** Plot of  $\ln(-dH/dt)$  versus  $\ln(1-x)$  of ALPNR1 combined with Darocur 1173 by various amount of TPGDA, carried out at 30°C

- ♦- A1T5D3 (ALPNR1:TPGDA:Darocue= 100:5:3.15)
- A1T10D3 (ALPNR1:TPGDA:Darocue=100:10:3.3)
- ▲-A1T20D3 (ALPNR1:TPGDA:Darocue=100:20:3.6)
- x-A1T30D3 (ALPNR1:TPGDA:Darocue=100:30:3.9)

## 5.2 Parameters affecting the photopolymerization

It has been known that the surface coating materials contain various chemical reagents including reactive diluents and photoinitiators. Various parameters affecting the photopolymerization by using double beam photocalorimeter were investigated.

The general equation for photopolymerization by radical initiator can be expressed as in eq. (5.37) [109]:

$$R_p = k_p [M]_0 \left( \frac{\phi \epsilon I_0 [A]_0}{k_t} \right)^{1/2} \quad (5.37)$$

$R_p$  is rate of polymerization ( $\text{mol l}^{-1} \cdot \text{s}^{-1}$ )

$[M]_0$  is the initial active functional material concentration ( $\text{mol l}^{-1}$ )

$[A]$  is photoinitiator concentration ( $\text{mol l}^{-1}$ )

This eq. (5.37) indicates that the rate of polymerization depends on the monomer concentration but a half-order of initiator concentration as shown in eq. (5.38) and (5.39).

$$R_p \propto [M]_0 \quad 5.38$$

$$R_p \propto [A]^{1/2} \quad 5.39$$

From eq. (5.38) and eq.(5.39), the amount of reactive functional groups on the acrylated rubbers, the diluents and photoinitiators will effect on the photocrosslinking reaction.

### 5.2.1 Amount of acrylate function on the rubber molecule

The purpose of using the rubber containing the acrylate function grafted on the rubber chain before mixing with the diacrylate compounds such as HDDA and TPGDA is to be able to achieve the final product having 3-dimensional network linked the rubber chain with the polyacrylate formed. Generally, a few molecules of the photosensitive groups fixed on the rubber chain are needed for the photocrosslinking reaction. Two different types of acrylated rubbers containing 11% acrylate function (ALPNR1) and 5% acrylate function (ALPNR2) were compared in this section. It was found in Figure 5.68 (A) that increasing the amount of acrylate function on the rubber chain increased the %conversion at various irradiation times. General mechanism of

the photocrosslinking reaction is proposed to be the formation of active radical from the photoinitiator under irradiation that initiate the propagation. Therefore, the active radical generated will move to react with both the acrylate function on the rubber chain and the HDDA. Higher amount of the acrylate function of the ALPNR1 than the ALPNR2 should render higher rate of initiation and propagation. The kinetic rate constant shown in Table 5.21 revealed the  $k$  values of A1H20I3 and A2H20I3 to be 136.99 and 95.40 respectively. These results supported that higher amount of the acrylate function on the rubber will enhance the formation of network in the material. The rate of polymerization ( $R_p$ ) of A1H20I3 ( $8.51 \text{ mole.l}^{-1} \text{ sec}^{-1}$ ) is higher than A2H20I3 ( $4.05 \text{ mole.l}^{-1} \text{ sec}^{-1}$ ). Similar results were obtained in the case of using Darocur 1173 initiator. (A1H20D3 and A2H20D3) [128,129]. It was also found that the higher rate of photoreaction of A1T20I3 than that of A2T20I3 corresponds to the higher ultimate yield of A1T20I3 than A2T20I3 as shown in Table 5.21.

**Table 5.21** Photocrosslinking results of acrylated rubber (ALPNR1 and ALPNR2) using different amounts acrylate units on the rubber chain, carried out at 30°C

Codes	Rubber (part)	HDDA (part)	TPGDA (part)	Irgacure 184 (part)	Darocur 1173 (part)	Ultimate Yield (%)	Time onset (min.)	$k$ ( $\text{min}^{-1}$ )	$R_p$ mole/l sec
A1H20I3	100	20	-	3.6	-	64.08	0.115	136.989	8.51
A2H20I3	100	20	-	3.6	-	60.87	0.152	95.402	4.05
A1H20D3	100	20	-	-	3.6	46.44	0.194	90.649	5.64
A2H20D3	100	20	-	-	3.6	62.11	0.187	83.722	3.54
A1T20I3	100	-	20	3.6	-	54.34	0.139	120.349	6.65
A2T20I3	100	-	20	3.6	-	47.92	0.221	49.171	1.74
A1T20D3	100	-	20	-	3.6	61.59	0.141	111.553	6.17
A2T20D3	100	-	20	-	3.6	32.81	0.179	30.141	1.09

A1 containing 11% acrylate units, and  $\overline{M}_v = 25,500$

A2 containing 5% acrylate units, and  $\overline{M}_v = 26,900$

### 5.2.2 Molecular weight of the acrylated rubber

The viscosity of acrylated rubber may directly influence on the rate of reaction as it controlled the movement of the acrylate function on the rubber chain to be

encountered by the reactive radical species as well as the diffusion of the diacrylate diluents. Two different molecular weights of similar acrylate content were prepared; ALPNR1 (11% acrylate functions with  $\overline{M}_v = 25,500$ ) and ALPNR3 (10% acrylate functions with  $\overline{M}_v = 38,000$ ). HDDA and TPGDA (20% by weight of rubber) were used with the rubbers in the presence of Irgacure 184 and Darocur 1173 (3 % by weight of rubber and diluent). The results of % conversion, and rate of polymerization are shown in Table 5.23. Figure 5.73 shows the plots of %conversion of various compound formulations at different irradiation times. It was shown in Figure 5.73 (A) that the %conversion of A1H20I3 at the same irradiation time is very much higher than A3H20I3. Similar results were also observed in the case of changing of the initiator to be Darocur 1173 that lower molecular weight ALPNR1 resulted in better rate of photopolymerization as shown in Figure 5.73 (B). This may be due the fact that the use of high molecular weight acrylated rubber (ALPNR3) may increase the viscosity of the formulations, therefore this will retard the movement of the active diluents as well as the acrylate function on the rubber chain to be encountered by the propagating species.

The use of the bigger molecule of diluent such as TPGDA did not help in better movement of the photoactive function in the system. %Conversion of A1T20I3 is higher than A3T20I3 at various reaction times. The  $k$  value of A1H20I3 ( $136.99 \text{ min}^{-1}$ ) is higher than A3H20I3 ( $87.6 \text{ min}^{-1}$ ) which is higher than A3T20I3 ( $61.33 \text{ min}^{-1}$ ). It can be concluded in this part that higher molecular weight of the acrylated rubber may slower the rate of photocrosslinking reaction. The results of  $R_p$  shown in Table 5.22 supported this conclusion as it was found that the  $R_p$  of A1H20I3 and A3H20I3 were 8.51 and 5.30  $\text{mole.l}^{-1}\text{sec}^{-1}$ , respectively. The increase of the molecular weight of the acrylated rubber indicated also the decrease of ultimate yield and increase the time onset of gel formation. The rate of propagation controlled by the diffusion of monomer was decreased.

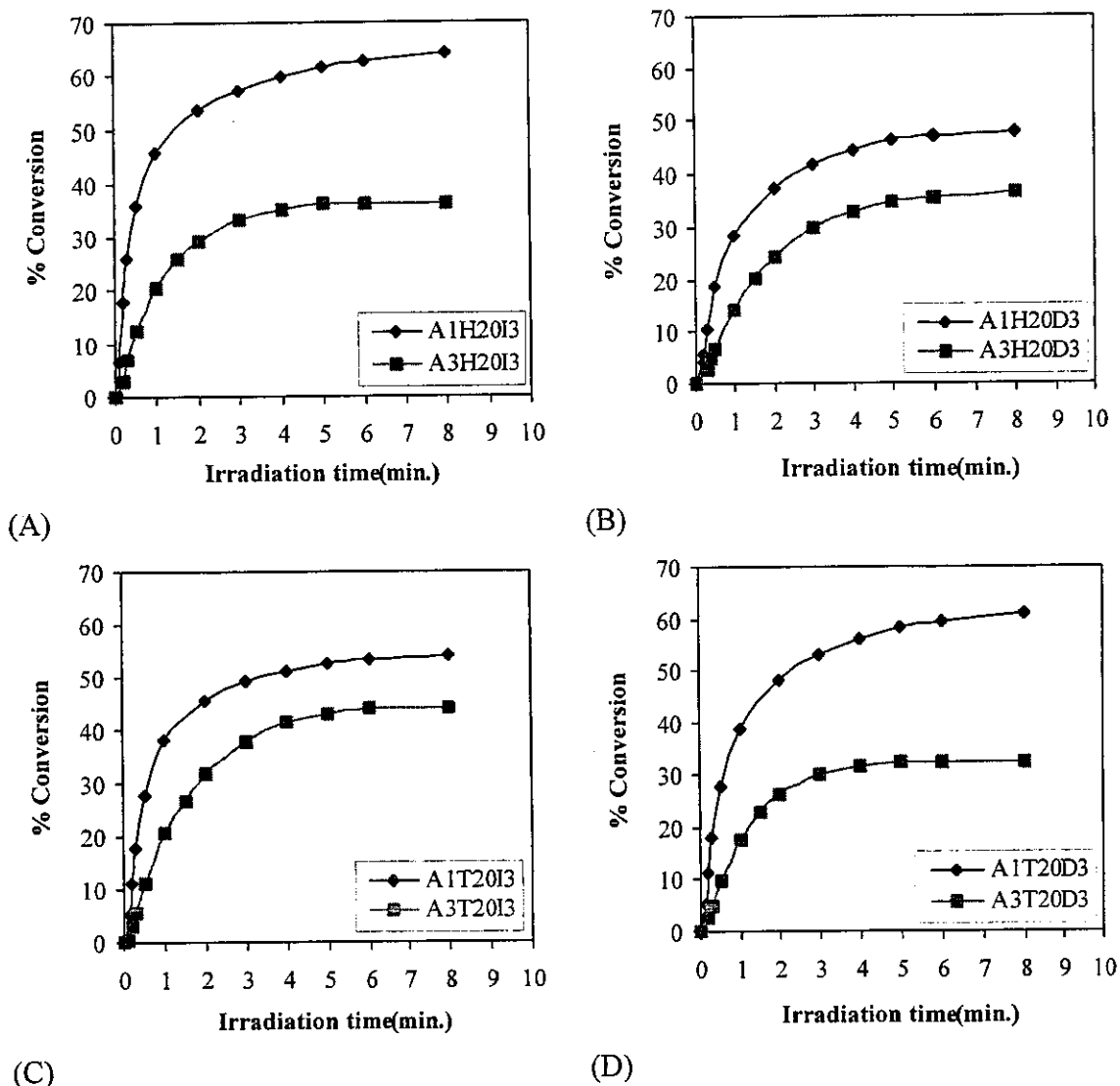


**Figure 5.73** Plots of % conversion of photocrosslinking reaction versus irradiation time of ALPNR1 (11%acrylate function,  $\bar{M}_v = 25,500$ ) and ALPNR3 (9.9%acrylate function,  $\bar{M}_v = 38,000$ ), carried out at 30°C,

(A) -◆- A1H20I3 (ALPNR1:HDDA:Irgacure = 100:20:3.6),

-■- A3H20I3 (ALPNR3:HDDA:Irgacure = 100:20:3.6)

(B) -◆- A1H20D3 (ALPNR1:HDDA:Darocur = 100:20:3.6),

-■- A3H20D3 (ALPNR3:HDDA: Darocur = 100:20:3.6)

(C) -◆- A1T20I3 (ALPNR1:TPGDA:Irgacure = 100:20:3.6),

-■- A3T20I3 (ALPNR3:TPGDA:Irgacure = 100:20:3.6)

(D) -◆- A1T20D3 (ALPNR1:TPGDA:Darocur = 100:20:3.6),

-■- A3T20D3 (ALPNR3:TPGDA:Darocur = 100:20:3.6)

**Table 5.22** Photocrosslinking results of acrylated rubber (ALPNR1 and ALPNR3) using different molecular weight of acrylated rubber, carried out at 30°C

Codes	Rubber (part)	HDDA (part)	TPGDA (part)	Irgacure 184 (part)	Darocur 1173 (part)	Ultimate Yield (%)	Time onset (min.)	k (min <sup>-1</sup> )	Rp mole/l sec
A1H20I3	100	20	-	3.6	-	64.08	0.115	136.989	8.51
A3H20I3	100	20	-	3.6	-	36.63	0.166	87.60	5.30
A1H20D3	100	20	-	-	3.6	46.44	0.194	90.649	5.64
A3H20D3	100	20	-	-	3.6	36.84	0.284	52.50	3.14
A1T20I3	100	-	20	3.6	-	54.34	0.139	120.349	6.65
A3T20I3	100	-	20	3.6	-	41.38	0.202	61.33	3.30
A1T20D3	100	-	20	-	3.6	61.59	0.141	111.553	6.17
A3T20D3	100	-	20	-	3.6	32.77	0.206	65.83	3.50

A1 containing 11% acrylate units, and  $\bar{M}_v = 25,500$

A3 containing 9.9 % acrylate units, and  $\bar{M}_v = 38,000$

### 5.2.3 Effect of reactive diluents

The reactive diluents are usually added to UV-curable resins as they play roles as viscosity modifier and crosslinker for the system and have also influence on both the polymerization rate and the properties of the final product obtained [130,131]. Di- or polyfunctional monomers are often employed such as diacrylate and triacrylate monomers. In this study, HDDA and TPGDA are two diacrylate monomers with different chain length between the diacrylate functions. The kinetic of reaction of the use of these diluents at various amounts in the acrylated rubber was investigated.

It was found in Table 5.23 and Figure 5.74 that increasing the amount of HDDA, the ultimate yield is increased. The ultimate yields of A1H5I3, A1H10I3, A1H20I3 and A1H30I3 are 29.50, 43.46, 64.08 and 70.06, respectively. It seems likely that the amount of HDDA may act as a plasticizer in the curing compound, leading to an enhancement of the mobility of active propagating species that facilitate the crosslinking reaction. Increasing the concentration of reactive diluent will also increase the segment density of active acrylate function around the radical site, leading to reduction of time for the movement of the active site as well as the reduction of the termination reaction brought by the autopolymerization. Then, the high values of rate of photopolymerization and the ultimate yield were obtained. Similar results were

obtained in the case of using TPGDA that increasing the amount of the TPGDA, the ultimate yield was increased as shown in Table 5.23. The  $R_p$  of the polymerization in both systems were also increased with increasing the amount of the diluents.

Comparing the different types of the diluent but the same amount, it was found that the  $k$  value and the  $R_p$  of the photocrosslinking reaction depend on the type as well as the amount considered as shown in Table 5.23. In the case of A1H5I3 compared with A1T5I3, it was found that the  $k$  and  $R_p$  of the former samples are lower than the later. This can be explained by the fact that the longer of the chain length between the diacrylate of TPGDA than the HDDA plays a better role as diluent than the HDDA. However, increasing the amount of the diluent to 20 and 30 % by weight of rubber, the HDDA may play a role of diluent as good as the TPGDA but now the longer the chain length between the diacrylate of the TPGDA displayed the disadvantage over the HDDA as the  $k$  and  $R_p$  values of the A1H30I3 are greater than the A1T30I3 as well as in the case of 20 % of the diluents. This can be explained that at the beginning of the reaction time the crosslinking may be already occurred, then the material became fast to the solid stage, the diffusion of diluent were also frozen with the polymeric radical, then the propagation rate controlled by diffusion of monomers were decreased. Rate of polymerization and yield obtained from the longer chain length between diacrylate (TPGDA) were decreased more than the HDDA.

**Table 5.23** Photocrosslinking results of acrylated rubber (ALPNR1) using different types and amounts of diluents.

Codes	Rubber (part)	HDDA (part)	TPGDA (part)	Irgacure (part)	Yield (%)	n	k ( $\text{min}^{-1}$ )	$R_p$ mole/l sec
A1H5I3	100	5	-	3.15	29.50	1.106	38.791	1.86
A1H10I3	100	10	-	3.30	43.46	1.221	68.889	3.66
A1H20I3	100	20	-	3.60	64.08	1.204	136.989	8.50
A1H30I3	100	30	-	3.90	70.06	1.393	270.291	18.73
A1T5I3	100	-	5	3.15	45.59	1.128	65.281	3.00
A1T10I3	100	-	10	3.30	51.82	1.207	72.327	3.57
A1T20I3	100	-	20	3.60	54.34	1.292	120.349	6.65
A1T30I3	100	-	30	3.90	62.93	1.372	145.897	8.79

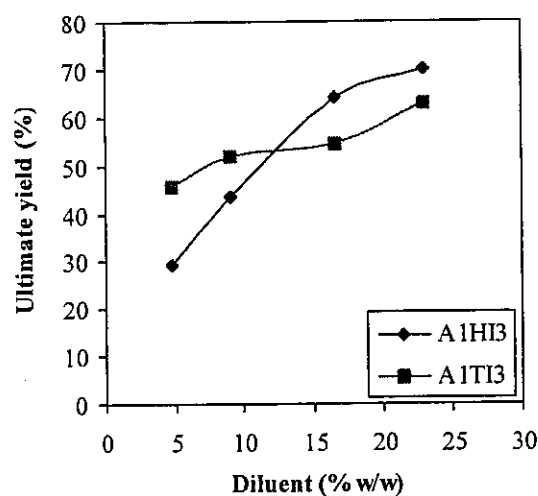


**Figure 5.74** Plots of ultimate yield (%) versus diluent concentration (% by weight of HDDA and TPGDA) of ALPNR1 as oligomer with Irgacure 184 and Daracur 1174 as photoinitiator (3 % by weight of rubber and diluent), carried out at 30°C; (-♦-) A1HI3 (ALPNR1:HDDA:Irgacure = 100:(5, 10, 20, 30):3) and (-■-) A1TI3 (ALPNR1:TPGDA:Irgacure = 100:(5, 10, 20, 30):3)

### 5.2.3 Types of initiator

Photoinitiator was added to the compound formulation and it was decomposed under irradiation into highly reactive species for initiation toward the acrylate double bond as shown in Figure 5.75 and 5.76.

Efficiency of initiator on photopolymerization is normally concerned with the competition between the reactions of the primary radical with the acrylate double bond during the initiation stage,  $[A^{\cdot}][M]$  and the coupling of two primary radicals  $[A^{\cdot}]^2$ . This competition is also related to the amount of initiator used. Increasing the concentration of active radicals will directly increase the number-consuming reactive species in the system, the rate of reaction and ultimate yield should be increased. However, the high opportunity on encountering of radical species or rate of termination reaction will also be increased. Moreover, in the crosslinking polymerization, initiator efficiency may be decreased at high conversion of reaction

because of the increase of the viscosity of the reaction medium. The diffusion of primary radical out of their cages may be hindered, then, the coupling of two radicals may be easily produced.

As shown in eq. (5.39) that the rate of propagation depends on a half order of initiator concentration. The effect of the amount and type of initiator were studied in our system by using ALPNR1 and ALPNR2 in the presence of 20 part of reactive diluents (HDDA and TPGDA) and various amounts (0.5, 1, 3 and 5 % by weight of rubber and diluent) and types of initiator (Irgacure 184 and Darocur 1173).

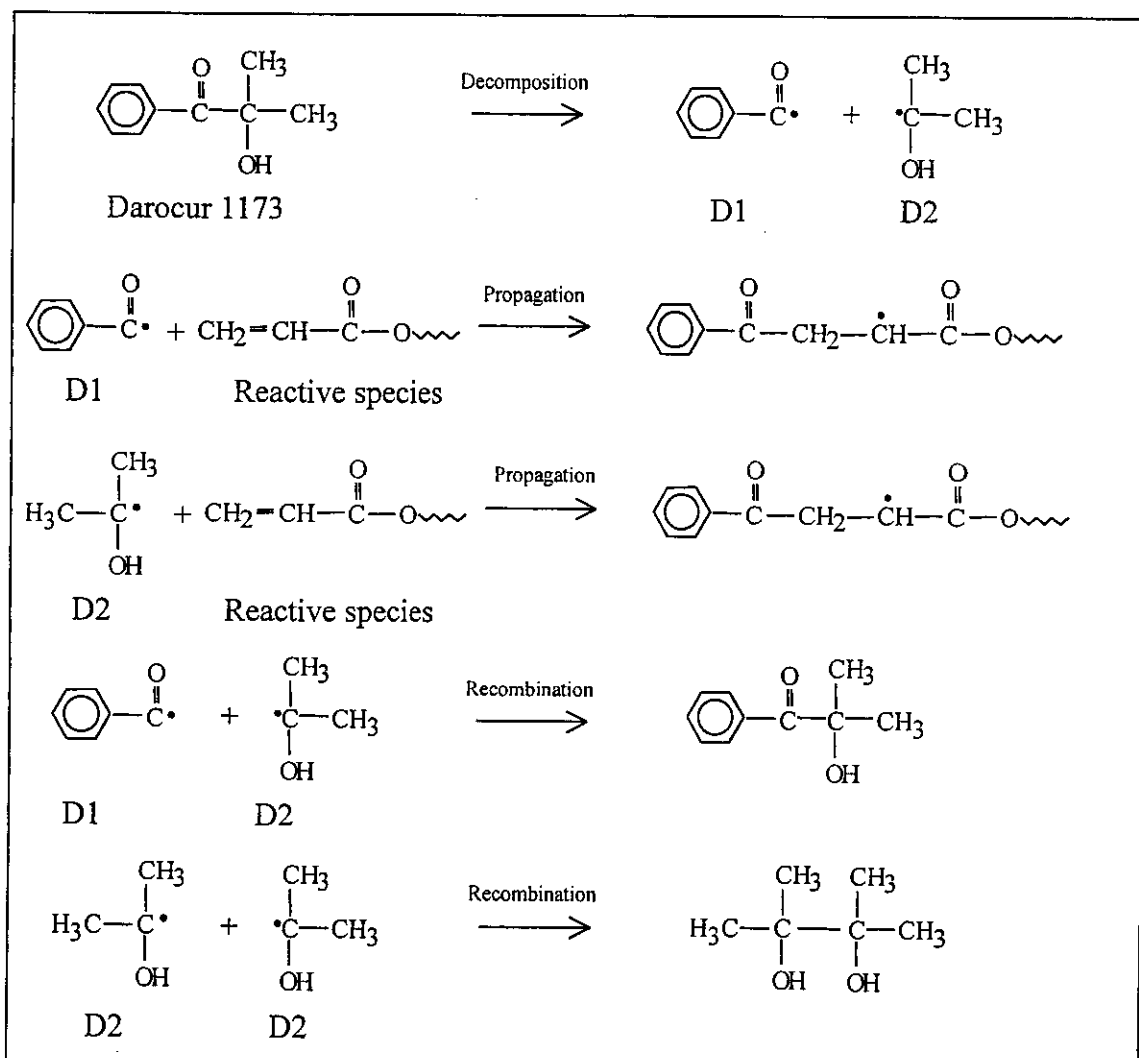


**Figure 5.75** Photolysis of 2,2-dimethyl-2-hydroxy acetophenone (Darocur 1173) and its initiation reaction

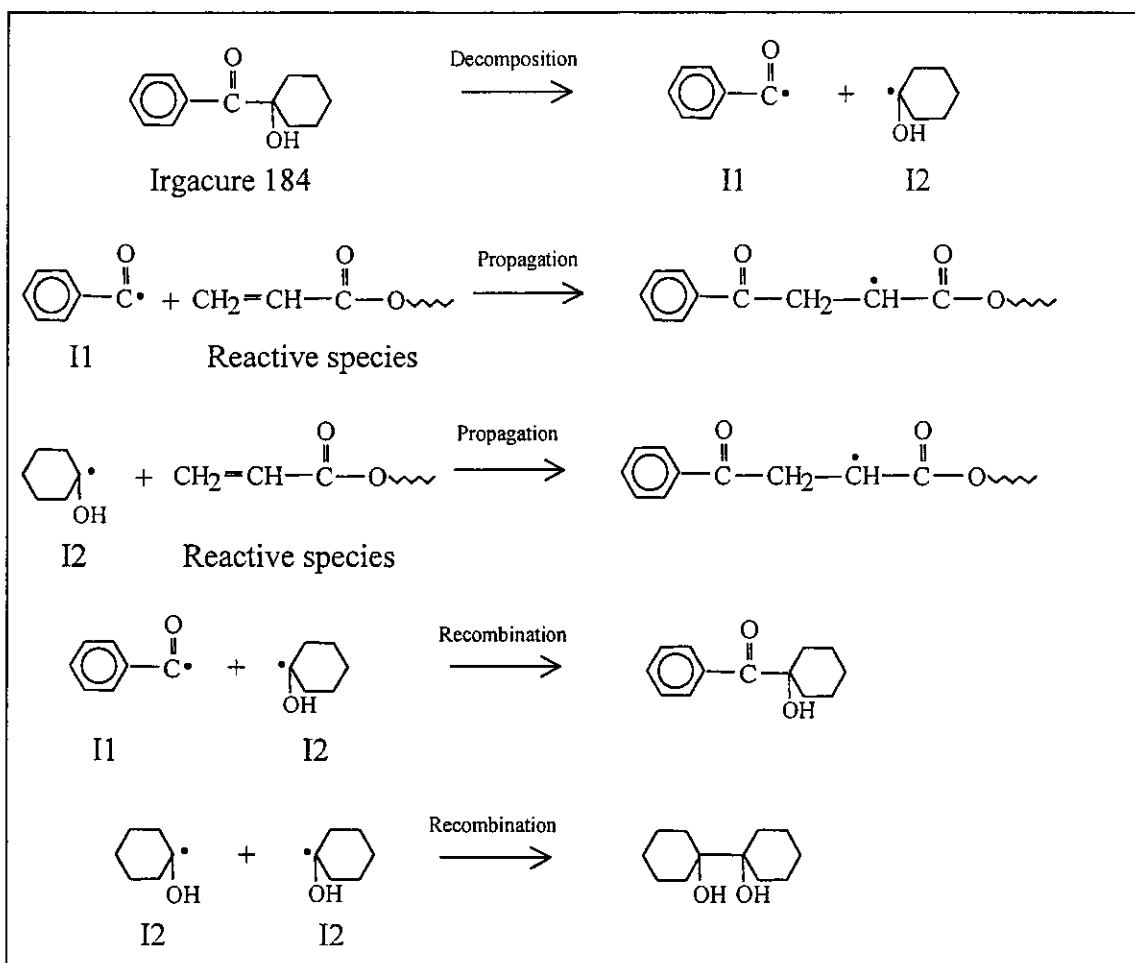


**Figure 5.76** Photolysis of 1-benzoyl-1-hydroxycyclohexane (Irgacure 184) and its initiation reaction.

**Table 5.24** Results of photocrosslinking of acrylated rubber (ALPNR1) in the presence of HDDA, using various amounts of initiator, carried out at 30°C

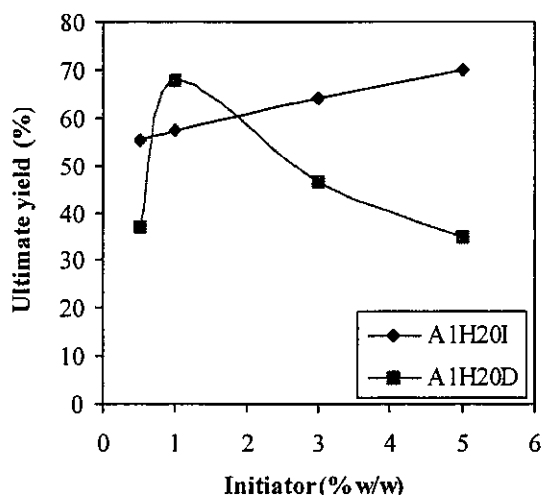
Codes	Rubber (part)	HDDA (part)	Irgacure 184 (part)	Darocur 1173 (part)	Yield (%)	Time onset (min)	k (min <sup>-1</sup> )	Rp <sup>c</sup> mole/l sec
A1H20I.5	100	20	0.6	-	55.47	0.149	104.293	6.62
A1H20I1	100	20	1.2	-	57.49	0.140	127.230	8.06
A1H20I3	100	20	3.6	-	64.08	0.115	136.989	8.51
A1H20I5	100	20	6	-	70.07	0.097	158.920	9.67
A1H20D.5	100	20	-	0.6	36.86	0.163	69.847	4.43
A1H20D1	100	20	-	1.2	67.80	0.136	155.571	9.84
A1H20D3	100	20	-	3.6	46.44	0.194	90.649	5.64
A1H20D5	100	20	-	6	34.96	0.308	53.229	3.23

Table 5.24 shows the results of time onset, ultimate yield, kinetic rate constant ( $k$ ) and rate of photocrosslinking reaction ( $R_p$ ) of ALPNR1. It can be seen that increasing the Irgacure 184 initiator effects in increasing of ultimate yield,  $k$  and  $R_p$  of the reaction. These results are in accordance with the kinetic eq. (5.37). Increasing the amount of the initiator affected also the decrease of time onset of the polymerization. The time onset for utilization of Irgacure 184 (0.5, 1, 3 and 5 %by weight of rubber and diluent) were found to be 0.149, 0.140, 0.115 and 0.097, respectively. However, it was found that increasing the amount of Darocur 1173 initiator from 0.5 % to 1% (by weight of rubber and diluent) effected in increasing the rate of photocrosslinking but increasing the amount of initiator to 3% and 5% (by weight of rubber and diluent), the rate of polymerization and ultimate yield were decreased. This may be proposed that at high amount of initiator resulted in generation of high amount of reactive species, which increased the rate of recombination of the radical initiator rather than the initiation reaction. Therefore, time onset of photopolymerization and rate of the reaction were decreased. The active radical generated from the decomposition of Darocur 1173 resulted in smaller molecule than in the case of the Irgacure 184 initiator, it is assumed that the rate of recombination of the radical initiators species ( $D_2$ ) is higher than the radical species ( $I_2$ ).

Figure 5.77 showed the ultimate yield and  $R_p$  results as a function of initiator concentration of photocrosslinking of ALPNR1. It was observed that the ultimate yield was increased with the increased of initiator concentration in the case of Irgacure 184 initiator. But the optimum values of ultimate yield and  $R_p$  were found in the case of Darocur 1173 initiator.

The effect of type and amount of photoinitiator on photocrosslinking of ALPNR1 in the presence of TPGDA were also investigated. The results are shown in Table 5.25

Table 5.25 shows that increasing the amount of the Irgacure initiator for the compound formulation containing TPGDA (0.5, 1 and 3 % by weight of rubber and diluent) results in increasing the ultimate yield, rate of photocrosslinking reaction ( $k$  and  $R_p$ ). The time onset was decreased as increasing the amount of initiator. These results are in accordance with the compound formulation of ALPNR1 using the HDDA. However, it was found that increasing the amount of Irgacure to 5% (by



**Figure 5.77** Plots of ultimate yield (%) versus initiator concentration (0.5, 1, 3 and 5 % by weight of rubber and diluent) of photopolymerization of ALPNR1 as oligomer with HDDA and TPGDA as diluent carried out at 30°C; (-◆-) A1H20I (ALPNR1:HDDA:Irgacure = 100:20:(0.6, 1.2, 3.6, 6)) and (-■-) A1H20D (ALPNR1:HDDA:Darocur = 100:20:(0.6, 1.2, 3.6, 6))

**Table 5.25** Results of photocrosslinking of acrylated rubber (ALPNR1) in the presence of TPGDA, using various amounts of initiator, carried out at 30°C

Codes	Rubber (part)	TPGDA (part)	Irgacure 184 (part)	Darocur 1173 (part)	Yield (%)	Time onset (min)	k (min <sup>-1</sup> )	Rp <sup>c</sup> mole/l sec
A1T20I.5	100	20	0.6	-	33.78	0.231	47.808	2.71
A1T20I1	100	20	1.2	-	40.32	0.134	69.297	3.91
A1T20I3	100	20	3.6	-	54.34	0.139	120.349	6.65
A1T20I5	100	20	6	-	44.75	0.213	78.218	4.25
A1T20D.5	100	20	-	0.6	62.37	0.117	117.672	6.66
A1T20D1	100	20	-	1.2	36.46	0.295	52.102	2.94
A1T20D3	100	20	-	3.6	61.59	0.141	111.553	6.17
A1T20D5	100	20	-	6	70.71	0.100	113.511	6.14

weight of rubber and diluent) the rate of polymerization was decreased in stead of increasing as in the case of the use of HDDA. This indicated that the effect of the amount of the initiator on the photocrosslinking reaction of ALPNR1 compound formulation depended not on the amount of the radical species generated from the

initiator but also the molecular structure of the diluent. The optimum amount of the Irgacure was found to be 3% (by weight of rubber and diluent) for the use of TPGDA in the compound formulations. The time onsets of the formulation using 1% and 3% (by weight of rubber and diluent) of initiator were also similar. However, the ultimate yield and rate of photocrosslinking were highest at the formulation using 3 part of the TPGDA.

In the system using TPGDA as diluent and Darocur 1173 as initiator i.e. A1T20D(0.5, 1, 3 and 5 % by weight of rubber and diluent), the results in Table 5.25 indicated that the rate of photocrosslinking reaction did not depend linearly on the amount of the initiator. It was assumed that the formation of the three dimensional network of the rubber and the TPGDA was complicated, it might depend on the rate of the dissociation of the initiator, the recombination of the radical species and the diffusion of the reactive diluent to the radical species.

The influences of the type and the amount of the initiator (Irgacure 184 and Darocur 1173) on the photocrosslinking reaction of the ALPNR2 (5% of acrylate function) containing HDDA and TPGDA were also investigated and the results are shown in Table 5.26 and 5.27. It was found in the case of using HDDA that the rate of the photocrosslinking did not relate directly on the amount and type of the initiator. This may be assumed that the ALPNR2 contained only 5% acrylate function on the molecular chain, therefore very small amount of the reactive function. can be found during the propagation reaction, leading to fluctuation of the time onset, ultimate yield and rate of photocrosslinking reaction. The optimum amount of the initiator used for the ALPNR2 containing 20 part of HDDA (20% by weight of rubber) in the case of using Irgacure 184 and Darocur 1173 were 3 and 5% by weight of rubber and diluent, respectively.

In the case of using TPGDA, it seems that the long chain length between the diacrylate helps in better uniformity of the system. The time onset of the photocrosslinking was decreased when the amount of the initiator was increased. The rate of reaction and the ultimate yield were also increased as the increase of the amount of the initiator both in the case of Irgacure 184 and Darocur 1173 initiators.

**Table 5.26** Results of photocrosslinking of acrylated rubber (ALPNR2) in the presence of HDDA, using various amounts of initiator, carried out at 30°C

Codes	Rubber (part)	HDDA (part)	Irgacure 184 (part)	Darocur 1173 (part)	Ultimate Yield (%)	Time onset (min.)	k (min <sup>-1</sup> )	Rp mole/l sec
A2H20L5	100	20	0.6	-	29.04	0.195	42.815	1.85
A2H20I1	100	20	1.2	-	42.00	0.190	34.336	1.48
A2H20I3	100	20	3.6	-	60.87	0.152	95.402	4.05
A2H20I5	100	20	6	-	53.67	0.212	79.790	3.33
A2H20D.5	100	20	-	0.6	32.87	0.292	36.683	1.59
A2H20D1	100	20	-	1.2	36.87	0.464	50.149	2.16
A2H20D3	100	20	-	3.6	62.11	0.187	83.722	3.54
A2H20D5	100	20	-	6	69.76	0.179	114.537	4.77

**Table 5.27** Results of photocrosslinking of acrylated rubber (ALPNR1) in the presence of TPGDA, using various amounts of initiator, carried out at 30°C

Codes	Rubber (part)	TPGDA (part)	Irgacure 184 (part)	Darocur 1173 (part)	Ultimate Yield (%)	Time on set (min.)	k (min <sup>-1</sup> )	Rp mole/l sec
A2T20I.5	100	20	0.6	-	19.57	0.377	16.188	0.59
A2T20I1	100	20	1.2	-	32.88	0.232	34.956	1.28
A2T20I3	100	20	3.6	-	47.92	0.221	49.171	1.74
A2T20I5	100	20	6	-	74.96	0.149	80.576	2.86
A2T20D.5	100	20	-	0.6	12.76	0.495	7.101	0.26
A2T20D1	100	20	-	1.2	16.84	0.410	13.366	0.49
A2T20D3	100	20	-	3.6	32.81	0.179	30.141	1.09
A2T20D5	100	20	-	6	43.27	0.160	52.589	1.87

#### 5.2.4 Effect of reaction temperature

It has been known that the reaction temperature has influence on the rate of dissociation of the initiator and the mobility of the polymer chain as well as the diffusion rate of the reactive diluents. The results of the rate of photocrosslinking reaction of ALPNR1 in the presence of the HDDA and TPGDA using Irgacure 184 and Darocur 1173, carried out at 30 and 60°C are compared in Figure.5.78. It was

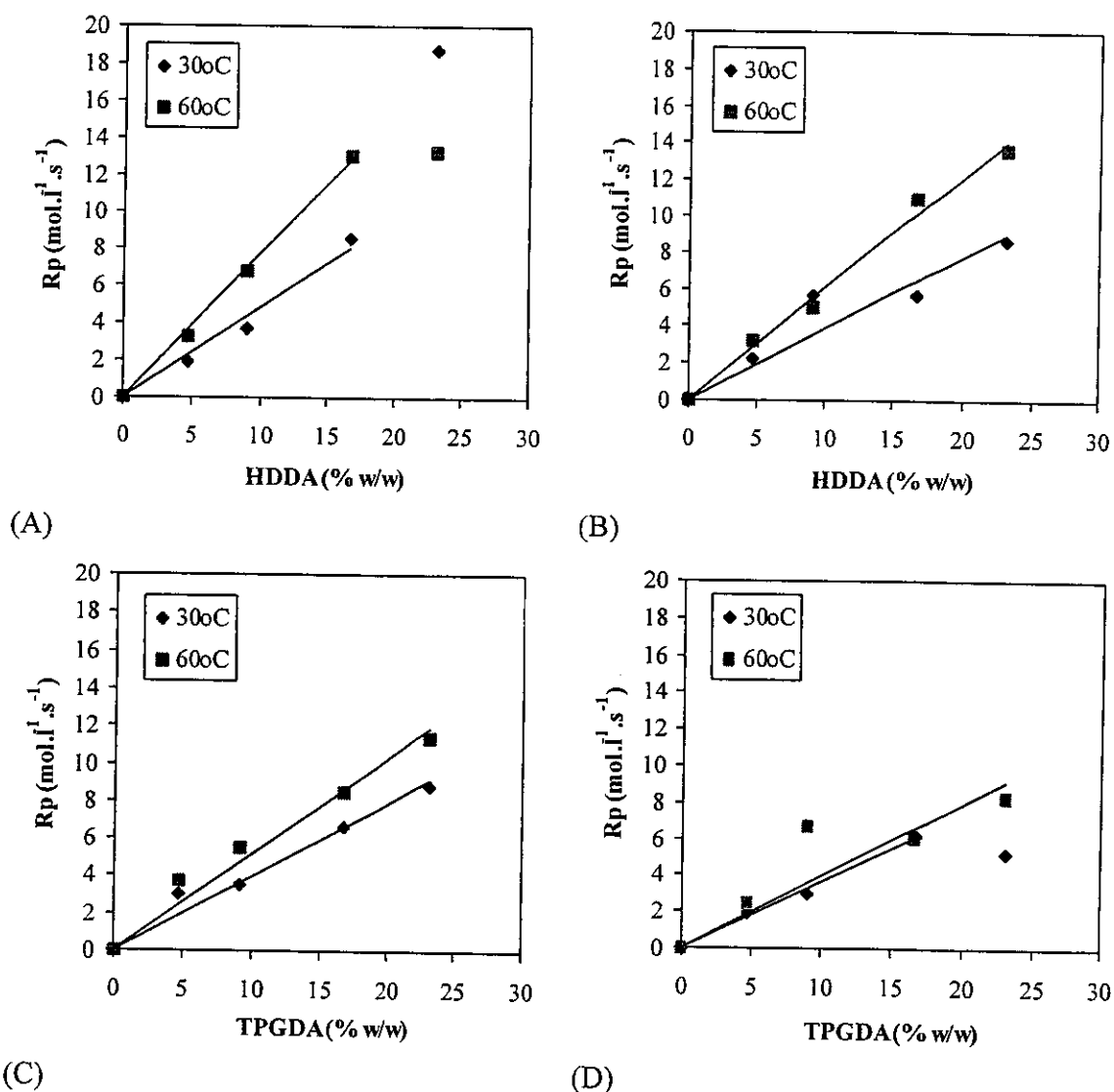


**Figure 5.78** Plots of rate of photopolymerization ( $R_p$ ) versus various amount of diluent of ALPNR1 as oligomer with Irgacure 184 and Daracur 1174 as photoinitiator (3% by weight of rubber and diluent), carried out at 30°C and 60°C;

- (A) A1HI3 (ALPNR1:HDDA:Irgacure = 100:(5, 10, 20, 30):3)
- (B) A1HD3 (ALPNR1:HDDA:Darocur = 100:(5, 10, 20, 30):3)
- (C) A1TI3 (ALPNR1:TPGDA:Irgacure = 100:(5, 10, 20, 30):3)
- (D) A1TD3 (ALPNR1:TPGDA:Darocur = 100:(5, 10, 20, 30):3)

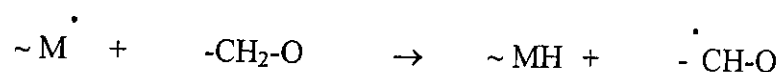
clearly seen that the rate of the photocrosslinking reaction was higher at higher temperature used at all different amount of the initiator added.

The effect of temperature on the photocrosslinking of acrylated rubber (ALPNR3) was studied by isothermal DSC in the range of 30-90°C with four formulations i.e. 100 parts of acrylated rubber in the presence of 20 part of diacrylate diluents (HDDA and TPGDA) and Irgacure 184 as well as Darocur 1173 (3% by weight of rubber and diluent). The plots of %conversion at various irradiation times of different temperatures of ALPNR3 containing HDDA (20 % by weight of rubber) and Irgacure 184 and Darocur 1173 are illustrated in Figure 5.79. It was found that %conversion was increased as increase of irradiation time as well as the reaction temperature. These results were anticipated that the raised temperature stimulated the mobility of monomer molecules, leading to increasing the propagation rate of photopolymerization. Moreover, the increased temperature may effect on reduction of the viscosity of the system which will facilitate the movement of the rigid network and also increase the generation and diffusion of initiator. Then the yield and  $R_p$  were increased with increasing the temperature [Ref.]. However, it was found a little difference in Figure 5.80 that the compound formulation containing the TPGDA both in the case of Irgacure 184 or Darocur 1173 did not show the same principle as in the case of Figure 5.79. It seems likely that the reaction at 60°C resulted in highest rate and %conversion.

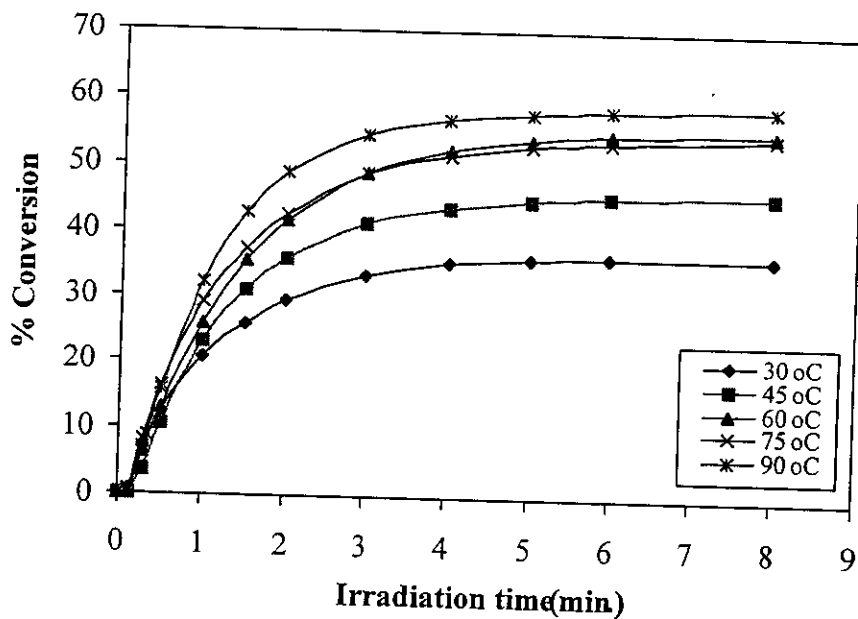
In axiom, the propagation completely stops when the system reached the solidification. Figure 5.81 shows the plots of ultimate yield of the compound formulation of ALPNR3 obtained from UV irradiation at various reaction temperatures. It was found in all cases that the maximum of the ultimate yield was about 60%. This may be due to the effect of autoacceleration which brought about the fast formation of chemical linkage, leading to fast increase of % ultimate yield and rate of polymerization at the initial of reaction [Ref.]. After that, the increased network density hampered both diffusion of monomer and radical propagating chain, then the propagation reaction become quickly slower and less photocrosslinking could be proceeded until the reaction stops due to solidification. It was found that the ultimate yield was increased with increasing the reaction temperature. It is possible that the increase of temperature put forward the ceiling of glassy state of the system, therefore

the propagation could continue further. However, it was found in Figures 5.81(A) and (B) that at 75°C of irradiation the ultimate yield dropped and increased again at 90°C. It was assumed to be due to the existence of transfer reaction which caused acceleration of crosslinked structure, inhibiting further propagation at 70°C. The chain transfer reaction normally uses energy higher than the propagation, it will interfere at high temperature [Ref]. While at 90°C, the temperature is high enough to melt the gel structure and put forward the polymerization [Ref]. However, it was found in the case of A3T20D3 that the maximum ultimate yield was at 75°C and beyond this temperature the ultimate yield dropped significantly. This may be due to slow rate of initial reaction ( $k=89 \text{ min}^{-1}$ ) which may cause evaporation of the reactants (TPGDA), therefore decrease of ultimate yield.

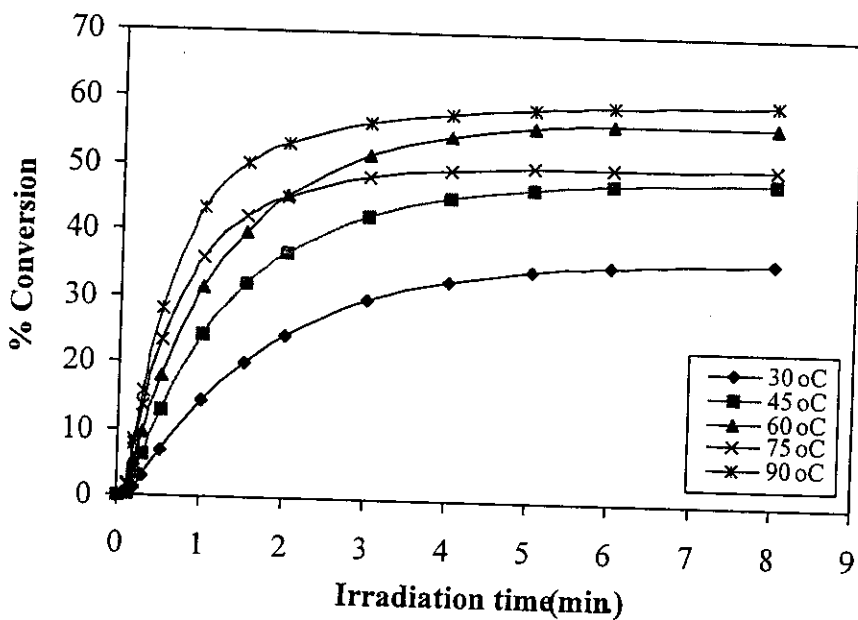
Rates of polymerization of different compound formulations at various temperatures are shown in Figure 5.82. It can be noticed that the increase of reaction temperature, the rate of polymerization was increased (see A3H20I3 and A3H20D3). This may be due to the higher the temperature, the more the diluents and reactive species can be moved. However, the presence of TPGDA and Darocur 1173 in Figure 5.82 (C) and (D) did not follow this hypothesis. This can be assumed that the complexity may come from the nature of the TPGDA and the Darocur 1173 initiator in A3T20I3 and A3T20D3. The dissociated species generated from Darocur 1173 in A3T20D3 may proceed the recombination reaction easier than the Irgacure 184 in A3T20I3 as pointed out in section 5.2.3, therefore the initiation rate is probably more complicated. The longer chain length of the TPGDA than the HDDA may facilitate the chain transfer reaction than in the case of using HDDA (comparing the A3H20D3 and A3T20D3). The TPGDA consists of long chain ether unit, which has tendency for hydrogen abstraction.



Where  $\sim \overset{\cdot}{\text{M}}$  is active radical specy



(A)

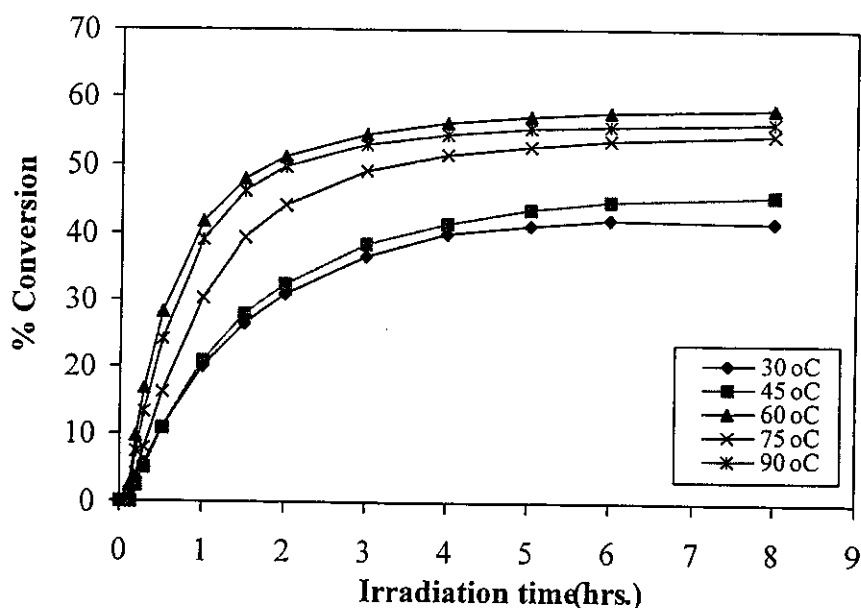


(B)

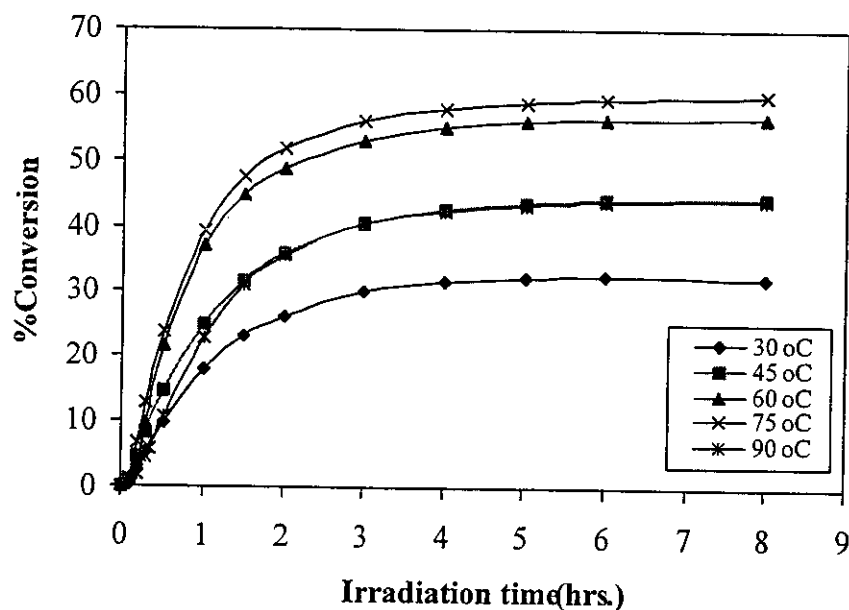
**Figure 5.79** Plot of % conversion versus irradiation time at various reaction temperature (30°C to 90°C) of photopolymerization of ALPNR3 as oligomer, HDDA as diluent and Irgacure 184 and Darocur 1173 as photoinitiators;

(A) A3H20I3 (ALPNR3:HDDA:Irgacure = 100:20:3.6)

(B) A3H20D3 (ALPNR3:HDDA:Darocur = 100:20:3.6)



(A)



(B)

**Figure 5.80** Plot of % conversion versus irradiation time at various reaction temperature(30°C to 90°C) of photopolymerization of ALPNR3 as oligomer, TPGDA as diluent and Irgacure 184 and Darocur 1173 as photoinitiators;

(A) A3T20I3 (ALPNR3:TPGDA:Irgacure = 100:20:3.6)

(B) A3T20D3 (ALPNR3:TPGDA:Darocur = 100:20:3.6)

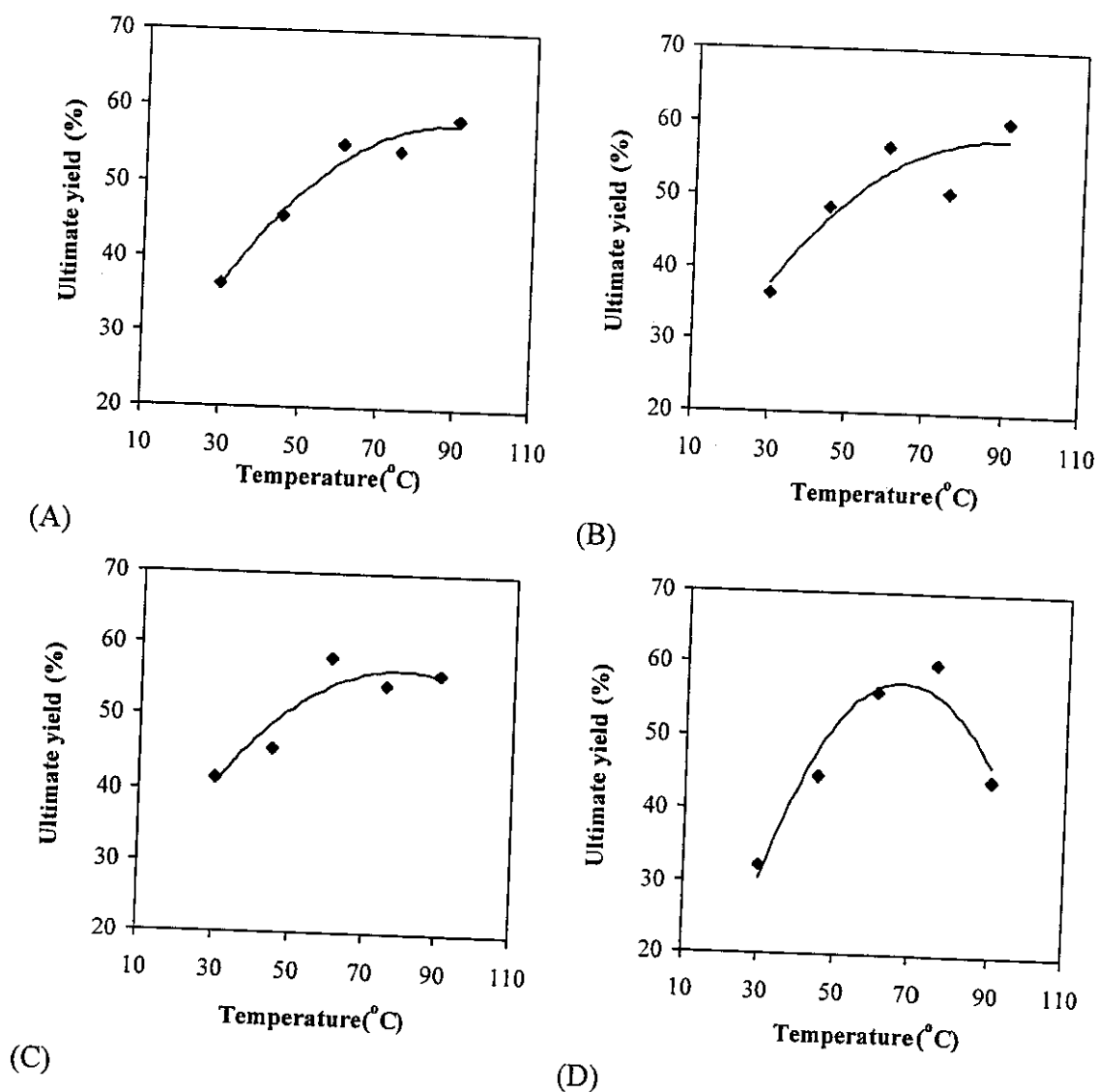
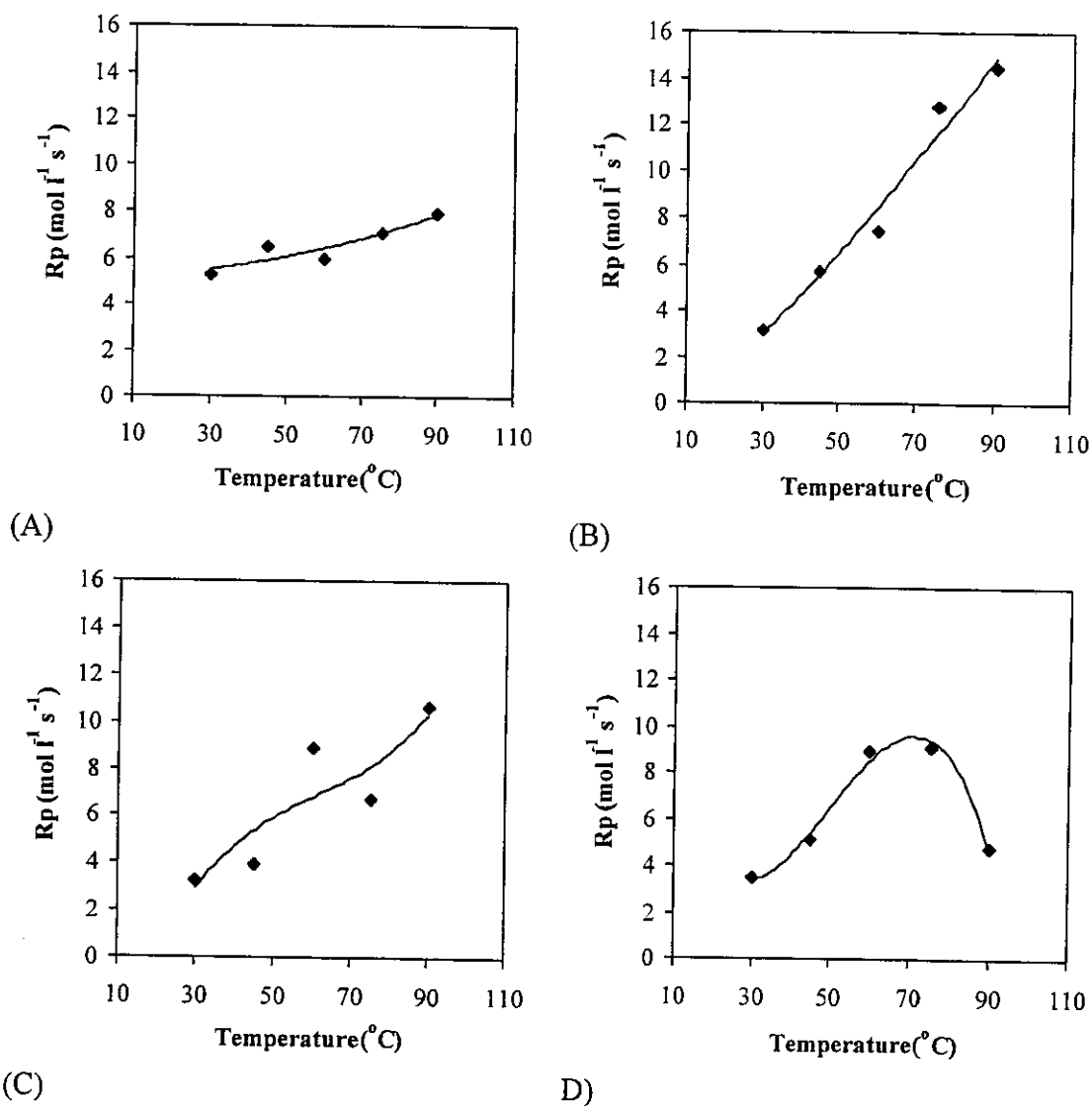


Figure 5.81 Plot of ultimate yield (%) versus temperature of photopolymerization of ALPNR3 with 4 formulations;

- (A) A3H20I3 (ALPNR3:HDDA:Irgacure = 100:20:3.6)
- (B) A3H20D3 (ALPNR3:HDDA:Darocur = 100:20:3.6)
- (C) A3T20I3 (ALPNR3:TPGDA:Irgacure = 100:20:3.6)
- (D) A3T20D3 (ALPNR3:TPGDA:Darocur = 100:20:3.6)





**Figure 5.82** Temperature dependence on polymerization rate of ALPNR 3 with 4 formulations;

(A) A3H20I3 (ALPNR3:HDDA:Irgacure = 100:20:3.6)

(B) A3H20D3 (ALPNR3:HDDA:Darocur = 100:20:3.6)

(C) A3T20I3 (ALPNR3:TPGDA:Irgacure = 100:20:3.6)

(D) A3T20D3 (ALPNR3:TPGDA:Darocur = 100:20:3.6)

The radical generated from chain transfer may offer both grafting and termination but at a reduced rate of propagation. At 75°C for A3T20I3 system, this temperature is sufficiently high to generate the chain transfer effect but it was not enough for movement of monomer to react with the generated radicals. Then the trapped radicals have tendency to termination. However, the raised temperature, 90°C, encouraged the network mobility and monomer movement which brought about the increase of yield and  $R_p$  of the A3T20I3.

The ultimate yield and  $R_p$  of A3T20D3 were increased at increased temperature upto the highest at 75°C, then dropped at the temperature of 90°C. It is assumed that at 90°C, there were the competition of chain transfer and thermal depropagation which was supported by its negative value of activation energy [ref.].

The activation energy ( $E_a$ ) for creating the network structure was calculated from the Arrhenius Law. In the polymerization of multifunctional monomer to network structure, the activation energy cannot respect relatively on the basic equation [Ref]:

$$E_a = E_p - 0.5 E_t \quad (5.28)$$

When  $E_i$  is close to 0

However, in this work, the calculation was done under steady state condition and first order assumption, derived for bimolecular termination.

From this assumption, the  $E_a$  can be obtained from the plots of the  $k$  values versus reaction temperature from Arrhenius equation:

$$k = A e^{-E_a/RT} \quad (5.7)$$

Arrhenius plot of  $\ln k$  with  $1/T$  are given in Figure 5.83. It can be noticed that most of the system showed a straight line. However, the plots of A3T20D3, two distinguish lines were detected. Then, the calculation was divided into two separated regions, 30-60°C and 75-90°C. The  $E_a$  values obtained for these formulations are demonstrated in Table 5.18. It can be seen that the energy needed for photopolymerisation of the ALPNR3 in different formulations are in the order of A3H20I3 < A3T20I3 < A3H20D3 < A3T20D3. It can be proposed and concluded that

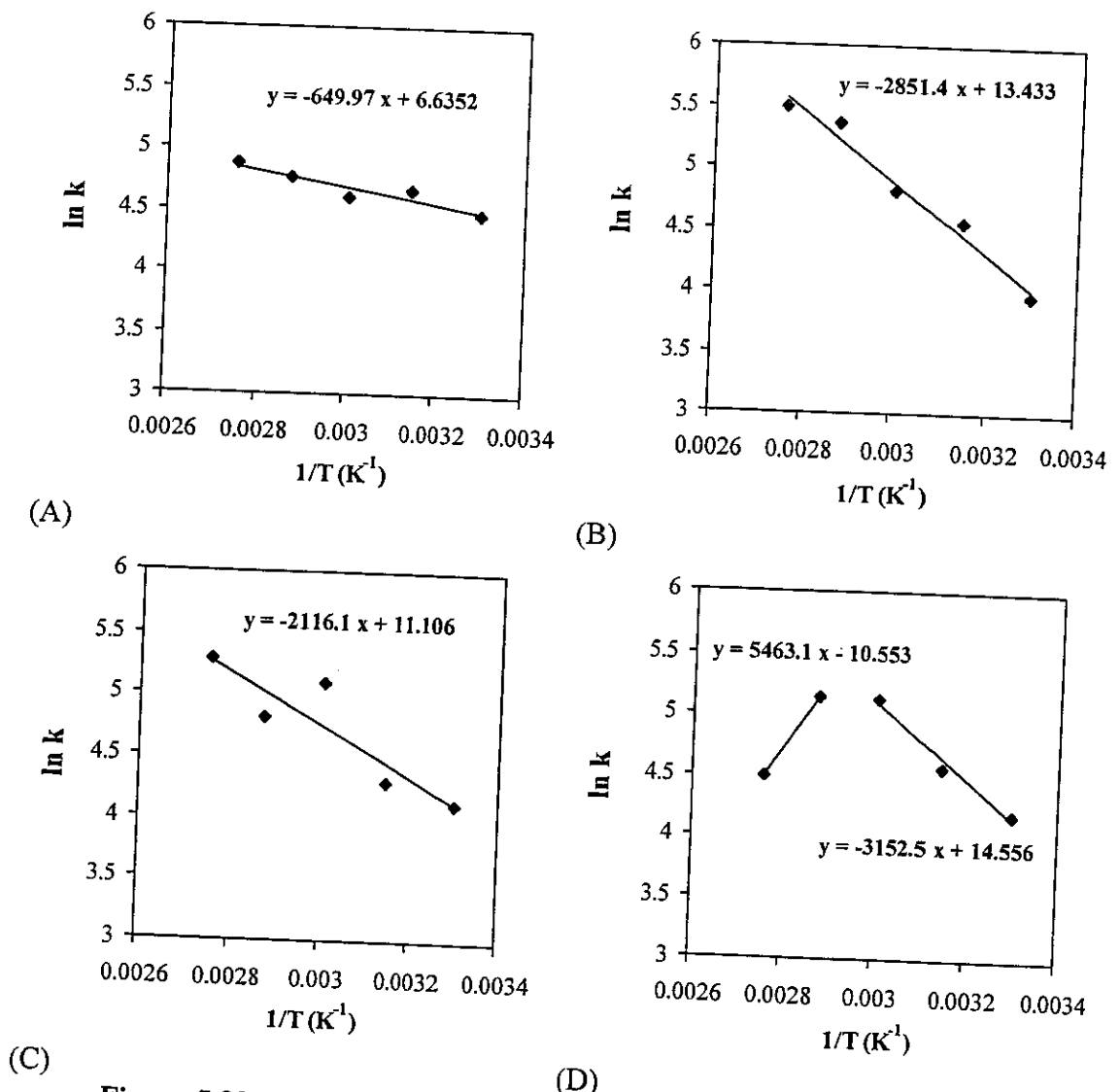


**Figure 5.83** Arrhenius plots of ALPNR 3 with 4 formulations;

- (A) A3H20I3 (ALPNR3:HDDA:Irgacure = 100:20:3.6)
- (B) A3H20D3 (ALPNR3:HDDA:Darocur = 100:20:3.6)
- (C) A3T20I3 (ALPNR3:TPGDA:Irgacure = 100:20:3.6)
- (D) A3T20D3 (ALPNR3:TPGDA:Darocur = 100:20:3.6)

the energy needed for initiation of HDDA is lower than the TPGDA and the energy needed for dissociation of Darocur is higher than the Irgacure. The negative value of  $E_a$  obtained from A3T20D3 may come from both the chain transfer from polyacrylate backbone and or depropagation of the polymerization chain [Ref.].

**Table 5.28** Activation energy of photopolymerization of ALPNR3 carried out 30-90°C

Formulation	A3H20I3	A3H20D3	A3T20I3	A3T20D3	
Ea (kJ mol <sup>-1</sup> )	5.40 <sup>a</sup>	23.71 <sup>a</sup>	16.46 <sup>a</sup>	26.21 <sup>b</sup>	-45.42 <sup>c</sup>

a : measured between 30-90°C;

b : measured between 30-60°C

c : measured between 75-90°C

### 5.3 Comparison of photocrosslinking of liquid, epoxidized and acrylated purified natural rubbers

Generally, photocrosslinking reaction of acrylic monomer with di- and polyfunctional acrylate monomer can be carried out under irradiation. However, the final product might not offer appropriate elastic property. Therefore, it is proposed that the addition of the liquid rubber into the compound formulation may render this property. However, the rubber should participate in the crosslinked structure. Figure 5.84 shows the plots of %conversion of liquid natural rubber (LPNR), epoxidized liquid natural rubber (ELPNR) and acrylated rubber (ALPNR1) in the presence of HDDA (20% by weight of rubber) and Irgacure 184 initiator (3% by weight of rubber and diluent), carried out at 30°C. It can be noticed that the initial rate of conversion of ALPNR1 is similar to the ELPNR which higher than LPNR. This might be due to the incompatibility of the HDDA and the LPNR that retard the photopolymerisation of the HDDA dispersed in the LPNR. The %conversion in the case of LPNR and ELPNR were much higher than the ALPNR. This can be assumed that the crosslink density of the ALPNR is higher than the LPNR and ELPNR, which may come from the reaction of the HDDA with the acrylate function fixed on the ALPNR. The HDDA may be trapped in the rigid structure of ALPNR, leading to lower %conversion in the case of ALPNR than LPNR and ELPNR. However, it may be possible that the radicals which were generated on the rubber chain of LPNR or ELPNR by UV irradiation or H-abstraction from transfer reaction participate in the chain propagation but at a very slow rate compared to the propagation of acrylate function. If there were the incorporation of the LPNR or ELPNR in chain polymerization of diacrylate diluent, the intermolecular network should have not enough to interrupt the movement of

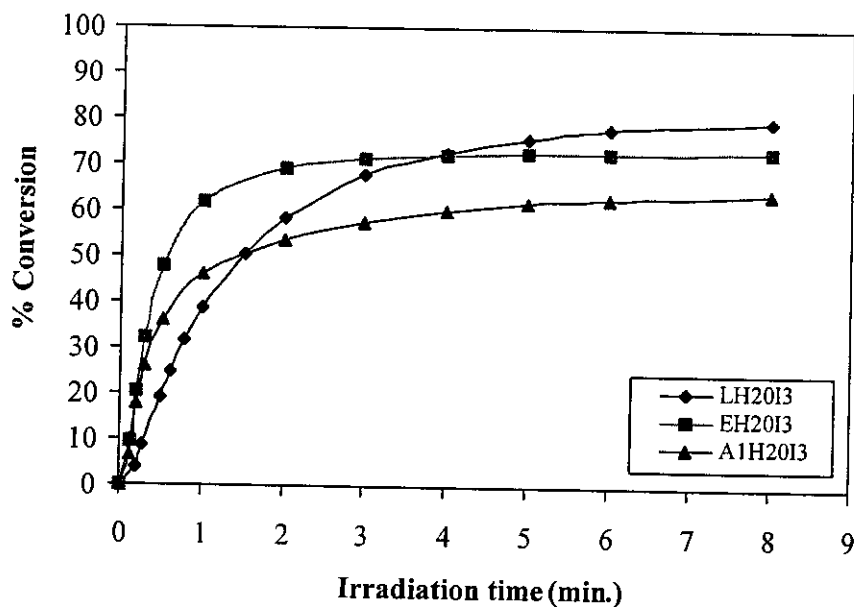
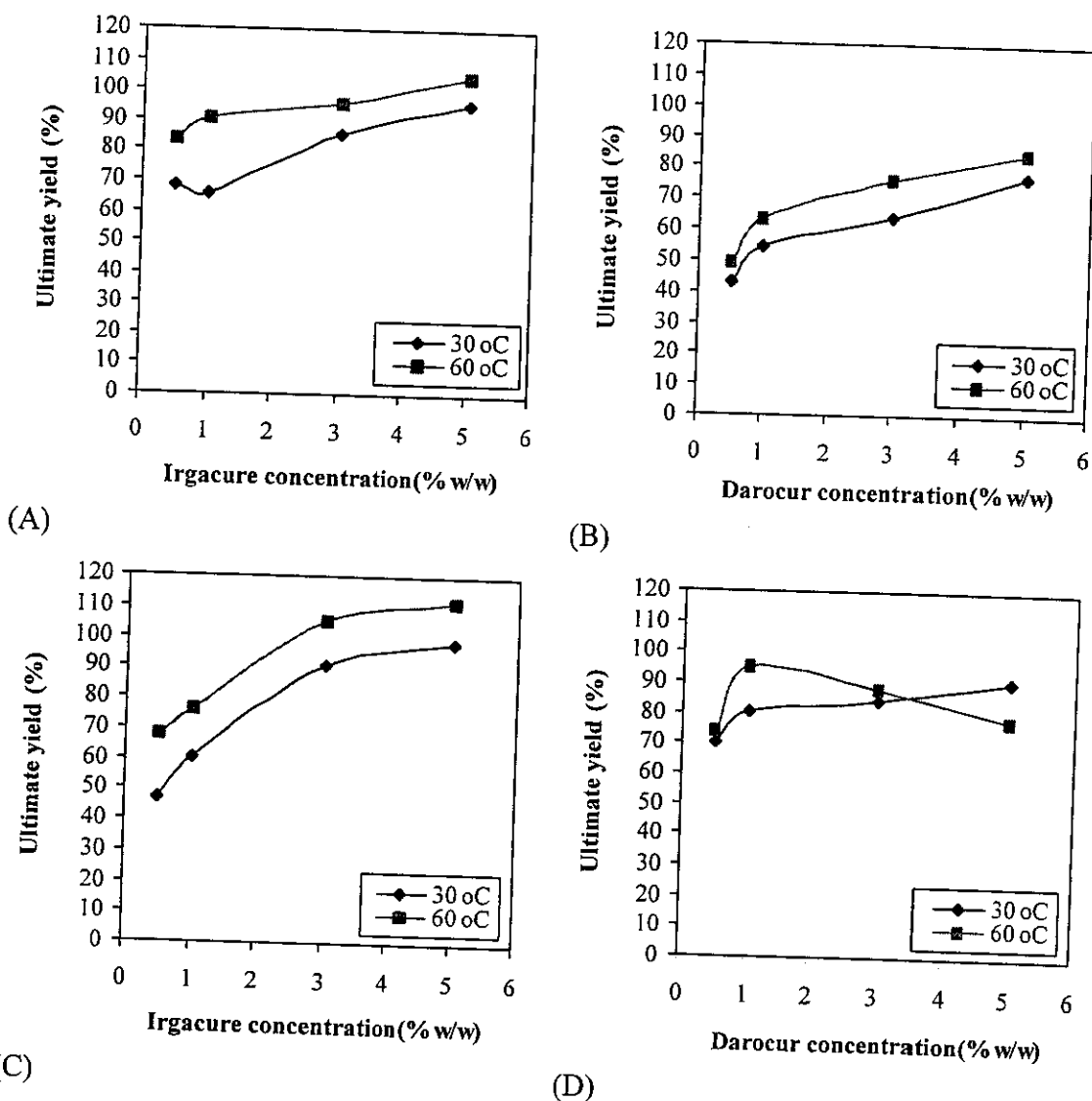


**Figure 5.84** Graft polt between % conversion versus irradiation time of LPNR, ELPNR and ALPNR1 with HDDA (20% by weight of rubber) and Irgacure 184 (3% by weight of rubber and diluent), carried out at 30°C

monomer and radical species, then high yield was achieved. The  $R_p$  values of LH20I3, EH20I3 and A1H20I3 were 1.46, 3.51 and 8.51 respectively.

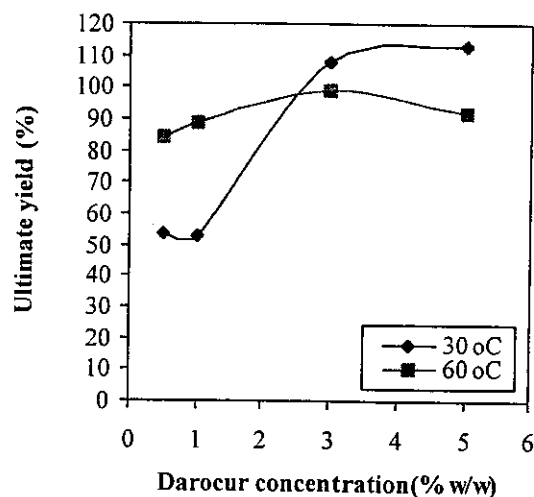
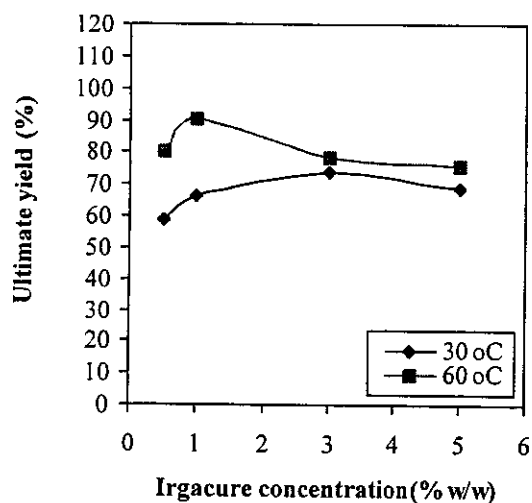
While the photopolymerization of acrylated function on acrylated rubber is too stiff to permit a complete polymerization of reactive diluent, because the high amount of intermolecular crosslinking between acrylated monomer and acrylated rubber reduced the flexibility of rubbers chain, prohibited the movement of radical species and also the movement of reactive diluent.

Figure 5.85 shows the ultimate yield of LPNR with HDDA and TPGDA at 30 and 60°C. It was found that increasing the reaction temperature for LPNR as well as the amount of the initiator, the ultimate yield was increased and each 100% in some cases. This may be supported that the liquid rubber may not participate in the crosslinked structure as a chemical linkage of the system but rather the long chain may interpenetrate in the network of polyacrylate. Similar results were obtained in the case of irradiation of ELPNR at 30 and 60°C, in the presence of HDDA or TPGDA that at 60°C, the ultimate yield reached 100% (see Figure5.86). However, in some cases, it



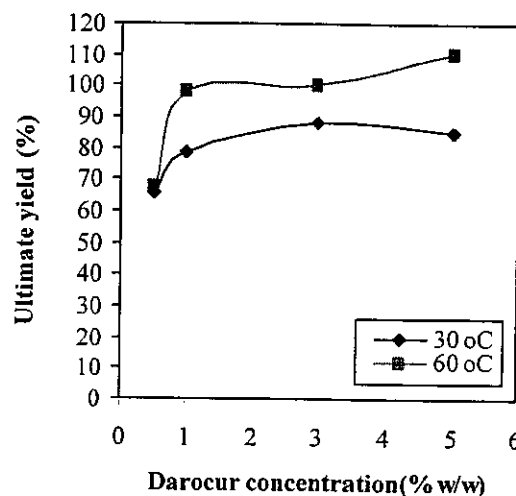
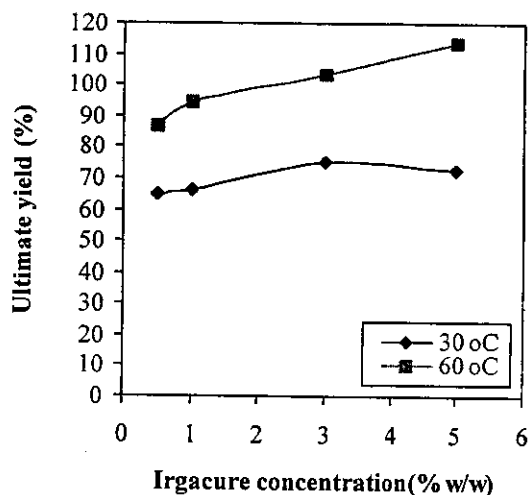
**Figure 5.60** Plots of ultimate yield (%) versus initiator concentration (0.5, 1, 3 and 5% by weight of rubber and diluent) of photopolymerization of LPNR as oligomer with HDDA and TPGDA as diluents carried out at 30°C and 60°C;

- (A) LH20I (LPNR:HDDA:Irgacure = 100:20:(0.6, 1.2, 3.6, 6))
- (B) LH20D (LPNR:HDDA:Darocur = 100:20:(0.6, 1.2, 3.6, 6))
- (C) LT20I (LPNR:TPGDA:Irgacure = 100:20:(0.6, 1.2, 3.6, 6))
- (D) LT20D (LPNR:TPGDA:Darocur = 100:20:(0.6, 1.2, 3.6, 6))



(A)

(B)



(C)

(D)

**Figure 5.61** Plots of ultimate yield (%) versus initiator concentration (0.5, 1, 3 and 5% by weight of rubber and diluent) of photopolymerization of ELPNR as oligomer with HDDA and TPGDA as diluents carried out at 30°C and 60°C;

(A) ELH20I (ELPNR:HDDA:Irgacure = 100:20:(0.6, 1.2, 3.6, 6))

(B) ELH20D (ELPNR:HDDA:Darocur = 100:20:(0.6, 1.2, 3.6, 6))

(C) ELT20I (ELPNR:TPGDA:Irgacure = 100:20:(0.6, 1.2, 3.6, 6))

(D) ELT20D (ELPNR:TPGDA:Darocur = 100:20:(0.6, 1.2, 3.6, 6))

was noticed that the ultimate yield passed the 100%, it may be assumed the occurrence of chain transfer reaction or reaction of ring opening unit of the epoxide that might react with the acrylate function of the HDDA which generated the heat of the reaction. Therefore, heat released was increasing.

It was found in Table 5.29 and 5.30 that the rates of polymerization ( $R_p$ ) in the case of LPNR and EPNR compound formulations were smaller than in the case of ALPNR1. This may be assumed that the presence of the acrylate function on the rubber chain accelerated the photocrosslinking reaction while the presence of the LPNR and ELPNR retarded the propagation of the HDDA or TPGDA. While the ultimate yields of irradiated LPNR and EPNR compound formulations were significantly higher than the ALPNR1. This may be due to the HDDA or TPGDA were not trapped by the crosslinked structure of the ALPNR participated in the photocrosslinking reaction.

The addition of the acrylic acid in the system of LPNR and ELPNR in the presence of HDDA or TPGDA were carried out and the results are shown in Table 5.34 and 5.35. It appeared that the addition of acrylic acid in the LPNR and ELPNR did not help in increasing the rate of polymerization. However, it was found that the ultimate yield was decreased, compared to the use of only the diluent (HDDA or TPGDA). The presence of the acrylic acid which is a smaller molecule than the HDDA or TPGDA, may play a role of better plasticizer. The ultimate yield was decreased with increasing of acrylic acid concentration. This may be assumed that increasing of acrylic acid, the viscosity of the system was reduced, leading to enhancement of the mobility of active chain, in contrast, it reduced the possible interaction between reactive functional groups. In addition, high amount of acrylic acid (15 part) in LPNR system may generate phase separation of diluents and oligomer that caused the gel effect of the acrylic acid and the HDDA and TPGDA.

All the results obtained from the photopolymerization were calculated and showed in Table 5.29-5.35.

**Table 5.29** The kinetic parameters from photopolymerization of photocurable materials, using oligomers (ALPNR1, ALPNR2, ALPNR3, LPNR and ELPNR) and reactive diluents (HDDA and TPGDA) as 20 % by weight of rubber, by various amount of photoinitiators (Irgacure 184 and Darocur 1173) as 0.5, 1, 3 and 5 % by weight of rubber and diluent, carried out at 30°C

Codes	$\Delta H_{\text{photo}}$ (J/g)	$\Delta H_{\text{theory}}$ (J/g)	Ultimate Yield (%)	Time onset (min.)	n	k (min <sup>-1</sup> )	$M_0$ (mole/kg)	Rp mole/kg min	$M_0$ (mole/l)	Rp mole/l sec
A1H20I.5	156.587	282.28	55.47	0.149	1.122	104.293	3.27	341.04	3.81	6.62
A1H20I1	161.470	280.89	57.49	0.140	1.295	127.230	3.26	414.77	3.80	8.06
A1H20I3	176.505	275.43	64.08	0.115	1.204	136.989	3.20	438.37	3.73	8.51
A1H20I5	189.324	270.18	70.07	0.097	1.173	158.920	3.13	497.42	3.65	9.67
A1H20D.5	104.042	282.29	36.86	0.163	1.069	69.847	3.27	228.40	3.81	4.43
A1H20D1	190.449	280.89	67.80	0.136	1.235	155.571	3.26	506.99	3.79	9.84
A1H20D3	127.915	275.44	46.44	0.194	1.162	90.649	3.20	290.08	3.72	5.64
A1H20D5	94.458	270.18	34.96	0.308	1.127	53.229	3.13	166.61	3.64	3.23
A1T20I.5	84.804	251.08	33.78	0.231	1.091	47.808	2.91	139.12	3.40	2.71
A1T20I1	100.723	249.84	40.32	0.134	1.228	69.297	2.90	200.96	3.39	3.91
A1T20I3	133.117	244.99	54.34	0.139	1.292	120.349	2.84	341.79	3.31	6.65
A1T20I5	107.539	240.33	44.75	0.213	1.138	78.218	2.79	218.23	3.26	4.25
A1T20D.5	156.599	251.09	62.37	0.117	1.285	117.672	2.91	342.43	3.40	6.66
A1T20D1	91.087	249.83	36.46	0.295	1.160	52.102	2.91	151.10	3.38	2.94
A1T20D3	150.898	244.99	61.59	0.141	1.284	111.553	2.84	316.81	3.32	6.17
A1T20D5	169.923	240.32	70.71	0.100	1.150	113.511	2.79	316.70	3.24	6.14
A2H20I.5	59.397	204.54	29.04	0.195	1.233	42.815	2.37	101.47	2.60	1.85
A2H20I1	85.552	203.69	42.00	0.190	1.023	34.336	2.36	81.03	2.58	1.48
A2H20I3	121.936	200.31	60.87	0.152	1.288	95.402	2.32	221.33	2.55	4.05
A2H20I5	105.766	197.05	53.67	0.212	1.262	79.790	2.29	182.72	2.51	3.33
A2H20D.5	67.230	204.55	32.87	0.292	1.057	36.683	2.37	86.94	2.59	1.59
A2H20D1	75.099	203.69	36.87	0.464	1.080	50.149	2.36	118.35	2.59	2.16
A2H20D3	124.410	200.31	62.11	0.187	1.124	83.722	2.32	194.24	2.54	3.54
A2H20D5	137.462	197.05	69.76	0.179	1.246	114.537	2.29	262.29	2.50	4.77
A2T20I.5	33.920	173.32	19.57	0.377	1.050	16.188	2.01	32.54	2.21	0.59
A2T20I1	56.753	172.60	32.88	0.232	1.093	34.956	2.00	69.91	2.19	1.28
A2T20I3	81.330	169.73	47.92	0.221	1.169	49.171	1.97	96.87	2.16	1.74
A2T20I5	125.147	166.96	74.96	0.149	1.117	80.576	1.94	156.32	2.13	2.86
A2T20D.5	22.122	173.34	12.76	0.495	1.076	7.101	2.01	14.27	2.20	0.26
A2T20D1	29.063	172.62	16.84	0.410	1.138	13.366	2.00	26.73	2.19	0.49
A2T20D3	55.719	169.81	32.81	0.179	1.042	30.141	1.97	59.38	2.16	1.09

Codes	$\Delta H_{\text{photo}}$ (J/g)	$\Delta H_{\text{theory}}$ (J/g)	Ultimate Yield (%)	Time onset (min.)	n	k (min <sup>-1</sup> )	$M_0$ (mole/kg)	Rp mole/kg min	$M_0$ (mole/l)	Rp mole/l sec
A2T20D5	72.296	167.10	43.27	0.160	1.283	52.589	1.94	102.02	2.13	1.87
A3H20I3	97.606	266.50	36.63	0.166	1.13	87.60	3.09	270.69	3.60	5.30
A3H20D3	98.177	266.49	36.84	0.284	1.11	52.50	3.09	162.22	3.59	3.14
A3T20I3	97.667	236.04	41.38	0.202	0.99	61.33	2.74	168.05	3.20	3.30
A3T20D3	77.353	236.04	32.77	0.206	1.16	65.83	2.74	180.38	3.19	3.50
LH20I.5	85.656	126.50	67.71	0.425	1.010	47.219	1.47	69.41	1.27	1.00
LH20I1	82.536	125.88	65.57	0.172	1.197	44.871	1.46	65.51	1.26	0.94
LH20I3	105.482	123.44	85.45	0.277	1.600	71.016	1.43	101.55	1.24	1.46
LH20I5	115.893	121.08	95.72	0.133	1.652	155.043	1.40	217.06	1.23	3.17
LH20D.5	54.430	126.51	43.02	0.468	1.377	31.287	1.47	45.99	1.26	0.66
LH20D1	68.291	125.88	54.25	0.518	1.056	34.647	1.46	50.58	1.26	0.73
LH20D3	79.087	123.43	64.07	0.340	1.464	65.200	1.43	93.24	1.24	1.35
LH20D5	93.130	121.08	76.92	0.184	1.344	107.533	1.40	150.55	1.22	2.19
LT20I.5	44.481	95.30	46.67	0.340	1.169	33.096	1.11	36.74	0.95	0.53
LT20I1	57.431	94.83	60.56	0.117	1.452	65.628	1.10	72.19	0.95	1.04
LT20I3	84.522	92.98	90.90	0.096	1.610	149.396	1.08	161.348	0.94	2.33
LT20I5	89.597	91.22	98.22	0.099	1.408	123.569	1.06	130.98	0.92	1.90
LT20D.5	67.140	95.30	70.45	0.250	1.158	47.337	1.11	52.54	0.95	0.75
LT20D1	76.359	94.83	80.52	0.177	1.256	67.094	1.10	73.80	0.95	1.06
LT20D3	78.520	92.99	84.44	0.172	1.299	55.701	1.08	60.16	0.94	0.87
LT20D5	82.752	91.22	90.72	0.159	1.776	93.822	1.06	99.45	0.92	1.44
E1H20I.5	74.357	126.51	58.78	0.220	1.048	63.669	1.47	93.59	1.31	1.39
E1H20I1	83.098	125.88	66.01	0.179	1.470	124.549	1.46	181.84	1.30	2.71
E1H20I3	91.127	123.43	73.83	0.143	1.543	163.842	1.43	234.29	1.29	3.51
E1H20I5	83.257	121.08	68.76	0.157	1.296	86.306	1.40	120.83	1.27	1.83
E1H20D.5	67.562	126.50	53.41	0.276	1.319	67.330	1.47	98.98	1.31	1.47
E1H20D1	66.550	125.88	52.87	0.232	1.440	79.321	1.46	115.81	1.31	1.73
E1H20D3	133.326	123.44	108.01	0.129	1.583	297.555	1.43	425.50	1.29	6.38
E1H20D5	136.444	121.09	112.68	0.095	1.954	268.997	1.40	376.60	1.26	5.67
E1T20I.5	61.651	95.30	64.69	0.176	1.264	66.82	1.11	74.17	0.99	1.10
E1T20I1	62.902	94.83	66.33	0.211	1.333	61.461	1.10	67.61	0.98	1.01
E1T20I3	69.916	92.99	75.19	0.111	1.656	162.439	1.08	175.43	0.97	2.62
E1T20I5	66.423	91.21	72.82	0.094	1.805	117.202	1.06	124.23	0.96	1.87
E1T20D.5	62.573	95.30	65.66	0.094	1.764	148.950	1.11	165.33	0.99	2.45
E1T20D1	74.172	94.83	78.22	0.168	1.427	76.165	1.10	83.78	0.99	1.25
E1T20D3	82.009	92.99	88.19	0.084	2.107	112.247	1.08	121.23	0.97	1.82
E1T20D5	77.415	91.22	84.87	0.090	1.885	168.899	1.06	179.03	0.95	2.68

**Table 5.30** The kinetic parameters from photopolymerization of photocurable materials, using oligomers (ALPNR1, ALPNR2, ALPNR3, LPNR and ELPNR) and reactive diluents (HDDA and TPGDA), as 20 % by weight of rubber, by various amount of photoinitiators (Irgacure 184 and Darocur 1173) as 0.5, 1, 3 and 5 % by weight of rubber and diluent, carried out at 60°C

Codes	$\Delta H_{\text{photo}}$ (J/g)	$\Delta H_{\text{theory}}$ (J/g)	Ultimate Yield (%)	Time onset (min.)	n	k (min <sup>-1</sup> )	$M_0$ (mole/kg)	Rp mole/kg min	$M_0$ (mole/l)	Rp mole/l sec
A1H20I.5	145.733	282.29	51.63	0.298	1.104	82.517	3.27	269.83	3.81	5.24
A1H20I1	145.763	280.89	51.89	0.249	1.210	102.535	3.26	334.26	3.80	6.49
A1H20I3	231.097	275.43	83.90	0.119	1.455	210.377	3.20	673.21	3.72	13.05
A1H20I5	203.063	270.18	75.16	0.113	1.148	172.967	3.13	541.39	3.65	10.53
A1H20D.5	128.115	282.28	45.39	0.122	1.128	62.085	3.27	203.02	3.81	3.94
A1H20D1	190.182	280.38	67.83	0.166	1.170	129.918	3.25	422.23	3.79	8.20
A1H20D3	222.152	275.44	80.65	0.119	1.260	177.718	3.20	568.70	3.71	10.99
A1H20D5	156.763	270.19	58.02	0.321	1.259	106.548	3.13	333.50	3.64	6.46
A1T20I.5	148.962	251.08	59.33	0.195	1.261	125.036	2.91	363.85	3.40	7.08
A1T20I1	131.203	249.84	52.51	0.219	1.201	105.858	2.90	306.99	3.39	5.98
A1T20I3	169.325	244.98	69.12	0.116	1.262	152.811	2.84	433.98	3.32	8.45
A1T20I5	184.670	240.31	76.85	0.116	1.326	192.328	2.79	536.60	3.25	10.43
A1T20D.5	207.312	251.08	82.57	0.109	1.394	182.966	2.91	532.43	3.40	10.36
A1T20D1	173.530	249.83	69.46	0.178	1.179	134.075	2.90	388.82	3.39	7.56
A1T20D3	147.379	244.98	60.16	0.204	1.210	110.145	2.84	312.81	3.31	6.07
A1T20D5	200.864	240.32	83.58	0.122	1.081	158.064	2.79	441.00	3.24	8.53
A2H20I.5	81.806	204.55	39.99	0.334	1.060	33.901	2.37	80.11	2.60	1.46
A2H20I1	99.365	203.69	48.78	0.262	1.096	62.165	2.36	146.71	2.58	2.68
A2H20I3	126.547	200.31	63.87	0.171	1.819	264.119	2.32	612.76	2.55	11.21
A2H20I5	133.732	197.05	67.87	0.183	1.264	104.136	2.29	238.47	2.51	4.36
A2H20D.5	84.638	204.55	42.20	0.321	1.046	42.398	2.37	100.48	2.59	1.83
A2H20D1	95.415	203.69	46.84	0.257	1.062	40.703	2.36	96.06	2.59	1.76
A2H20D3	140.519	200.31	70.15	0.296	1.033	82.550	2.32	191.52	2.54	3.49
A2H20D5	115.762	197.05	58.75	0.213	1.796	185.991	2.29	425.92	2.50	7.75
A2T20I.5	90.027	173.32	51.94	0.333	1.193	62.784	2.01	126.20	2.21	2.31
A2T20I1	58.694	172.59	34.01	0.204	1.077	31.284	2.00	62.57	2.20	1.14
A2T20I3	97.564	169.73	57.48	0.303	1.142	65.059	1.97	128.17	2.16	2.35
A2T20I5	98.016	166.96	58.71	0.193	1.104	60.099	1.94	116.59	2.13	2.14
A2T20D.5	39.304	173.34	22.67	0.258	1.122	16.920	2.01	34.01	2.20	0.62
A2T20D1	29.059	172.62	16.83	0.422	1.316	14.698	2.00	29.40	2.19	0.54
A2T20D3	74.515	169.81	43.88	0.247	1.198	44.460	1.97	87.59	2.16	1.60

Codes	$\Delta H_{\text{photo}}$ (J/g)	$\Delta H_{\text{theory}}$ (J/g)	Ultimate Yield (%)	Time onset (min.)	n	k ( $\text{min}^{-1}$ )	$M_0$ (mole/kg)	Rp mole/kg min	$M_0$ (mole/l)	Rp mole/ sec
A2T20D5	105.058	167.09	62.88	0.158	1.123	69.255	1.94	134.36	2.13	2.46
A3H20I3	147.379	266.49	55.30	0.272	1.10	99.12	3.09	306.27	3.60	6.00
A3H20D3	151.557	266.49	56.87	0.182	1.05	123.35	3.09	381.14	3.59	7.38
A3T20I3	138.436	236.04	58.65	0.162	1.45	165.29	2.74	452.89	3.20	8.90
A3T20D3	134.230	236.05	56.87	0.270	1.31	168.68	2.74	462.18	3.19	8.97
LH20I.5	105.881	126.50	83.70	0.263	1.176	67.728	1.47	99.56	1.27	1.43
LH20I1	113.654	125.88	90.29	0.201	1.019	99.554	1.46	145.35	1.26	2.10
LH20I3	118.171	123.44	95.73	0.222	1.388	80.858	1.43	115.63	1.24	1.67
LH20I5	126.825	121.09	104.74	0.144	1.888	188.124	1.40	263.37	1.22	3.83
LH20D.5	62.112	126.50	49.10	0.407	1.230	40.964	1.47	60.22	1.26	0.86
LH20D1	79.739	125.88	63.35	0.371	1.200	30.499	1.46	44.53	1.26	0.64
LH20D3	93.465	123.43	75.72	0.299	1.235	82.195	1.43	117.54	1.24	1.70
LH20D5	102.513	121.09	84.66	0.159	1.476	112.056	1.40	156.88	1.22	2.29
LT20I.5	65.012	95.30	68.22	0.113	1.887	161.855	1.11	179.66	0.95	2.57
LT20I1	72.111	94.83	76.04	0.158	1.525	67.518	1.10	74.270	0.95	1.07
LT20I3	98.244	92.98	105.66	0.244	1.609	182.948	1.08	197.58	0.94	2.86
LT20I5	101.855	91.22	111.66	0.089	1.410	184.805	1.06	195.89	0.92	2.85
LT20D.5	70.491	95.30	73.97	0.328	1.130	55.562	1.11	61.67	0.96	0.89
LT20D1	90.117	94.83	95.03	0.190	1.328	90.985	1.10	100.08	0.95	1.44
LT20D3	81.913	92.99	88.09	0.232	2.150	66.540	1.08	71.86	0.94	1.04
LT20D5	70.749	91.22	77.56	0.330	1.438	63.606	1.06	67.42	0.92	0.98
E1H20I.5	101.113	126.50	79.93	0.195	1.239	97.827	1.47	143.81	1.31	2.14
E1H20I1	114.051	125.88	90.60	0.119	1.863	268.932	1.46	392.64	1.31	5.86
E1H20I3	96.599	123.43	78.26	0.198	1.336	115.008	1.43	164.46	1.29	2.47
E1H20I5	92.073	121.09	76.04	0.131	1.691	151.411	1.40	211.98	1.01	2.55
E1H20D.5	106.471	126.51	84.16	0.117	1.536	207.867	1.47	305.56	1.31	4.54
E1H20D1	111.429	125.88	88.52	0.127	1.668	180.152	1.46	263.02	1.30	3.90
E1H20D3	122.182	123.44	98.98	0.086	1.716	169.881	1.43	242.93	1.29	3.64
E1H20D5	111.332	121.09	91.94	0.112	1.811	260.734	1.40	365.03	1.27	5.50
E1T20I.5	82.290	95.30	86.35	0.098	1.811	175.720	1.11	195.05	0.99	2.89
E1T20I1	89.588	94.83	94.47	0.104	1.644	153.915	1.10	169.31	0.99	2.53
E1T20I3	96.276	92.99	103.53	0.094	1.490	186.457	1.08	201.37	0.97	3.01
E1T20I5	103.491	91.22	113.45	0.088	1.772	5.379	1.06	229.87	0.96	3.46
E1T20D.5	64.332	95.30	67.50	0.160	1.134	50.390	1.11	55.93	0.99	0.83
E1T20D1	93.186	94.83	98.27	0.132	1.805	154.625	1.10	170.09	0.98	2.53
E1T20D3	93.199	92.99	100.22	0.098	1.970	139.561	1.08	150.73	0.97	2.25
E1T20D5	100.777	91.22	110.48	0.109	1.810	162.098	1.06	171.82	0.95	2.58

**Table 5.31** The kinetic parameters from photopolymerization of photocurable material using oligomers (ALPNR3), reactive diluents (HDDA and TPGDA) as 20 % by weight of rubber and photoinitiators (Irgacure 184 and Darocur 1173) as 3 % by weight of rubber and diluent, by various reaction temperatures as 30, 45, 60, 75 and 90 °C

Codes	$\Delta H_{\text{photo}}$ (J/g)	$\Delta H_{\text{theory}}$ (J/g)	Ultimate Yield (%)	Time onset (min.)	n	k ( $\text{min}^{-1}$ )	$M_0$ (mole/kg)	Rp mole/kg min	$M_0$ (mole/l)	Rp mole/l sec
A3H20I3-30	97.606	266.50	36.63	0.166	1.13	87.60	3.09	270.69	3.60	5.30
A3H20I3-45	122.695	266.49	46.04	0.371	1.25	107.05	3.09	330.79	3.60	6.48
A3H20I3-60	147.379	266.49	55.30	0.272	1.10	99.12	3.09	306.27	3.60	6.00
A3H20I3-75	145.354	266.49	54.54	0.231	1.20	116.73	3.09	360.71	3.60	7.06
A3H20I3-90	170.930	266.49	64.14	0.349	1.08	130.93	3.09	404.59	3.60	7.92
A3H20D3-30	98.177	266.49	36.84	0.284	1.11	52.50	3.09	162.22	3.59	3.14
A3H20D3-45	129.538	266.49	48.61	0.236	1.13	94.63	3.09	292.41	3.59	5.66
A3H20D3-60	151.557	266.49	56.87	0.182	1.05	123.35	3.09	381.14	3.59	7.38
A3H20D3-75	135.855	266.49	50.98	0.164	1.44	213.32	3.09	659.16	3.59	12.76
A3H20D3-90	161.407	266.49	60.57	0.201	1.43	241.63	3.09	746.63	3.59	14.46
A3T20I3-30	97.667	236.04	41.38	0.202	0.99	61.33	2.74	168.05	3.20	3.30
A3T20I3-45	108.457	236.04	45.95	0.266	1.20	73.32	2.74	200.89	3.20	3.95
A3T20I3-60	138.436	236.04	58.65	0.162	1.45	165.29	2.74	452.89	3.20	8.90
A3T20I3-75	129.871	236.04	55.02	0.258	1.33	124.15	2.74	340.17	3.20	6.68
A3T20I3-90	133.460	236.05	56.54	0.189	1.44	197.61	2.74	541.45	3.20	10.64
A3T20D3-30	77.353	236.04	32.77	0.206	1.16	65.83	2.74	180.38	3.19	3.50
A3T20D3-45	106.188	236.04	44.99	0.151	1.25	96.20	2.74	263.58	3.19	5.11
A3T20D3-60	134.230	236.05	56.87	0.270	1.31	168.68	2.74	462.18	3.19	8.97
A3T20D3-75	142.296	236.04	60.28	0.204	1.34	171.62	2.74	470.25	3.19	9.12
A3T20D3-90	104.776	236.05	44.39	0.354	1.20	89.71	2.74	245.81	3.19	4.77

**Table 5.32** The kinetic parameters from photopolymerization of photocurable materials, using oligomers (ALPNR1) and photoinitiators (Irgacure 184 and Darocur 1173) as 3 % by weight of rubber and diluent, by various amount of reactive diluents (HDDA and TPGDA) as 5, 10, 20 and 30 % by weight of rubber, carried out at 30°C

Codes	$\Delta H_{\text{photo}}$ (J/g)	$\Delta H_{\text{theory}}$ (J/g)	Ultimate Yield (%)	Time onset (min.)	n	k (min <sup>-1</sup> )	$M_0$ (mole/kg)	Rp mole/kg min	$M_0$ (mole/l)	Rp mole/l sec
A1H5I3	61.640	208.97	29.50	0.176	1.106	38.791	2.42	93.87	2.87	1.86
A1H10I3	101.337	233.15	43.46	0.167	1.221	68.889	2.70	186.00	3.19	3.66
A1H20I3	176.505	275.43	64.08	0.115	1.204	136.989	3.20	438.37	3.73	8.51
A1H30I3	218.028	311.22	70.06	0.114	1.393	270.291	3.61	975.75	4.16	18.73
A1H5D3	61.466	208.97	29.41	0.322	1.170	46.109	2.42	111.58	2.86	2.20
A1H10D3	97.398	233.15	41.77	0.174	1.199	105.752	2.70	285.53	3.17	5.59
A1H20D3	127.915	275.44	46.44	0.194	1.162	90.649	3.20	290.08	3.72	5.64
A1H30D3	181.465	311.22	58.31	0.100	1.021	125.286	3.61	452.28	4.15	8.67
A1T5I3	91.303	200.28	45.59	0.177	1.128	65.281	2.32	151.45	2.76	3.00
A1T10I3	112.212	216.53	51.82	0.133	1.207	72.327	2.51	181.54	2.96	3.57
A1T20I3	133.117	244.99	54.34	0.139	1.292	120.349	2.84	341.79	3.31	6.65
A1T30I3	169.323	269.06	62.93	0.111	1.372	145.897	3.12	455.20	3.61	8.79
A1T5D3	73.876	200.28	36.89	0.193	1.098	42.237	2.32	97.99	2.76	1.94
A1T10D3	76.270	216.54	35.22	0.137	1.175	61.399	2.51	154.11	2.96	3.02
A1T20D1	91.087	249.83	36.46	0.295	1.160	52.102	2.91	151.10	3.38	2.94
A1T30D3	120.165	269.06	44.66	0.118	1.287	87.628	3.12	273.40	3.60	5.26

**Table 5.33** The kinetic parameters from photopolymerization of photocurable materials, using oligomers (ALPNR1) and photoinitiators (Irgacure 184 and Darocur 1173) as 3 % by weight of rubber and diluent, by various amount of reactive diluents (HDDA and TPGDA) as 5, 10, 20 and 30 % by weight of rubber, carried out at 60°C

Codes	$\Delta H_{\text{photo}}$ (J/g)	$\Delta H_{\text{theory}}$ (J/g)	Ultimate Yield (%)	Time onset (min.)	n	k ( $\text{min}^{-1}$ )	$M_0$ (mole/kg)	Rp mole/kg min	$M_0$ (mole/l)	Rp mole/l sec
A1H5I3	100.820	208.98	48.24	0.213	1.181	67.775	2.42	164.02	2.88	3.25
A1H10I3	149.999	233.15	64.34	0.229	1.241	126.735	2.70	342.18	3.19	6.73
A1H20I3	231.097	275.43	83.90	0.119	1.455	210.377	3.20	673.21	3.72	13.05
A1H30I3	242.298	311.22	77.85	0.100	1.117	191.101	3.61	689.87	4.16	13.25
A1H5D3	79.419	208.98	38.00	0.344	1.287	68.825	2.42	159.30	2.87	3.15
A1H10D3	152.374	233.15	65.35	0.138	1.388	95.507	2.70	257.87	3.17	5.05
A1H20D3	222.152	275.44	80.65	0.119	1.260	177.718	3.20	568.70	3.71	10.99
A1H30D3	201.762	311.22	34.83	0.118	1.444	197.098	3.61	711.52	4.15	13.65
A1T5I3	104.778	200.28	52.32	0.177	1.329	80.826	2.32	187.52	2.76	3.72
A1T10I3	124.233	216.54	57.37	0.122	1.149	110.112	2.51	276.38	2.97	5.45
A1T20I3	169.325	244.98	69.12	0.116	1.262	152.811	2.84	433.98	3.32	8.45
A1T30I3	156.832	269.06	58.29	0.205	1.404	189.275	3.12	590.54	3.61	11.39
A1T5D3	90.325	200.28	45.10	0.116	1.097	53.383	2.32	123.85	2.75	2.45
A1T10D3	125.802	216.54	58.10	0.167	1.454	137.126	2.51	344.19	2.96	6.75
A1T20D3	147.379	244.98	60.16	0.204	1.210	110.145	2.84	312.81	3.31	6.07
A1T30D3	183.936	269.06	68.36	0.183	1.081	137.428	3.12	428.78	3.60	8.26

**Table 5.35** The kinetic parameters from photopolymerization of photocurable materials, using oligomers (LPNE and ELPNR) and photoinitiators (Irgacure 184 and Darocur 1173) as 1% by weight of rubber and diluent, by various type and amount of reactive diluents (acrylic acid as mono-reactive function and HDDA and TPGDA as di-reactive functions) as 5, 10 and 15 % by weight of rubber, carried out at 60°C

Codes	$\Delta H_{\text{photo}}$ (J/g)	$\Delta H_{\text{theory}}$ (J/g)	Ultimate Yield (%)	Time onset (min.)	n	k ( $\text{min}^{-1}$ )	$M_0$ (mole/kg)	Rp mole/kg min	$M_0$ (mole/l)	Rp mole/l sec
LH10a10I1	39.116	151.63	25.80	0.526	1.081	12.643	1.15	14.54	1.62	0.34
LH10a10D1	59.177	151.64	39.02	0.333	1.638	45.961	1.15	52.86	1.62	1.24
LT10a10I1	42.544	136.11	31.26	0.532	1.375	17.761	1.15	20.43	1.47	0.44
LT10a10D1	31.814	136.11	23.37	0.158	1.514	51.951	1.15	59.74	1.47	1.27
LH5a15I1	36.057	164.51	21.92	0.293	1.283	28.763	1.72	49.47	1.80	0.86
LH5a15D1	21.788	164.51	13.24	0.165	1.307	30.766	1.72	52.92	1.80	0.92
LT5a15I1	32.309	156.78	20.61	0.173	1.276	28.755	1.72	49.46	1.73	0.83
LT5a15D1	20.611	156.78	13.15	0.315	1.615	23.843	1.72	41.01	1.72	0.69
EH10a10I1	60.963	151.64	40.20	0.116	1.654	79.036	1.15	90.89	1.68	2.21
EH10a10D1	62.581	151.63	41.27	0.177	1.616	86.965	1.15	100.01	1.68	2.44
ET10a10I1	37.282	136.10	27.39	0.178	1.706	49.181	1.15	56.56	1.52	1.25
ET10a10D1	55.567	136.11	40.83	0.121	1.396	47.651	1.15	54.80	1.52	1.21
EH5a15I1	57.154	164.51	34.74	0.122	1.734	60.166	1.72	103.49	1.87	1.87
EH5a15D1	49.125	164.51	29.86	0.127	1.816	74.106	1.72	127.461	1.86	2.30
ET5a15I1	36.144	156.78	23.05	0.126	1.975	55.114	1.72	94.80	1.79	1.61
ET5a15D1	43.534	156.78	27.77	0.123	1.666	55.556	1.72	95.56	1.78	1.65

## CHAPTER VI

### CONCLUSIONS

From the study of modification of purified natural rubber (PNR) into photosensitive materials and studied of photocrosslinking reaction of prepared photosensitive rubber by photocalorimetry under ultraviolet irradiation, the following conclusion could be made:

1. The preparation of light color photosensitive rubber could be carried out by three-step chemical modification of PNR i.e. degradation, epoxidation and addition reaction. The purified of natural rubber (NR) as PNR by enzymatic treatment, surfactant washing and ultracentrifugation resulted in reduction of protein and other non-rubber dispersed in latex phase and bounded with the rubber particles. FTIR spectrum of PNR showed the disappearance of characteristic amide signals, corresponding to the presentation of protein comparing with the spectrum of NR. Micro-Kjeldahl technique reported the decrease of the nitrogen content (%) of NR and PNR from 0.4 to 0.03% respectively.

2. The oxidative degradation of PNR in latex phase, using potassium persulfate ( $K_2S_2O_8$ ) and propanal could be achieved. The results found that amount of  $K_2S_2O_8$ , propanal, temperature, dry rubber content, amount of oxygen and types of surfactant affect the intrinsic viscosity and kinetic rate constant of chain degradation of liquid rubber obtained. The highest kinetic rate constant was found to be  $11.33 \times 10^{-2} \text{ sec}^{-1}$ , when the degradation reaction was carried out at  $80^\circ\text{C}$ , 5% DRC of PNR latex, 1 phr of  $K_2S_2O_8$ , 32 phr of propanal and 0.34 phr of  $Na_3PO_4$ . By using the condition of 5% DRC of PNR latex, 1 phr of  $K_2S_2O_8$ , 32 phr of propanal and 0.34 phr of  $Na_3PO_4$ , the activation energy for oxidative degradation was found to be  $76.56 \text{ kJ.mol}^{-1}$ .

3. The epoxidation reaction of liquid PNR (LPNR) could be carried out by 2 methods, in organic phase using *m*-chloroperbenzoic acid and in latex phase using *in-situ* peroxyformic acid. The preparation of epoxidized LPNR (ELPNR) in organic phase showed the controllable of amount of epoxide content and could not detected of the secondary products. The preparation of ELPNR in latex phase was found that type and amount of surfactant, amount of hydrogen peroxide ( $H_2O_2$ ) and formic acid ( $HCOOH$ ) affect the epoxidation reaction and the secondary reaction. When the epoxidation reaction was carried out in cationic surfactant, the secondary reactions especially ether linkage were found to be higher than in non-ionic surfactant, the increase of molecular weight of ELPNR was detected.
4. Increase amount of  $H_2O_2$  from 0.3 to 1.2 moles per mole of isoprene unit (PI), the epoxide content was found to be increased as well as the secondary products contents. The effect of  $HCOOH$  was found in the same tread that increasing amount of  $HCOOH$ , the secondary products contents increased. The kinetic rate constant of the formation of epoxide structure showed the decreased with increasing amount of  $H_2O_2$  and  $HCOOH$ . It may be due to the formation of secondary products might reduce the rate of the epoxide formation.
5. The epoxidized liquid rubber could be prepared by another way using the degradation of epoxidized PNR (EPNR) with periodic acid ( $H_5IO_6$ ). The telechelic ELPNR obtained showed the same amount of epoxide content with the starting EPNR. It was found that amount of epoxide units on the rubber chain and amount of  $H_5IO_6$  did not effect to the molecular weight of liquid rubber obtained.
6. The degradation reaction by using  $H_5IO_6$  could be also with NR and PNR latex. Then, the degradation reaction pathway was proposed vie the formation of vic-diols on the carbon-carbon double bond of rubber by  $H_5IO_6$  and then degradation by another  $H_5IO_6$ .
7. The fixation of acrylate groups onto epoxidized molecules could be achieved. The addition of acrylic acid (10 fold per mole of epoxied unit) on 4,5-epoxy-

4-methyloctane was obviously observed the presentation of four additional adducts of two types of acrylate structures and two type of allyl alcohol i.e. 4-methyl-5-acrylated-4-octanol (compound 2), 5-methyl-5-acrylated-4-octanol (compound 3), 2-propyl-1-hexene-3-ol (compound 4) and 5-methyl-5-octene-4-ol (compound 5) respectively. The epoxide structure showed the total disappearance after 34 hours of addition time, the whole acrylate adducted (compound 2 and 3) and two types of secondary products (compound 4 and 5) represented 74%, 12% and 12% yields after 34 hours respectively, detected by  $^1\text{H}$  NMR spectroscopy.

8. High molecular weight as epoxidized liquid synthetic rubber (ELIR) and epoxidized liquid purified natural rubber (ELPNR) showed lower levels of modification comparing with addition onto 4,5-epoxy-4-methyloctane. However, four mains adducts were also observed. By using 10 fold of acrylic acid per mold of epoxidized unit, ELPNR (17% epoxide content) as mostly cis-1,4-polyisoprene structure showed the whole acrylate adducts as 39 % yield, at 34 hours of reaction. In the same condition, ELIR (17% epoxide content) constructed of the mixture of 1,4-polyisoprene structure (cis- and trans- structure) and 3,4-polyisoprene structure exhibited the lower yield (%) of the whole acrylate adducts as 11% after 34 hours of the addition time respectively.

9. On the addition reaction, it was found that temperature and amount of acrylic acid affect the fixation of acrylic acid onto ELPNR. 40% yield of the whole acrylate adducts were carried out at 70°C and 10 fold of acrylic acid per mold of epoxidized unit in toluene solution after 34 hours of reaction. Decreasing the reaction temperature to 60°C, the addition reaction was found to be 23% yield of acrylate adducts at the same time. It can be concluded that the reaction temperature was effect on stimulate the addition reaction as the kinetic of the addition reaction and yield (%) of acrylate adducts increased with increasing of the reaction temperature.

In our condition, excess amount of acrylic acid (10 fold per mold of epoxide unit) was found to act as self-acid catalyst for the addition reaction. The kinetic rate constant and yield (%) of acrylate adducts of addition reaction of acrylic acid onto ELPNR (17% epoxide content) were found to increase from  $4.69 \times 10^{-8}$  and 8% to

$2.54 \times 10^{-7}$  and 40% with the amount of acrylic acid increased from 2 fold to 10 fold after 34 hours of reaction respectively.

10. The NMR technique was found to be acceptable method for the determination of acrylate adducts constants and the secondary adducts as well as the progression of the addition reaction than the determination by FTIR technique. Because of the disappearance of the peak area ratio of epoxide to methyl detected by FTIR technique could not refer to the modification to acrylate structure. Moreover, the secondary adducts were difficult to observed.

11. The photopolymerization of acrylated liquid purified natural rubber (ALPNR) to produced highly crosslinked rubber depended on amount of acrylate function on the rubber chain, molecular weight of ALPNR, types and amount of reactive diluents and photoinitiator. Increase of the amount of acrylate function on the rubber chain observed the increase of the rate of polymerization ( $R_p$ ). The decrease of molecular weight of rubber showed also the increased of rate and conversion of polymerization. It may be due to the increase of acrylate units on the rubber chain and decrease of molecular weight as the increase of the dense of active function resulted to the increase of the density of network structure, brought about autopolymerization. Then, the rate of reaction found to be increased.

12. The photopolymerization of ALPNR was found to be faster in HDDA than TPGDA (in the condition of 20% by weight of rubber) under the presence of Irgacure 184 as a photoinitiator. It may be due to the shorter chain length of HDDA could be faster on the formation of network structure. However, in the condition of using small amount of reactive diluents (5 and 10% by weight of rubber), TPGDA showed the higher rate of polymerization. It may be due to in the high viscosity condition, the long chain of TPGDA could help the encounter of the end active functional groups more than HDDA.

13. On the effect of photoinitiator, it was found that rate of polymerization was increased with increasing of amount of photoinitiator, especially Irgacure 184. In

the case of Darocur 1173, the  $R_p$  was found to be decrease, when the amount of Darocur was more than 3% by weight of rubber and diluent. It was also found that Irgacure 184 was a more effective initiator than Darocur 1173 when combined with HDDA diluent.

14. By changing the reaction temperature from 30 to 90°C, the photopolymerization reaction was found to be higher. It might be due to the increase of reaction temperature could be increased the mobility of active functional groups and the network structure, the encountering of active groups increased, then the ultimate yield and rate of polymerization were found to be increased.